DETERMINATION OF THE HEAT OF SOME AEROBIC FERMENTATIONS

© HA THANH LUONG

Submitted to the Faculty of Graduate Studies and Research of McGill University in partial fulfillment of the requirements for the degree DOCTOR OF PHILOSOPHY

Thesis Supervisor : Dr. B. Volesky

Department of Chemical Engineering
McGill University, Montreal, Canada

August 1979

RESUME

Nous avons developpé une nouvelle technique pour la mesure continue du taux de production de chaleur durant un procédé de fermentation. La technique basé sur un système spécial de contrôle de température a été utilisé pour mesurer la quantité de chaleur métabolique produite par activité microbienne. La quantité de chaleur mesurée a été quantitativement évaluée et corrigée pour les pertes et gains de chaleur sur la base d'un bilan de chaleur sur l'appareil de fermentation. Etant donné que la chaleur d'agitation n'est pas connue, et qu'elle a une grande influence sur le bilan de chaleur, cette variable a été examinée en détail. Ona ainsi pu élaborer une meilleure corrélation générale entre le rapport des puissances requises pour l'agitation avec ou sans gaz et les nombres d'aeration et de Weber pour l'agitateur . Spécifiquement cette technique a été employée pour déterminer avec précision le taux d'évolution de chaleur de *l'Aspergillus niger, l'Escherichia coli, la Candida lipolytica, la Candida utilis, et la Candida intermedia* cultivés sur différentes sources de carbone : hydrates de carbones, hydrocarbures et ethanol .

Avec les donnés expérimentales que nous avons obtenues, une corrélation du taux de chaleur dégagée et du taux d'oxygène consommé a été établie : $Q_{ferm} = 0.111\ \Delta O_2$. La chaleur totale dégagée correspond bien à la quantité d'oxygène consommée par les micro-organismes en croissance . La constante de proportionalité pour cette corrélation est 0.111 kcal/mmol O_2 . Les résultats expérimentaux sont en accord avec ceux obtenus par la technique dynamique calorimétrique et avec les prédictions théoriques .

Les corrélations rapportées dans cette étude sont très utiles pour le calcul, le contrôle et l'optimisation de processus de fermentation .

ABSTRACT

An accurate continuous technique has been developed and applied to continuous measuring of the rate of heat production during a fermentation process. A special temperature control system was used to monitor the amount of metabolic heat produced by microbial activity. The results were corrected for heat losses and gains based on the overall heat balance on the fermentor. Since the heat of agitation represented a major unknown in the heat balance, it was examined for the given system in more detail. This part of the study yielded an improved general correlation between the gassed-to-ungassed mixing power consumption ratio and the aeration number and the impeller Weber number. The technique was used for precisely determining the rate of heat evolution of *Aspergillus niger*, *Escherichia coli*, *Candida lipolytica*, *Candida intermedia* , and *Candida utilis* grown on ethanol and different carbohydrate and hydrocarbon carbon sources .

Based on the experimental data, a correlation between the rate of heat released and the rate of oxygen consumed has been determined as $Q_{ferm} = 0.111\ \Delta O_2$. The total heat released also correlated well with the total oxygen consumed by the growing culture . The proportionality constant for this correlation was 0.110 kcal/mmol O_2 . The experimental results agreed well with the theoretical predictions and with those developed by the dynamic calorimetric technique .

The derived correlations reported in this study are useful for fermentation process design, optimization and control .

ACKOWLEGEMENTS

I would like to express my sincere appreciation and gratitude to Dr. B. Volesky who suggested this project and provided helpful advice and encouragement throughout the investigation .

I am grateful to Dr. T. J. Boyle for his generous help and advice .

Thanks is also due to Mr. W. Hoogendoorn for his assistance in the construction and implementation of equipment .

I desire to extend my appreciation to Dr. J. Little and his associates of the Montreal Neurological Hospital and Dr. H. G. Robson of the Royal Victoria Hospital who saved my life in the final stage of this research ; without them this project could never have been completed .

I owe a debt of thanks to my parents who have been a source of encouragement throughout my education .

Last but not least, this dissertation is lovingly dedicated to my wife, Thien-Huong whom I love, honor and cherish. Her unique love, her outstanding patience and her infinite generosity permitted her to constantly bear my depressed behavior and also to share the pain with me during the most discouraging moment of this research .

TABLE OF CONTENTS

Page

Page

CHAPTER IV - RESULTS

CHAPTER V - DISCUSSION

CHAPTER VI - CONCLUSIONS AND RECOMMENDATIONS

LIST OF TABLES

LIST OF FIGURES

CHAPTER I

INTRODUCTION AND LITERATURE REVIEW

A. INTRODUCTION

One of the important aspects of a number of microbial processes used in industry is the removal of heat from the bulk liquid broth in order to maintain an optimal temperature for desired microbial activity. Efficient heat removal is specially important in aerobic hydrocarbon fermentations where the heat released is estimated to be 2½ times that of conventional carbohydrate fermentations[1] (Table I) .

Relatively little useful information is available on the microbial thermogenesis. Information on the amount of heat being produced during the fermentation process is crucial for a proper design of a cooling system and can be also used for assessing the degree of microbial activity. The problem of heat removal is very important in fermentation industry where the capital cost of the heat removal system always represents a significant proportion of the overall cost of plant items. In terms of operating expenses, the cost of power for oxygen transfer and heat removal represents typically 15-20% of the manufacturing costs[2]. The heat removal techniques should be optimized in order to improve the overall project profitability.

The problem of biological heat generation is also of great interest since no reliably accurate and convenient method has been available which would provide criteria for predicting the heat evolved and thus

TABLE I

GENERAL STOICHIOMETRIC RELATIONS FOR FERMENTATIONS

CARBOHYDRATES :

$$1.8n\ CH_2O + 0.8n\ O_2 + 0.19n\ NH_4^+ + \text{(essential elements as P,K,S,etc.)} \longrightarrow$$

$$n(CH_{1.7}O_{0.5}N_{0.19}\ \text{Ash}) + 0.8n\ CO_2 + 1.3n\ H_2O + 80{,}000\ n\ \text{Kcal}$$

HYDROCARBONS :

$$2n\ CH_2 + 2n\ O_2 + 0.19n\ NH_4^+ + \text{(essential elements as P,K,S,etc.)} \longrightarrow$$

$$n(CH_{1.7}O_{0.5}N_{0.19}\ \text{Ash}) + n\ CO_2 + 1.5n\ H_2O + 200{,}000\ n\ \text{Kcal}$$

facilitating the scale-up of heat removal systems .

B. LITERATURE REVIEW

A literature review indicated that much of the early work concerning the measurement of the heat of fermentation was discussed briefly by Winzler and Baumberger.[3] The approaches taken by most of the investigators involved the use of crude calorimeters to measure the heat evolved in their respective fermentations.

A more recent method for heat measurements in microbial cultures was reported by Sedlaczek and co-workers.[4] These investigators presented a dynamic micro-calorimetric technique to measure the heat during fermentation. Basically, this procedure involves measuring the temperature difference between the fermentor and the surroundings when the surroundings temperature is accurately controlled.

Other different procedures have also been used to measure the heat of fermentation. In most cases, as Cooney et al[5] pointed out, the techniques require relatively complicated apparatus and/or procedures for determining the heat produced during growth and product formation[6,7].

A successful attempt was reported by Cooney[5] et al based on a simple technique for measuring the rate of heat production during a fermentation process by monitoring the broth temperature rise when the temperature controller was turned off. The heat accumulation measured in this manner was then corrected for heat losses and gains on the bio-reactor. Volesky[8] et al

applied this "dynamic calorimetry" to natural gas fermentation. The authors pointed out that the use of the dynamic calorimetric technique posseses a certain advantage in its relative simplicity. The approach, however, requires continuous attention during fermentation and may not be compatible with the application of automatic process control monitoring the heat of fermentation. The procedure also does not take into account the changing physical properties of the fermentation broth. Extra-cellular surface active agents change the gas hold-up thus affecting the fluid density. Apart from viscosity and density changes during the fermentation process, some types of broths are known to exhibit highly non-Newtonian rheological properties. These factors can appreciably change the mixing power input requirements for the culture broth even though the external factors such as agitation speed and aeration rate are maintained constant. Error in the measurement of agitation power contributes significantly to the error in the overall heat balance on the bioreactor.

Recently, Eriksson and co-workers[9,10] described a flow calorimeter which can measure heat evolution independent of the disturbances caused by stirring or the addition of gas, alkali, or nutrients. Mou and Cooney[11] commented that this technique suffers from the problems of wall growth in the measuring cell and oxygen deficiency with increasing cell densities. It may also be difficult to use with filamentous organisms or non-Newtonian fluids. In a recent study, Mou and Cooney[11] also applied the dynamic calorimetric technique for monitoring fermentation processes. The rate of heat evolution in mycelial fermentations for novobiocin and cellulase production with media containing non-cellular solids was measured by this technique.

Thermal data obtained were proved significant both in monitoring the cell concentration during a trophophase(growth phase) and in serving as an additional physiological variable in the fermentation process. The validity of this technique was demonstrated by closing the overall material and energy balances.

Based on the elemental stoichiometric equations, Minkevich and Eroshin[12] developed a semi-theoretical correlation between the heat released and the culture oxygen uptake rate under oxygen limitation conditions. Imanaka and Aiba[13] recently also established a convenient method to evaluate the rate of heat evolution based on total oxygen demand. In order for these correlations and their principles to be employed, more supporting experimental data are required.

The practical significance of the heat of fermentation is illustrated by the failure of a project in the West Indies which failed to produce food yeast because of the problems in removal of heat from the fermentation vessel[14]. Furthermore, Guenther[15], in an analysis of aerobic hydrocarbon fermentations,noted that the cost of heat removal could very well cause the growth of yeast on hydrocarbons to be an uneconomical venture.

More fundamental and reliable criteria for predicting the heat of fermentation would be most useful for the design and scale-up operations as well as for the optimization of the manufacturing costs of fermentation products in the fermentation industry.

For the purpose of easily developing laboratory data on the heat of fermentation this work has focused on the development of an appropriate

temperature control system whose action can be monitored as it varies in response to the amount of heat produced by microbial activity. This enables determination of heat of fermentation with high accuracy without undue disturbance to the culture. The technique has been shown to be applicable to measure the rate of heat evolution which in turn was correlated well with oxygen consumption by the growing culture .

CHAPTER II

THEORETICAL ASPECTS

The theoretical aspects of this work are divided into three parts: The mathematical basis for calculating the heat released during the growth in a batch fermentor, the relationship between the heat evolution and the oxygen uptake during fermentation, and estimation of the oxygen uptake rate based on the measurements of oxygen and carbon dioxide concentrations in an outgoing gas stream.

II-1. MATHEMATICAL BASIS FOR CALCULATING THE HEAT RELEASED DURING FERMENTATION

II-1.1. The Overall Heat Balance On The Fermentor

An expression of the heat balance around the fermentor was attempted. A control element LJKL will be considered containing an operating volume V_L in which the concentration of cells is X g/ℓ. During operation the temperature of the control element is maintained at a preset value T (Fig. II.1). An aerobically growing culture requires a flow rate of Q ℓ/min of air which is characterized by its temperature T and humidity Y_o. The flow of the air stream through the volume V_L of the control element results in the removal of sensible heat and evaporative heat loss from the control element. The heat input into the control element is provided by the agitation required for maintaining the volume homogeneous and well aerated. A further

Figure II.1. The Overall Heat Balance on the Fermentor

Q_{ferm} : The Rate of Heat Production of Fermentation

Q_{sen} : The Rate of Sensible Heat Loss

Q_{evp} : The Rate of Evaporative Heat Loss

Q_{surr} : The Rate of Heat Loss to the Surroundings

Q_{agi} : The Rate of Heat of Agitation

Q_{con} : The Rate of Heat Removal by the Temperature Controller

Q_{bub} : The Rate of Heat Dissipated by the Sparged Gas

All terms in the heat balance equation have the units of kcal/ℓ.h

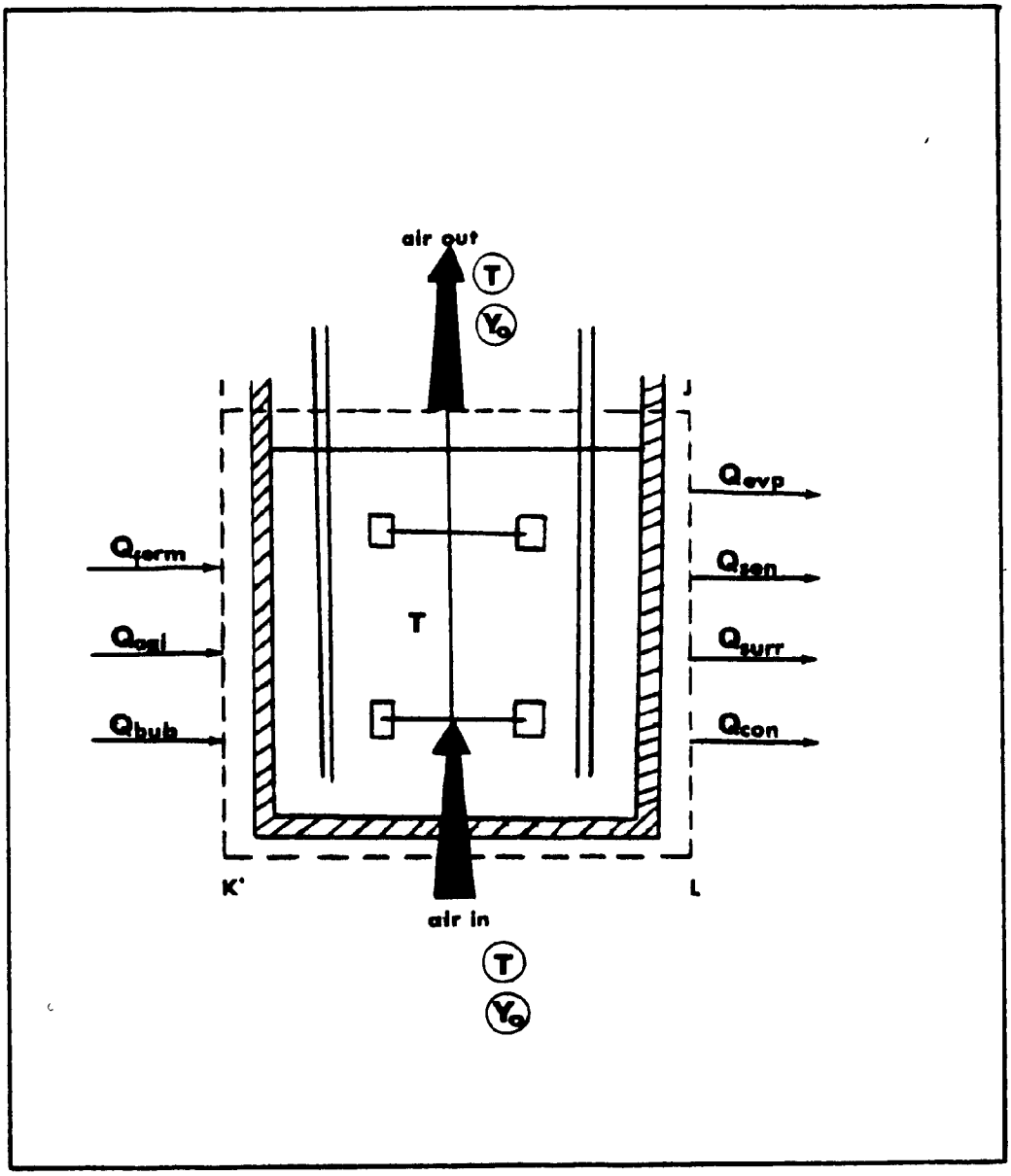
air out
T
Y_o
Q_{evp}
Q_{conv}
Q_{sen}
Q_{cond}
T
Q_{surr}
Q_{bub}
Q_{con}
K'
L
air in
T
Y_o

heat input into the control volume is due to the bubbling gas. The difference in temperature of the control element T and that of the ambient T_{amb} leads to the heat exchange between the two localities. Finally the heat removal from fermentor during exothermic growth is considered as another heat loss from the control element. Considering the exothermic growth and respiration processes of the micro-organism, the following heat balance on the control element can be written:

$$\text{Total heat input} = \text{Total heat output} \quad \ldots\ldots\ldots (1)$$

Substitution of the component heat terms yields:

$$Q_{ferm} + Q_{agi} + Q_{bub} = Q_{sen} + Q_{evp} + Q_{surr} + Q_{con} \quad \ldots (2)$$

The overall heat balance above is based on the following assumptions:

- No spatial variations of temperature in the bio-reactor.
- Homogeneous biomass distribution throughout the fermentor volume.
- Constant gas flow rate through the fermentor.

Another arrangement of equation (2) is as follows:

$$Q_{ferm} = Q_{sen} + Q_{evp} + Q_{surr} - Q_{con} - Q_{agi} - Q_{bub} \quad \ldots (3)$$

Equation (3) shows that Q_{ferm} , the heat evolution during the fermentation, can be completely specified by experimentally measuring and/or estimating the six remaining heat terms .

II-1.2. The Determinations of The Evaporative and Sensible Heat Loss

When the air stream passes through the control element of fermentation broth, it is carrying away a certain volume of vaporized liquid. This results in the removal of the latent heat of vaporization from the control element. The heat loss by evaporation can be expressed :

$$Q_{evp} = \frac{\lambda W_{air}}{V_L} (Y_{out} - Y_{in}) \quad \ldots\ldots\ldots\ldots\ldots\ldots (4)$$

Where

W_{air}	:	Mass flow rate of air (kg/h)
Q_{evp}	:	Heat of evaporation (kcal/l.h)
λ	:	Latent heat of evaporation (kcal/kg)
Y_{in}, Y_{out}	:	Humidity of air in and out of the fermentor (kg water/kg dry air)

The humidity of air is calculated from the following formula :

$$Y = \frac{18 P_w}{29(760-P_w)} \quad \ldots\ldots\ldots\ldots\ldots\ldots\ldots\ldots (5)$$

Where P_w = vapor pressure of water (mm Hg)

The sensible heat loss from the control element can be evaluated by

calculating the difference in the inlet and outlet temperatures of the air stream, i.e.,

$$Q_{sen} = \frac{W_{air}}{V_L} (T_{out} - T_{in}) (C_{air} + C_w Y_{out}) \quad \ldots\ldots\ldots (6)$$

Where

Q_{sen} : Sensible heat loss (kcal/l.h)

C_{air} : Heat capacity of air (kcal/kg.^{o}C)

C_w : Heat capacity of water (kcal/kg.^{o}C)

Y_{out} : Humidity out of fermentor as defined previously

Equations (4) to (6) can be used to estimate the sensible heat loss as well as the evaporative heat loss. However, if the incoming gas is saturated with water at the operating temperature of the fermentor before being introduced into the fermentor, the evaporative and sensible heat loss can safely be neglected[8,11] . The overall heat balance therefore becomes :

$$Q^{*}_{ferm} = Q_{con} + Q_{surr} - Q_{agi} - Q_{bub} \quad \ldots\ldots\ldots\ldots\ldots\ldots (7)$$

II-1.3. <u>The Determination of The Heat Dissipated by The Sparged Gas</u>

The energy input to the liquid phase by a sparged gas consists of the jet energy at the sparger hole which is transmitted to the bulk liquid and of the energy required to move the gas through the static liquid head above the sparger.

The application of the First Law of Thermodynamics to an ideal gas system results in the following expression :

$$Q_{bub} = W_{air} \left[(KE_{out} - KE_{in}) + (PE_{out} - PE_{in}) \right] \quad \ldots\ldots\ldots (8)$$

Where

Q_{bub}	:	Rate of heat transfer to the system
W_{air}	:	Mass flow rate of gas
KE	:	Kinetic energy per unit mass of gas
PE	:	Potential energy per unit mass of gas

The kinetic energy change can be estimated by the basic formula :

$$(KE_{out} - KE_{in}) = U_{out}^2/2 - U_{in}^2/2 \quad \ldots\ldots\ldots\ldots\ldots (9)$$

In normal case $U_{out} << U_{in}$, equation (9) then becomes :

$$(KE_{out} - KE_{in}) = - U_{in}^2/2 \quad \ldots\ldots\ldots\ldots\ldots (10)$$

The potential energy change is the work required to push the bubble from the sparger to the top of the liquid height. The work required becomes constant if the operation is performed at low pressure, i.e., $\rho_G << \rho_L$

$$W = V_b \rho_D g h \quad \ldots\ldots\ldots\ldots\ldots\ldots\ldots (11)$$

Where V_b is volume of a bubble

The work required per unit mass of gas then becomes

$$\frac{W}{V_b \rho_G} = \frac{\rho_D g h}{\rho_G} \quad \ldots\ldots\ldots\ldots\ldots\ldots\ldots\ldots \quad (12)$$

From equations (8) to (12) the result is

$$Q_{bub} = - W_{air} U_{in}^2/2 - W_{air} \rho_D g h/\rho_G \quad \ldots\ldots\ldots\ldots \quad (13)$$

If it is assumed further that $\rho_D \simeq \rho_L$, and $W_{air}/\rho_G A$ is the superficial velocity V_s , the rate of heat transfer becomes :

$$Q_{bub} = - W_{air} U_{in}^2/2 - V_s A \rho_L g h \quad \ldots\ldots\ldots\ldots \quad (14)$$

It is evident that $Q_{bub} < 0$ and thus heat must be removed to keep the bio-reactor isothermal. From equation (14) , the energy dissipated by the bubbling gas can be expressed as follows :

$$Q_{bub} = \frac{Q \rho_G}{V_L} (U_{in}^2/2) + V_s A \rho_L g h/V_L \quad \ldots\ldots\ldots \quad (15)$$

The energy dissipated by the bubbling gas can be found from the work of Lehrer[16] and Miller[17] .

II-1.4 The Determination of Heat Exchange to the Surroundings

The temperature difference between the control element and its surroundings results in heat transfer to or from the element. The schematic diagram of a simple model for the heat exchange to the surroundings is shown in Figure II.2 .

In order to derive a relationship for estimating the heat loss to the surroundings, the following assumptions were made :

- Steady state heat transfer
- Uniform temperature T throughout the bulk liquid phase of the control element .
- The interfacial resistance between region (1) and (2) is negligible
- Constant thermal conductivities k_{01} and k_{02} in region 1 and 2
- Newton's Law of cooling at the fluid-solid interface apply
- Radiation heat loss is negligible

The total heat loss to the ambient air includes the heat loss in radial and axial directions and the heat loss through the supported stainless steel headplate of the fermentor (the stainless steel structure includes the baffles, impeller shaft, thermocouple and thermistor well, and sampling tube as well as the headplate itself). The headplate rests on a steel on a steel supporting fin which is part of the fermentor frame. The whole structure represents a complicated heat sink arrangement. The total heat loss to the surroundings may be written as follows :

$$Q_{surr} = Q^1_{surr} + Q^2_{surr} + Q^3_{surr} \quad \ldots\ldots\ldots\ldots\ldots (16)$$

Figure II.2 A Model for the Heat Loss to the Surroundings

Region 01 - Fermentor Wall

Region 12 - Insulating Material

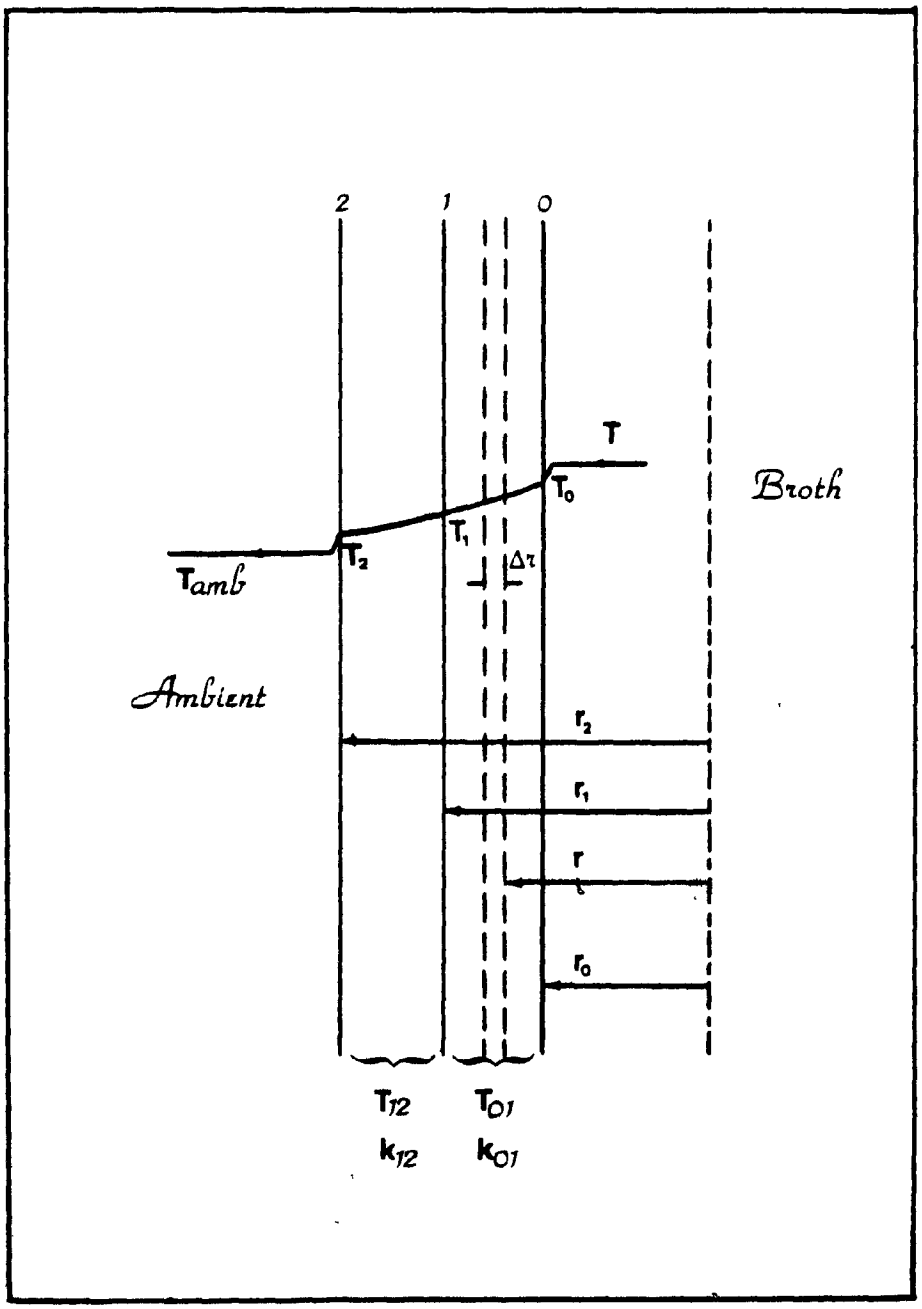
2
1
0
T
T_0
Broth
T_1
T_2
Δr
T_{amb}
Ambient
r_2
r_1
r
r_0
T_{12}
T_{01}
k_{12}
k_{01}

* The heat loss in radial direction

A heat balance on a element Δr of length L (the axial length of the control element) yields :

$$\text{Heat in} - \text{Heat out} = 0 \quad \ldots\ldots\ldots\ldots \quad (17)$$

If q_{01} is the heat flux per unit area per unit time equation (17) then becomes :

$$2\pi rL\, q_{01}\Big|_{r=r} - 2\pi rL\, q_{01}\Big|_{r=r+\Delta r} = 0 \quad \ldots\ldots\ldots \quad (18)$$

Dividing by $2\pi L\Delta r$ with the limit $\Delta r \to 0$ gives the following differential expression

$$\frac{d}{dr}\left(r\, q_{01}\right) = 0 \quad \ldots\ldots\ldots\ldots\ldots\ldots \quad (19)$$

Integrating equation (19) for constant thermal conductivity k_{01} ,

$$r\, q_{01}^{r} = r_o\, q_o \quad \ldots\ldots\ldots\ldots\ldots\ldots \quad (20)$$

Since the primary mode of heat transfer occurs by a conductive mechanism, the Fourier's Law[18] of conductive heat transfer can be applied

$$q_{01}^{r} = -k_{01}\frac{dT_{01}}{dr} \quad \ldots\ldots\ldots\ldots\ldots\ldots \quad (21)$$

Substitution of (21) into (20) gives

$$-k_{01}\frac{dT}{dr} = \frac{r_o q_o}{r} \qquad \text{..... (22)}$$

or

$$dT = -\frac{r_o q_o}{k_{01}}\left(\frac{dr}{r}\right) \qquad \text{..... (23)}$$

Integrating with boundary condition $T = T_o$ at $r = r_o$, and $T = T_1$ at $r = r_1$

$$\int_{T_o}^{T_1} dT = \frac{r_o q_o}{k_{01}} \int_{r_o}^{r_1} \frac{dr}{r} \qquad \text{..... (24)}$$

After integrating, equation (24) becomes

$$T_o - T_1 = \left(\frac{r_o q_o}{k_{01}}\right) \ln (r_1/r_o) \qquad \text{..... (25)}$$

From Newton's Law[19] of cooling at the fluid-solid interface, it follows that

$$T - T_o = q_o/h_o \qquad \text{..... (26)}$$

$$T_2 - T_{amb} = \frac{r_o}{r_2}\left(\frac{q_o}{h_r}\right) \qquad \text{..... (27)}$$

In equations (26) and (27), h_o and h_r are the heat transfer coefficients at the fermentor wall and the ambient insulation interface. An expression

for q_o results from the addition of equation (26) and (27) .

$$\text{Heat Flux} \quad q_o = U_1^* \left(T - T_{amb} \right) \quad \ldots\ldots\ldots\ldots\ldots \quad (28)$$

where U_1^* , the overall heat transfer coefficient used in equation (28), is defined by

$$U_1^* = \frac{1}{\left\{ 1/h_o + (r_o/k_{01}) \ln(r_1/r_o) + (r_o/k_{12}) \ln(r_2/r_1) + r_o/r_2 h_\infty \right\}} \quad (29)$$

Hence from the heat flux per unit time , the heat loss per unit volume of fermentation broth can be evaluated as follows :

$$Q_{surr}^1 = \frac{2\pi L \left(T - T_{amb} \right)}{V_L \left[1/h_o r_o + \ln(r_1/r_o)/k_{01} + \ln(r_2/r_1)/k_{12} + 1/r_2 h_\infty \right]} \quad (30)$$

where $A_o = 2\pi r_o L$ is chosen as the base area for heat transfer.

* <u>The determination of the film heat transfer coefficient for the liquid side</u>

Almost all successful studies have correlated the film heat transfer coefficient h_o by a correlation of the form[20]

$$\left(\frac{h_o D}{k_f} \right) = K_1 \left(\frac{d^2 N \rho}{\mu} \right)^{2/3} \left(\frac{c_p \mu}{k_f} \right)^{1/3} \left(\frac{\mu_w}{\mu} \right)^{0.14} \quad \ldots\ldots\ldots\ldots\ldots \quad (31)$$

where μ_w and μ are viscosities of the fluid at the vessel walls and in

the bulk liquid respectively. If it is further assumed that $\mu_w \approx \mu$, equation (31) becomes :

$$\left(\frac{h_o D}{k_f}\right) = K_1 \left(\frac{d^2 N \rho}{\mu}\right)^{2/3} \left(\frac{c_p \mu}{k_f}\right)^{1/3} \quad \ldots\ldots\ldots\ldots\ldots\ldots (32)$$

According to Brooks and Su[21] the value of K_1 is equal to 0.74 for a disk flat blade turbine-type agitated reactor with 1,2, or 4 baffles. Equation (32) is considered to represent more closely to test data from available sources[21].

Where

$$300 < N_{Re} < 3 \times 10^5 \quad \ldots\ldots\ldots\ldots\ldots (33)$$

* <u>The determination of the film heat transfer coefficient for the ambient side</u>

The heat transfer from the wall of the insulating material to the ambient air can be considered as a free convection heat transfer on a vertical cylinder. Many experimental investigations have been conducted to determine the heat transfer from various surfaces to fluids in free-convection. The data are usually correlated by an equation of the form

$$\left(\frac{h_\infty L}{k_f}\right) = Nu_f = C \left(Gr_f Pr_f \right)^m \quad \ldots\ldots\ldots\ldots\ldots\ldots (34)$$

where the subscript f indicates that the properties in the dimensionless groups are evaluated at the mean film temperature

$$T_f = \frac{T_\infty + T_w^*}{2} \qquad \text{..... (35)}$$

McAdams[22] has summarized available experimental data for free convection from vertical cylinders, and recommended values of C and m to be used with equation (34) (Table II)

TABLE II

CONSTANTS FOR USE WITH EQUATION (34) FOR FREE CONVECTION FROM VERTICAL PLANES AND CYLINDERS

$Gr_f \times Pr_f$	(C)	(m)
$10^4 - 10^9$	0.59	1/4
$10^9 - 10^{12}$	0.13	1/3

In equation (34), h_∞ is the film heat transfer coefficient on the ambient side where Pr and Gr are the Prandtl and Grashof numbers respectively, which are usually defined as follows :

$$Pr = \frac{c_p \mu}{k_f} \quad \text{.....} \quad (36)$$

$$Gr = \frac{g \beta \rho^2}{\mu^2} (T_w^* - T_\infty) L^3 \quad \text{.....} \quad (37)$$

The constant β in equation (37) is so-called volume expansion of the temperature coefficient and defined as

$$\beta = \left(\frac{1}{V}\right)\left(\frac{\partial V}{\partial T}\right)_p = \frac{\rho_\infty - \rho}{\rho(T - T_\infty)} \quad \text{.....} \quad (38)$$

The heat loss to the surroundings in the radial direction, therefore, can be estimated since two unknown parameters h_o and h_∞ have already been specified .

* The heat loss in the axial direction

Equation (30) is only expected to yield an accurate result in estimating the heat loss to the surroundings when the length of reactor is relatively large, i.e. the bulk of the heat flow will be through the walls in a radial direction. For the sake of simplicity, it is necessary to assume that the heat flow from the top plate and the bottom of the reactor in an axial direction is identical and proportional to the heat exchange in the radial direction through the following relationship

$$Q^2_{surr} = Q^T_{surr} + Q^B_{surr} = Q^1_{surr} * \left[\frac{\pi R_3^2}{2\pi L R_3}\right] \quad \text{.....} (39)$$

where $2\pi LR_3$ and πR_3^2 are the heat transfer area of the system in radial and axial direction respectively. The heat loss to the surroundings in both radial and axial directions, therefore becomes :

$$Q^1_{surr} + Q^2_{surr} = Q^1_{surr} (1 + R_3/L) \quad \ldots\ldots\ldots\ldots\ldots\ldots (40)$$

The heat loss in radial and axial directions per unit volume of fermentation broth can be estimated as follows :

$$Q^1_{surr} + Q^2_{surr} = \frac{2\pi L(1 + R_3/L)(T - T_{amb})}{V_L\left\{1/r_o h_o + \ln(r_1/r_o)/k_{01} + \ln(r_2/r_1)/k_{12} + 1/r_2 h_\infty\right\}} \quad (41)$$

* <u>The heat sink</u>

There was a heat loss to the surroundings through the steel fermentor head support which could be considered as a heat sink. The stainless steel fermentor head includes the baffles, thermometer well, impeller shaft, and sampling tube. These act as heat conducting elements connected with the head plate and the fermentor console which make the estimation of the heat lost very difficult. The evaluation of the heat loss to the surroundings can only be determined experimentally. However, according to equations (16) to (41) the heat loss to the surroundings does not change appreciably during the course of fermentation even though the physical properties of fluid may vary significantly. The evaluation of the heat loss to the surroundings before inoculation could safely be used for the estimate of the heat of fermentation during the culture

period. It is, of course, corrected for the differing temperature difference driving forces during experiments .

II-1.5. The Determination of The Heat Dissipated by The Impeller Shaft

The semi-theoretical formula for predicting the mixing power input in non-aerated systems is available from the work of Rushton et al[23]

$$P = \frac{N_p \rho_L N^3 d^5}{g_c} \qquad \ldots\ldots\ldots\ldots\ldots\ldots\ldots (42)$$

Equation (42) has been developed for fully baffled systems, and in the turbulent regime ($N_{Re} > 10^4$) where the power number N_p is a constant dependent on the particular impeller configuration .

The power dissipated by the impeller into the liquid phase of an aerated agitated system cannot be determined from equation (42) simply by replacing ρ_D for ρ_L[24] . No universally applicable correlation has been available for predicting accurately the power input of a gas-liquid system. There are only a limited number of empirical correlations for this purpose such as those of Ohyama and Endoh[25], Michel and Miller[26], Pharamond et al[27], Clark and Vermeulen[28], and a recent contribution of Hassan and Robinson[29].

i- Correlation of Ohyama and Endoh[25]

$$P_g/P = f\left(N_A = \frac{Q}{N d^3}\right) \qquad \ldots\ldots\ldots\ldots\ldots\ldots (43)$$

Calderbank[30,31] applied this correlating method and found the following relationship :

$$P_g/P = K_2 \quad \text{..... (44)}$$

If $N_A < 0.035 \longrightarrow K_2 = 1 - 12.6\, N_A$ ..... (45)

If $N_A > 0.035 \longrightarrow K_2 = 0.62 - 1.85\, N_A$ ..... (46)

The correlations of Ohyama and Endoh[25] and Calderbank[30,31] do not uniquely characterize the interaction of gas flow rate and rotational speed which was pointed out by Michel and Miller[26].

ii- Correlation of Michel and Miller[26]

$$P_g = C_1 \left(\frac{P^2 N d^3}{Q^{0.56}} \right)^{0.45} \quad \text{..... (47)}$$

In MKSA system the proportionality constant C_1 equals to 0.72 . The correlation of Michel and Miller could not be reliably applied to large scale equipment and also failed at extreme values of gas flow rate. Furthermore, this correlation does not appear to be applicable to gas dipersions in aqueous electrolyte solutions as pointed out by Hassan and Robinson[29].

iii- Correlation of Clark and Vermeulen[28]

The power ratio was given by Clark and Vermeulen[28] as

$$P_g/P = f\left(\Phi\, N_{We}^{1/4}\, G_v^{-1/2} \right) \quad \text{..... (48)}$$

The correlation of Clark and Vermeulen[28] appears to have the most merit since the authors used the impeller Weber number and the measured gas hold-up as a basis for calculating the gassed-to-ungassed power ratio . However, their method of gas sparging was unusual in that a perforated plate covering the entire bottom of the vessel was used to distribute the gas . Equation (48) thus may not be safely applied to a one-single orifice sparger system .

iv- Correlation of Pharamond et al[27]

$$1 - P_g/P = 96 \left(Q/V_L \right) D^{0.63} \quad \text{..... (49)}$$

Equation (49) is only applicable for $\left(Q/V_L \right) D^{0.63} < 0.3$; above this value , P_g/P is more or less constant at 0.5 to 0.55 . The correlation of Pharamond et al[27] is restricted to correlating only their experimental data developed with six-blade turbine impeller .

v- Correlation of Hassan and Robinson[29]

The power ratio was proposed by Hassan and Robinson[29] as

$$P_g/P = C_2 N_{We}^{-0.25} N_A^{-0.38} (\rho_L/\rho_D) \quad \text{..... (50)}$$

The proportionality constant C_2 of the correlation of Hassan and Robinson[29] may vary with different tank sizes and the correlation is restricted to

Newtonian fluids . It also requires the measurement of gas hold-up therefore it is not practically applicable for fermentation experiments where the aseptic conditions pose a serious restriction .

vi- Present Study

* The Principle of Strain-Gauge Dynamometer

Most of the aforementioned correlations are not expected to yield satisfactorily accurate estimates of the heat dissipated by the impeller shaft during the course of a fermentation process because the changes of fluids properties can alter the power drawn into the fermentation broth and the deviation of geometry of the fermentor may have some effects on the heat of mixing .

In this study, a mixing power measurement based on a strain gauge device was employed to measure the torque of the impeller shaft. Four identical strain-gauge were connected as shown in Fig.II.4 . Each gauge is exposed to a longitudinal stress, σ , resulting in a strain $\pm\varepsilon$. It is readily shown that the value of the potential, de, generated between the terminals of the bridge is[32]

$$de = V_1 K_s \varepsilon \qquad \text{..... (51)}$$

where V_1 = Electric potential applied

K_s = Gauge factor

The magnitude of the shaft shear strain, $\gamma/2$, is composed of longitudinal

Figure II.3 Principle of Strain Gauge Dynamometer for Measuring the Torque of Impeller Shaft

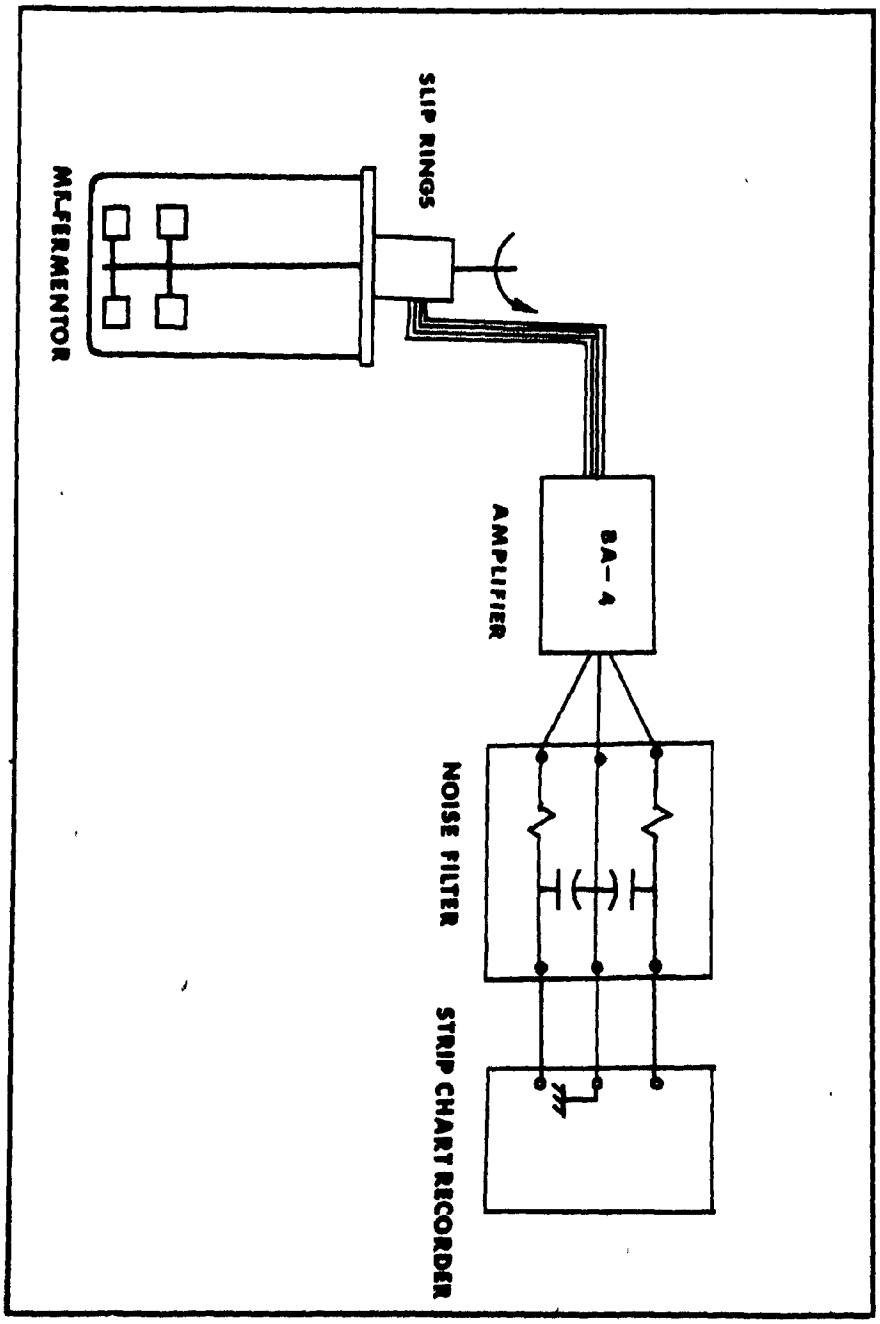
MF-FERMENTOR
SLIP RINGS
AMPLIFIER
BA-4
NOISE FILTER
STRIP CHART RECORDER

Figure II.4 Strain Gauge Dynamometer Arrangement

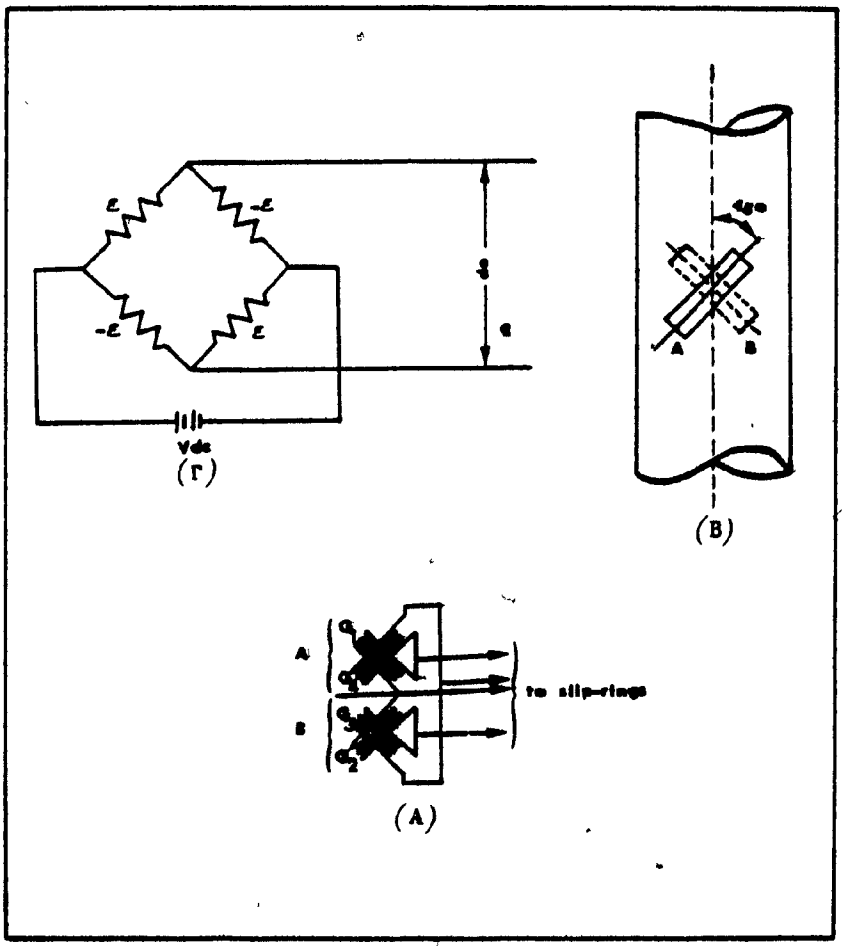
ε
-ε
-ε
ε
Vdc
(C)
A
B
(B)
A
B
to slip-rings
(A)

and transverse strains in the rotating shaft, σ/E and $-\sigma/mE$, respectively.

$$\gamma/2 = \sigma/E - (-\sigma/m.E) = \frac{\sigma}{E}(1 + 1/m) \quad \ldots\ldots (52)$$

In order to measure the torque of a rotating shaft, the gauges are mounted on the shaft at a 45° angle to the axis (Fig. II.4). The angle of 45° is selected because the shearing strain, ε, is maximum at this plane .

The value of ε in (51) can be substituted by $\gamma/2$ for the specific arrangement of strain-gauges on the shaft. Namely,

$$de = V_i K_s (\gamma/2) \quad \ldots\ldots\ldots\ldots\ldots\ldots (53)$$

where

E = Young's Modulus

m = Reciprocal of Poisson's ratio

For a shaft twisted by an imposed torque, the angle of twist ϕ is proportional to the distance x of the cross-section from the fixed-end and hence $d\phi/dx$ is a constant. This constant represents the angle of twist per unit length of the shaft and will be called θ :

$$\gamma = r\frac{d\phi}{dx} = r\,\theta \quad \ldots\ldots\ldots\ldots\ldots\ldots (54)$$

The maximum stress occurs on the outer surface of the shaft where $r = d_o/2$. Therefore,

$$\gamma_{max} = \theta \, d_o/2 \qquad \ldots\ldots\ldots\ldots\ldots\ldots\ldots\ldots \quad (55)$$

The total moment M about the axis of the shaft is the summation, taken over the entire cross-sectional area of these moments on the individual elements, i.e., :

$$M = \int_{d_i/2}^{d_o/2} G \, \theta \, \rho^2 \, dA = G \, \theta \int_{d_i/2}^{d_o/2} \rho^2 \, dA \qquad \ldots\ldots\ldots\ldots \quad (56)$$

$$= G \, \theta \, I_p \qquad \ldots\ldots\ldots\ldots\ldots\ldots \quad (56b)$$

Where

$$I_p = \int_{d_i/2}^{d_o/2} \rho^2 \, dA = \frac{\pi}{32} \left(d_o^4 - d_i^4 \right) \qquad \ldots\ldots\ldots \quad (57)$$

I_p is the polar moment of inertia of the ring section. From (56) and (57) results

$$\theta = \frac{M}{G \, I_p} = \frac{32 \, M}{\pi \left(d_o^4 - d_i^4 \right) G} \qquad \ldots\ldots\ldots\ldots\ldots\ldots \quad (58)$$

or

$$2 \, \gamma_{max}/d_o = \frac{32 \, M}{\pi \left(d_o^4 - d_i^4 \right) G} \qquad \ldots\ldots\ldots\ldots\ldots\ldots \quad (59)$$

Hence

$$\gamma_{max} = \frac{16\ M}{\pi\ (\ d_o^4 - d_i^4\ )G} \qquad \ldots\ldots\ldots\ldots\ldots\ (60)$$

From (51) and (60) yields

$$de = V_1 K_s \frac{\gamma_{max}}{2} = V_1 K_s \frac{8\ M\ d_o}{\pi(\ d_o^4 - d_i^4\ )G} \quad \ldots\ldots\ (61)$$

When the value of torque is obtained, the power consumption can be calculated by the following relation :

$$P \text{ or } P_g = M\omega = 2\pi N M \qquad \ldots\ldots\ldots\ldots\ldots\ (62)$$

* <u>The Correlating Procedure for The Mixing Power Input</u>

Based on the experimental data as well as the work of Ohyama and Endoh[25], Michel and Miller[26], Clark and Vermeulen[28], and Hassan and Robinson[29], the following correlation is proposed here to correlate the mixing power ratio :

$$P_g/P = C_1^* \left(\frac{Q}{N\ D^3}\right)^{m^*} \left(\frac{N^2\ \rho\ D^3}{\sigma}\right)^{n^*} \qquad \ldots\ldots\ldots\ldots\ (63)$$

The constants C_1^*, m^*, and n^* are to be determined experimentally by measuring the mixing power input and the physical properties of the fluids studied .

II-1.6 The Determination of the Heat Removal by the Action of Temperature Controller

During the isothermal fermentation process, the amount of heat removed from the fermentor can be evaluated by measuring the cooling water inlet and outlet temperatures and its flow-rate through two hollow baffles inside the bio-reactor. However, in bench scale fermentors, it is very difficult to control an exact amount of water flow rate required for cooling. Furthermore, it is not practical to record the flow rate of cooling water continuously .

In this study, the fermentation broth was overcooled by a given constant cooling water flow rate. The excess heat removed from the fermentor is then made-up by the action of an immersion electrical heater. The temperature of the fermentation broth is measured by a thermocouple and compared with the set-point temperature of an electrical proportional controller. The difference between these two signals is used to control the programmable direct current (dc) power supply which activates the immersion heater at the proper power level. The rate of heat removed from the fermentor, therefore, can be evaluated as the difference between the rate of heat transfer from the fermentation broth to the cooling water baffles and the compensating heat produced by the immersion heater (Fig. II.5).

Mathematically, the rate of heat removal can be expressed as follows :

$$Q_{con} = \frac{U_2 A_2 K Q_c}{V_L (K Q_c + 1)} (T - T_c) - 0.8604 \; V_2 I / V_L \quad \ldots\ (64)$$

Figure II.5 A Temperature Control System for Measuring the Heat of Fermentation

HI = Heat Indicator

PI = Proportional Plus Reset Controller

FM = Flow Meter

TC = Thermocouple

H = Immersion Heater

PPS = Programmable Power Supply

HCV = Hand Control Valve

CW = Cooling Water

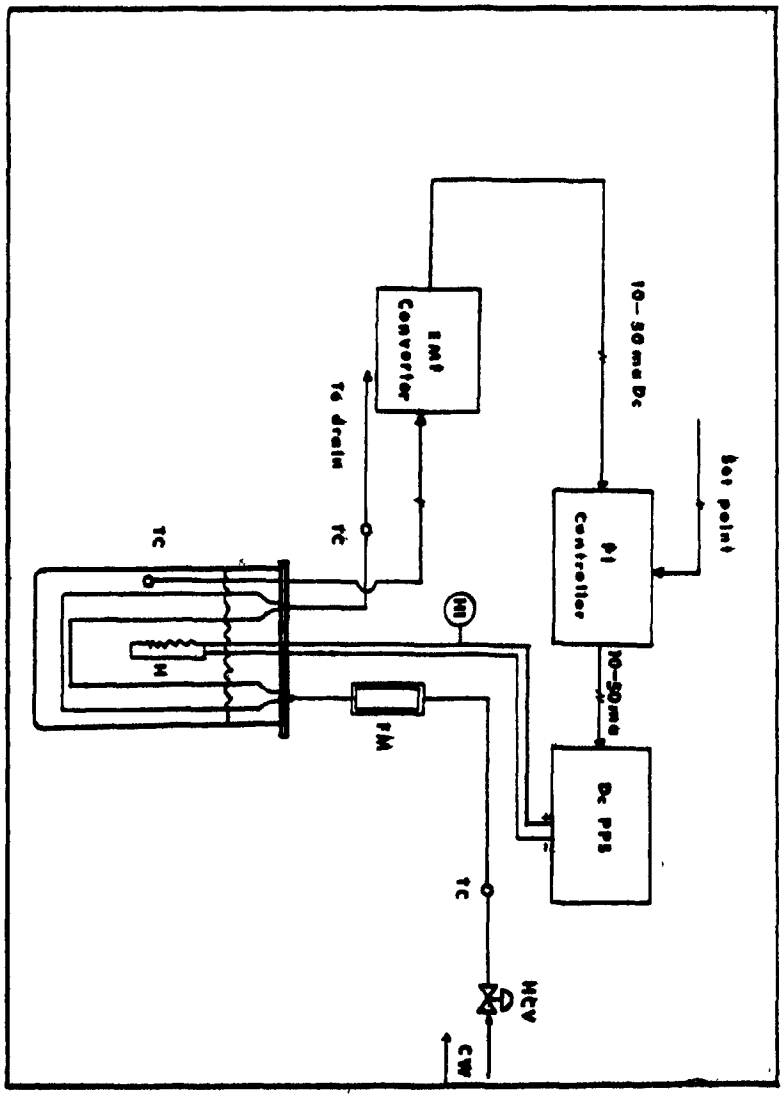
EMF Converter
To drain
TC
FC
10-50 ma Dc
Set point
PI Controller
4-20ma
Dc PPS
TC
HCV
CW
PM
H

Where

$$K = 2 C_c \rho_c / U_2 A_2 \qquad \ldots\ldots\ldots\ldots\ldots (65)$$

The first term in equation (64) refers to the rate of heat transfer between the perfectly mixed reactor fluid and the metal walls of the cooling surfaces. This energy exchange term was firstly developed by Amundson and co-workers[33] and has been used extensively for modelling the dynamic behavior of the CSTR's [34,35,36] . The second term in equation (64) describes the compensating heat produced by the immersion heater. This heat term is obviously the product of the voltage (V) and current (I) crossing the resistance of the immersion heater where 0.8604 is the conversion factor which converts the compensating heat term from W/ℓ to kcal/ℓ.h

* Process Modeling and Controller Tuning

1. Transient Energy Balance

An energy balance for the perfectly mixed vessel gives

$$\Sigma_i M_i C_{pi} \left[\frac{dT}{dt}\right] = Q_{pss}(t) + Q_{agi} + U_1 A_1 (T_{amb} - T) + U_2 A_2 (T_w - T) \;..\; (66)$$

Equation (66) describes the transient energy balance for the system before inoculation where the heat of fermentation is equal to zero .

The average coolant temperature T_w and the inlet coolant temperature T_c are related by :

$$T_w = \frac{(\alpha/Q_c)T + T_c}{(\alpha/Q_c) + 1} \quad \ldots\ldots\ldots\ldots\ldots\ldots \quad (67)$$

Where

$$\alpha = \frac{U_2 A_2}{2\, C_c \rho_c} \quad \ldots\ldots\ldots\ldots\ldots\ldots \quad (68)$$

Substituting (67) and (68) into (66) yields :

$$\Sigma_i M_i C_{pi}\left[\frac{dT}{dt}\right] = Q_{pss}(t) + Q_{agi} + U_1 A_1 (T_{amb} - T) + \frac{U_2 A_2\, Q_c}{\alpha + Q_c}(T_c - T) \ldots (69)$$

or

$$\Sigma_i M_i C_{pi}\left[\frac{dT}{dt}\right] = Q_{pss}(t) + Q_{agi} - U_1 A_1 (T - Tamb) - \frac{U_2 A_2\, K\, Q_c}{1 + K\, Q_c}(T - T_c)$$

$$\ldots\ldots\ldots\ldots\ldots\ldots \quad (70)$$

Where

$$K = 2\, \rho_c\, C_c / U_2 A_2 \quad \ldots\ldots\ldots\ldots\ldots\ldots \quad (71)$$

The rearrangement of equation (70) gives :

$$\Sigma_i M_i C_{pi}\left[\frac{dT}{dt}\right] + \left[U_1 A_1 + \frac{U_2 A_2\, K\, Q_c}{1 + K\, Q_c}\right] T = Q_{pss}(t) + Q_{agi} + U_1 A_1 T_{amb} + \left[\frac{U_2 A_2\, K\, Q_c}{1 + K Q_c}\right] T_c \quad \ldots (72)$$

The time constant τ of the process, therefore, depends on the cooling water flow rate

$$\tau = \left(\frac{1 + K Q_c}{K Q_c}\right)\left(\frac{\Sigma_i M_i C_{pi}}{U_1A_1 + U_2A_2}\right) \quad \text{.....(73)}$$

The incremental model for equation (72) becomes :

$$\Sigma_i M_i C_{pi}\left[\frac{d\tilde{T}}{dt}\right] + \left[\frac{U_1A_1 + U_2A_2 K Q_c}{1 + KQ_c}\right]\tilde{T} = \bar{Q}_{pss} + \tilde{Q}_{pss} + Q_{agi} + U_1A_1 T_{amb} - \left[\frac{U_1A_1 + U_2A_2 K Q_c}{1 + K Q_c}\right]\bar{T} + \left[\frac{U_2A_2 K Q_c}{1 + K Q_c}\right]T_c \quad \text{.....(74)}$$

Or

$$\Sigma_i M_i C_{pi}\left[\frac{d\tilde{T}}{dt}\right] + \left[\frac{U_1A_1 + U_2A_2KQ_c}{1 + K Q_c}\right]\tilde{T} = \bar{Q}_{pss} + \tilde{Q}_{pss} + Q_{agi} + U_1A_1(T_{amb} - \bar{T}) + \left[\frac{U_2A_2 K Q_c}{1 + K Q_c}\right](T_c - \bar{T}) \quad \text{.....(75)}$$

Where $\bar{T}$ is the steady state temperature ($T = \bar{T} + \tilde{T}$, $Q_{pss} = \bar{Q}_{pss} + \tilde{Q}_{pss}$)

Moreover ,it is observed that :

$$\left[U_1A_1 + \frac{U_2A_2 K Q_c}{1 + K Q_c}\right]\bar{T} = \bar{Q}_{pss} + Q_{agi} + U_1A_1T_{amb} + \left[\frac{U_2A_2 K Q_c}{1 + K Q_c}\right]T_c \quad \text{.....(76)}$$

Equation (75) therefore becomes :

$$\Sigma_i M_i C_{pi}\left[\frac{d\tilde{T}}{dt}\right] + \left[U_1A_1 + \frac{U_2A_2\,K\,Q_c}{1 + K\,Q_c}\right]\tilde{T} = \tilde{Q}_{pss} \quad \ldots\ldots\ldots (77)$$

or

$$\left[\frac{\Sigma_i M_i C_{pi}}{U_1A_1 + \frac{U_2A_2\,K\,Q_c}{1 + K\,Q_c}}\right]\frac{d\tilde{T}}{dt} + \tilde{T} = \frac{\tilde{Q}_{pss}}{U_1A_1 + \frac{U_2A_2\,K\,Q_c}{1 + K\,Q_c}} \quad (78)$$

Hence

$$\tau\,\frac{d\tilde{T}}{dt} + \tilde{T} = K_\alpha\,\tilde{Q}_{pss} \quad \ldots\ldots\ldots (79)$$

Where

$$\tau = \frac{\Sigma_i M_i C_{pi}}{U_1A_1 + \frac{U_2A_2\,K\,Q_c}{1 + K\,Q_c}} \quad \ldots\ldots\ldots (80)$$

$$K_\alpha = \frac{1}{U_1A_1 + \frac{U_2A_2\,K\,Q_c}{1 + K\,Q_c}} \quad \ldots\ldots\ldots (81)$$

Taking the Laplace transform of equation (79) yields :

$$\frac{\tilde{T}}{\tilde{Q}_{pss}} = \frac{K_\alpha}{\tau\,s + 1} \quad \ldots\ldots\ldots (82)$$

The transfer function of the incremental energy equation describes first order behavior .

2. Controller Tuning and Stability

A block diagram of the system (Fig.II.6) is presented to assist in the study of the controller . From the block diagram , the following relationships can be derived :

$$e = K_M (\tilde{X} - \tilde{T}) \qquad \ldots\ldots\ldots\ldots\ldots\ldots \quad (83)$$

$$\tilde{T} = \frac{K_C K_P K_\alpha e}{\tau s + 1} \qquad \ldots\ldots\ldots\ldots\ldots\ldots \quad (84)$$

From (83) and (84) the following is obtained :

$$\frac{\tilde{T}}{\tilde{X}} = \frac{K_M K_C K_P K_\alpha \left(\frac{1}{\tau s + 1} \right)}{1 + K_M K_C K_P K_\alpha \left(\frac{1}{\tau s + 1} \right)} \qquad \ldots\ldots\ldots\ldots\ldots \quad (85)$$

$$\frac{\tilde{T}}{\tilde{X}} \quad \frac{K_M K_C K_P K_\alpha}{\tau s + (K_M K_C K_P K_\alpha)} = \frac{K^*_\alpha}{\tau^* s + 1} \qquad \ldots\ldots\ldots \quad (86)$$

Where

$$\tau^* = \frac{\tau}{1 + K_M K_C K_P K_\alpha} \qquad \ldots\ldots\ldots\ldots\ldots\ldots \quad (87)$$

$$K^*_\alpha = \frac{K_M K_C K_P K_\alpha}{1 + K_M K_C K_P K_\alpha} \qquad \ldots\ldots\ldots\ldots\ldots\ldots \quad (88)$$

Figure II.6 The Block Diagram for the Temperature Control System

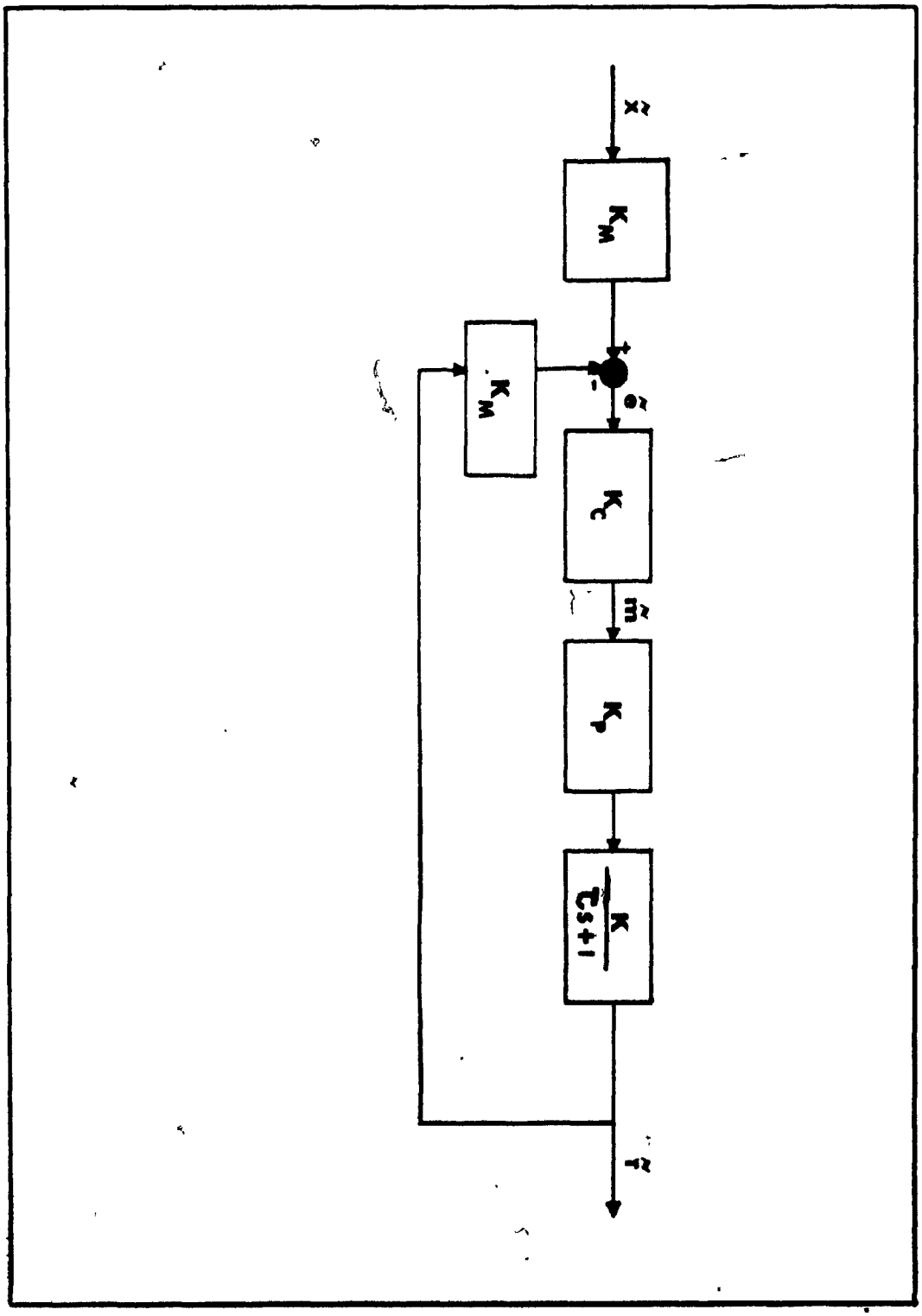
x_2
K_M
K_M
e_2
K_c
m_2
K_p
$\frac{K}{\tau s+1}$
z_2

The behavior of the closed loop system is analogous to the open loop system; the system is always stable regardless the value of K_C . The gain of the controller should, however, be tuned at the maximum value in order to reduce the offset which is the difference between the set point and the steady state controlled value .

II-2. CORRELATION OF THE HEAT OF FERMENTATION AND OF THE CULTURE OXYGEN UPTAKE

The elemental balance equation for an aerobic fermentation process is :

$$CH_mO_\ell + a\,NH_3 + b\,O_2 \longrightarrow \underset{\text{(Biomass)}}{y\,CH_pO_nN_q.Ash} + \underset{\text{(Product)}}{z\,CH_rO_sN_t} + c\,H_2O + (1-y-z)CO_2 \quad ..(89)$$

Upon application of the law of mass conservation, the balancing of both parts of equation (89) with respect to N, H, and O results in

$$b = 1/4(\gamma_s - y\gamma_b - z\gamma_p) \quad .....(90)$$

Where

$$\gamma_s = 4 + m - 2\ell \quad .....(91)$$

$$\gamma_b = 4 + p - 2n - 3q \quad .....(92)$$

$$\gamma_p = 4 + r - 2s - 3t \quad .....(93)$$

According to Minkevich and Eroshin[12] γ_s, γ_b, and γ_p are referred to as

the reducing power of substrate, biomass, and products respectively. The elemental balance equations of the combustion of substrate, biomass, and product are thus respectively expressed as follows :

$$* \underset{\text{(Substrate)}}{CH_mO_\ell} + (4+m-2\ell)1/4\ O_2 \longrightarrow CO_2 + m/2\ H_2O \quad \ldots\ldots\ldots\ldots (94)$$

$$* \underset{\text{(Biomass)}}{CH_pO_nN_q.Ash} + (4+p-2n-3q)1/4\ O_2 \longrightarrow CO_2 + 1/2(p-3q)H_2O + qNH_3 \quad (95)$$

$$* \underset{\text{(Product)}}{CH_rO_sN_t} + (4+r-2s-3t)1/4\ O_2 \longrightarrow CO_2 + 1/2(r-3t)H_2O + tNH_3 \quad (96)$$

The combustion heats of substrate, biomass, and product per 1 gram-equivalent of O_2 are denoted as Q_{os}, Q_{ob}, and Q_{op} respectively. From equations (89) to (96), the heat of combustion per gram-atom carbon equal $\gamma_s Q_{os}$, $\gamma_b Q_{ob}$, and $\gamma_p Q_{op}$ respectively. The heat of combustion per gram of substrate, biomass, and product then becomes respectively :

$$Q_s = (\sigma/12)\gamma_s Q_{os} \quad \ldots\ldots\ldots\ldots (97)$$

$$Q_b = (\sigma_1/12)\gamma_b Q_{ob} \quad \ldots\ldots\ldots\ldots (98)$$

$$Q_p = (\sigma_2/12)\gamma_p Q_{op} \quad \ldots\ldots\ldots\ldots (99)$$

where σ, σ_1, σ_2 are the weight part of carbon in substrate, dried biomass and product respectively.

From the above equations, it follows that the yields of biomass and product per oxygen consumed on weight basis are :

$$Y_{xo} = \frac{12\,y}{32\,b\,\sigma_1} = \left(\frac{3}{2\,b\,\sigma_1}\right)\left[\frac{y}{\frac{\gamma_s - z\,\gamma_p}{\gamma_b} - y}\right] \quad \ldots\ldots(100)$$

$$Y_{po} = \frac{12\,y}{32\,b\,\sigma_2} = \left(\frac{3}{2\,b\,\sigma_2}\right)\left[\frac{z}{\frac{\gamma_s - z\gamma_p}{\gamma_b} - y}\right] \quad \ldots\ldots(101)$$

Equations (89) to (101) describe a fairly wide range of microbial culture behavior. In industrial biomass production only a very small formation of organic products is desirable (less than 1-3%) . Under such a condition the product formation can be safely neglected . Equation (100) therefore becomes :

$$Y_{xo} = \frac{3}{2\,b\,\sigma_1}\left[\frac{y}{\frac{\gamma_s}{\gamma_b} - y}\right] \quad \ldots\ldots(102)$$

Since the synthesis of biomass containing 1 gram-atom of carbon requires the consumption of 1/y gram atoms of substrate carbon, the metabolic heat generated by cells equals the difference between the heats of substrate combustion and the corresponding amount of biomass (heats of hydration have not been taken into account since they are negligible as compared with the heats of combustion). Hence metabolic heat generation per 1 gram of dried cells grown, denoted as ΔQ_{ferm} is :

$$\Delta Q_{ferm} = \left[\frac{\sigma\, \gamma_s\, Q_{os}}{12y} - \frac{\sigma_1 \gamma_s\, Q_{ob}}{12}\right] = \frac{1}{12}\left[\frac{\sigma\, \gamma_s\, Q_{os}}{y} - \sigma_1 \gamma_s\, Q_{ob}\right] \quad (103)$$

Since the amount of product formation is neglected, i.e., $\sigma_2 = 0$, it is shown that $\sigma = \sigma_1$. Equation(103) then becomes :

$$\Delta Q_{ferm} = \frac{\sigma}{12}\left[\frac{\gamma_s\, Q_{os}}{y} - \gamma_b\, Q_{ob}\right] \quad \ldots\ldots\ldots\ldots\ldots\ldots \quad (104)$$

Minkevich and Eroshin[12] also demonstrated that there are no appreciable differences between Q_{os} and Q_{ob} and found that $\bar{Q}_{os}$ = 26.92 kcal (relative deviation in Q_{os} = 4%) and $\bar{Q}_{ob}$ = 26.94 kcal (relative deviation in Q_{ob} is 3.9%) . Equations (102) and (104) result in :

$$\Delta Q_{ferm} = \frac{Q_{os}}{8}\frac{1}{Y_{xo}} + \frac{\sigma\, \gamma_b}{12}\left(Q_{os} - Q_{ob}\right) \quad \ldots\ldots\ldots\ldots \quad (105)$$

Therefore the fermentation heat generation per unit volume becomes :

$$Q_{ferm} = \Delta Q_{ferm} \cdot \Delta W \quad \ldots\ldots\ldots\ldots\ldots\ldots\ldots\ldots\ldots\ldots \quad (106)$$

where $\Delta W = Y_{xo} \cdot \Delta O_2$ is the amount of dried biomass produced by working volume unit per unit time and ΔO_2 is the rate of oxygen uptake by the micro-organisms.Substituting equation (105) into (106) results in :

$$Q_{ferm} = \left[\frac{Q_{os}}{8} + \frac{2\sigma\gamma_b}{3} \left(\frac{Q_{os} - Q_{ob}}{Q_{os}} \right) Y_{xo} \right] \Delta O_2 \quad \ldots\ldots\ldots\ldots\ldots (107)$$

Since the deviation of Q_{os} and Q_{ob} is 4% of their range, the ratio $(Q_{os} - Q_{ob})/Q_{os}$ varies in the range ±0.08 . According to Minkevich and Eroshin[12] , the value of σ and γ_b are fairly constant (σ = 0.455, relative deviation = 4.2%, γ_b = 4.182, relative deviation = 1.8%), therefore the factor $2\sigma\gamma_b/3$ equals 1.3; Y_{xo} equals 1.15 which can be considered as fairly high among values achieved in experimental practice. Therefore the second term in square brackets may vary in the interval ±0.12. Equation(107) then becomes :

$$Q_{ferm} = (0.106 \pm 0.004) \Delta O_2 \quad \ldots\ldots\ldots\ldots\ldots (108)$$

Equation(108) appears to agree very well with the one suggested by Imanaka and Aiba[13] who derived the following relationship :

$$Q_{ferm} = (- \Delta H_o^*) \Delta O_2 \quad \ldots\ldots\ldots\ldots\ldots (109)$$

where $(-\Delta H_o^*)$ = 0.106 kcal/mmol O_2 $\ldots\ldots\ldots\ldots\ldots (110)$

Cooney et al[5] , using the *in-situ* dynamic calorimetric technique for directly measuring the heat of fermentation and the oxygen uptake rate , found the following correlation :

$$Q_{ferm} = 0.124 \Delta O_2 \quad \ldots\ldots\ldots\ldots\ldots (111)$$

The above suggests a need for further investigation on the subject, so that the validity of the derived semi-theoretical equation can be confirmed. The existing dicrepances between the theoretical relationship and the experimental correlation obtained by Cooney et al[5] should also be explained.

II-3. THE OXYGEN UPTAKE RATE DURING FERMENTATION

The Oxygen Uptake Rate (OUR) was calculated by applying the following equation :

$$OUR = \frac{F_{in}\, p_{O_2}^{in} - F_{out}\, p_{O_2}^{out}}{V_L} \quad \ldots\ldots\ldots\ldots\ldots (112)$$

The exit gas flow rate F_{out} is not equal to the inlet gas flow rate due to the respiration activity of the cells[37] and it can be obtained by considering a material balance on the inert gas species in the inlet and exit gas streams :

$$F_N = F_{in}(1- p_{O_2}^{in} - p_w^{in} - p_{CO_2}^{in}) = F_{out}(1- p_{O_2}^{out} - p_w^{out} - p_{CO_2}^{out}) \quad \ldots\ldots\ldots\ldots\ldots (113)$$

From equations (112) and (113) it follows that

$$OUR = \frac{F_N}{V_L}\left[\frac{p_{O_2}^{in}}{1 - p_{O_2}^{in} - p_{CO_2}^{in} - p_w^{in}} - \frac{p_{O_2}^{out}}{1 - p_{O_2}^{out} - p_{CO_2}^{out} - p_w^{out}} \right] \ldots (114)$$

When the incoming air is fully saturated with water at the same temperature as the fermentation broth, i.e., $p_w^{in} = p_w^{out}$, equation (114) then becomes :

$$OUR = \frac{F_N}{V_L}\left[\frac{p_{O_2}^{in}}{1 - p_{O_2}^{in} - p_{CO_2}^{in}} - \frac{p_{O_2}^{out}}{1 - p_{O_2}^{out} - p_{CO_2}^{out}}\right] \quad \ldots\ldots\ldots\ldots \quad (115)$$

The concentration of oxygen and carbon dioxide could be determined analytically. When the gas flow rate is measured the oxygen balance on the gas stream can be completed .

CHAPTER III

MATERIALS AND METHODS

A. INSTRUMENTS AND CALIBRATIONS

* Fermentor

A "Microferm" laboratory fermentor (New Brunswick, New Jersey) with a 14-liter total capacity Pyrex glass vessel was used in this study. This fermentor has an internal diameter of 22.2 centimeters, and stands 45.7 centimeters high. Inside are four baffles, two temperature measurement wells and an extra extended broth sampling tube. All internal parts of the fermentor are constructed of type 316 stainless steel. The fermentation broth was agitated by two, six bladed turbine impellers, each 7.4 centimeters in diameter. The impeller shaft was driven by a variable 1/4 HP direct current motor capable of speeds between 0 and 1000 rpm. The rotational speed of impeller shaft was measured by an optical tachometer device connected to a digital read-out indicator (Figures III.1 and III.2) The rotational speed was kept constant at 700 rpm during the experiments .

* Aeration

A schematic diagram of the fermentor aeration arrangement is shown in Figure III.3. The inlet air was introduced through a 0-30 psig pressure gauge, a Brooks rotameter no. R-6-15-A, an inlet air filter, a saturation column, and it was then bubbled into the culture medium through a single orifice sparger.The outlet air was passed through a moisture

Figure III.1 Agitation Device Arrangement for 14 liter Fermentor

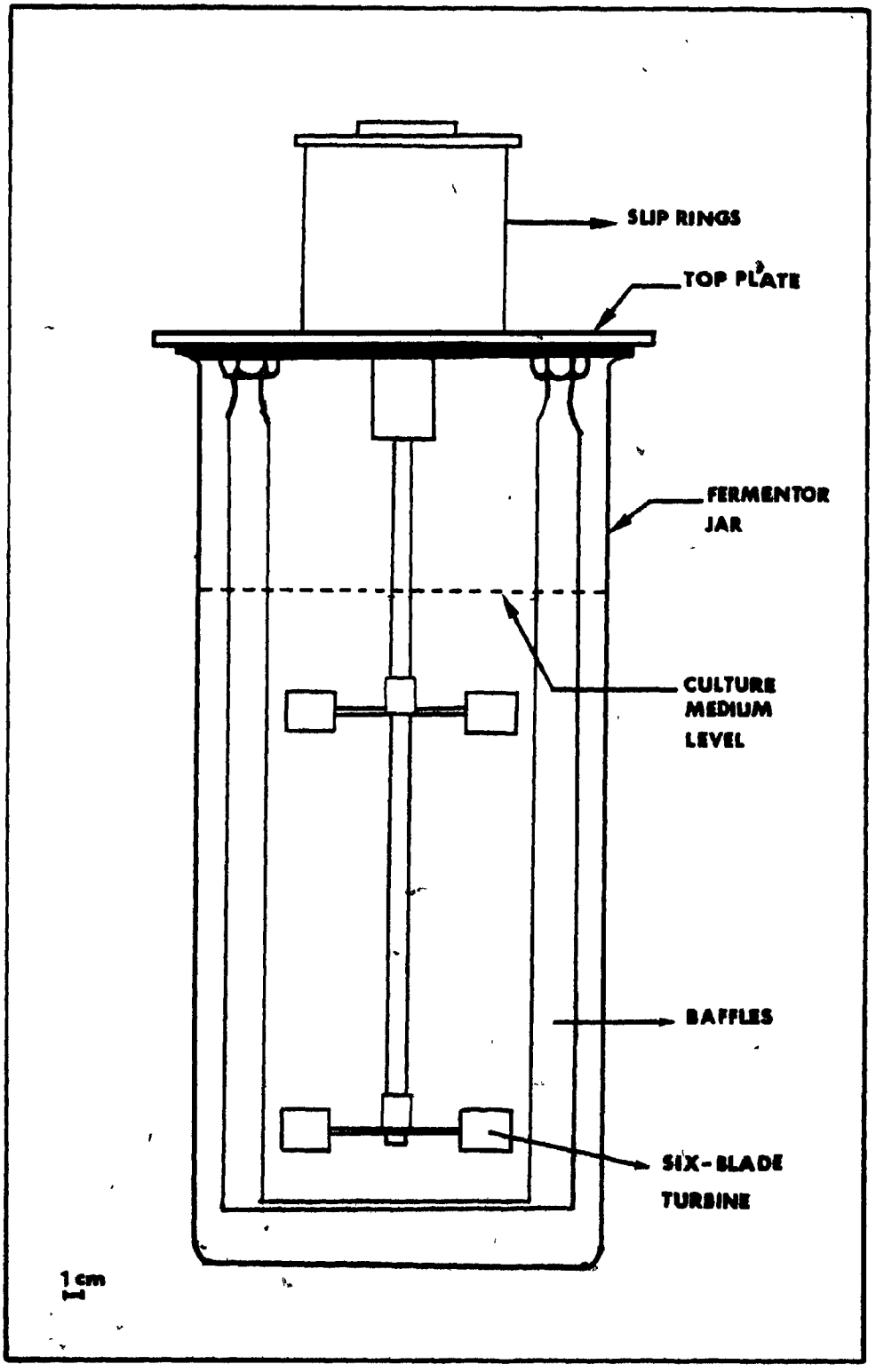
SLIP RINGS
TOP PLATE
FERMENTOR JAR
CULTURE MEDIUM LEVEL
BAFFLES
SIX-BLADE TURBINE
1 cm

Figure III.2 The Agitation Device and Measurement

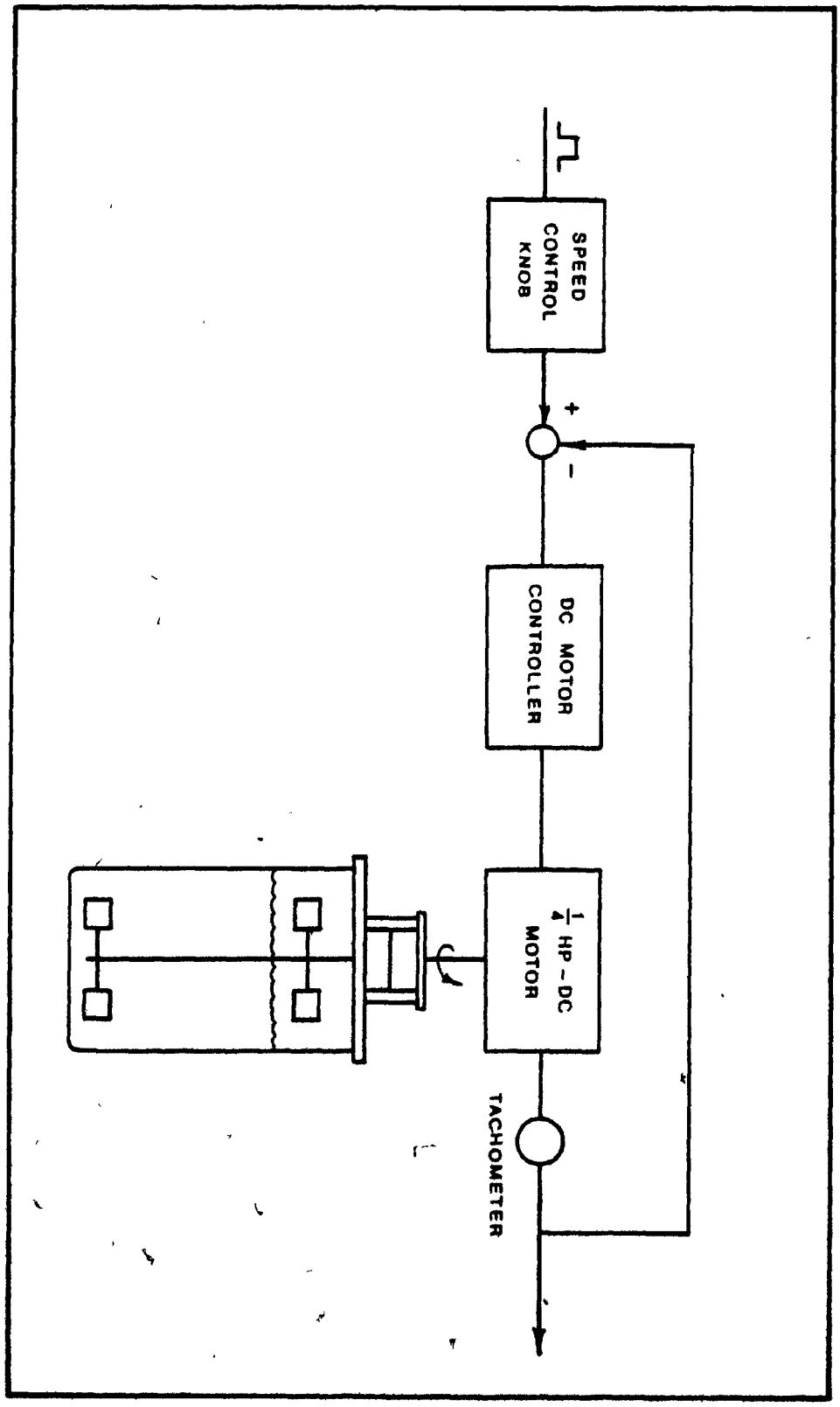
SPEED CONTROL KNOB
+
-
DC MOTOR CONTROLLER
1/4 HP - DC MOTOR
TACHOMETER

Figure III.3 The Aeration Arrangement

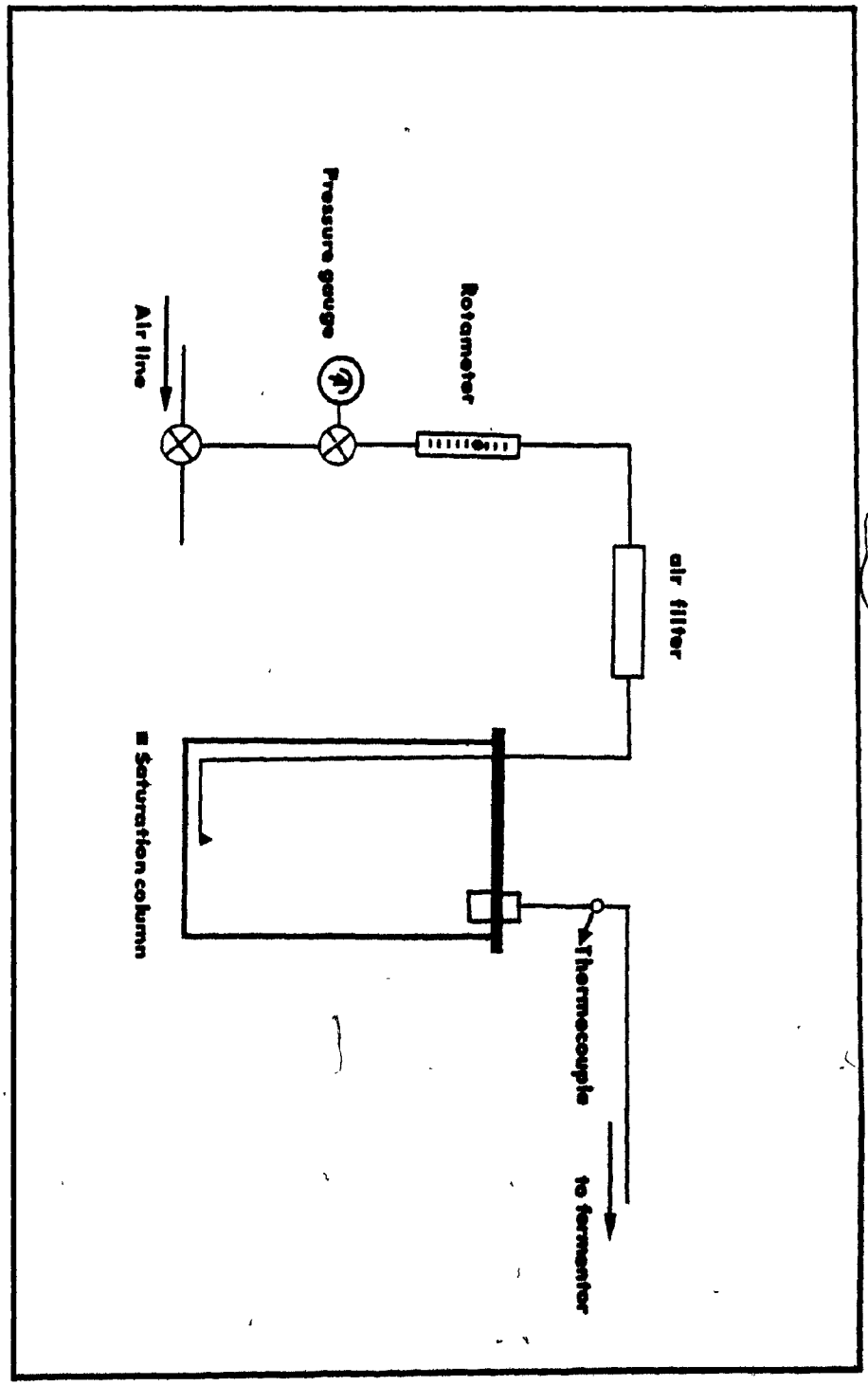
Air line
Pressure gauge
Rotameter
air filter
Saturation column
Thermocouple
to fermenter

condenser. The aeration rate was set at the desired value by the pressure gauge and the rotameter valve. The calibration of the rotameter was accomplished through the on-line installation of a wet test gas meter. The outlet air flow, after entering the rotameter passed through the wet test gas meter and was discharged to the atmosphere.

The calibration procedure consisted of the passage of constant volumes of air through the rotameter at specified temperature, pressure and time interval. Volume flow rate were then measured at the prevailing flow conditions (pressure, temperature) for different rotameter settings .

During the fermentation studies, the gas flow rate was corrected for the mean conditions of delivery air by using the ideal gas equation of state (Figure III.4), and kept constant at 8.4 l/min .

* Air Stream

Figure III.3 represents a schematic diagram of the constant temperature saturation column. The air stream was saturated with water at the temperature of the fermentation broth by passing it through a temperature controlled 7 liter fermentor filled with water. The temperature of the inlet air stream to fermentor was measured by a thermistor. The total pressure of the inlet air stream was measured using U-tube mercury manometers open to the atmosphere. The accuracy of the pressure measurements was within ±1 mm of mercury .

* Cooling

During experiments the amount of cooling water passed through the

Figure III.4 The Calibration for Air Rotameter

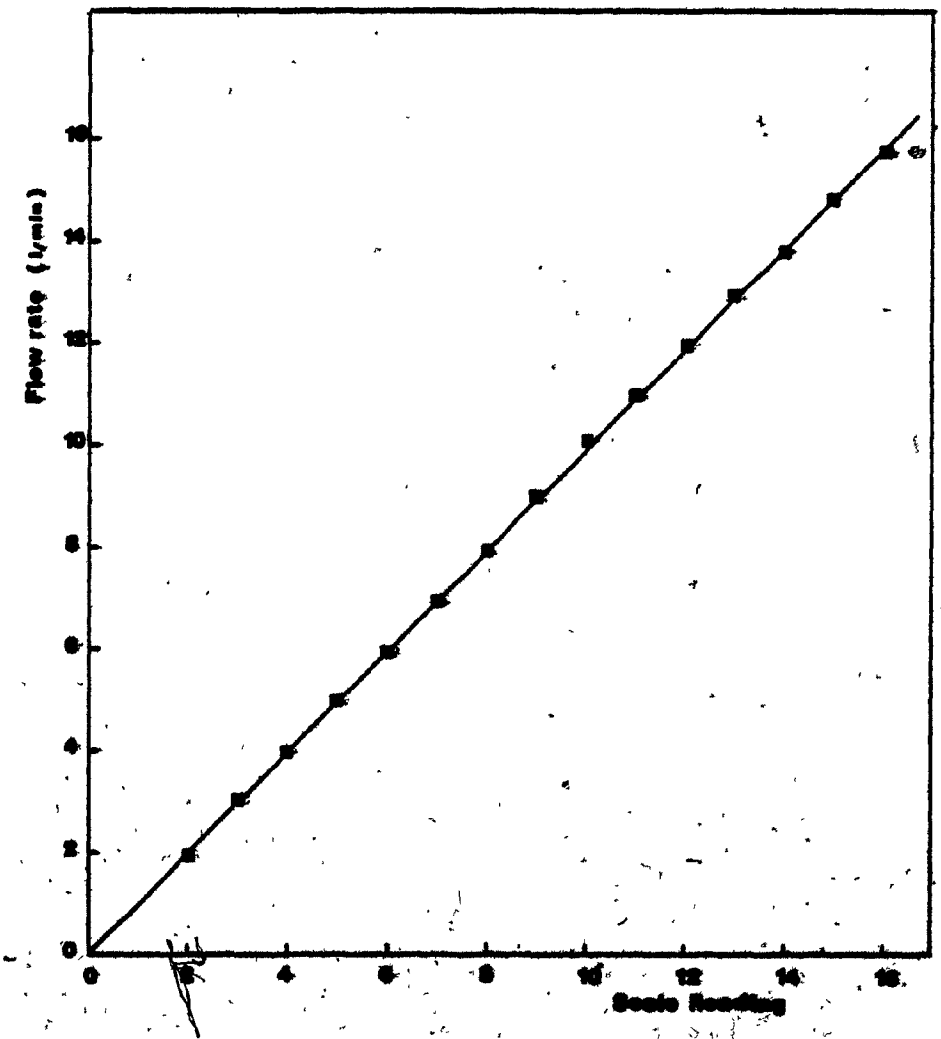
Flow rate (l/min)
0
2
4
6
8
10
12
14
16
Scale Reading

hollow cooling baffles of the fermentor was maintained constant and measured by a rotameter (the Brooks rotameter, no. R-6-15-A). To counter over-cooling, the temperature of fermentation broth was maintained at the set-point value of a controller by a submersible heater with variable power input, supplied by a programmable power supply .

* Broth Temperature

An Iron-Constantan thermocouple with a 304 stainless steel sheath was used to measure the temperature of the fermentation broth. The thermocouple was connected with a thermocouple reference junction which represented the temperature of fermentation broth. The thermocouple provided the input to an EMF (electro-motive force) converter. The calibration curve for the thermocouple and its reference junction is shown in Figure III.6 . During the calibration the temperature of the culture medium was measured by a digital thermometer indicator. The EMF converter (Model 693A, Foxboro, Mass.) was used to change a dc millivolt signal fed to an electronic controller. The converter was calibrated to operate within span of 1.6 mV. The minimum signal to the converter was set for 20 ^{o}C(0.96 mV) and the maximum signal was set for a temperature of 50 ^{o}C (2.56 mV) .

The proportional electronic controller (Model 62H, Foxboro, Mass.) was employed to control the temperature of the culture broth at the desired value. The signal received from the EMF converter was compared to the set point value. If the measurement signal is equal to the set point, the control output will remain constant until corrective action is required . If the measurement does not equal the set point, the output will ramp to

Figure III.5 The Calibration for Water Rotameter

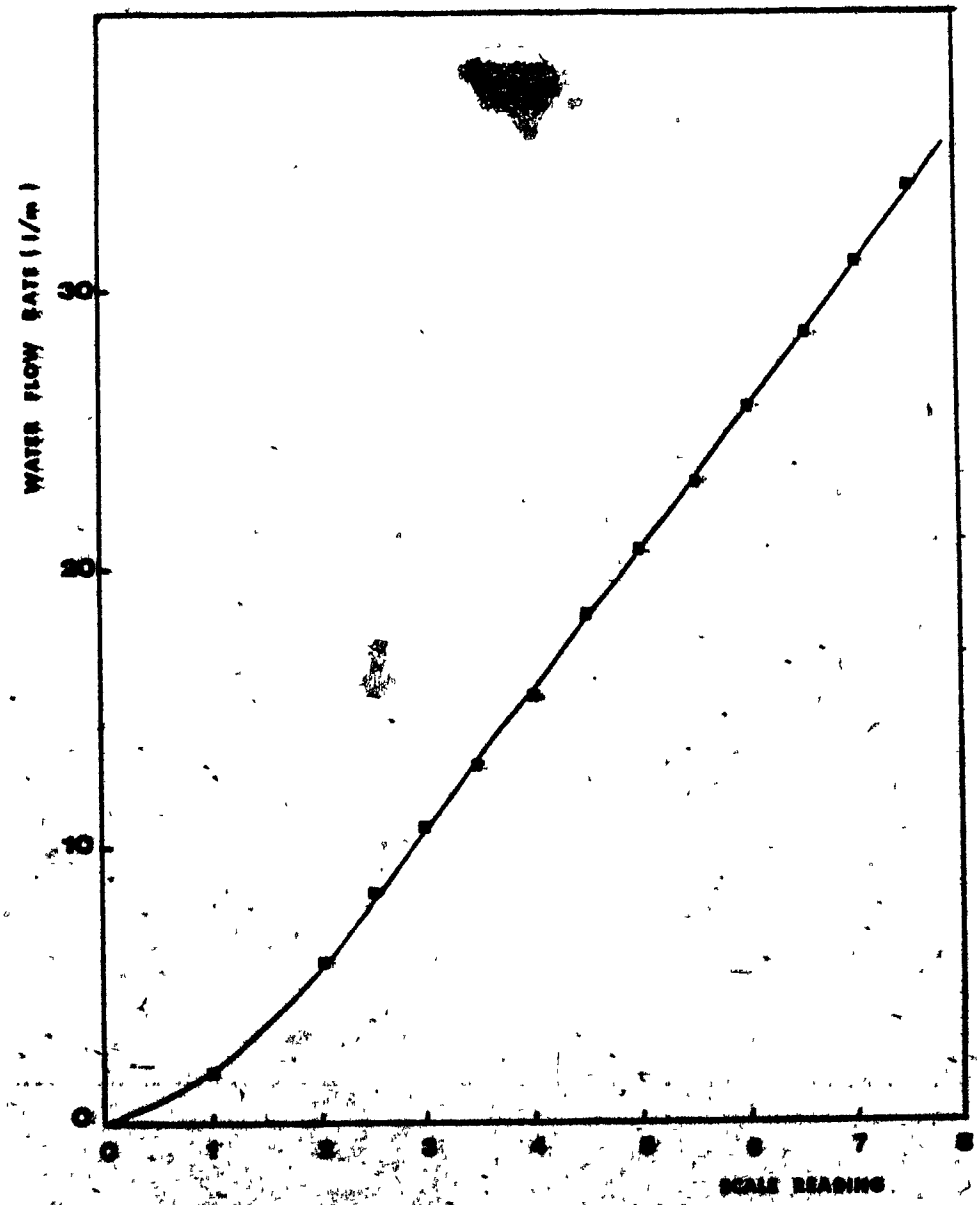
WATER FLOW RATE (l/m)
30
20
10
0
0
1
2
3
4
5
6
7
8
SCALE READING

Figure EII.6 The Calibration for the Thermocouple

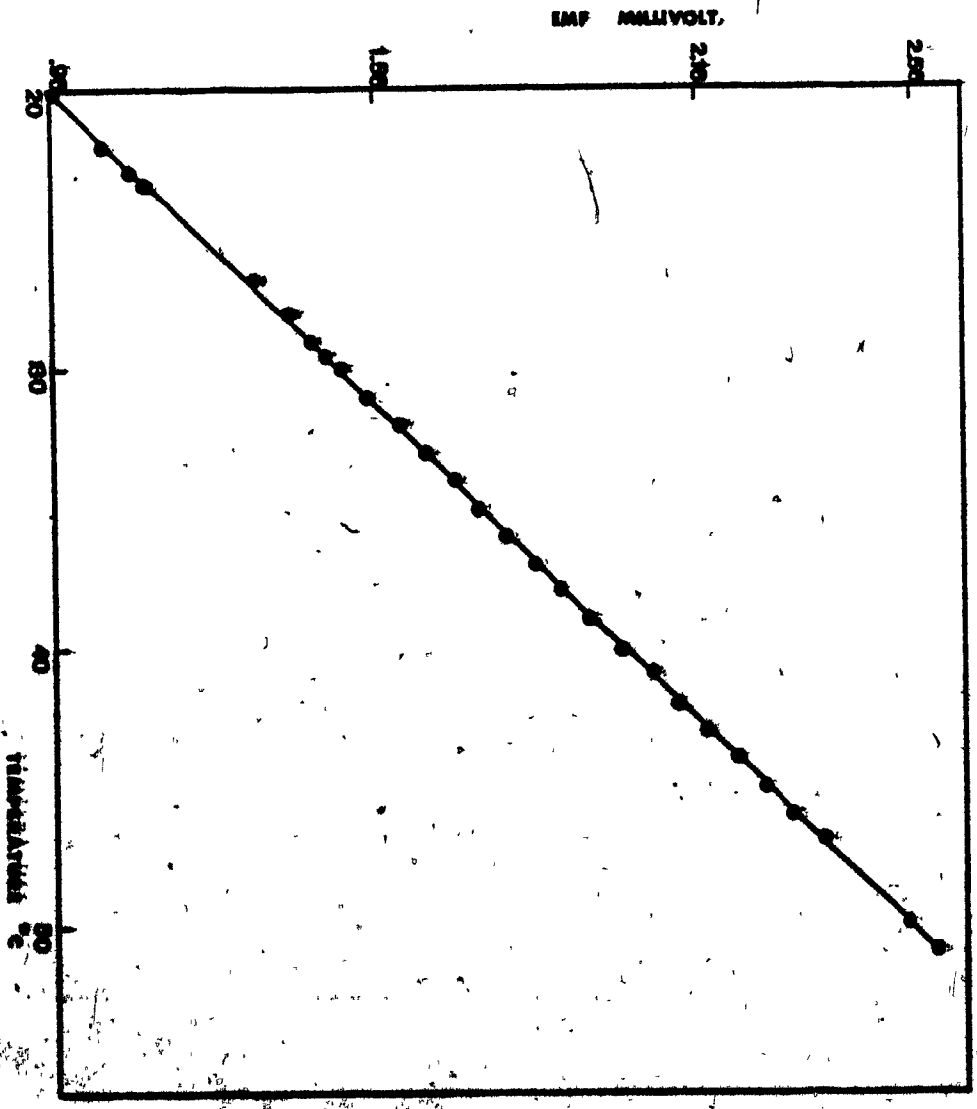
EMF MILLIVOLTS
TEMPERATURE °C
20
60
40
80
1.0
1.5
2.0
2.5

the level necessary to make the measurement equal to the set point. The output signal of the controller is from 10 to 50 mA dc where the proportional band can be varied between 5-300 % . The calibration for the EMF converter and the controller are shown in Figures III.7 and III.8 .

A programmable power supply (Model OPS 36-8M, Kepco Inc., Flushing, NY) was used to deliver stabilized voltage to activate an immersion heater (7.29Ω). The dc source voltage of the power supply is able to deliver from 0 to 288 W to the liquid broth .

To obtain a measurement of the broth temperature, a thermistor circuit was connected in a Wheatstone bridge arrangement with the fermentor temperature controller thermistor as one leg of the bridge (Appendix IX). The output of the bridge was recorded using a standard 10" Hewtlett Packard chart recorder to plot the temperature in the fermentor when the temperature controller was turned off. The thermistor circuit device was used in this study to evaluate the specific heat transfer coefficients U_1A_1 and U_2A_2 . The resulting calibration curves are shown in Figures III.9 and III.10 . The bridge used a 1.5 V dc power supply .

* The pH Controller Unit

A standard New Brunswick Scientific (Model pH 22) pH controller unit was used, incorporating the following equipment :

- a pH indicator/controller
- a pH recorder module
- a Ingold sterilizable pH probe (Model 465-25-PZ)
- Two peristaltic pumps for acid-base additions

Figure III.7 Calibration for Electronic Controller

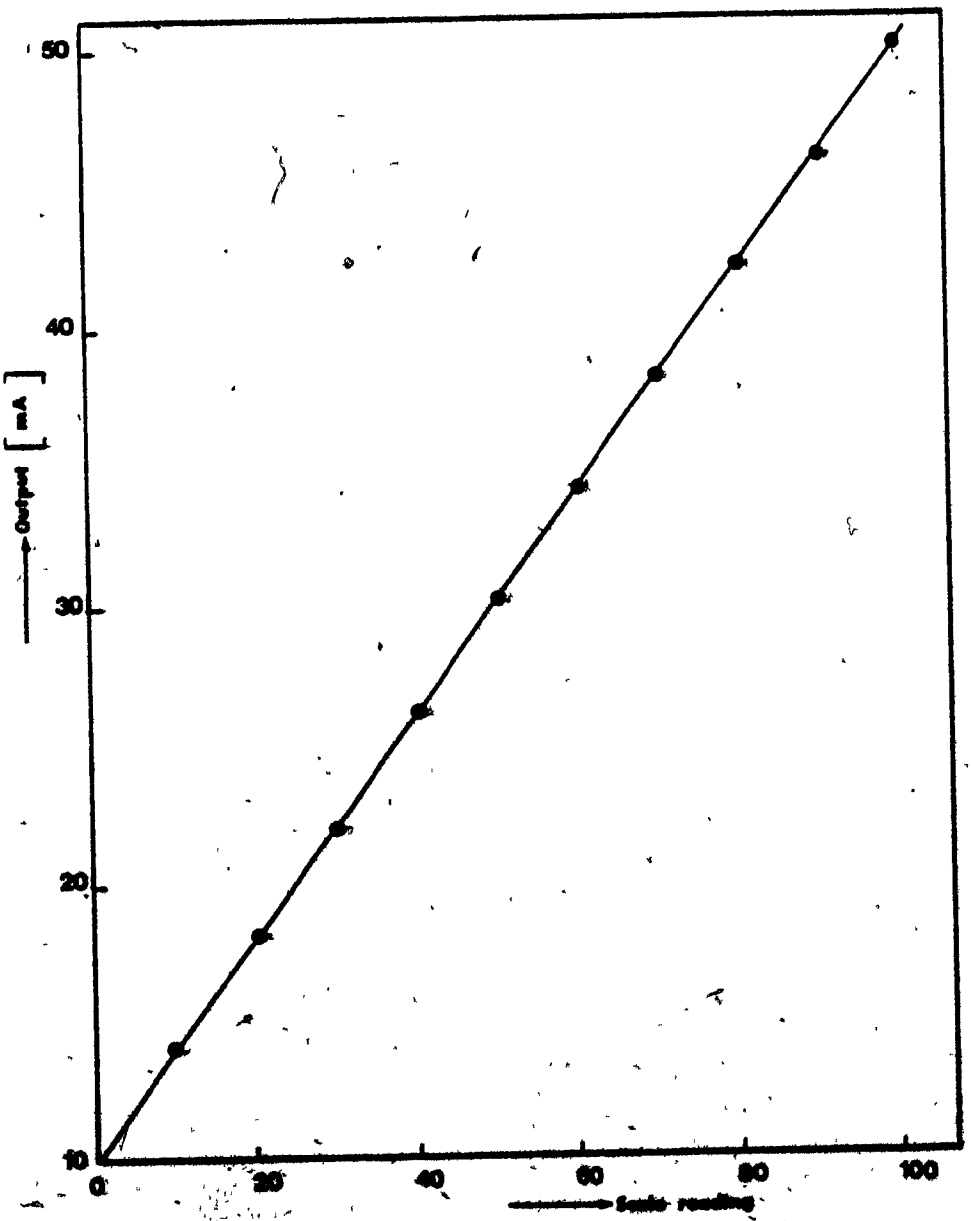
50
40
30
20
10
Output [mA]
0
20
40
60
80
100
Scale reading

Figure III.8 Calibration for the EMF Controller

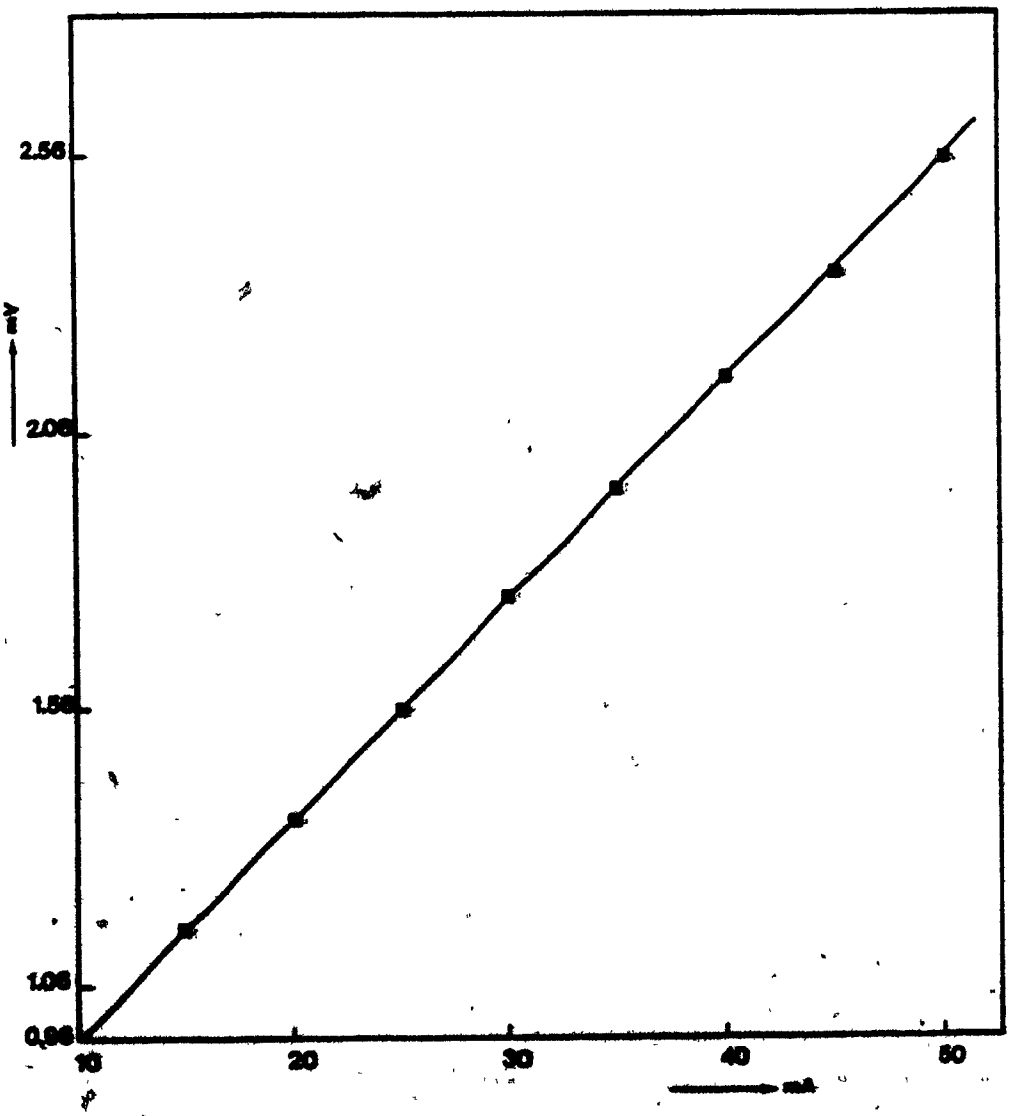
2.56
2.06
1.56
1.06
0.56
mV
10
20
30
40
50
mA

Figure III.9 Calibration for Thermistor

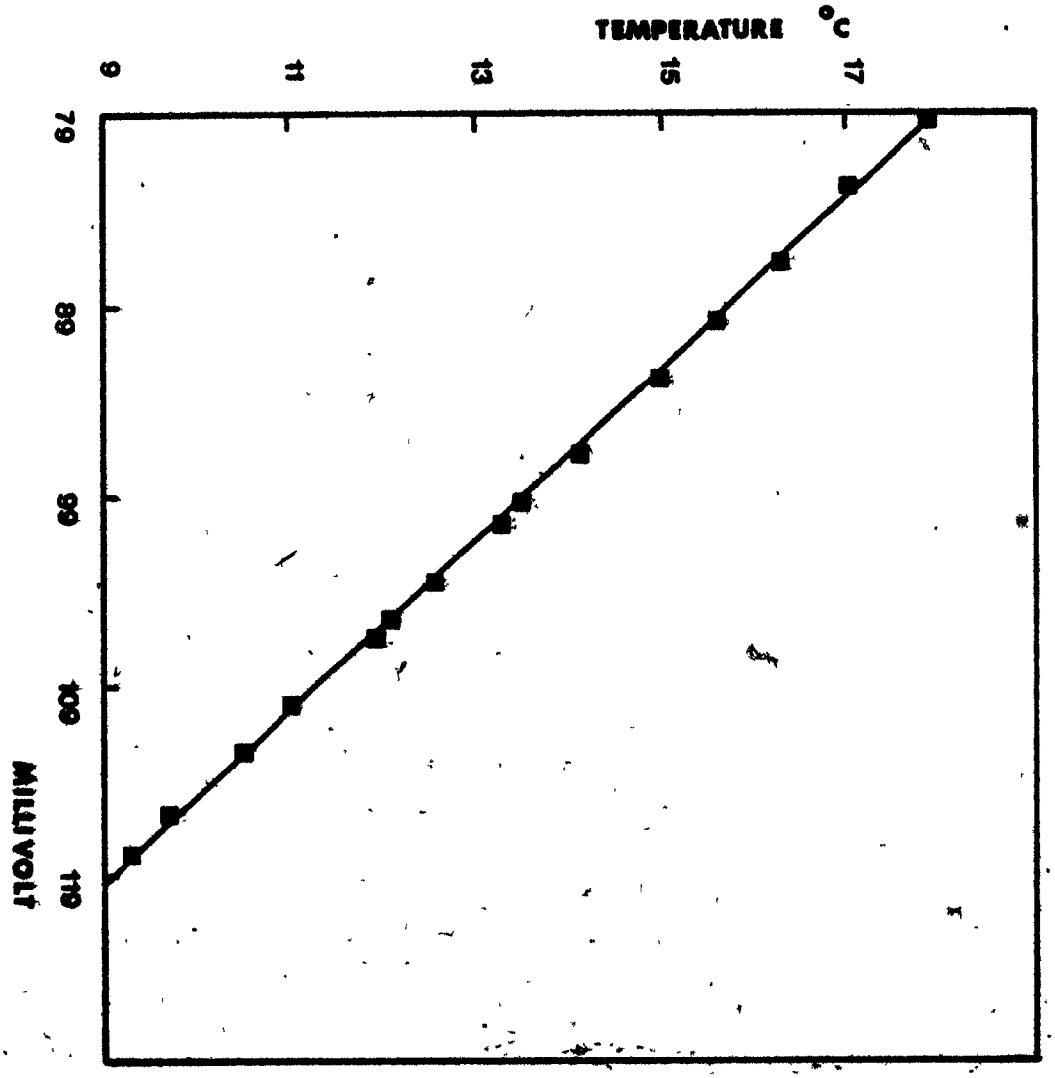
TEMPERATURE °C
9
11
13
15
17
MILLIVOLT
79
89
99
109
119

Figure III.10 Calibration for Thermistor

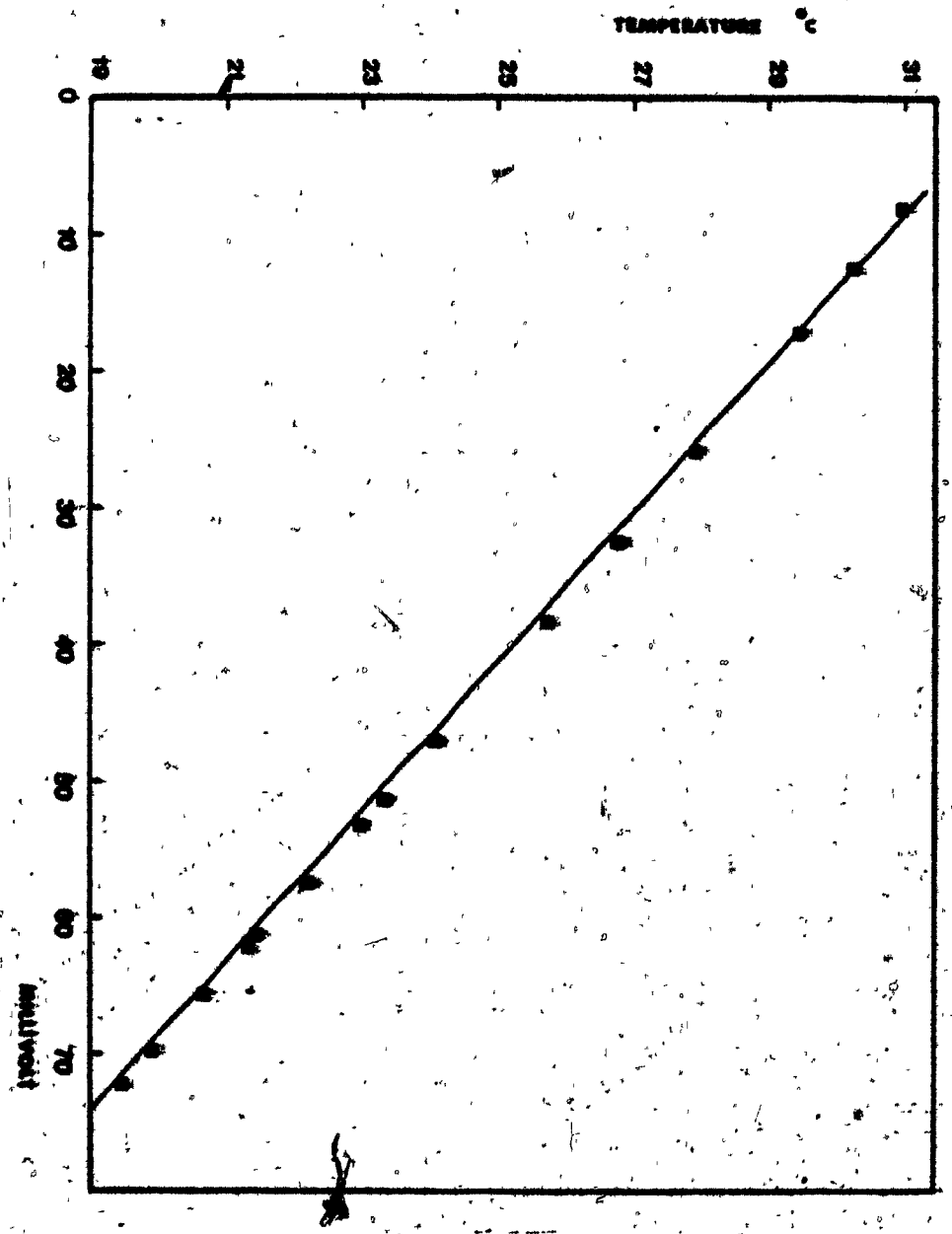
TEMPERATURE °C
0
10
20
30
40
50
60
70
MILLIVOLT

The pH controller was calibrated by using standard pH 4 and 7 buffer solutions. During the calibration procedure the temperature of the buffer solution used was taken into account by appropriately adjusting the temperature-slope setting of the pH controller . The ADD and MIX timer of the controller were proportionately adjusted throughout the fermentation in order to obtain a measured pH accuracy within ±0.2 units of the set point.

* The Oxygen Analyzer Unit

The oxygen concentration in the exit gas stream was monitored by a Taylor Servomex (Model OA 273) paramagnetic oxygen analyzer. The oxygen analyzer sample streams of a flow rate between 0-150 mℓ/min have to be dry gas mixtures . The bulk of the exit gas stream was by-passed from the oxygen analyzer as shown in Figure III.11 . The inlet gas to be analyzed was dried by passing it through a drying column (6.35 cm diameter, 28 cm length) packed with anhydrous calcium sulphate. The exhaust stream from the analyzer was vented to the atmosphere via a small rotameter which maintained the flow rate at 150 mℓ/min by adjustment of the pinch valves A and B . The zero (Nitrogen) gas and room air were used to calibrate the analyzer from 0 to 20.9 % . The output from the analyzer was fed to a recorder with a 0 to 10 mV full scale range (Hewlett Packard, Model 7127A) .

*, The Carbon Dioxide Analyzer Unit

A LIRA Model 303 infrared carbon dioxide analyzer (Mine Safety Appliances Co., Pittsburg, Penna.), was employed to monitor the exit gas stream CO_2 concentration . The equipment was installed in series with and

Figure III.11 Flow Arrangement for Oxygen Analyzer and Carbon Dioxide Analyzer Unit

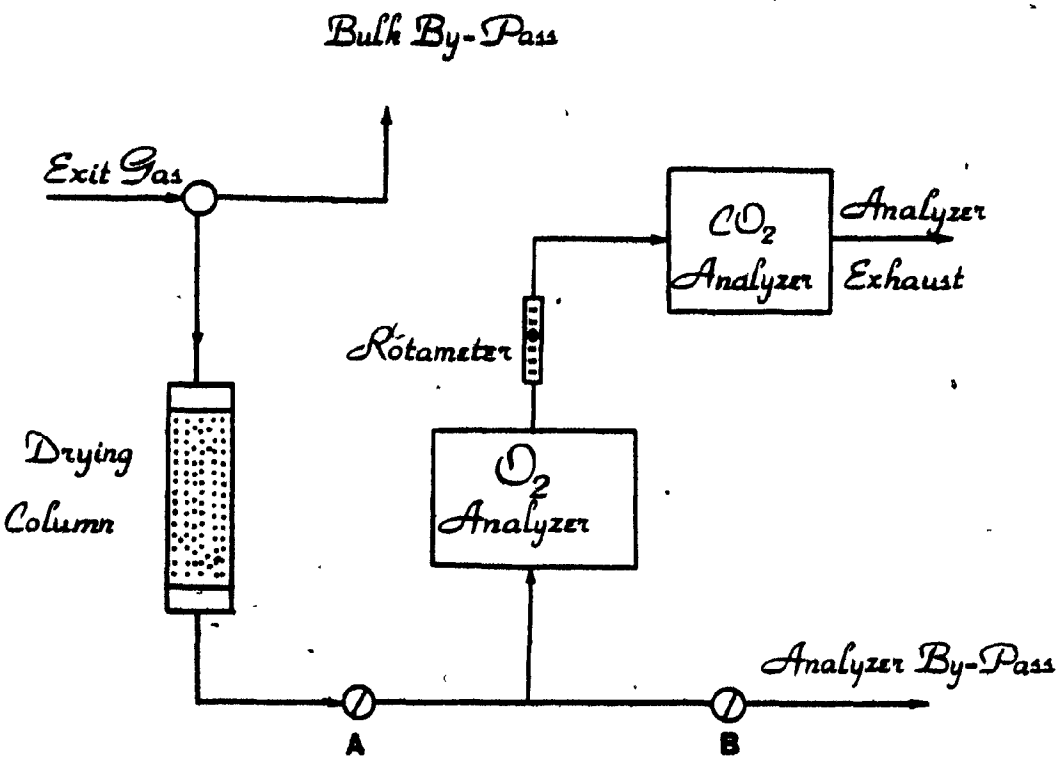
Bulk By-Pass
Exit Gas
CO_2 Analyzer
Analyzer Exhaust
Rotameter
Drying Column
O_2 Analyzer
Analyzer By-Pass
A
B

immediately after oxygen analyzer . The output from the CO_2 analyzer was also fed to the same recorder used for recording the output from the oxygen analyzer with a 0 to 100 millivolt full scale range. Before each fermentation run, the CO_2 analyzer was calibrated with known mixtures of carbon dioxide and nitrogen (0, 1.18%, 3.01%, 4.99%, and 5.45%). The calibration curves are shown in FiguresIII.12 and III.13 .

* A Strain Gauge Dynamometer

A modified strain gauge dynamometer was employed to measure the torque of the rotating impeller shaft . A schematic diagram of this device is shown in Figure II.3.

The electrical signal was transmitted from the rotating shaft via slip rings (IEC-4, Longhorn, Texas). The output signal was balanced and amplified by a signal condition (Model BA-4 Vishay, Pa) followed by a dc noise filter . The resulting signal was then recorded by a strip chart recorder (Hewlett Packard, Model 7127A). It was shown that the value of the potential de is proportional to the torque of the impeller shaft(Equation {61}). The calibration for the torque was performed by means of a cord, pulley, and weight arrangement. The resulting calibration curves of the torque versus the electrical potential generated are illustrated in Figures III.14 and III.15 .

The overall system used for continuous measurement of the fermentative heat is shown in Figure III.16

Figure III.12 Calibration for CO_2 Analyzer

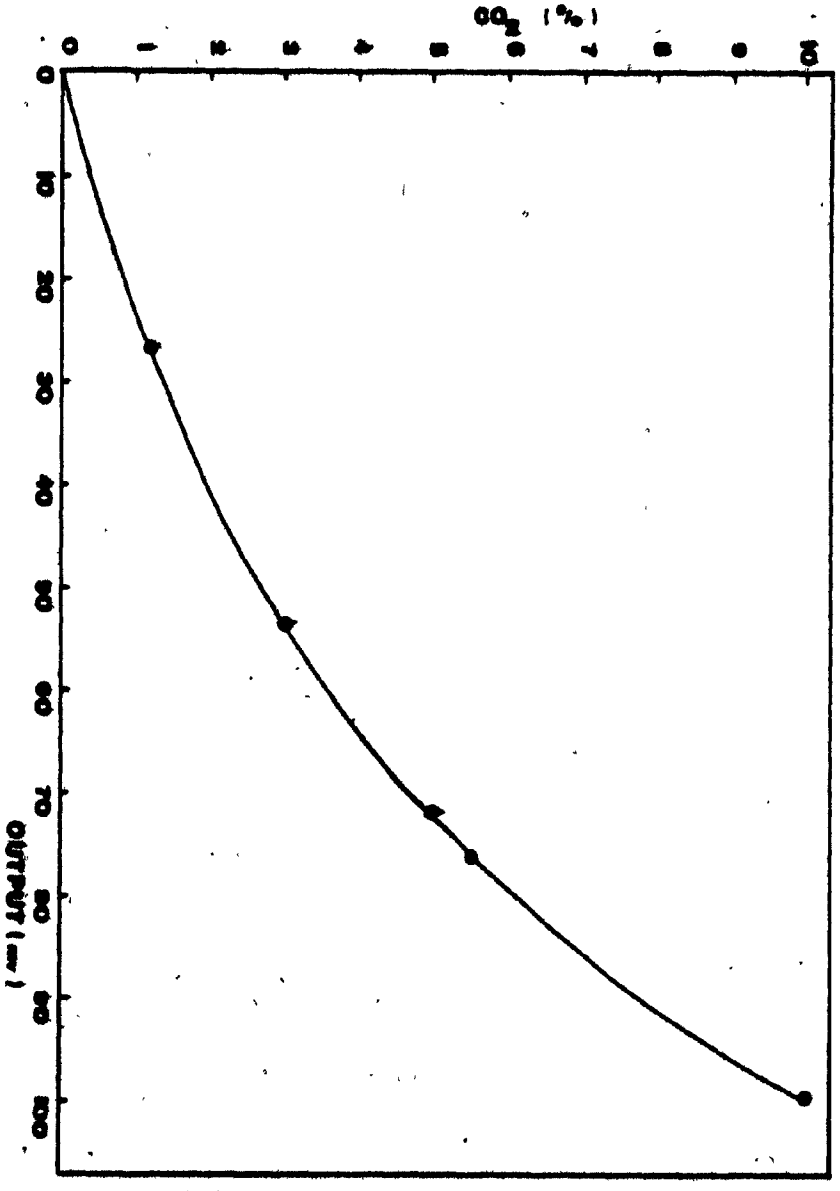
CO_2 (%)
0
2
4
6
8
10
OUTPUT (mA)
0.00
0.02
0.04
0.06
0.08
0.10
0.12
0.14
0.16
0.18
0.20

Figure III.13 Calibration for CO_2 Analyzer

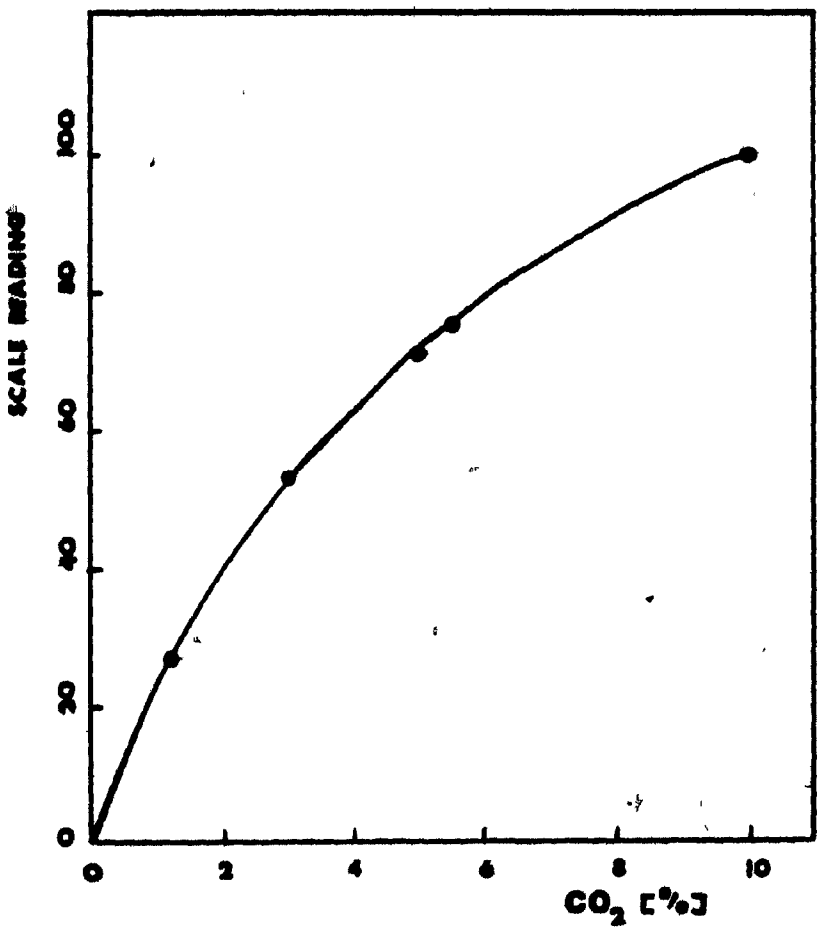
SCALE READING
0
20
40
60
80
100
0
2
4
6
8
10
CO_2 [%]

Figure III.14 Calibration for Strain Gauge Dynamometer

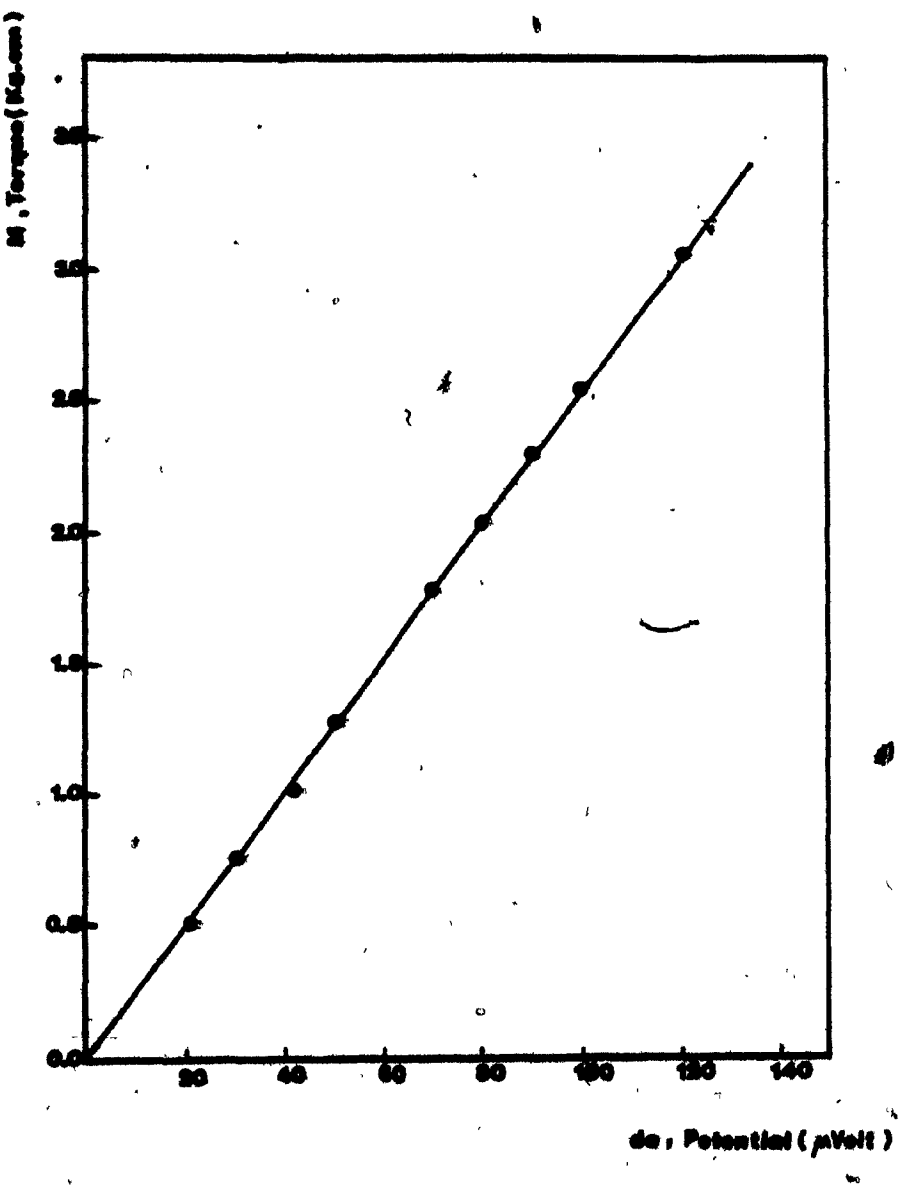
M , Torque (Kg.cm)
0.0
1.0
2.0
20
40
60
80
100
120
140
dø , Potential (μVolt)

Figure III.15 Calibration for Strain Gauge Dynamometer

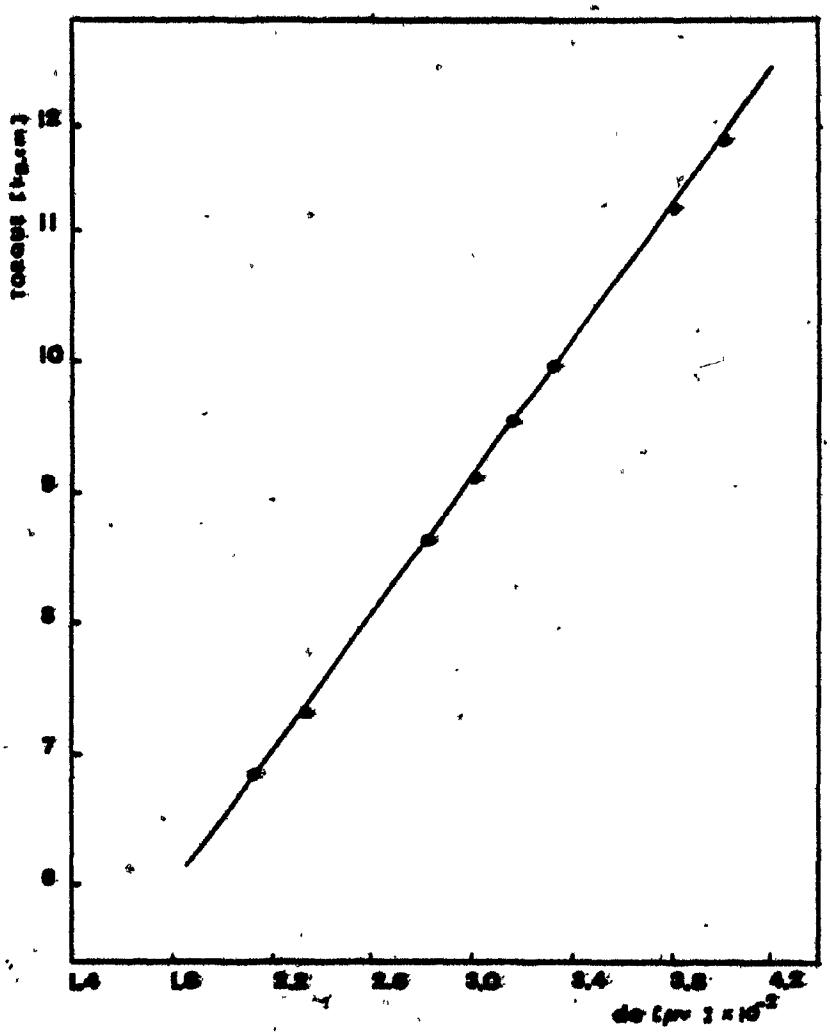
torque (lb-in)
12
11
10
9
8
7
6
1.4
1.6
2.2
2.6
3.0
3.4
3.8
4.2

Figure III.16 The Overall System Used for Continuous Measurement of the Fermentative Heat

A. Fermentor
B. Saturation Column
C. pH Controller
D. Oxygen Analyzer
E. Carbon Dioxide Analyzer
F. Digital Multimeter
G. Drying Column
H. Reference Gas Cylinders
I. Thermocouple Reference Junction
K. Proportional Controller
J. EMF Converter
L. Programmable Power Supply
M. Digital Thermistor Indicator
N. Digital Thermistor Indicator
O. Strip Chart Recorder
P. Mercury Manometer

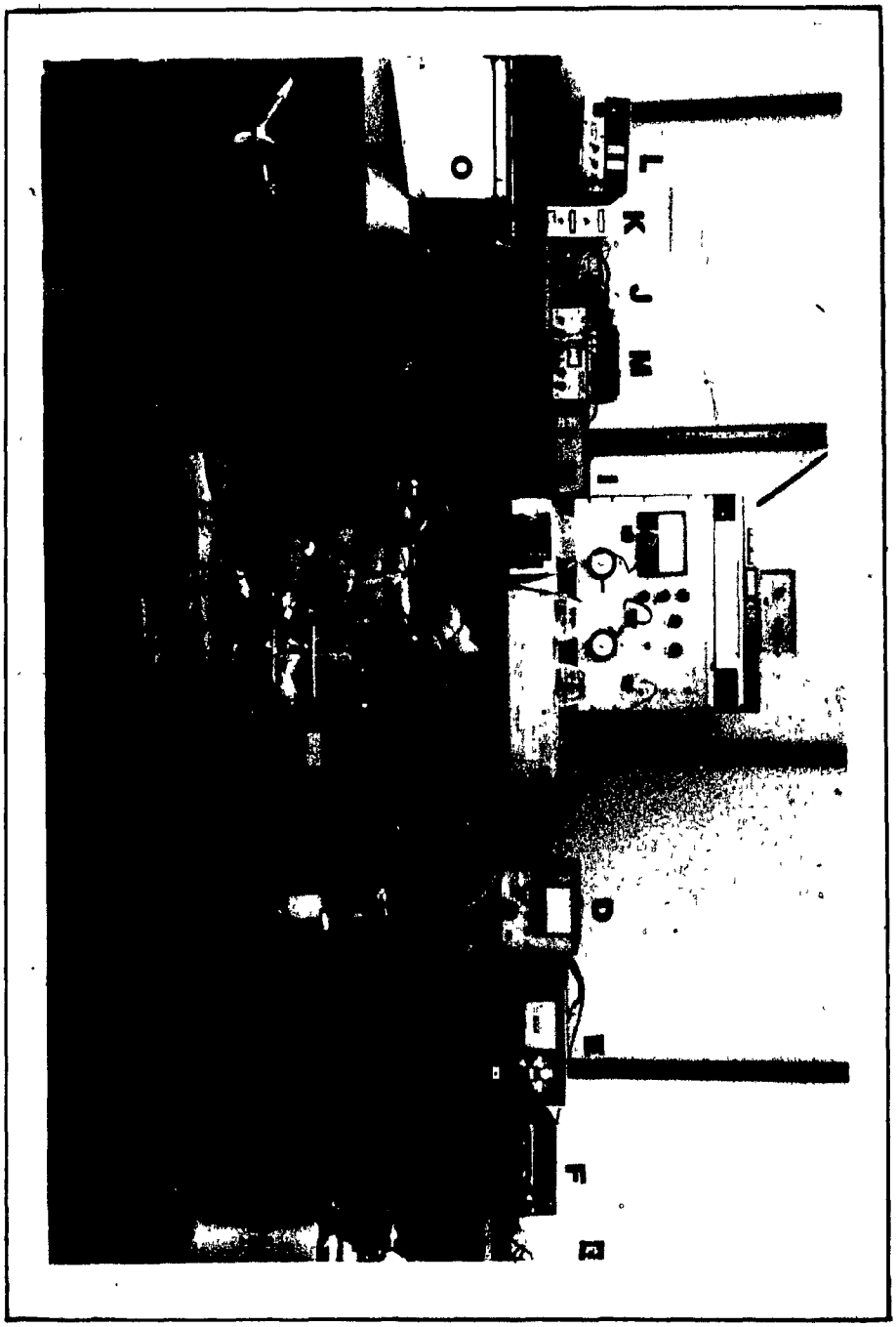

B. MICROBIAL CULTURES AND ANALYTICAL MEASUREMENTS

1. Organism

Experiments were performed using a mold (*A.niger*), a bacteria (*E.coli*), and three different yeasts (*C.lipolytica, C.intermedia, and C.utilis*) . Both the yeast hydrocarbon and carbohydrate fermentation systems were investigated extensively since they are important processes for the production of the single cell protein (SCP) .

The following table lists the micro-organisms used in this study and their sources .

Table III

Organism	Medium Used	Source
Aspergillus niger	I	Carolina Biological Supply Co. Burlington, North Carolina
Candida utilis	III	ATCC 9950
Candida intermedia	II	ATCC 20404
Candida lipolytica	IV	ATCC 8662
Escherichia coli	V	Department of Microbiology, McGill University, Montreal

2. Culture Media

A list of the culture media used in this study is compiled in Appendix I. All the components used were reagent grade except for the

glucose, sucrose, ethanol, cellobiose, hexadecane, and n-dodecane, which were technical grade .

3. Inoculum Preparation

The inoculum for each fermentation was prepared by the following standard procedure. Three 250 ml shake flasks with 50 ml of medium were inoculated from a slant or stock culture stored in the refrigerator. The cultures were allowed to grow from ten to eighteen hours . One ml of the resulting cell suspension was then used to inoculate six 500 ml shake flasks containing 160 ml of medium each. These flasks were shaken at 250 rpm at 25°C. After six to sixteen hours, when the cultures were in the exponential growth phase, they were used to inoculate the 14 liter fermentor .

4. Sterilization

All shake flasks with carbohydrate were steam sterilized in an autoclave at 10 psi. This temperature and time is not sufficient to caramelize the carbohydrates . Ethanol, n-dodecane, and hexadecane, which cannot be sterilized by steam were sterilized by means of a "millipore" filter (.45μ) connected with 50 ml syringe. All other sterilization was done with steam for 15 minutes at 15 psi. All mineral salt solutions were sterilized separately in order to prevent precipitation . The 7 liters of water were also steam sterilized at 15 psi for 15 minutes .

5. Sampling from the fermentor

The device shown in Figure III.17 was used to remove samples from the 14 liter fermentor . A 12 cm length of 32 mm Pyrex glass tubing was fitted with two number 6 rubber stoppers. Five ml gradations were marked on the glass tube to measure the volume of the sample removed .

Figure III.17 The Sampling Device

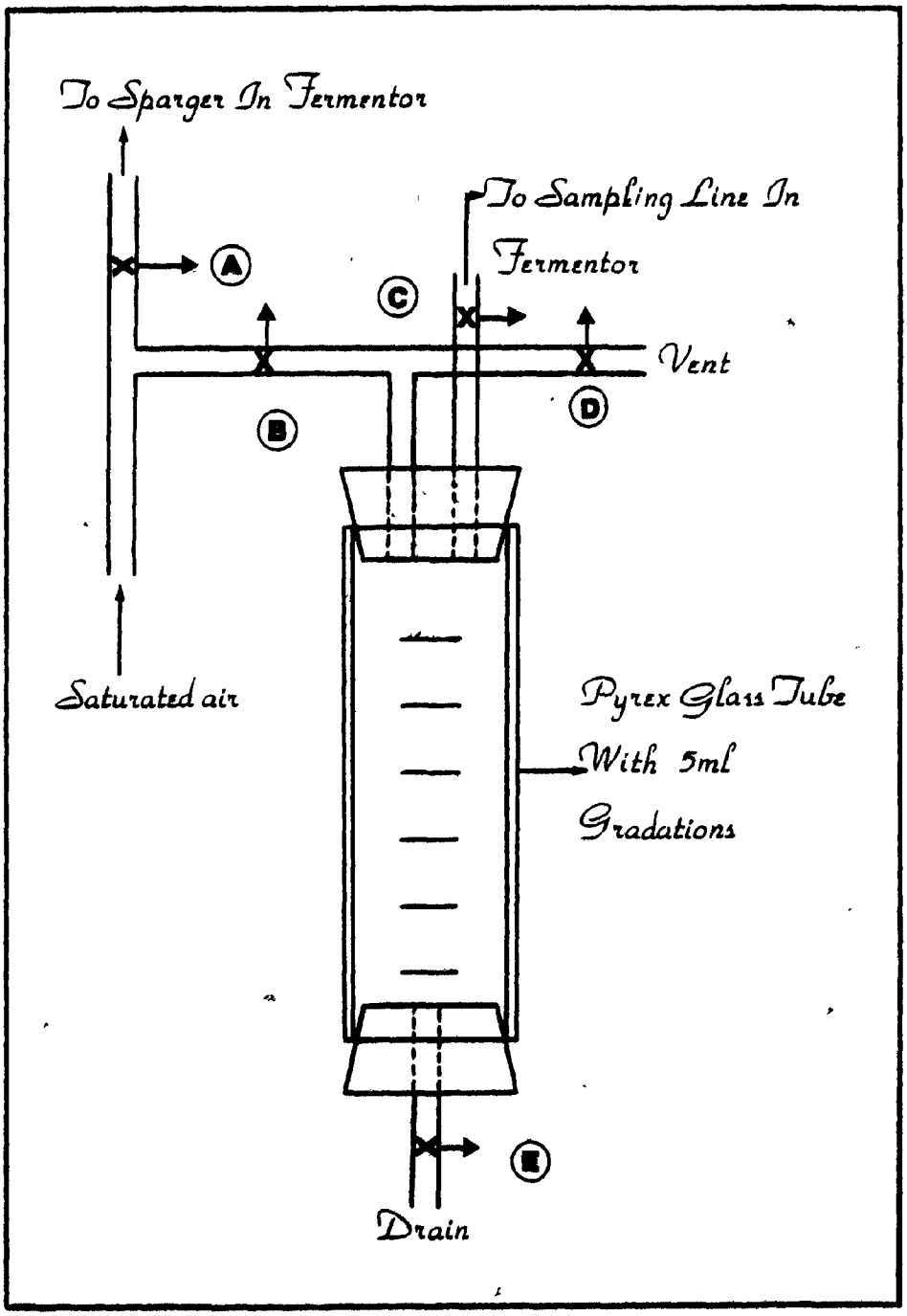
To Sparger In Fermentor
To Sampling Line In Fermentor
A
C
Vent
B
D
Saturated air
Pyrex Glass Tube With 5ml Gradations
E
Drain

When removing a sample, air from the water saturating column was first diverted to blow out the sampling line by closing the line to the sparger at (A) and opening valves (B) and (C). After clearing the sample line, the air was again allowed to flow to the sparger by opening (A), and closing (B). A portion of the fermentation broth was then forced into the collecting tube by closing the exit gas line of the fermentor and opening the vent at (D). After closing (D), the sample was discharged by opening (E) .

6. Density Measurement

The density of cell suspensions was determined by pipetting 50 ml of sample into a weighed 50 ml Erlenmeyer flask. An electronic balance was used to weigh the flasks with and without the culture sample. Care was taken to determine the densities at constant temperature. Density measurements were made in duplicate for each sample .

7. Dry Weight Determination

A 40 ml sample of cell suspension was centrifuged at 15,000 rpm for 15 minutes. The supernatant was discarded and the cells washed with 25 ml of distilled water. After a second centrifugation, the supernatant was again discarded, and the cells resuspended in 5ml of distilled water. These samples were placed in weighed aluminium tare dishes and put into an oven at 110^{o}C . At about 18 hours, the samples were weighed and then returned to the drying oven. The samples were weighed again in 2 to 4 hours. If their

weight remained constant, drying was stopped. This procedure was carried out at least twice for each determination .

8. Surface Tension Measurement

The Fisher Surface Tensiomat (Model 21) was used to measure the surface tension of liquids. The surface tensiomat consists of a torsion wire balance with a dial calibrated in dynes per centimeter, a weighted platinum-iridium ring, a movable table and a small reversible motor. Surface tension measurements were made in triplicate for each sample .

9. Glucose Concentration Determination

The determination of glucose levels in the culture broth was based on the method of Fisher Diagnostics Glucose Hexokinase (HK), utilizing the coupled enzyme reactions of hexokinase and glucose-6-phosphate dehydrogenase :

$$\text{Glucose} + \text{ATP} \longrightarrow \text{ADP} + \text{Glucose-6-Phosphate}$$

$$\text{Glucose-6-Phosphate} + \text{NAD}^+ \xrightarrow{\text{G-6-PDH}} \text{6-Phosphogluconate} + \text{NADH} + \text{H}^+$$

The first reaction involved phosphorylation of glucose by hexokinase (HK) and ATP to yield glucose-6-phosphate. This product is then oxidized by glucose-6-phosphate dehydrogenase (G-6-PDH) with concomittant reduction of NAD^+ to NADH. Since both reactions are essentially irreversible, the total amount of NADH formed in the second reaction, determined spectrophotometrically at 340 nm , is a direct measure of the glucose concentration.

CHAPTER IV

RESULTS

A. MIXING POWER INPUT STUDY

With the purpose of developing a semi-theoretical correlation for estimation of the mixing power input in a gassed agitated system, a strain gauge dynamometer was used to measure the torque of the fermentor impeller shaft. The stirred tank geometry and ranges of operating variables are given in Figure IV.1 and Table IV.1 respectively. The physio-chemical properties of liquid solutions used in this study are given in Table IV.2 .

The relationship between the mixing power input in gassed or ungassed systems and the impeller rotational speed for some Newtonian and non-Newtonian liquids was experimentally established. Figures IV.2 and IV.3 depict the mixing power per unit volume correlation with impeller rotational speed. In both cases, the impeller power input was proportional to the cube of the impeller rotational speed over the entire range of the rotational speed examined which was from 500 to 800 rpm. The mixing power number(N_p) was constant at 6.14 for a six-blade turbine impeller under turbulent conditions (Figure IV.4).

When the mixing power ratio (P_g/P) was plotted against the aeration number (N_A), a non-linear relationship was obtained (Figure IV.5). Cross plots of all the experimental data in the form of Figure IV.5 showed that (P_g/P) varied with $N_A^{-0.38}$ for the Newtonian solutions. A similar correlation also applies for the non-Newtonian solutions .

Finally, when the function $(P_g/P)N_A^{0.38}$ was plotted against the Weber number (N_{We}), a non-linear relationship also resulted (Figure IV.6). The behavior of the non-Newtonian liquids, however, was observed to be slightly different with respect to power consumption from that of Newtonian solutions.

All experimental data related to mixing power input are tabulated in Appendix III .

Figure IV.1 The Geometry of 14 liter "Microferm" Fermentor

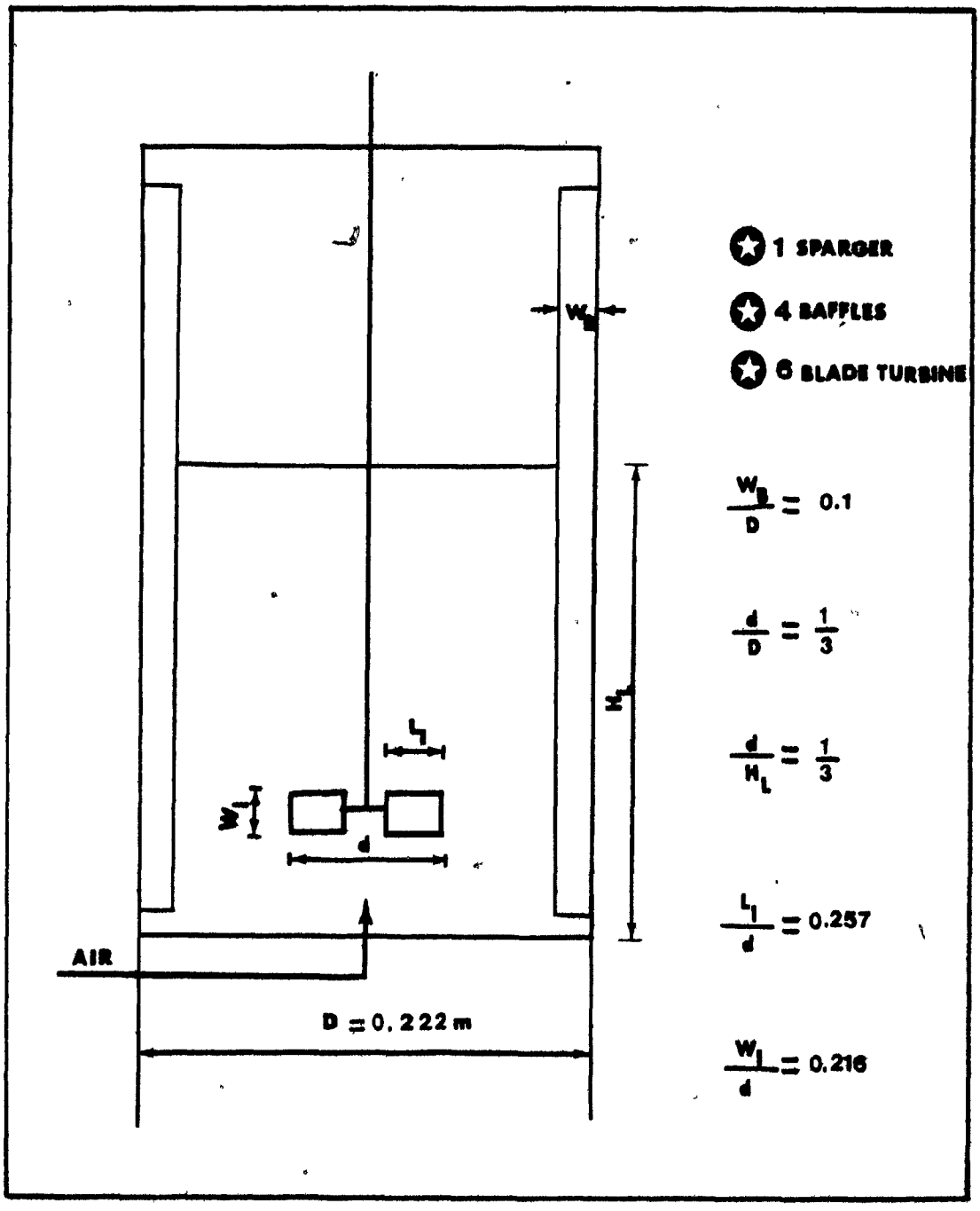
1 SPARGER
4 BAFFLES
6 BLADE TURBINE
$\frac{W_B}{D} = 0.1$
$\frac{d}{D} = \frac{1}{3}$
$\frac{d}{H_L} = \frac{1}{3}$
$\frac{L_1}{d} = 0.257$
$\frac{W_1}{d} = 0.216$
AIR
D = 0.222 m

TABLE IV.1

Stirred Tank Geometry, Ranges of Operating Variables and Geometric Ratios of Impeller

Internal Diameter of Tank (m)	0.222
Air Sparger	
* Number	1
* Orifice diameter (m)	0.002
Aeration Rate (m^3/sec) x 10^5	2.987-24.234
Baffles	
* Number	4
* W_B/D	0.1
Rotational Speed (rpm)	500-900
Impeller Type : Six Flat-Blade Turbine	
- d/D	1/3
- W_I/d	0.216
- L_I/d	0.257
- T_I/d	0.0135

TABLE IV.2

Physico-Chemical Properties of Aqueous Phases (25°C)

Liquid/Solution	Density (kg/m^3)	Viscosity ($N.s/m^2$)x10^3	Surface Tension (N/m)x10^3
* Newtonian Fluids			
Water	1000	0.89	72
Methanol (10% by volume)	983	0.85	58
Methanol (25% by volume)	963.5	0.80	46
Ethylene Glycol (8% by weight)	1008	1.72	55
* Non-Newtonian Fluids			
CMC (0.4%)	1000	-	68.5
CMC (0.67%)	1000	-	71.5

Figure IV.2 The Mixing Power Input versus the Rotational Speed for Newtonian Fluids

- Parameter is the aeration gas flow rate

* VVM : Volume of gas flow rate per volume of broth per minute

MIXING POWER INPUT

WATER and AIR

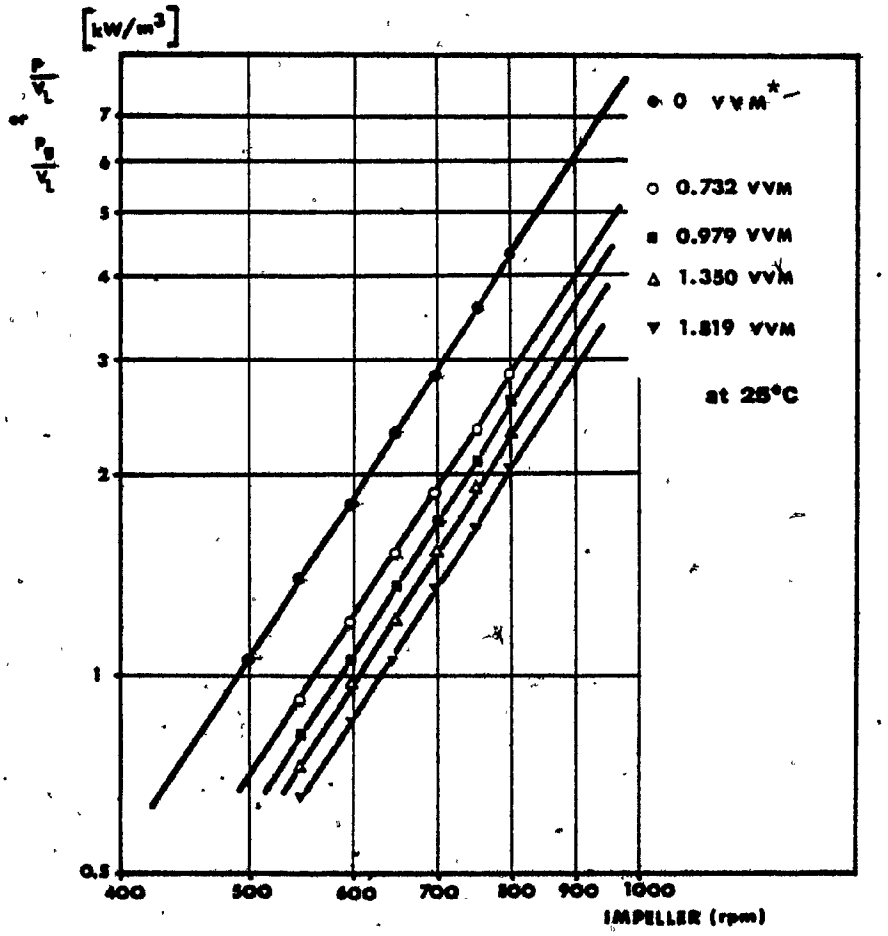

Figure IV.3 The Mixing Power Input versus the Rotational Speed for non-Newtonian Fluids

1. VVM : Volume of gas per volume of broth per minute
2. CMC : CarboxyMethylCellulose

N.B. Parameter is the aeration gas flow rate

MIXING POWER INPUT

NON-NEWTONIAN LIQUIDS at 25°C

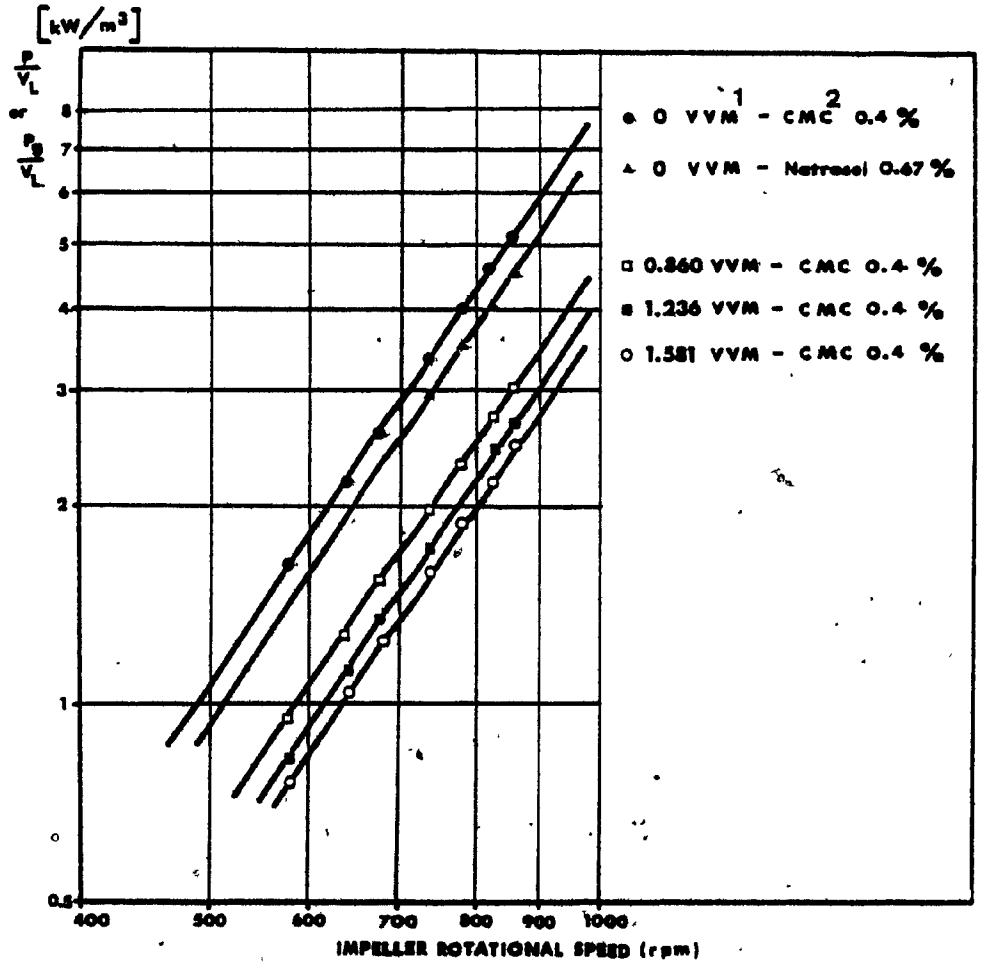

Figure IV.4 The Mixing Power Number for Some Newtonian Fluids at 25 °C

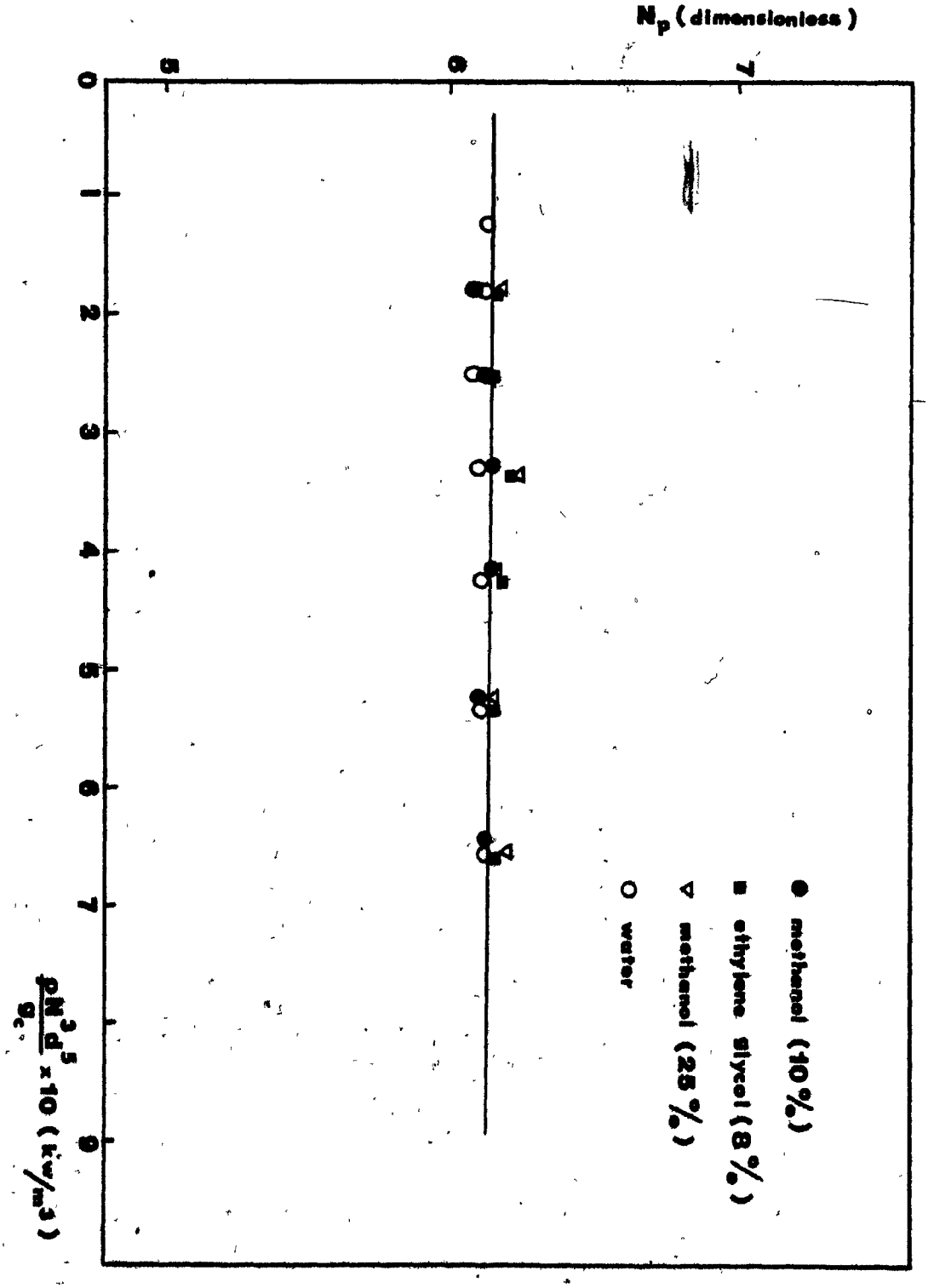
N_p (dimensionless)
8
9
7
0
1
2
3
4
5
6
7
8
9
$\frac{\rho N^3 d^5}{g_c} \times 10$ (kw/m³)
● methanol (10 %)
■ ethylene glycol (8 %)
▲ methanol (25 %)
○ water

Figure IV.5 The Correlation between the Aeration number (Q/Nd^3) and the Gassed-to-Ungassed Mixing Power Ratio (P_g/P)

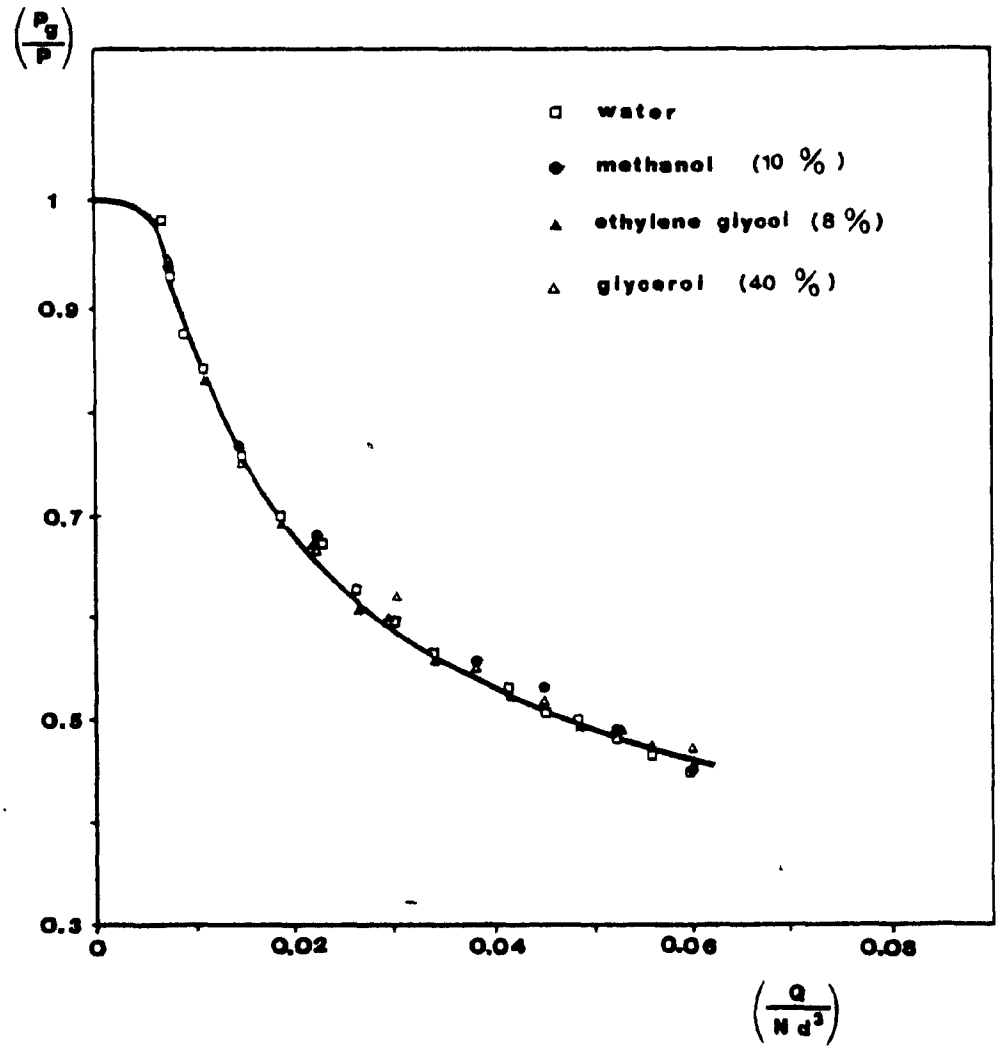
$\left(\frac{P_g}{P}\right)$
water
methanol (10 %)
ethylene glycol (8 %)
glycerol (40 %)
1
0.9
0.7
0.5
0.3
0
0.02
0.04
0.06
0.08
$\left(\frac{Q}{N d^3}\right)$

Figure IV.6 The Mixing Power Correlation for Newtonian and non-Newtonian Fluids

1. Newtonian Fluids

$$\frac{P_g}{P} = 0.497 \left(\frac{Q}{N d^3}\right)^{-0.38} \left(\frac{N^2 d^3 \rho_L}{\sigma}\right)^{-0.18}$$

* Correlation Coefficient = 0.985

2. Non-Newtonian Fluids

$$\frac{P_g}{P} = 0.514 \left(\frac{Q}{N d^3}\right)^{-0.38} \left(\frac{N^2 d^3 \rho_L}{\sigma}\right)^{-0.194}$$

* Correlation Coefficient = 0.989

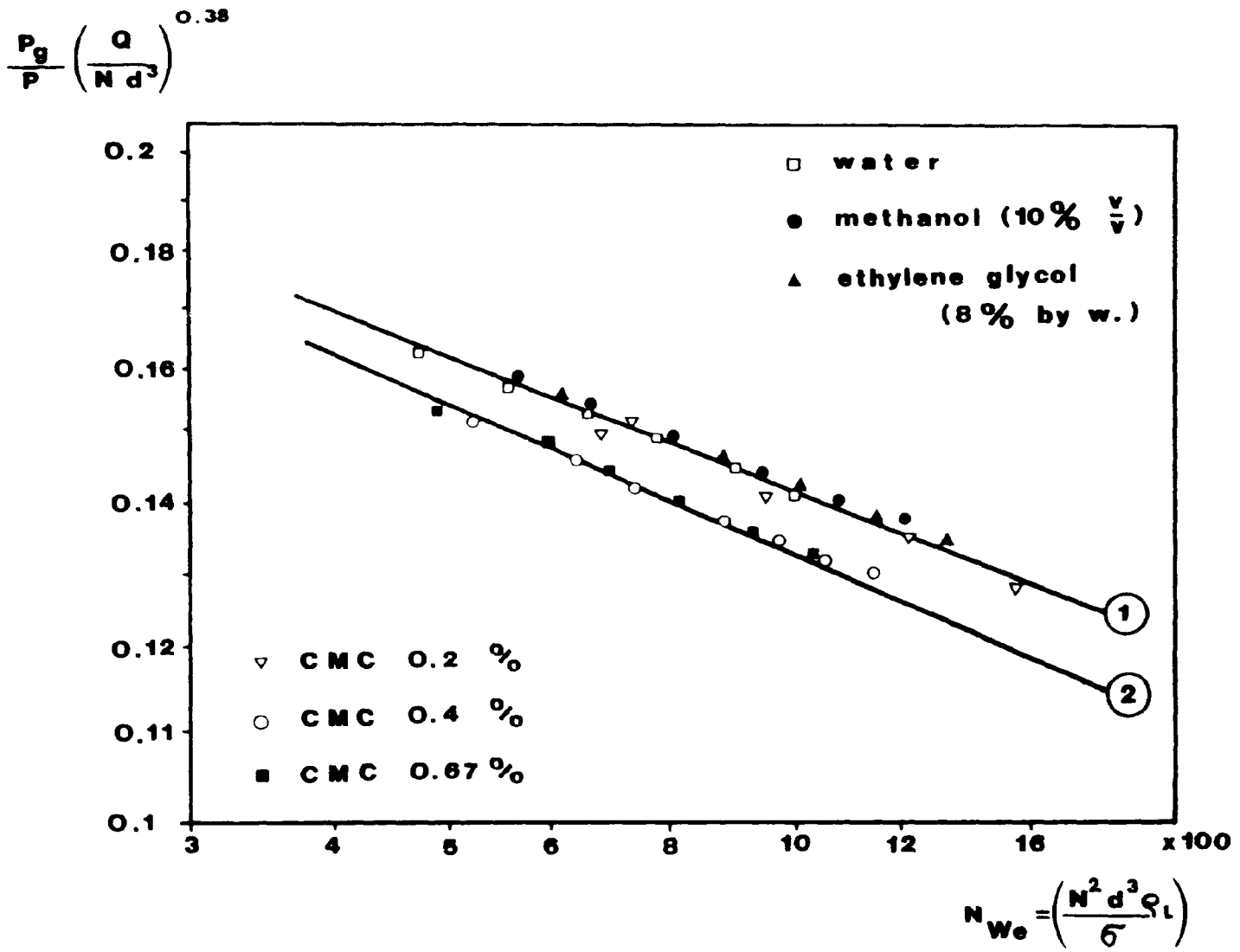
$\frac{P_g}{P}\left(\frac{Q}{N\,d^3}\right)^{0.38}$
0.2
0.18
0.16
0.14
0.12
0.11
0.1
3
4
5
6
8
10
12
16
x 100
$N_{We}=\left(\frac{N^2 d^3 \rho_L}{\sigma}\right)$
water
methanol (10% v/v)
ethylene glycol (8% by w.)
CMC 0.2 %
CMC 0.4 %
CMC 0.67 %
1
2

B. THE HEAT LOST TO THE SURROUNDINGS

Although the fermentor jar was insulated with 5 cm in thickness of polyurethane foam, some heat loss to the surroundings always occured, particularly through the head plate. An initial estimation of this heat loss term was necessary for the correction of the fermentative heat calculations. Equations (16) to (41) could be used to evaluate the heat loss to the surroundings theoretically. However, these calculations may not be quite accurate since some parameters in the equations could not be determined precisely. The theoretical model proved that the specific heat transfer coefficient U_1A_1 was almost independent of the mixing power input and the physical properties of the fluids studied. In this work, the specific heat transfer coefficient term(U_1A_1) was determined experimentally by measuring the slope of temperature rise versus time at constant agitation and aeration rates,with the temperature controller turned off .

A known amount of heat was introduced into the system through a resistance heater in order to increase the slope of the temperature versus time plot. The transient heat term $\Sigma_i M_i C_{pi} (dT/dt)$ values,determined by this procedure, were then plotted as a function of the temperature difference driving force ($T - T_{amb}$) yielding a straight line relationship with a slope ($=U_1A_1$) of 0.068 kcal/l.h.^{o}C (Figure IV.7) .

The value of the heat loss to the surroundings was only corrected for variation in the temperature difference driving forces as encountered during the experiment. The ambient air temperature, however, was fairly constant and the fluctuations of the heat loss to the surroundings were

Figure IV.7 The Determination of the Specific Heat Transfer Coefficient U_1A_1

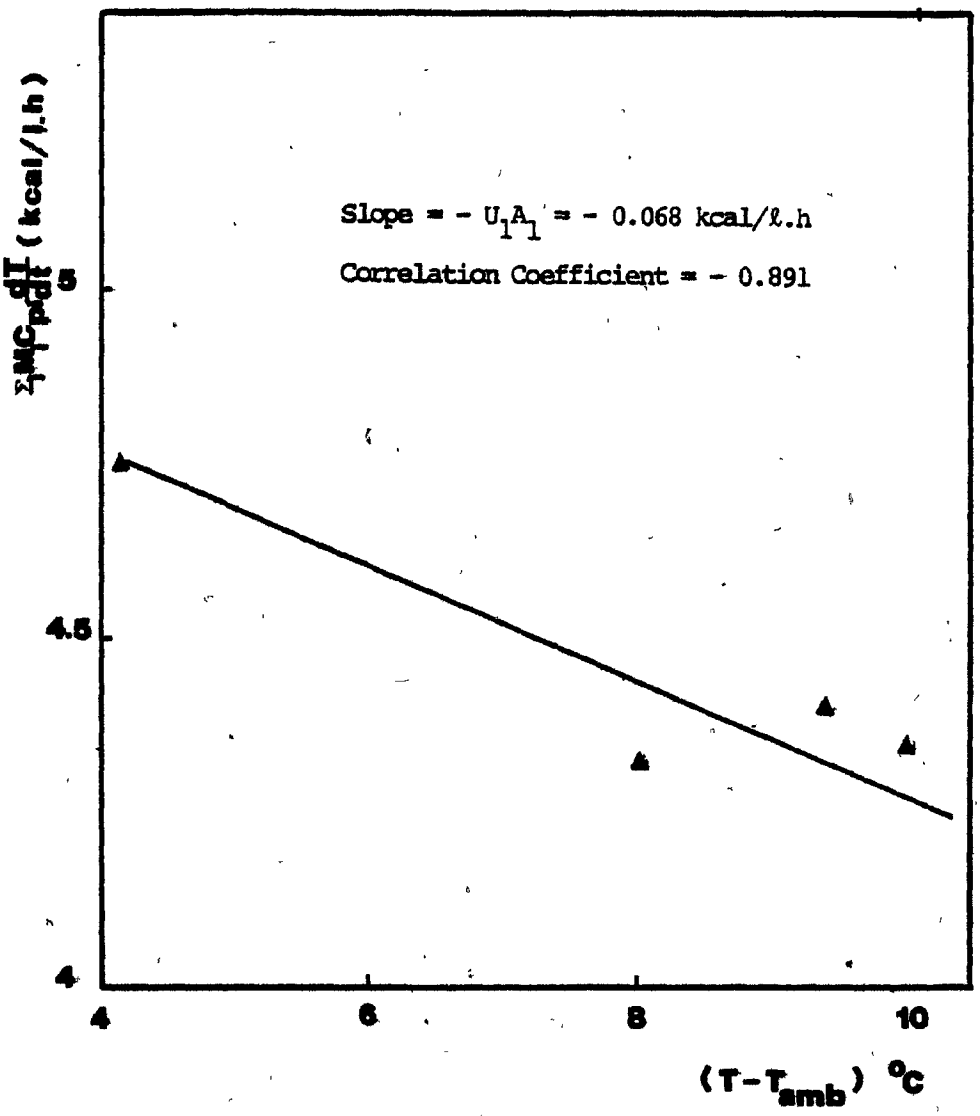
Slope = - $U_l A_l$ = - 0.068 kcal/ℓ.h
Correlation Coefficient = - 0.891
$\Sigma_l MC_p \frac{dT}{dt}$ (kcal/l.h)
5
4.5
4
4
6
8
10
(T-T_{amb}) °C

negligible in the overall calculation of the fermentative heat (Table IV.3).

The mixing power could be evaluated by using Equation (63). However, the operating conditions in this study were slightly different from the ideal conditions (D/d =3, H/d = 3). In accordance with the measured heat loss, the basic value of $Q_{agi} + Q_{bub} - U_l A_l (T - T_{amb})$ could be determined by measuring the temperature rise in the fermentor prior to inoculation for a given rate of agitation and gas flow rate. Subsequently, the measured value was used throughout the fermentation for the calculation of Q_{ferm}.

TABLE IV.3

THE HEAT LOSS TO THE SURROUNDINGS CALCULATION

Fermentation Time (Hour)	T_{amb} (°C)	T (°C)	$T - T_{amb}$ (°C)	Q_{surr} (kcal/l.h)
0	23.66	30.02	6.36	0.432
5	23.23	30.13	6.90	0.469
7	23.90	30.16	6.26	0.426
8	23.08	30.18	7.10	0.483
9	23.50	30.12	6.62	0.450
10	23.48	30.08	6.60	0.449

C. THE DETERMINATION OF THE SPECIFIC HEAT TRANSFER COEFFICIENT U_2A_2 FOR COOLING HOLLOW BAFFLES

A similar approach to the method of evaluation of heat transfer coefficient U_1A_1 was again employed to estimate the specific heat transfer coefficient for the hollow baffles U_2A_2 . Basically the slope of the temperature versus time curve was measured while the temperature controller was turned off, and agitation and cooling water flow rates were kept constant. The heat transfer rate from the fermentation broth to the cooling medium was calculated through the following dynamic energy balance:

$$\Sigma_i M_i C_{pi}\left(\frac{dT}{dt}\right) = Q_{agi} + Q_{bub} - U_1A_1(T - T_{amb}) - \frac{U_2A_2\, KQ_c}{1 + KQ_c}(T - T_c) \quad \ldots\ldots (116)$$

$$= Q_{agi} + Q_{bub} - U_1A_1(T - T_{amb}) - U_2A_2^*(T - T_c) \quad \ldots\ldots (117)$$

where

$$U_2A_2^* = \frac{U_2A_2\, K\, Q_c}{1 + KQ_c} \quad \ldots\ldots (118)$$

and

$$K = 2\, C_c \rho_c / U_2A_2 \quad \ldots\ldots (119)$$

The resulting values of $U_2A_2^*$ coefficient are reported in Table IV.4 for different cooling water flow rates . Figure IV.8 presents a graphical relationship between the cooling flow rate and the mean specific heat transfer coefficient $U_2A_2^*$ defined in Equation (118) .

This relationship was established as a linear correlation with values for $U_2A_2^*$ ranging from 1.0520 - 1.6039 kcal/l.h.^{o}C and cooling flow rates from 11.5326 - 18.5326 l/h .

Figure IV.8 The Determination of the Specific Heat Transfer Coefficient $U_2A_2^*$.

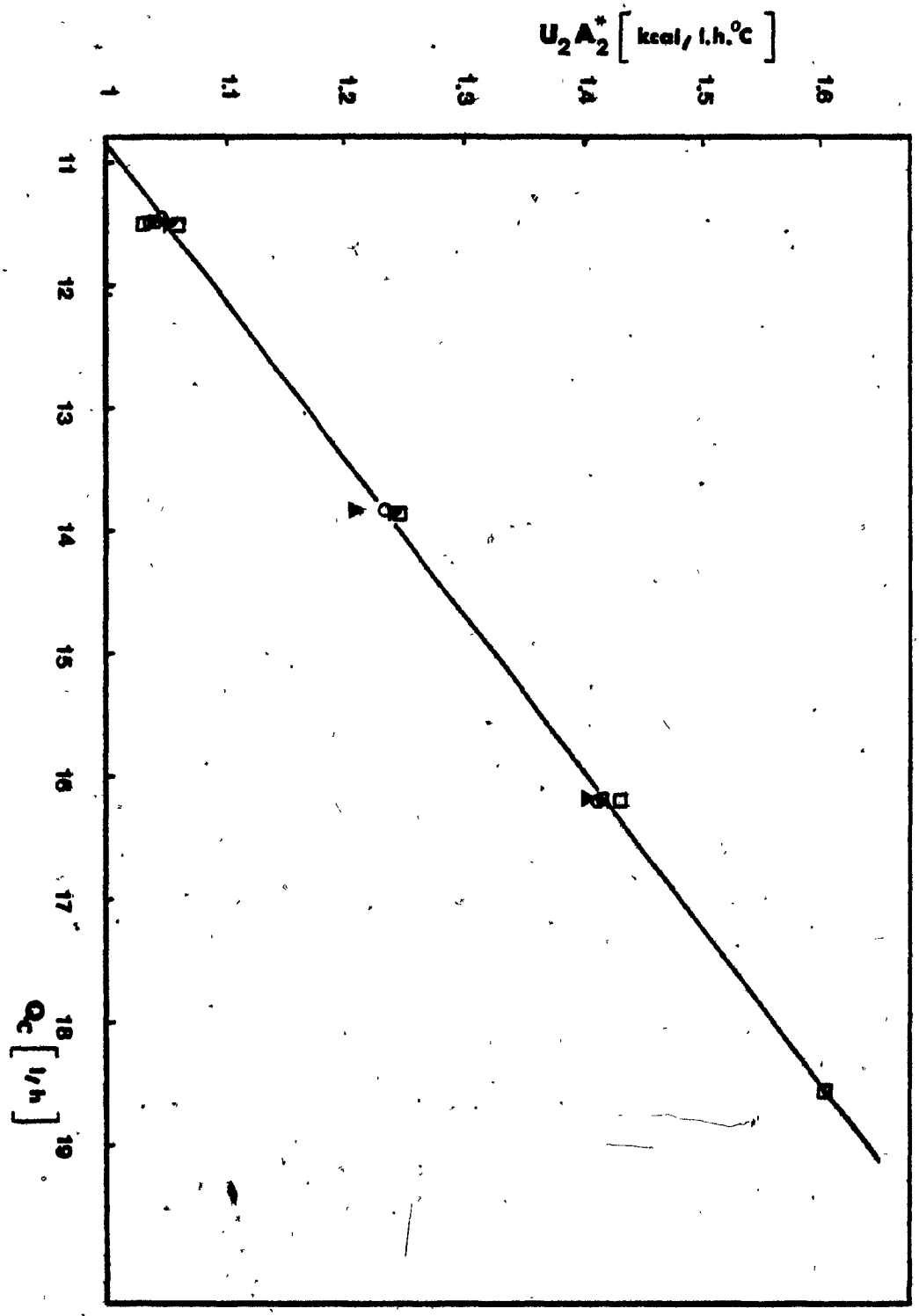
$U_2 A_2^*$ [kcal / l.h.°C]
1
1.1
1.2
1.3
1.4
1.5
1.6
11
12
13
14
15
16
17
18
19
Q_c [l/h]

TABLE IV.4

THE DETERMINATION OF SPECIFIC HEAT TRANSFER COEFFICIENT $U_2A_2^*$

Water Flow Rate (l/h)	$T - T_c$ (°C)	$U_2A_2^*(T - T_c)$ (kcal/l.h)	$U_2A_2^*$ (kcal/l.h.°C)
13.8147	9.9	12.2754	1.2399
-	11.48	14.3544	1.2504
-	10.70	13.3275	1.2456
-	11.51	13.9442	1.2115
-	12.15	14.7298	1.2123
		*Mean :	1.2320
16.1737	10.82	15.3071	1.4147
-	12.18	17.4985	1.4367
-	13.20	18.7064	1.4172
-	13.55	19.0304	1.4045
		*Mean :	1.4180
11.4558	13.25	13.9811	1.0552
-	14.03	14.9867	1.0682
-	14.28	14.8382	1.0391
-	13.91	14.3644	1.0477
-	14.23	14.7343	1.1354
-	14.44	15.2040	1.0529
-	14.12	15.0614	1.0667
		*Mean :	1.0520
18.5326	13.90	22.294	1.6039

D. THE APPLICABILITY, RELIABILITY, AND ACCURACY OF THE EXPERIMENTAL TECHNIQUE AND OF DYNAMIC CALORIMETRIC TECHNIQUE

The overall accuracy of the experimental technique used in this study to measure the heat of fermentation was established to be - 1.41% . This was determined by simulating the heat of fermentation through the introduction of a known amount of heat into the system via a submersible electric heater. In order to define the overall accuracy of the measuring technique, the set heat input was estimated by using the overall heat balance {Equation (7)} and compared to the actual value .

From Table IV.5, the discrepancy ranged from 0.12 to -7.5% of the known heat input. The overall accuracy of the measuring technique was thus determined to be - 1.41% .

A series of similar tests were carried out to determine the accuracy of the dynamic calorimetric technique (Table IV.6). The average percent difference between the known heat input and the amount of heat determined by the dynamic calorimetric technique was + 2.20% .

It is evident from Table IV.6 that the accuracy of the dynamic calorimetric technique is satisfactory only when the simulated heat input is high . In each experiment, the measured heat was smaller than the known heat input. The discrepancy ranged from 0.21 to 4.29% of the actual heat input .

TABLE IV.5

THE DETERMINATION OF THE OVERALL ACCURACY FOR THE NEW TECHNIQUE

Test No.	Heat Input (kcal/l.h)	Heat Measured (kcal/l.h)	Difference from Heat Input (%)
1	2.908	2.763	4.98
2	2.908	3.114	-7.5
3	2.908	3.092	-5.95
4	23.038	22.827	0.92
5	23.333	23.572	-1.02
6	23.378	23.350	0.12

TABLE IV.6

THE DETERMINATION OF THE OVERALL ACCURACY OF THE DYNAMIC CALORIMETRIC TECHNIQUE

Test No.	Heat Input (kcal/l.h)	Heat Measured (kcal/l.h)	Difference from Heat Input (%)
1	3.745	3.632	3.01
2	5.899	5.464	4.29
3	11.921	11.896	0.21
4	12.631	12.230	3.17
5	16.734	16.679	0.33

E. THE FLUCTUATION OF THE LIQUID BROTH TEMPERATURE AROUND THE CONTROLLED VALUE

Before inoculation, the compensating heat produced by the immersion heater remained unchanged (Figure IV.9) .

During the fermentation the amount of external heat supplied into the system varied in accordance to the quantity of heat produced by microbial activity in order to maintain an isothermal liquid broth (Figure IV.10). It was observed that the controlled temperature of liquid broth never deviated for more than ± 0.15 ^{o}C from the preset desired temperature (Table IV.7) .

Upon determining the overall accuracy, reliability, and applicability of the method, it was concluded that this technique should be adopted for the desired continuous monitoring of the heat of fermentation .

TABLE IV.7

THE DEVIATION OF THE CONTROLLED TEMPERATURE OF FERMENTATION BROTH AROUND THE SET POINT

No.	Time (hr)	Fermentation Broth Temperature (^{o}C)
0	0	30.02
1	2	30.16
2	4	30.10
3	6	30.12
4	8	30.17
5	10	30.08
6	12	29.98

*Data were for the growth of C. utilis on glucose (T = 30 ^{o}C)

Figure IV.9 The Response of the Heat Activated by the Programmable Power Supply before Inoculation

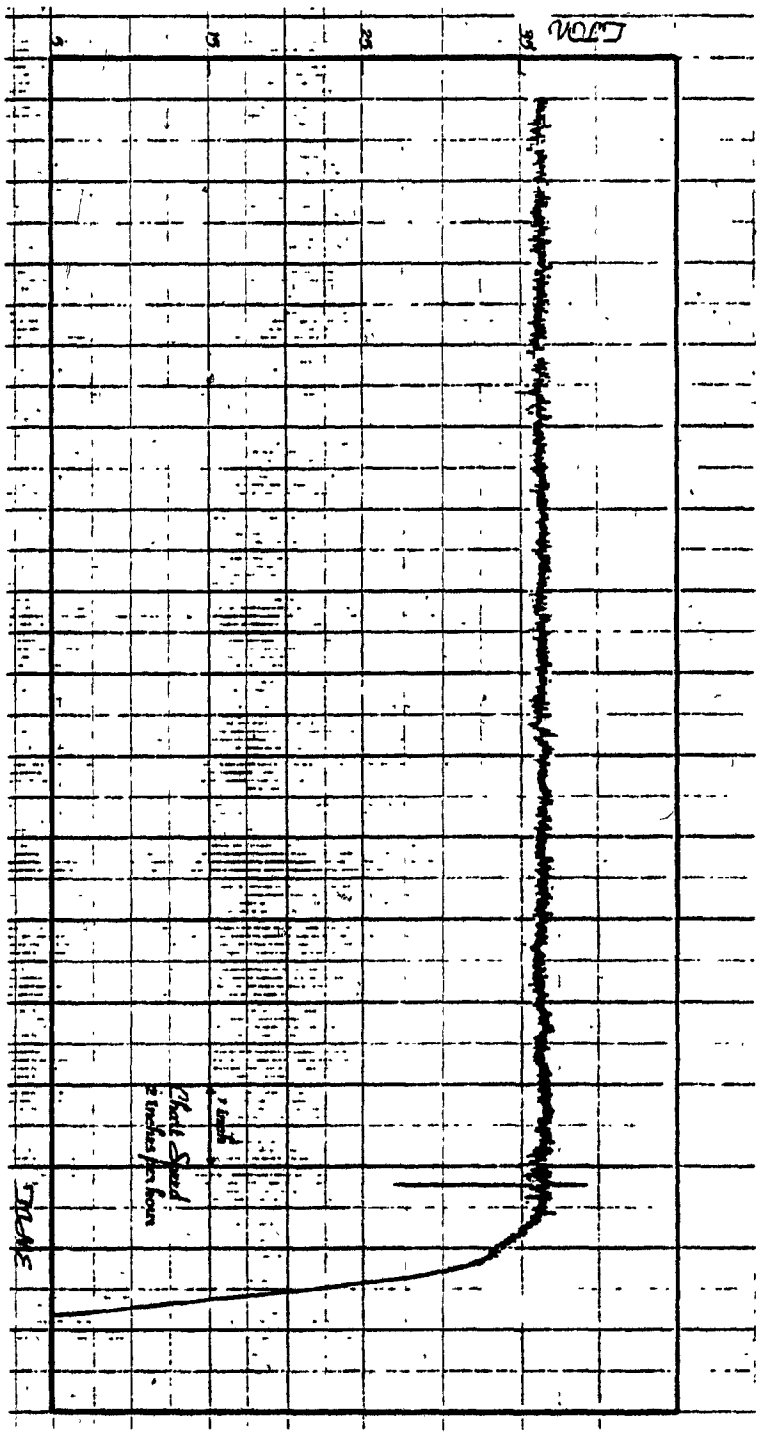
VOLTS
5
15
25
35
Chart Speed
2 inches per hour
TIME

Figure IV.10 The Variation of Heat Activated by the Programmable Power Supply in Response to the Amount of Heat Released by the Growing Culture during the Course of Fermentation

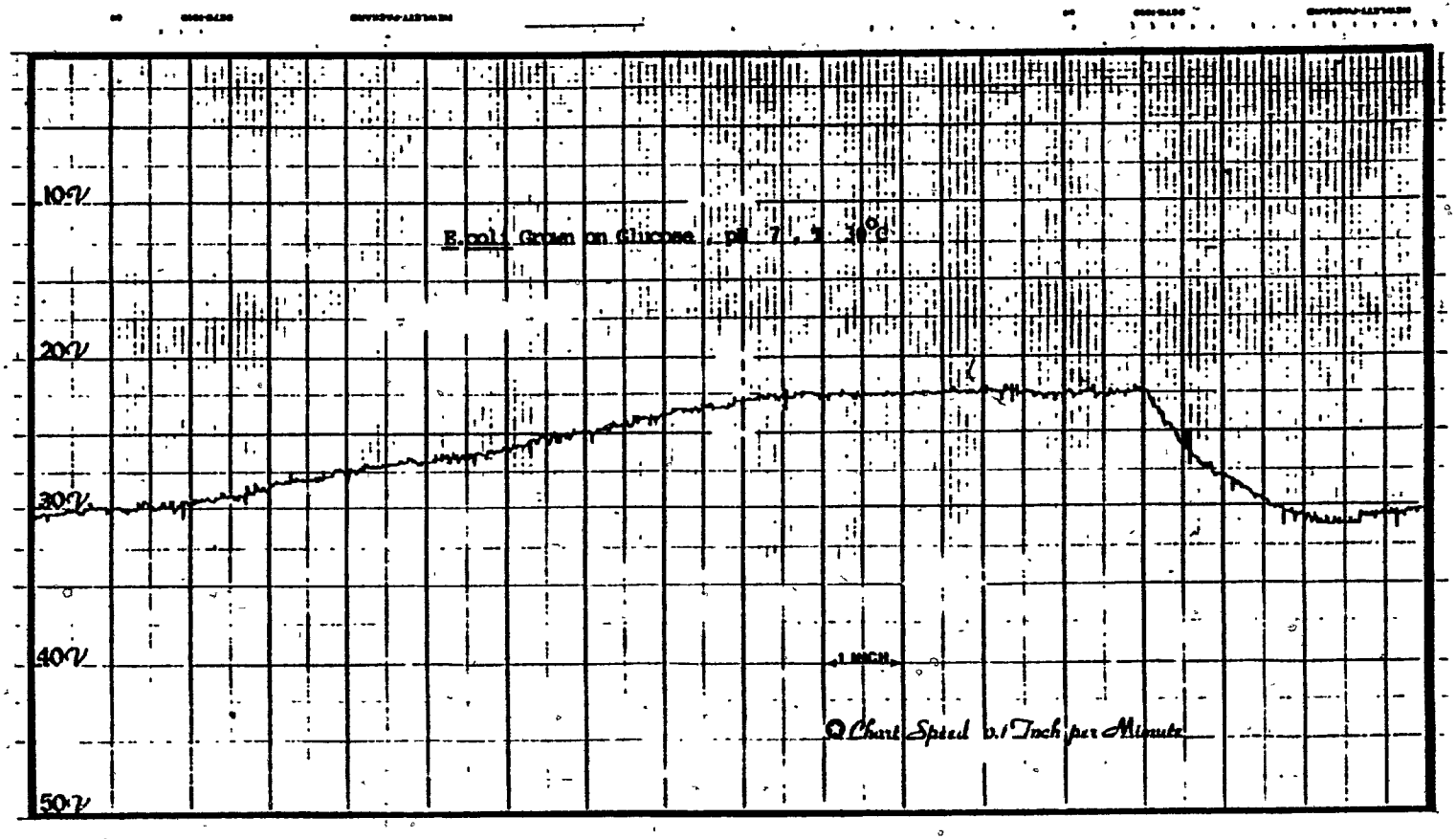
10V
20V
30V
40V
50V
E.coli Grown on Glucose, pH 7, 37°C
1 INCH
Chart Speed 0.1 Inch per Minute

F. PHYSIO-CHEMICAL PROPERTIES OF FERMENTATION BROTH

Since the mixing power ratio (P_g/P) was established to be dependent on the aeration number and the impeller Weber number, the density and the surface tension of the fermentation broth were measured periodically throughout the experiments in order to improve the correction for the agitation energy input . Usually, the density of the liquid broth does not change appreciably for both carbohydrate and hydrocarbon fermentations . The surface tension, therefore, is the only parameter which needs to be measured during the fermentation. The surface tension of the selected carbohydrate fermentation broth did not vary significantly during the experiment . Table IV.8 presents the physical properties of broth for a culture of C. utilis .

In the case of hydrocarbon fermentations, foaming occured several times during the experiments . Significant quantities of antifoam were added to the fermentation broth to improve the aeration and flow patterns. The interfacial tension was decreasing during the growth of C. lipolytica on hexadecane (Table IV.9) .

TABLE IV.8

PHYSIO-CHEMICAL PROPERTIES OF FERMENTATION BROTH

No.	Time (h)	Density (g/l)	Surface Tension (dyne/cm)
Before Inoculation	-	1.06636	32
0	0	1.06634	32
1	2.41	1.06860	31.5
2	3.75	1.06783	33
3	4.67	1.06759	33.5
4	5.67	1.06839	34.5
5	6.67	1.06565	36
6	7.67	1.06734	35
7	8.84	1.06629	34
8	9.50	1.06578	35
9	10.17	1.06354	37

The organism used for this experiment was C.utilis grown on a mixture of Glucose and Cellobiose .

TABLE IV.9

Time Course of the Growth of *Candida lipolytica* on Hexadecane

Fermentation Time (Hour)	Interfacial Tension (dyn-cm)
1	40.3
12	33.2
15	27
18	-
21	18.3

G. RATE OF HEAT PRODUCTION, OXYGEN CONSUMPTION, AND BIOMASS CONCENTRATION VERSUS TIME

Figures IV.11 through IV.25 are plots of the rate of heat production, oxygen consumption, and biomass concentration versus time for the following individual microbial culture and carbon sources :

Organisms	Substrate	Figure
Aspergillus niger[1]	Glucose	IV.11
Aspergillus niger[2]	Glucose	IV.12
Aspergillus niger	Glucose	IV.13
Candida intermedia	Glucose	IV.14
Escherichia coli	Glucose	IV.15
Escherichia coli	Glucose & Lactose	IV.16
Candida lipolytica	Glucose	IV.17
Candida lipolytica	n-Dodecane	IV.18
Candida lipolytica	Hexadecane	IV.19
Candida utilis[1]	Glucose	IV.20
Candida utilis	Glucose	IV.21
Candida utilis	Sucrose	IV.22
Candida utilis	Ethanol	IV.23
Candida utilis	Glucose & Cellobiose	IV.24
Candida utilis	Glucose & Cellobiose	IV.25

1. Dynamic Calorimetry
2. Wall Growth

The rate of oxygen consumption, when plotted against time, followed the trend of variation in the rate of heat evolution (Figures IV.11 through IV.25).

When the heat and oxygen curves were compared with the growth curves, two different types of behavior were indicated . In the first case, the rates of heat released and oxygen consumed drastically declined after the culture passed the peak of the exponential growth phase. In the second case, the two rate maxima coincided with the maximum culture growth rate, indicated by the inflection point on the growth curve. Experiments with *E. coli, C. lipolytica, and C. utilis* (Figures IV.15, IV.18, and IV.21) are illustrative of the first case while those with *A. niger, C. intermedia* (Figures IV.11, IV.13, and IV.14) exemplify the second .

In the case of diauxic growth of *E. coli* (Figure IV.16), it was observed that the heat and oxygen curves exhibit dual maxima , the first peaks occuring when the preferential glucose carbon source was completely utilized and the second ones corresponding to the end of the resumed log phase . The presence of lactose was probably responsible for a longer lag phase in comparison with *E. coli* growing on glucose only (Figure IV.15).

The parameters monitored during the growth of *C. utilis* on a mixture of glucose and cellobiose did not follow the expected diauxic growth pattern . The heat and oxygen curves both declined sharply when glucose was depleted by the growing culture . The experiment was executed in duplicate (Figures IV.24 and IV.25). Cellobiose was not utilized by the *C. utilis* culture for its growth . All the biomass was apparently produced at the expense of primary glucose only . This fact is confirmed

by comparing the cell concentrations of *C. utilis* in this experiment to the experiment where glucose was the sole carbon source (Figure IV.21) . The resulting final biomass concentration was 14.382 g/l for *C. utilis* grown on 30 g/l glucose as the only carbon source, while it was 7.63 g/l when 15.5 g/l glucose was combined with 15.5 g/l cellobiose . In the first case, the cell yield is approximately equal to 45% (g cell/ g glucose), while for *C. utilis* grown on a medium containing a 1 : 1 mixture of glucose and cellobiose, the cell yield was experimentally determined to be 48% (g cell/g primary glucose).

The experimental data showed that the rate of heat release and the rate of oxygen consumption depend on the type of organism and substrate used . The highest volumetric peak rate of heat released was observed to be 10.196 kcal/l.h for the growth of *E.coli* cultivated on a 1 : 1 mixture of glucose and lactose . The lowest peak volumetric peak rate of heat released for any culture examined was 2.641 kcal/l.h for *A.niger* grown on glucose . However, when the rate of heat released was represented as kcal/g cell.h , the result was different . The lowest peak rate of heat release was 0.512 kcal/g cell.h for the growth of *C. utilis* on glucose . The highest peak rate of heat release was 1.822 kcal/g cell.h for *E. coli* grown on glucose only . During the yeast-hydrocarbon and yeast-carbohydrate fermentations, the range of variation in the maximum rate of heat release was between 0.512 and 1.215 kcal/g cell.h . The maximum peak rate of heat release was higher for the bacterial culture than for the yeast culture . These values were 1.38 and 1.822 kcal/g cell.h for *E. coli* grown on a

1 : 1 mixture of glucose and lactose , and glucose respectively . The maximum rate of heat release for the mold culture was smaller than that for the yeast culture. The value of 0.60 kcal/g cell.h was observed for *A. niger* grown on glucose . In general, the cultures that exhibited the highest rate of heat production, in descending order, were : bacteria, yeast, and mold .

The maximum rate of oxygen consumption by the growing culture was also observed to be dependent on the type of organism and substrate used . The maximum rate of oxygen consumption by the growing culture varied from 4.36 to 13.32 mmol O_2/g cell.h for the growth of *C. utilis* on glucose and ethanol respectively .

Table IV.10 summarizes the maximum values of the rate of heat release and the rate of oxygen consumption for all microbial cultures examined in this study

1 : Dynamic Calorimetry

N.B. The Experimental Data for C. utilis grown on Glucose obtained by the Dynamic Calorimetry were not shown in this Table since the biomass concentration for this experiment were not taken.

TABLE IV.10

MAXIMUM VALUES OF THE RATE OF HEAT RELEASED AND THE RATE OF OXYGEN CONSUMED

Organism	Substrate	Maximum Rate of Heat Released		Maximum Rate of Oxygen Consumption	
		(kcal/l.h)	(kcal/g.h)	(mmol /l.h)	(mmol /g.h)
A. niger[1]	Glucose	2.641	0.60	28.725	6.53
A. niger	Glucose	3.297	-	31.339	-
C. intermedia	Glucose	3.444	1.125	24.939	8.797
E. coli	Glucose	6.925	1.822	48.448	12.749
E. coli	Glucose & Lactose	10.196	1.38	83.287	11.255
C. lipolytica	Glucose	3.469	0.598	35.973	6.20
C. lipolytica	n-Dodecane	5.598	0.888	51.429	8.163
C. lipolytica	Hexadecane	7.487	0.913	60.044	7.322
C. utilis	Glucose	7.085	0.512	64.380	4.359
C. utilis	Sucrose	3.221	0.767	31.303	7.453
C. utilis	Ethanol	6.923	1.442	63.918	13.32
C. utilis	Glucose & Cellobiose	7.410	0.972	51.278	6.727

1. Dynamic Calorimetry

Figure IV.11 Rate of Heat Production, Oxygen Uptake Rate, and Biomass Concentration for A. niger grown on Glucose

- Dynamic Calorimetry

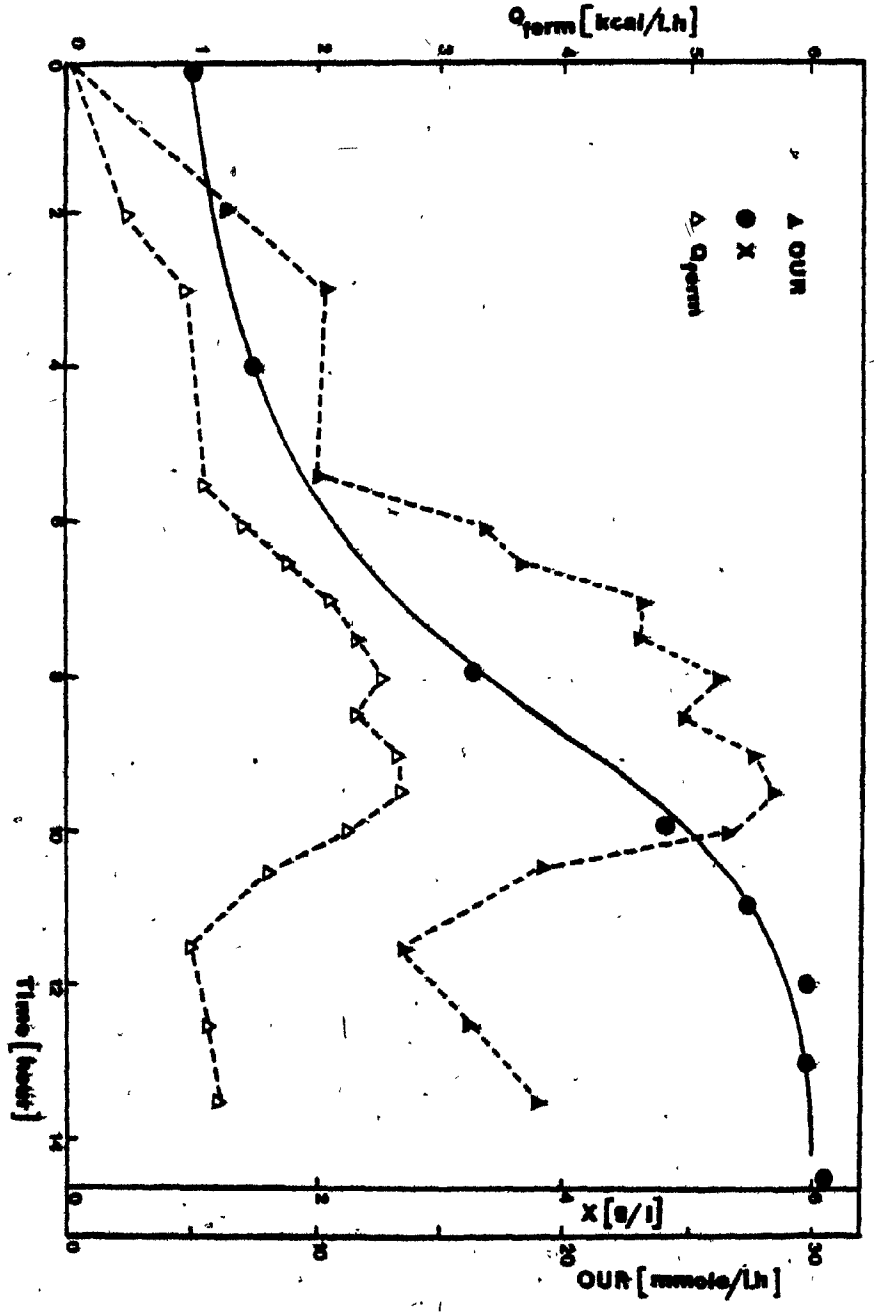
Q_{form} [kcal/l.h]
OUR
X
Q_{form}
Time [hours]
X [g/l]
OUR [mmole/l.h]

Figure IV.12 Rate of Heat Production and Oxygen Uptake Rate for *A. niger* grown on Glucose

- Dynamic Calorimetry

N.B. The Biomass Concentration data were not taken for this experiment

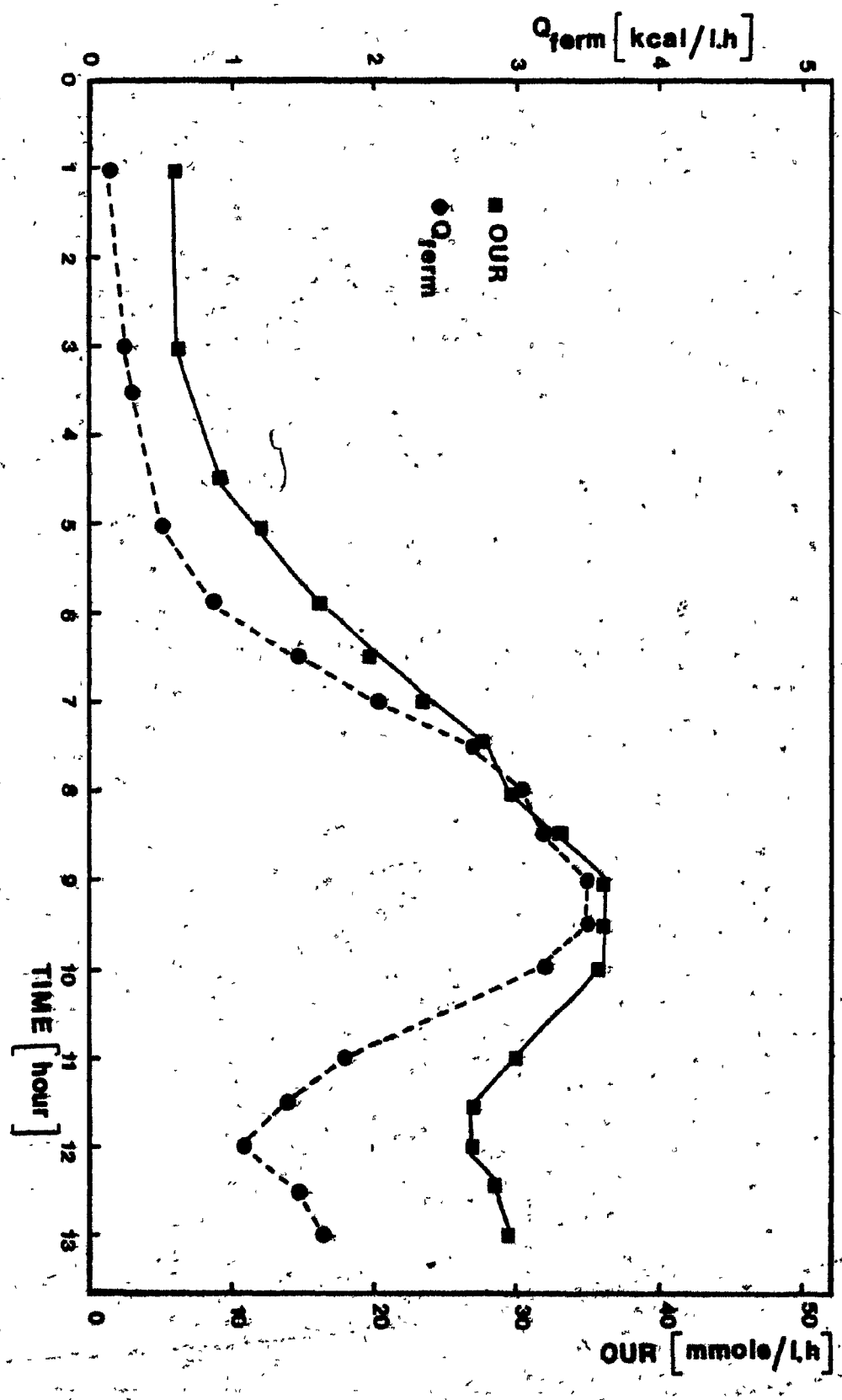
Q_{ferm} [kcal/l.h]
0
1
2
3
4
5
■ OUR
● Q_{ferm}
TIME [hour]
0
1
2
3
4
5
6
7
8
9
10
11
12
13
0
10
20
30
40
50
OUR [mmole/l.h]

Figure IV.13 Rate of Heat Production, Oxygen Uptake Rate, and Biomass Concentration for A. niger grown on Glucose

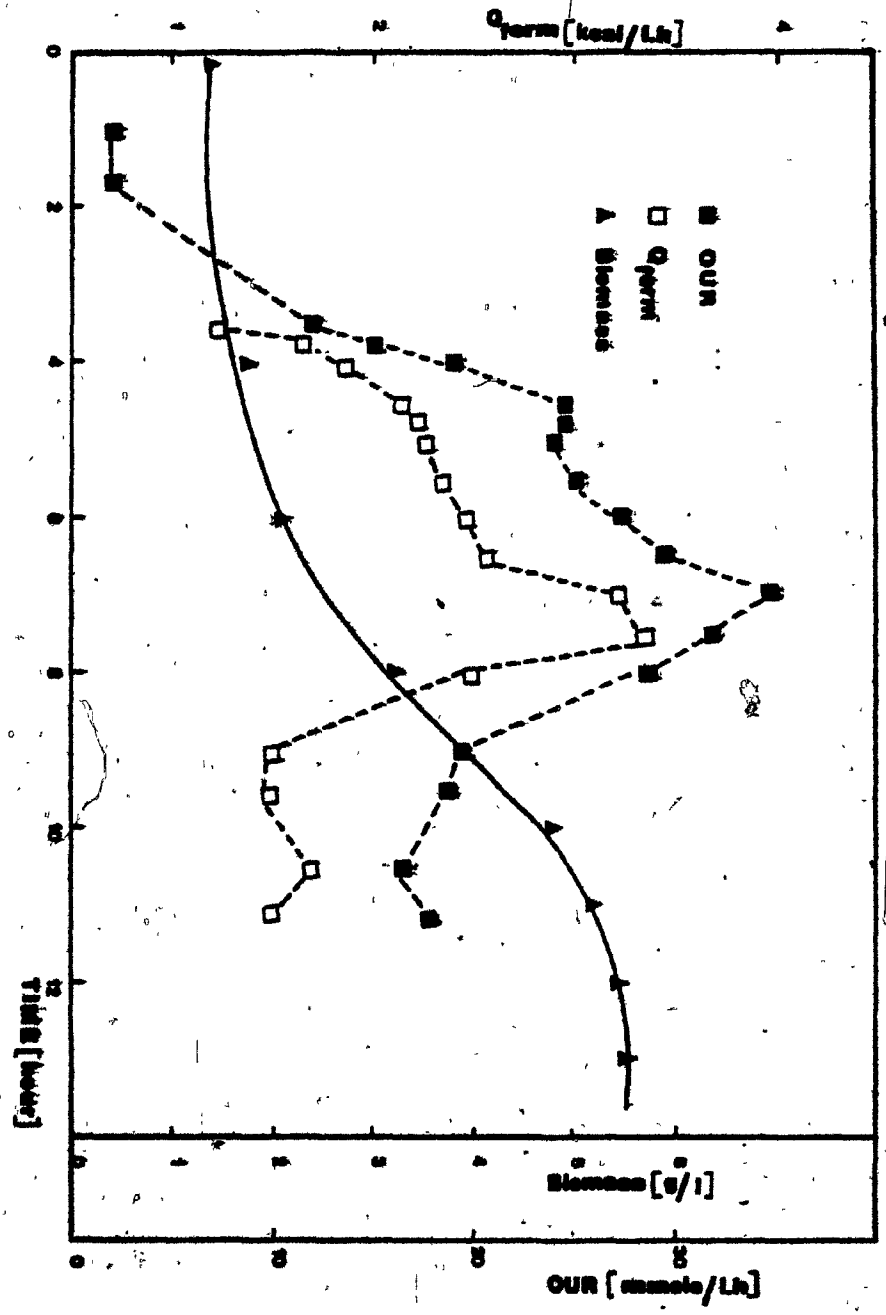
Q_{Term} [kcal/Lh]
OUR
Q_{Term}
Biomass
Time [hours]
Biomass [g/l]
OUR [mmole/Lh]

Figure IV.14 Rate of Heat Production, Oxygen Uptake Rate, and Biomass Concentration for C. intermedia grown on Glucose

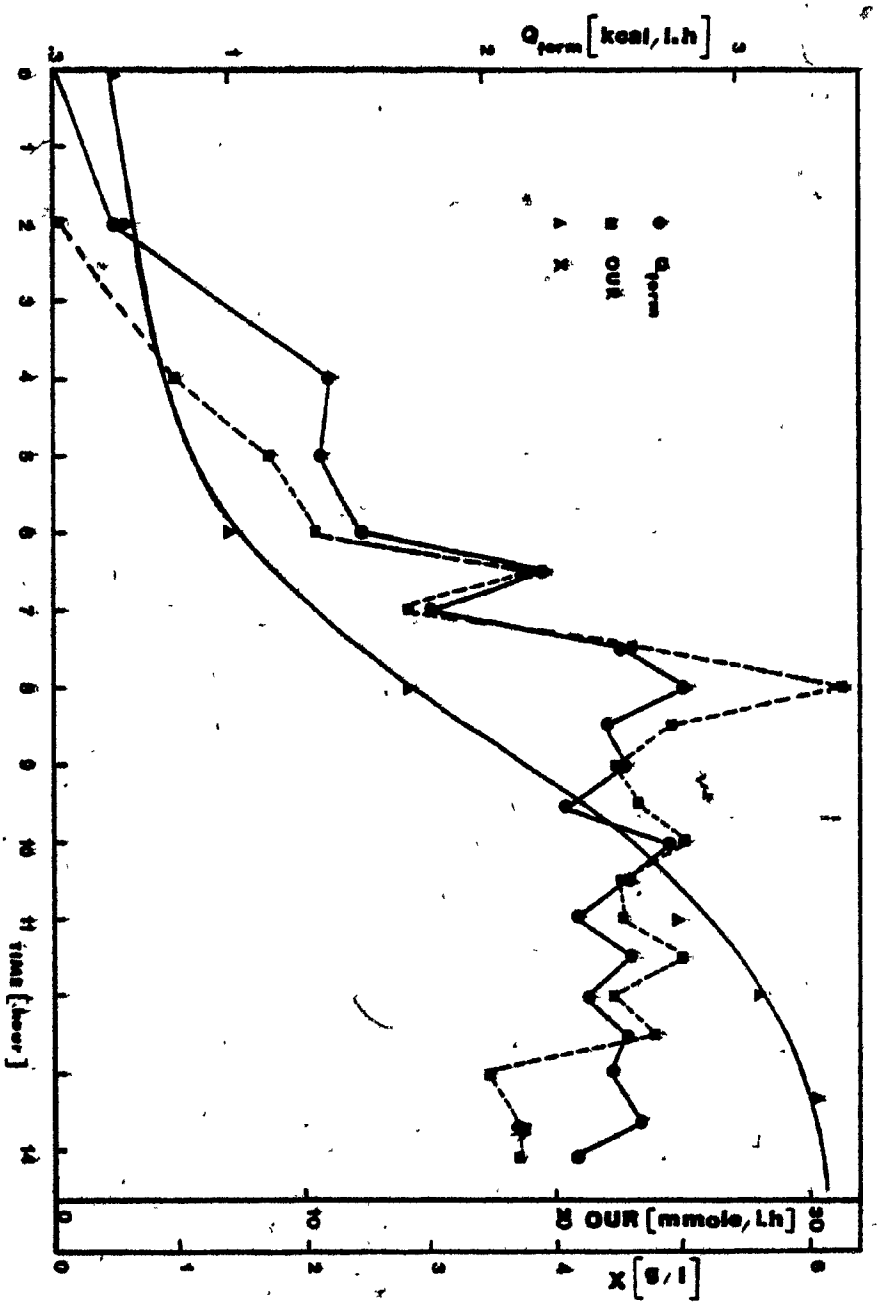
Q_{therm} [kcal/l.h]
Q_{therm}
OUR
time [hour]
OUR [mmole/l.h]
X [g/l]

Figure IV.15 Rate of Heat Production, Oxygen Uptake Rate, and Biomass Concentration for E. coli grown on Glucose

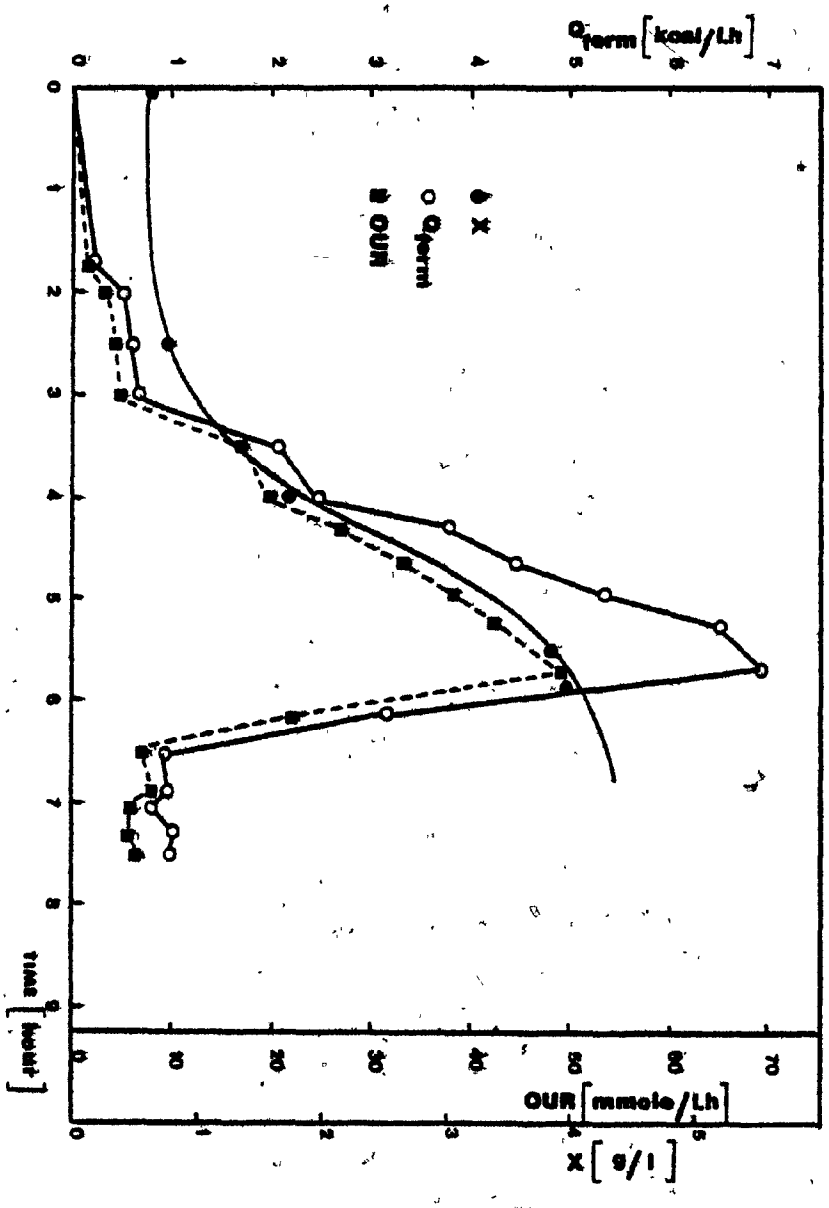
Q_{term} [kcal/Lh]
X
Q_{term}
OUR
time [hours]
OUR [mmole/Lh]
X [g/l]

Figure IV.16 Rate of Heat Production, Oxygen Uptake Rate, Carbon Dioxide Production Rate , Biomass Concentration, and Glucose Concentration for E. coli grown on a 1 : 1 Mixture of Glucose and Lactose

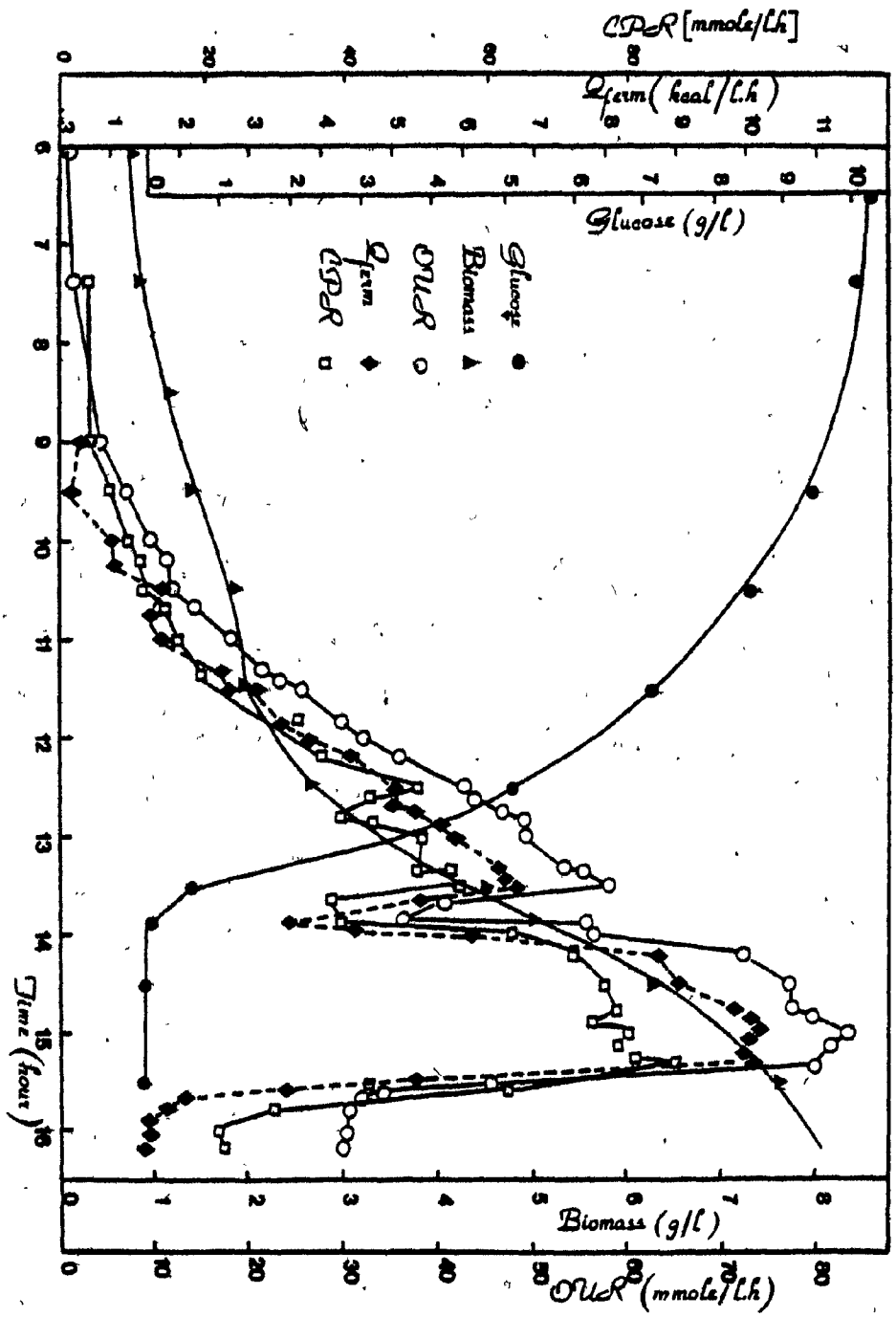
CPR [mmole/l.h]
Q_term (kcal/l.h)
Glucose (g/l)
Glucose
Biomass
OUR
Q_term
CPR
Time (hour)
Biomass (g/l)
OUR (mmole/l.h)

Figure IV.17 Rate of Heat Production, Oxygen Uptake Rate, and Biomass Concentration for C. lipolytica grown on Glucose

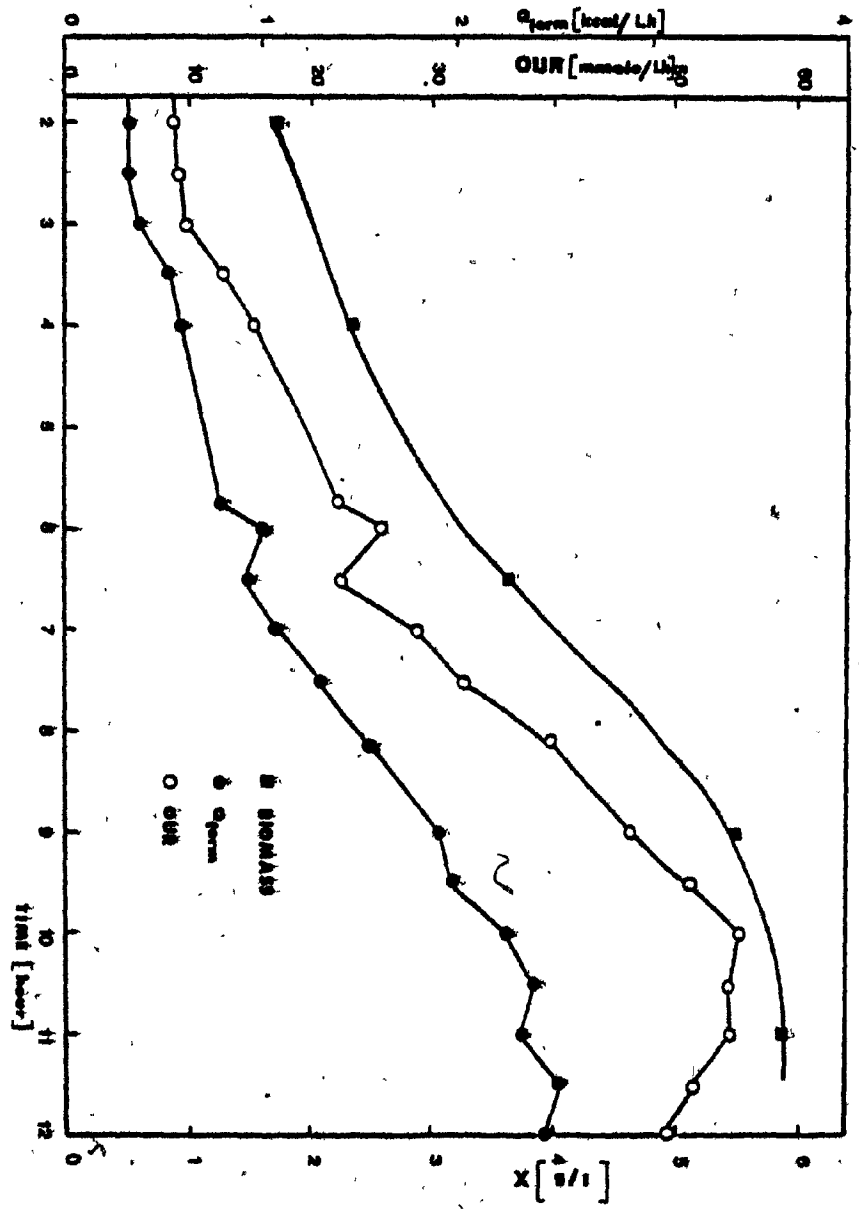
Q_{form} [kcal/ Lh]
OUR [mmole/ Lh]
BIOMASS
Q_{form}
OUR
time [hour]
X [g/l]

Figure IV.18 Rate of Heat Production , Oxygen Uptake Rate, and Biomass Concentration for C. lipolytica grown on n-Dodecane

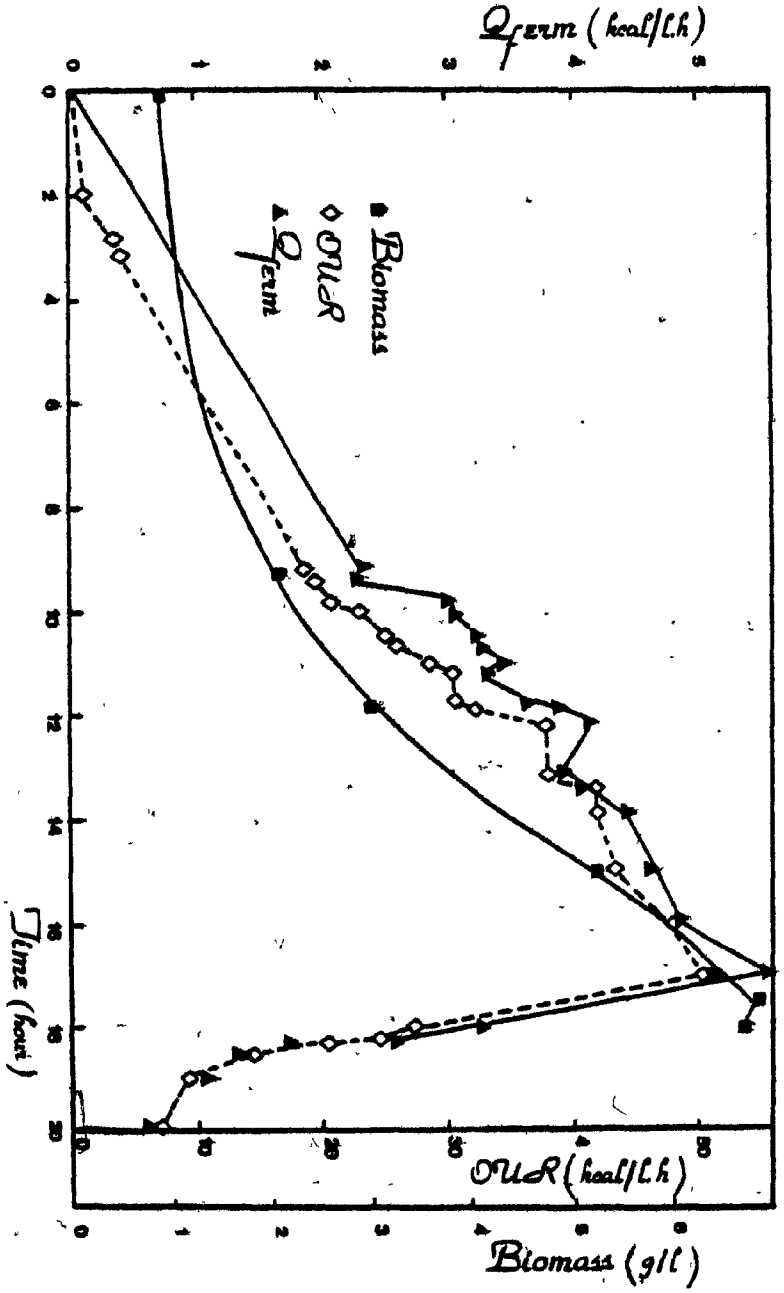
Qferm (kcal/l.h)
Biomass
OUR
Qferm
Time (hour)
OUR (kcal/l.h)
Biomass (g/l)

Figure IV.19 Rate of Heat Production, Oxygen Uptake Rate, and Biomass Concentration for C. lipolytica grown on Hexadecane

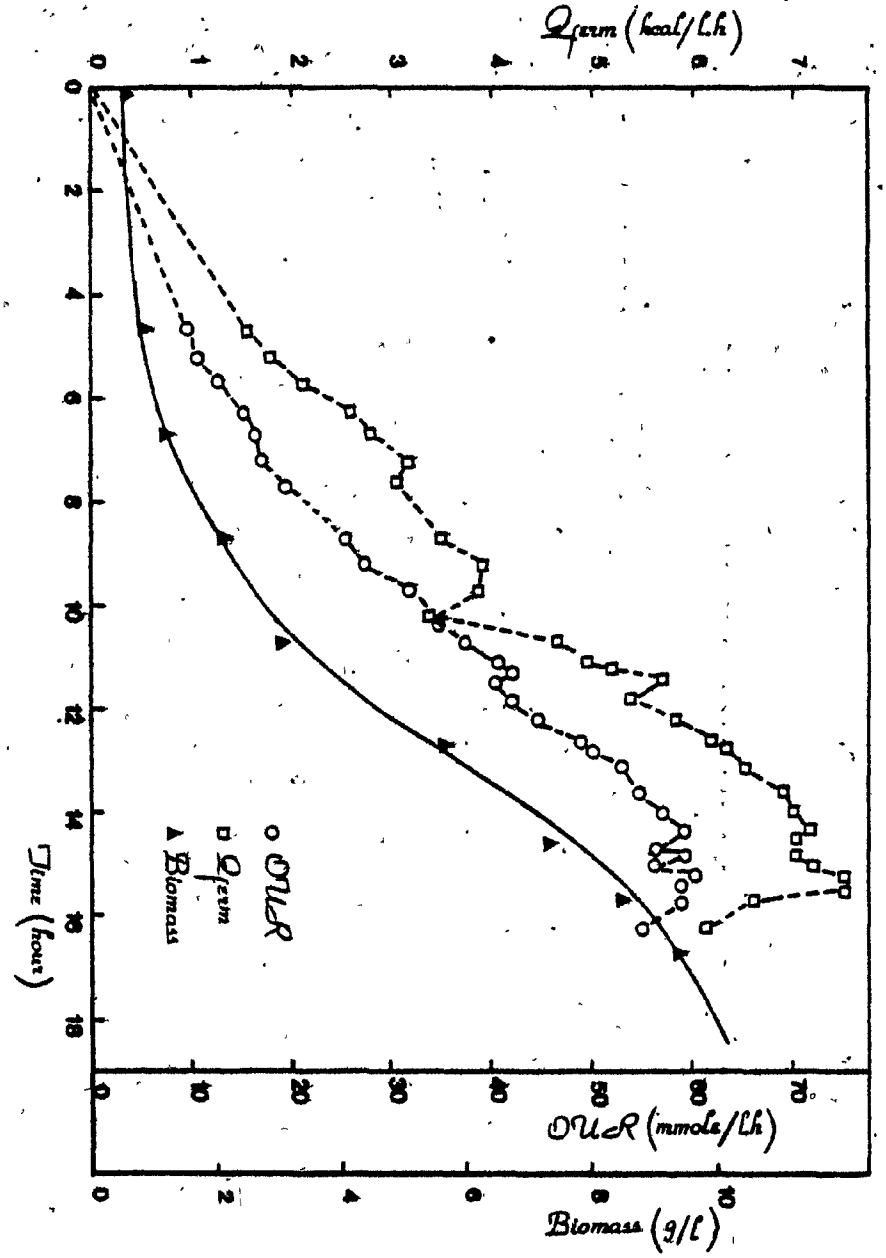
Qgerm (kcal/l.h)
Time (hour)
OUR
Qgerm
Biomass
OUR (mmole/l.h)
Biomass (g/l)

Figure IV.20 Rate of Heat Production and Oxygen Uptake Rate for *C. utilis* grown on Glucose (Dynamic Calorimetry)

N.B. The biomass concentration data were not taken for this experiment

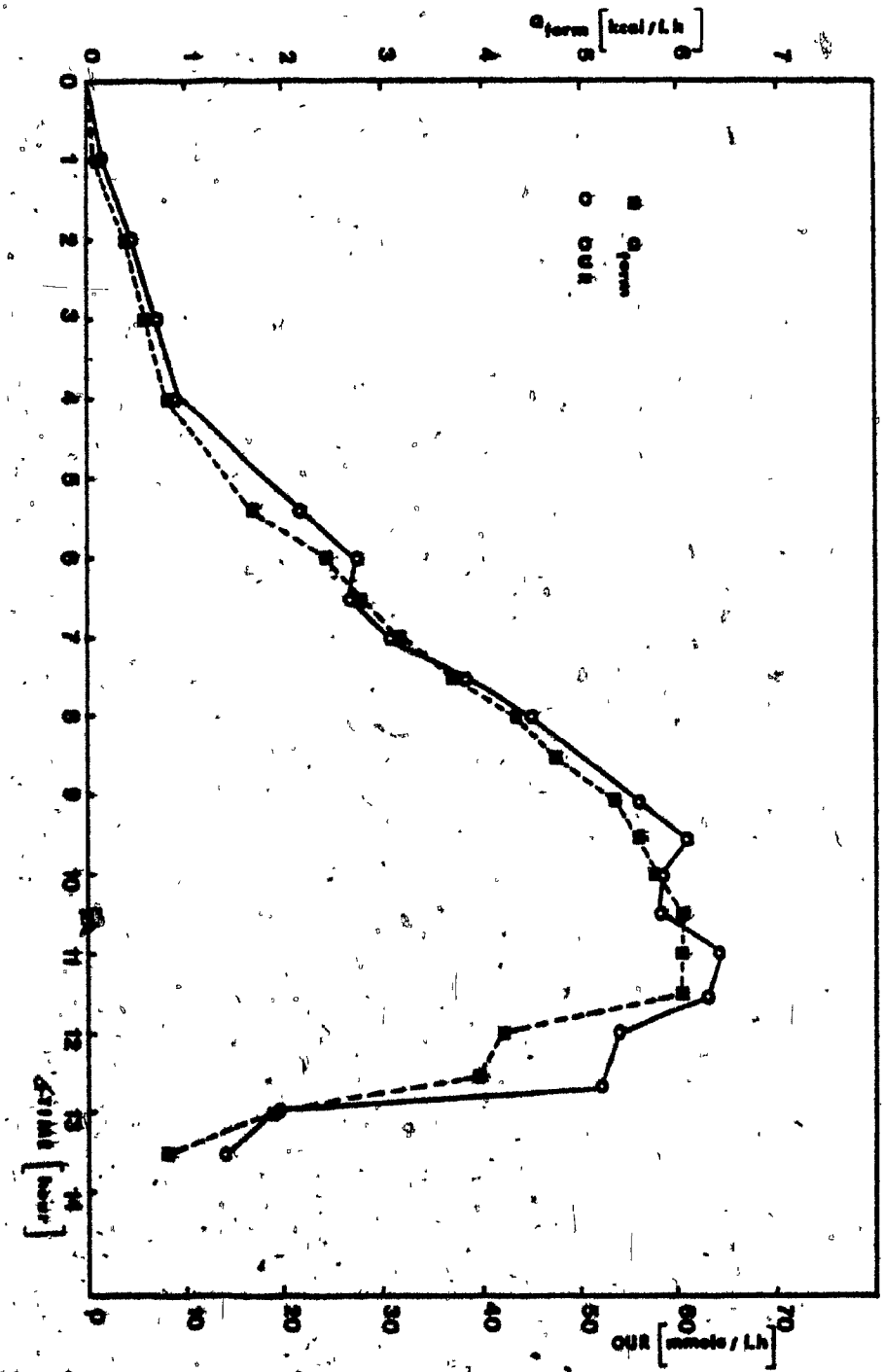
Q_{form} [kcal/L.h]
0
1
2
3
4
5
6
7
8
9
10
11
12
13
14
Q_{form}
Q_{cons}
OUR [mmole/L.h]
0
10
20
30
40
50
60
70
Cell mass [kg/m³]

Figure IV.21 Rate of Heat Production, Oxygen Uptake Rate, and Biomass Concentration for C. utilis grown on Glucose

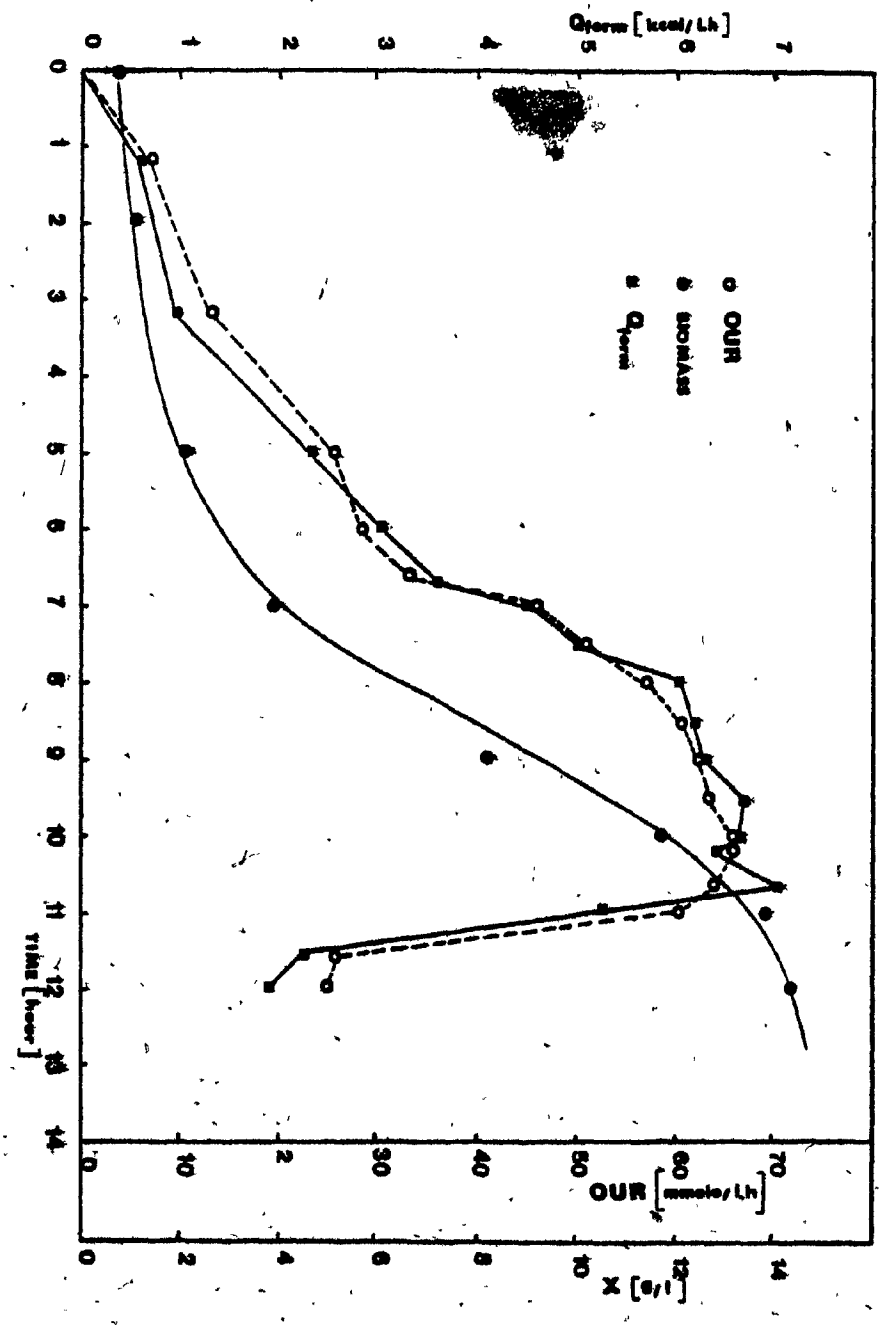
Q_{form} [kcal/ Lh]
o OUR
● BIOMASS
■ Q_{form}
TIME [hour]
OUR [mmole/ Lh]
X [g/l]

Figure IV.22 Rate of Heat Production, Oxygen Uptake Rate, and Biomass Concentration for C. utilis grown on Sucrose

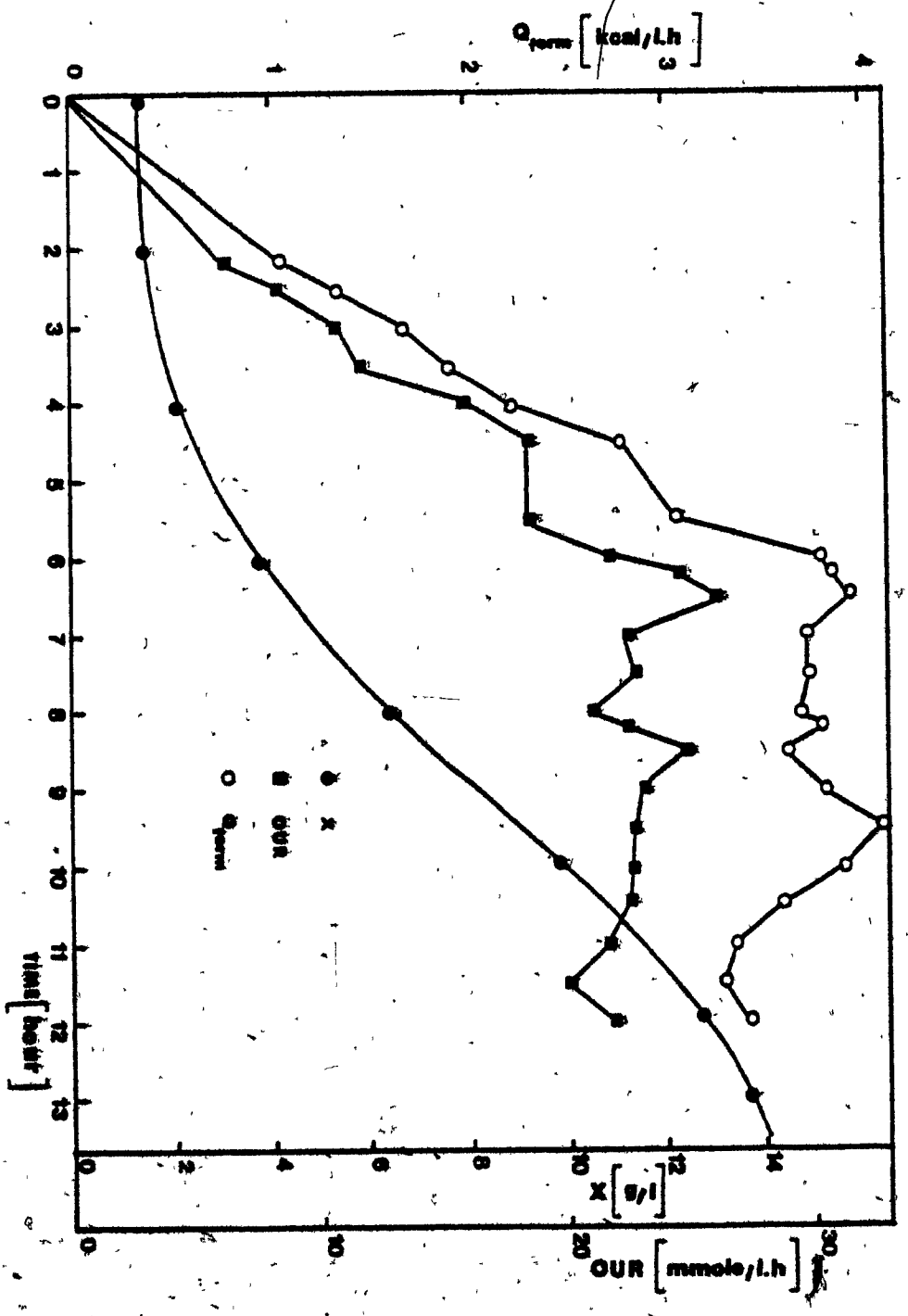
Q_{term} [kcal/l.h]
time [hour]
X [g/l]
OUR [mmole/l.h]
X
OUR
Q_{term}

Figure IV.23 Rate of Heat Production, Oxygen Uptake Rate, and Biomass Concentration for C. utilis grown on Ethanol

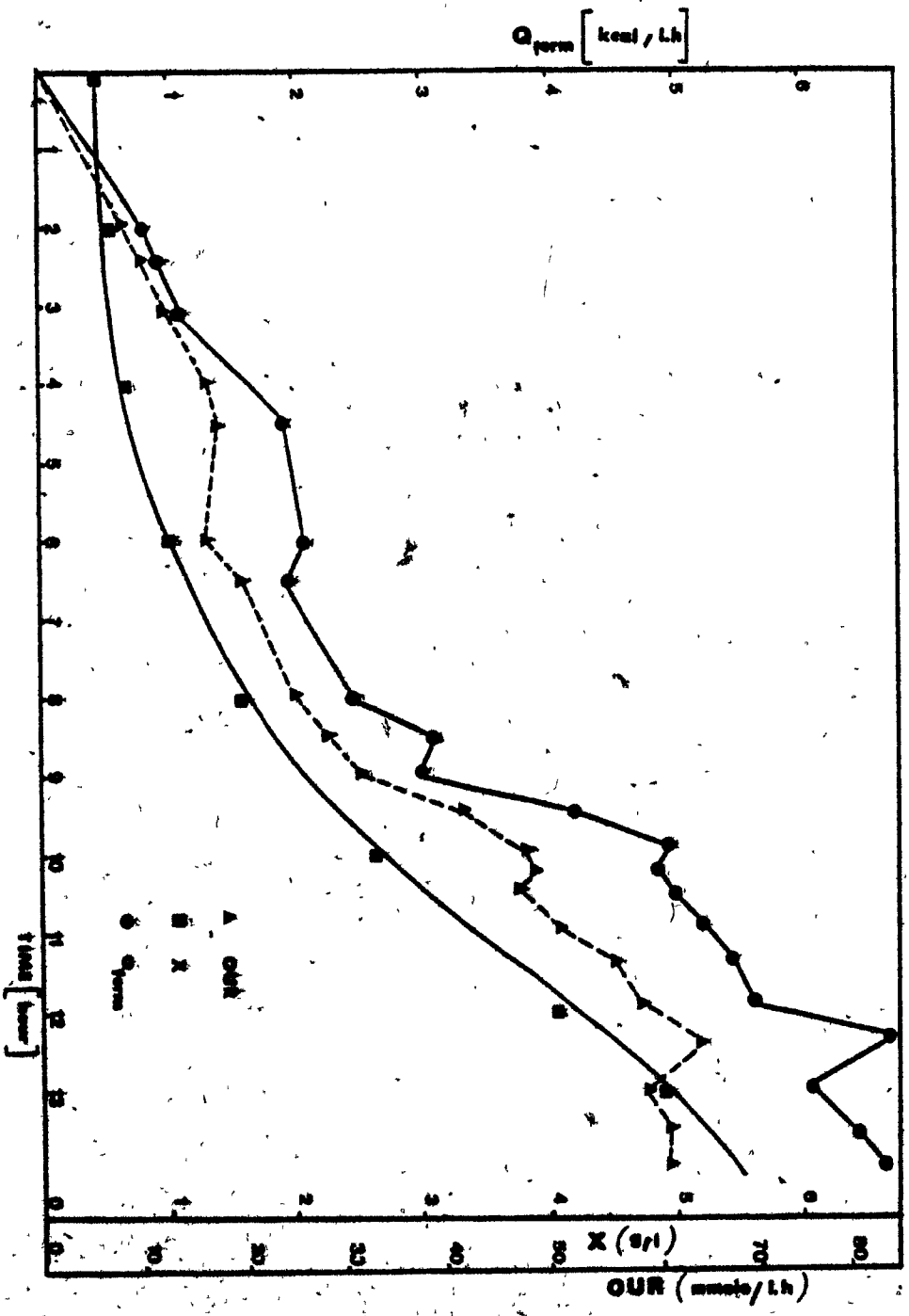
Q_{form} [kcal / l.h]
time [hour]
Q_{form}
X
OUR
X (g/l)
OUR (mmole/l.h)

Figure IV.24 Rate of Heat Production, Oxygen Uptake Rate, Biomass Concentration, and Glucose Concentration for C. utilis Grown on a 1 : 1 mixture of Glucose and Cellobiose

- Total Sugar Concentration : 30 g/l

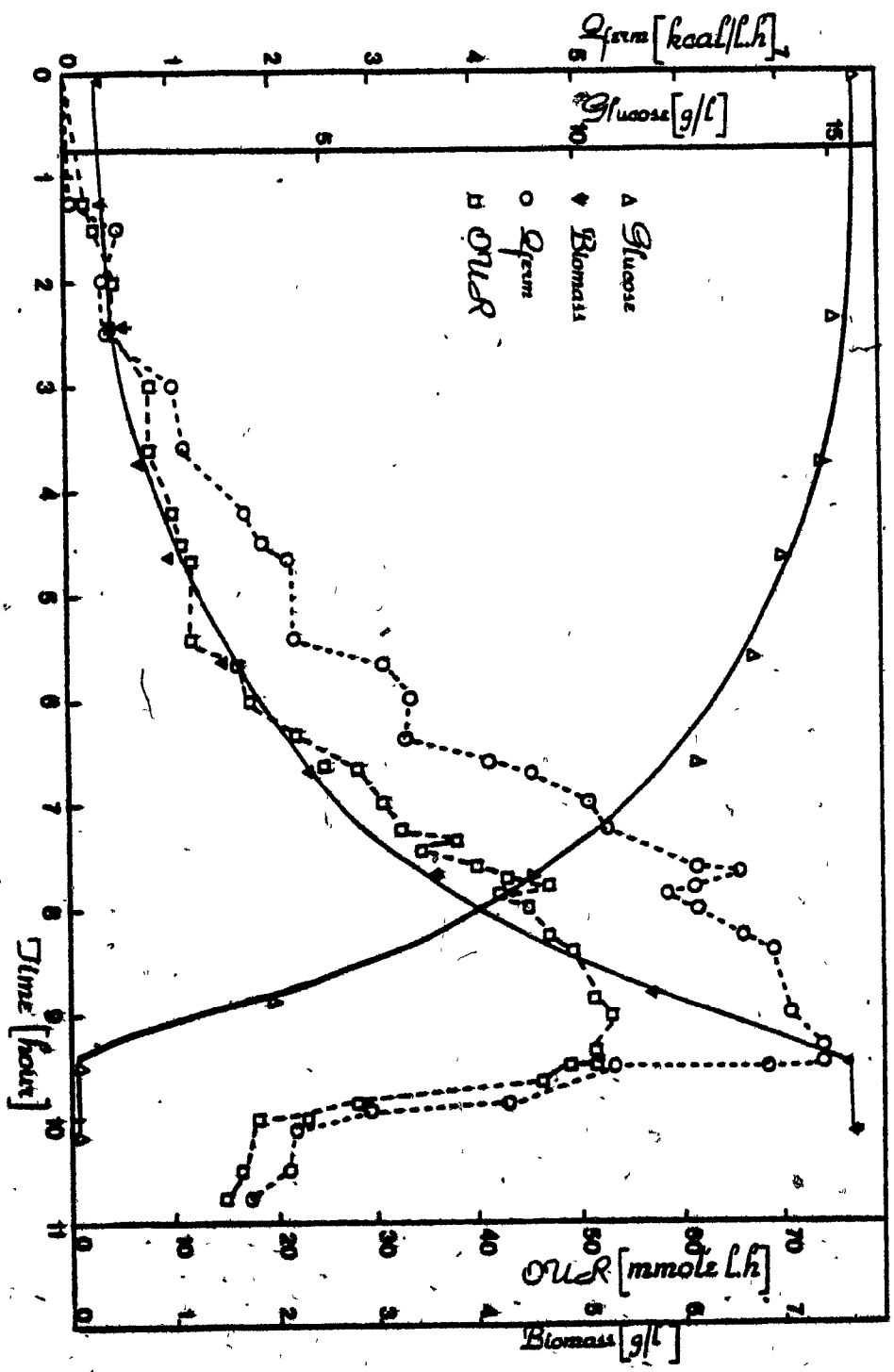
Qterm [kcal/l.h]
Glucose [g/l]
Glucose
Biomass
Qterm
OUR
Time [hour]
OUR [mmole/l.h]
Biomass [g/l]

Figure IV.25 Oxygen Uptake Rate, Biomass Concentration, and Glucose Concentration for C. utilis grown on 1 : 1 mixture of Glucose and Cellobiose

- Total Initial Sugar Concentration : 15 g/l

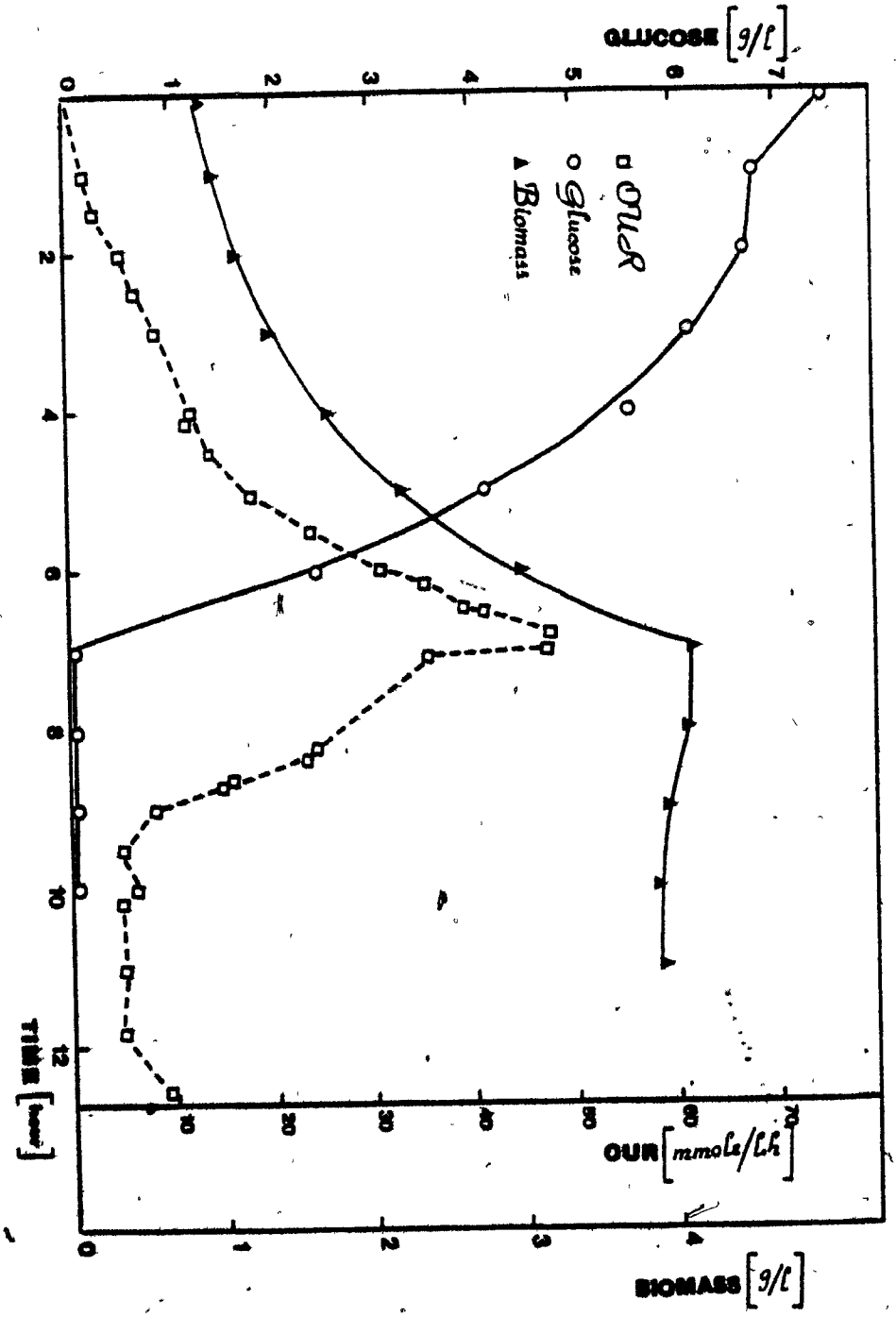
GLUCOSE [g/l]
OUR
Glucose
Biomass
TIME [hour]
OUR [mmole/l.h]
BIOMASS [g/l]

H. CORRELATION OF OXYGEN CONSUMPTION WITH THE HEAT OF FERMENTATION FOR INDIVIDUAL EXPERIMENTS

For practical purposes a correlation between the rate of oxygen consumption and the rate of heat production during growth is desirable . When these two quantities were plotted against each other a linear relationship resulted. The values of ΔH_{fo} (the ratio between the rate of heat release and the rate of oxygen consumption) slightly differ according to the micro-organism used (Table IV.11) .

The lowest value of ΔH_{fo} = 0.0917 kcal/mmol O_2 was recorded for *A. niger* grown on glucose while the highest ΔH_{fo} = 0.143 kcal/mmol O_2 was observed in *C. utilis* grown on a 1 : 1 mixture of glucose and cellobiose. The proportionality constant ΔH_{fo} appears to be dependent on the type of growth substrate and the organism used . This ratio , however, is almost independent of the growth rate . The data taken at the end of some experiments exhibited a large deviation from the general trend (Figures IV.27 and IV.32) .

Diagrams correlating the rate of oxygen consumption and the rate of heat production during microbial growth of selected cultures are shown in rectlinear coordinates for the following strains :

Organism	Substrate	Figure
Aspergillus niger[1]	Glucose	IV.26
Aspergillus niger[2]	Glucose	IV.27
Aspergillus niger	Glucose	IV.28
Candida intermedia	Glucose	IV.30
Escherichia coli	Glucose	IV.31
Escherichia coli	Glucose & Lactose	IV.32
Candida lipolytica	Glucose	IV.33
Candida lipolytica	n-Dodecane	IV.34
Candida lipolytica	Hexadecane	IV.35
Candida utilis[1]	Glucose	IV.36
Candida utilis	Glucose	IV.37
Candida utilis	Sucrose	IV.39
Candida utilis	Ethanol	IV.40
Candida utilis	Glucose & Cellobiose	IV.41

1. Dynamic Calorimetry
2. Wall Growth

The slopes of the regression lines ranged from 0.0917 to 0.143 (kcal/mmol O_2) . When the values of the respective rates were plotted for all the experimental data obtained in this study regardless of the type of substrate, microbial species and effectiveness of cell growth, a straight line with a slope of 0.111 ± 0.02 kcal/mmol O_2 resulted (Figure IV.42) .

TABLE IV. 11

THE RELATIONSHIP BETWEEN THE RATE OF HEAT RELEASED AND THE RATE OF OXYGEN CONSUMED FOR INDIVIDUAL EXPERIMENTS

Mirco-organisms	Substrate	ΔH_{fo} (kcal/mmol O_2)
A.niger[1]	Glucose	0.092
A.niger	Glucose	0.092
A.niger[2]	Glucose	0.082
C.intermedia	Glucose	0.112
E.coli	Glucose	0.135
E.coli	Glucose & Lactose	0.121
C.lipolytica	Glucose	0.104
C.lipolytica	n-Dodecane	0.112
C.lipolytica	Hexadecane	0.135
C.utilis[1]	Glucose	0.094
C.utilis	Glucose	0.096
C.utilis	Sucrose	0.098
C.utilis	Ethanol	0.105
C.utilis	Glucose & Cellobiose	0.143

1. Dynamic Calorimetry
2. Wall Growth

Figure IV.26 The Rate of Heat Production versus the Oxygen Uptake Rate for A. niger grown on Glucose

- Dynamic Calorimetry
- Correlation Coefficient : 0.976

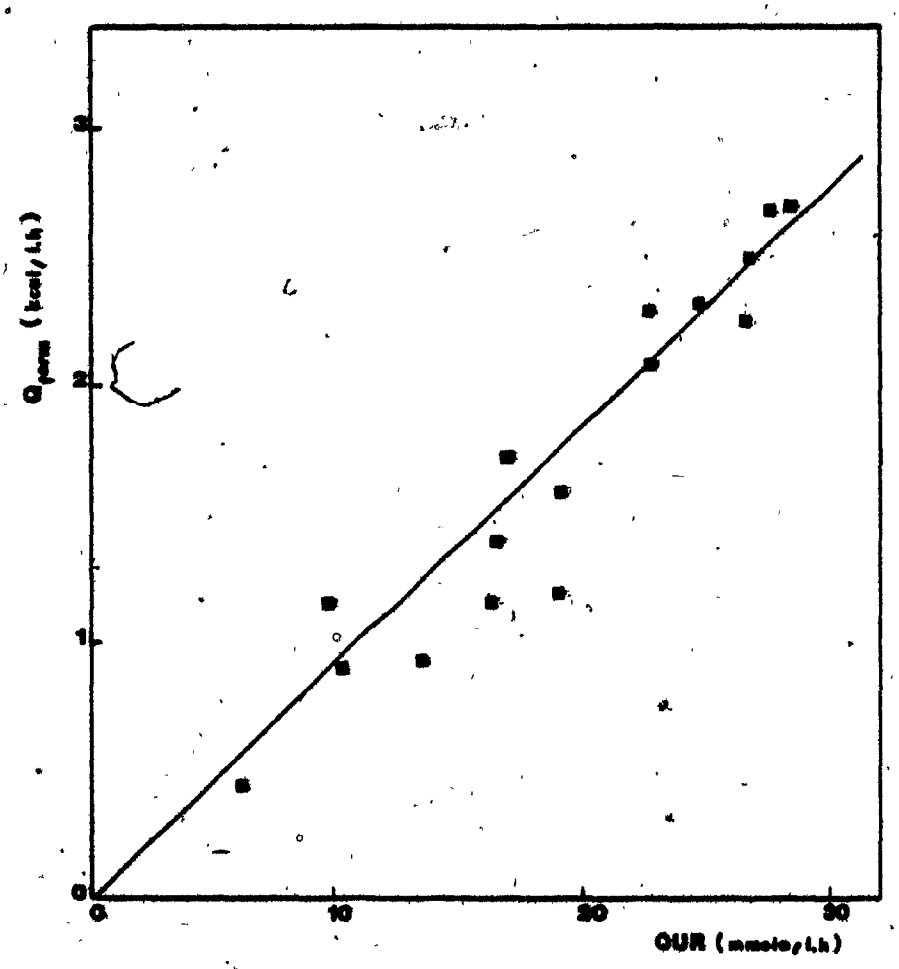
Q_{gross} (kcal/ l.h)
2
1
0
0
10
20
30
OUR (mmole/ l.h)

Figure IV.27 The Rate of Heat Production versus the Oxygen Uptake Rate for A. niger grown on Glucose

-Dynamic Calorimetry

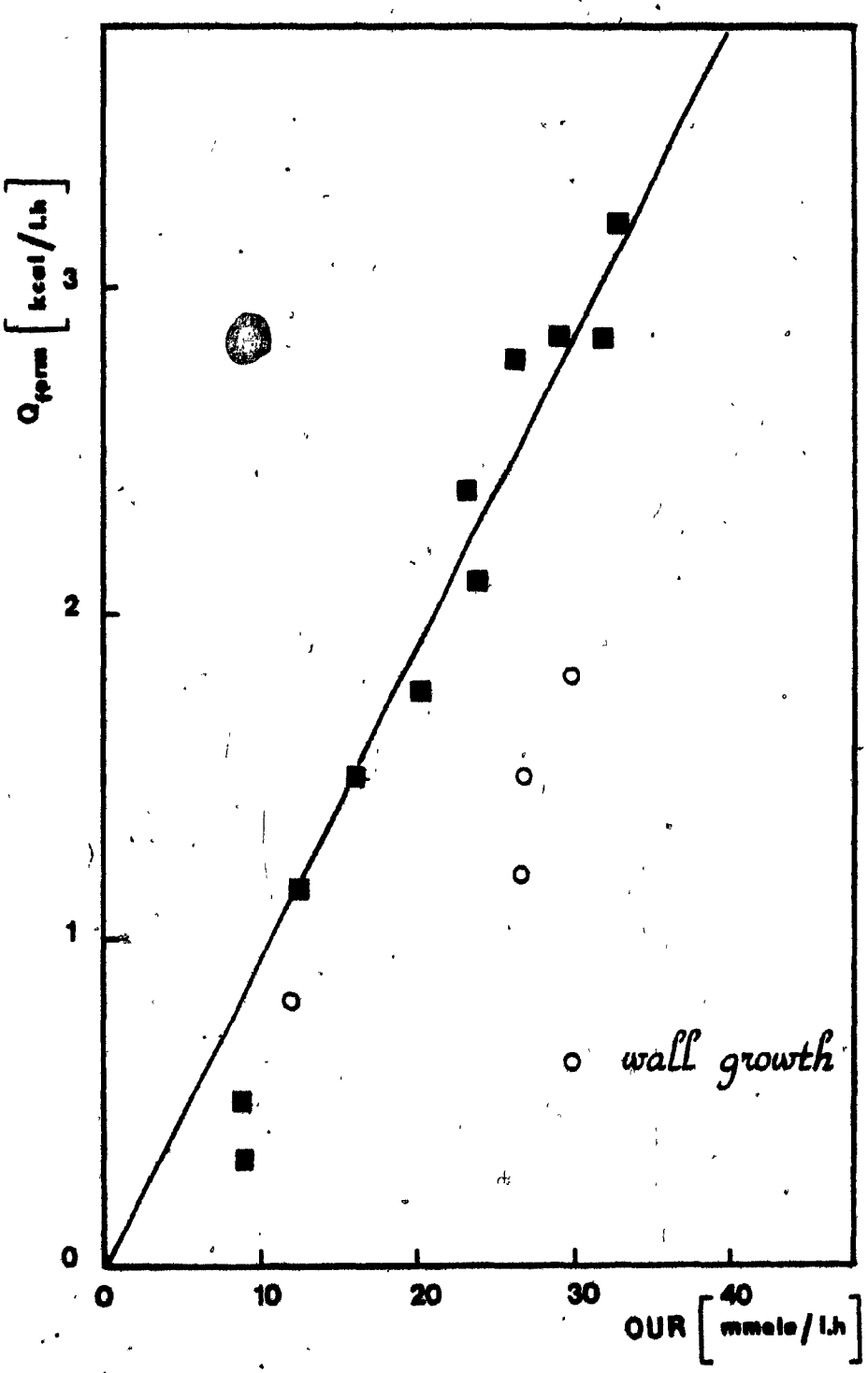
Q_{form} [kcal/l.h]
0
1
2
3
0
10
20
30
40
OUR [mmole/l.h]
wall growth

Figure IV.28 The Rate of Heat Production versus the Oxygen Uptake Rate for A. niger grown on Glucose

* Correlation Coefficient : 0.950

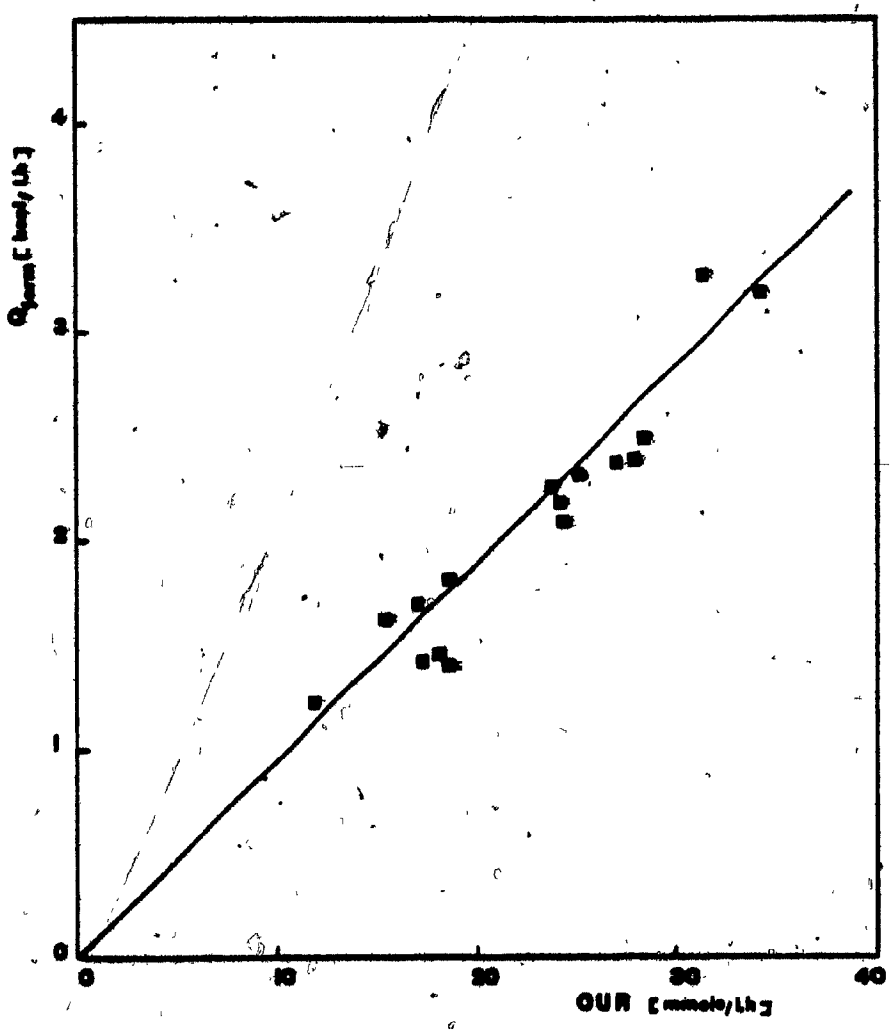
0
1
2
3
4
0
10
20
30
40
OUR [mmole/l.h]

Figure IV.29 The Rate of Heat Production versus the Oxygen Uptake Rate for A. niger grown on Glucose

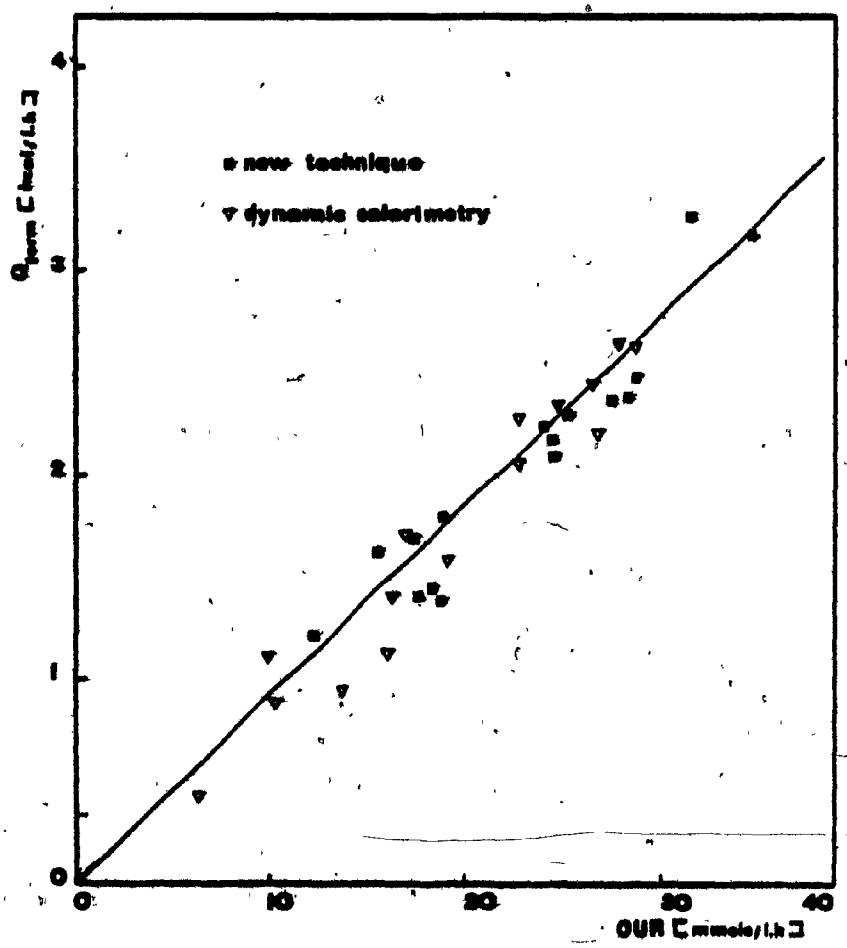
new technique
dynamic calorimetry
0
1
2
3
4
0
10
20
30
40
OUR (mmole/l.h)

Figure IV.30 The Rate of Heat Production versus the Oxygen Uptake Rate for C. intermedia grown on Glucose

* Correlation Coefficient : 0.973

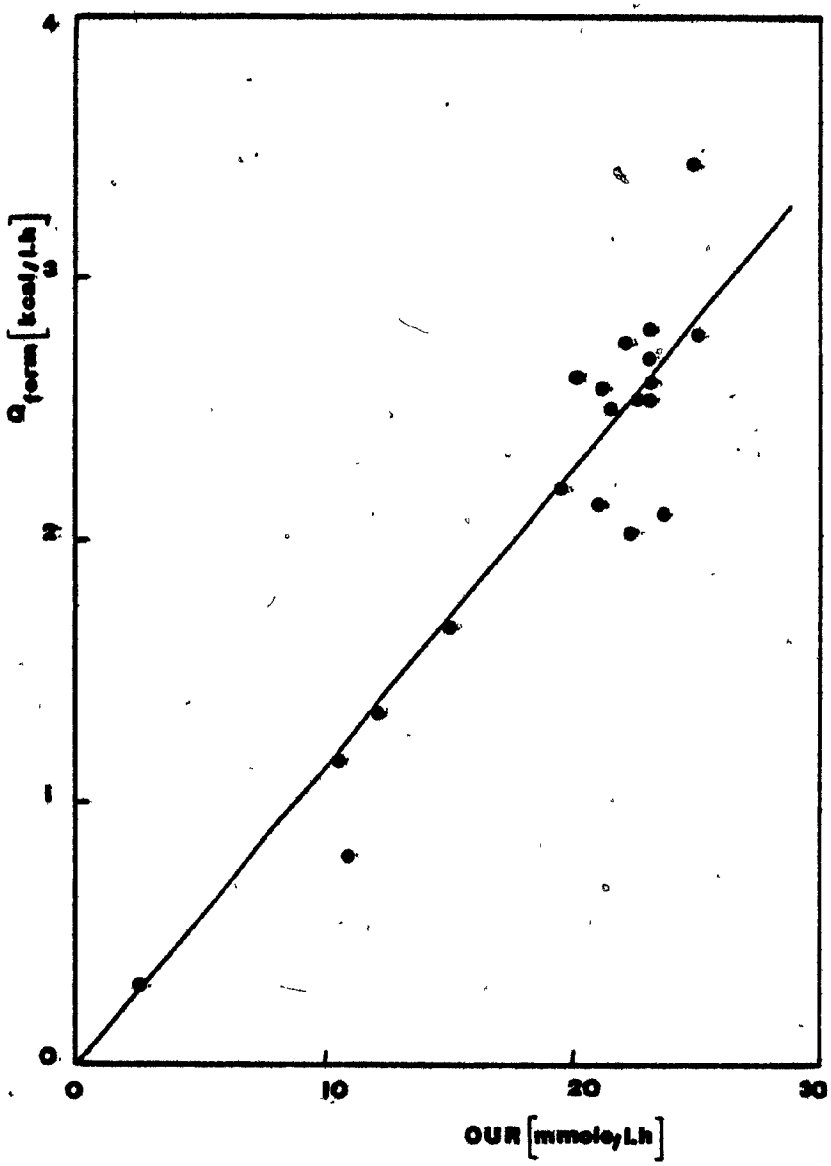
4
3
2
1
0
0
10
20
30
Q_{ferm} [kcal/L.h]
OUR [mmole/L.h]

Figure IV.31 The Rate of Heat Production versus the Oxygen Uptake Rate for *E. coli* grown on Glucose

* Correlation Coefficient : 0.996

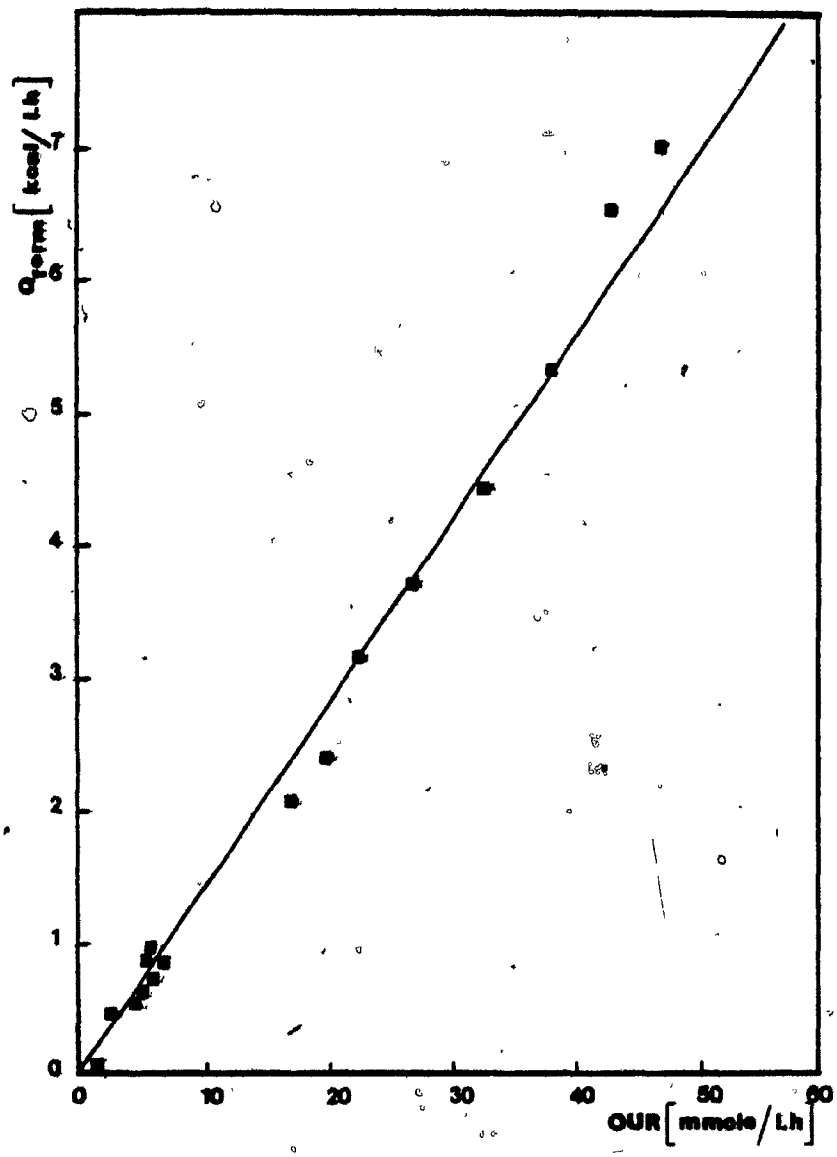
Q_{term} [kcal/ l.h]
0
1
2
3
4
5
6
0
10
20
30
40
50
60
OUR [mmole/ l.h]

Figure IV.32 The Rate of Heat Production versus the Oxygen Uptake Rate for E. coli grown on a 1 : 1 mixture of Glucose and Lactose

- Correlation Coefficient : 0.98

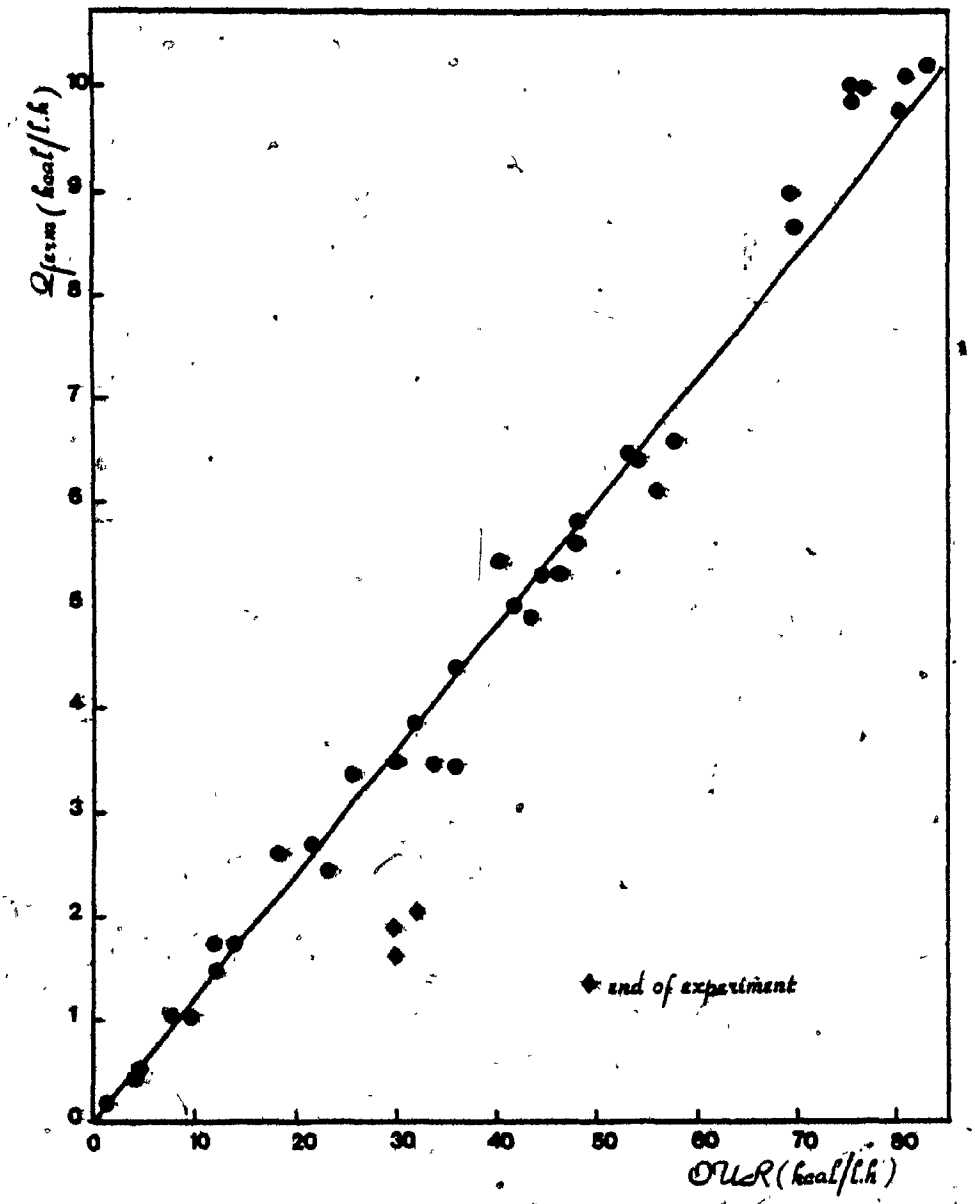
Q_{ferm} (kcal/l.h)
OUR (kcal/l.h)
0
10
20
30
40
50
60
70
80
1
2
3
4
5
6
7
8
9
end of experiment

Figure IV.33 The Rate of Heat Production versus the Oxygen Uptake Rate for C. lipolytica grown on Glucose

* Correlation Coefficient : 0.981

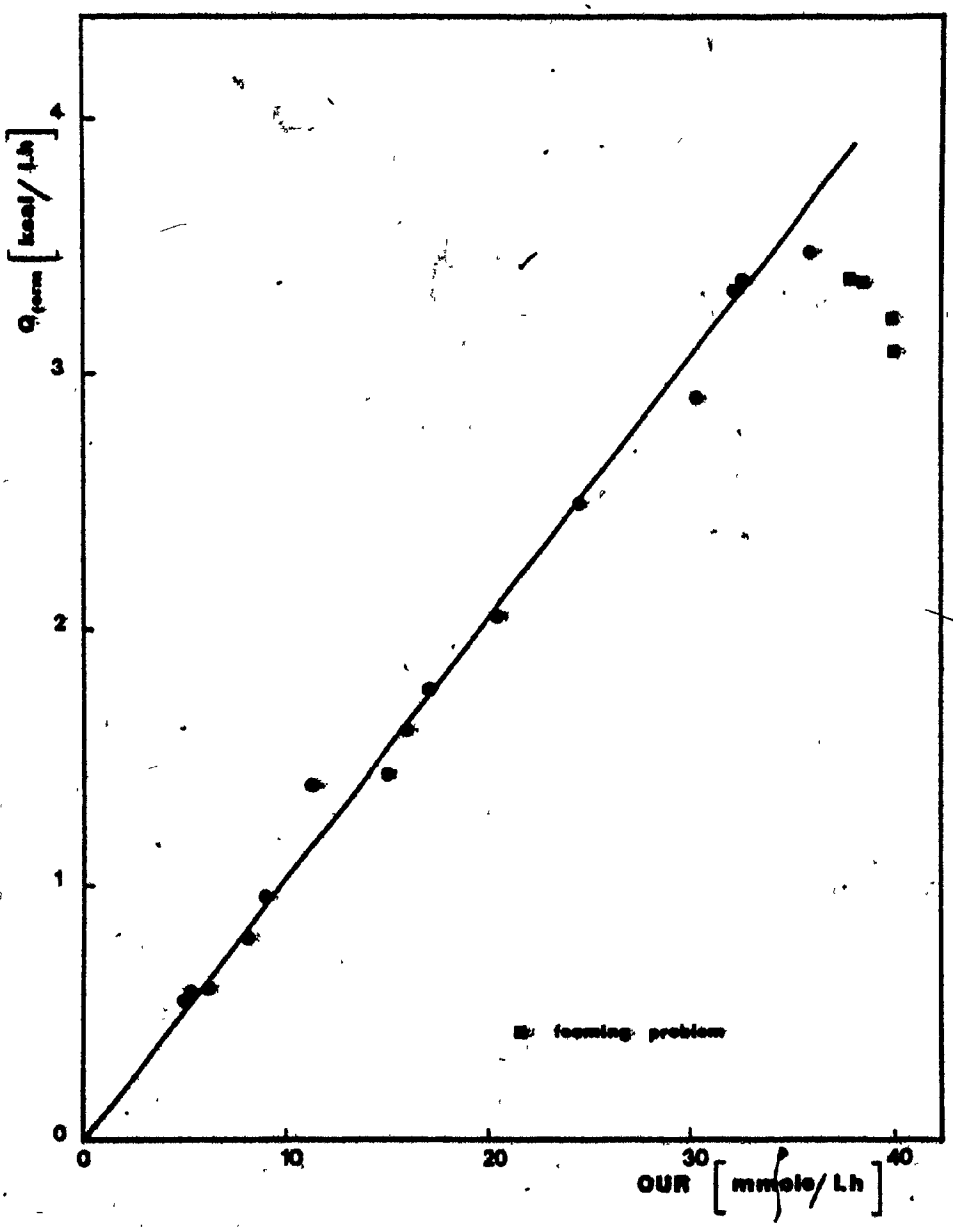
Q_{form} [kcal/ l.h]
0
1
2
3
0
10
20
30
40
OUR [mmole/ l.h]
foaming problem

Figure IV.34 The Rate of Heat Production versus the Oxygen Uptake Rate for C. lipolytica grown on n-Dodecane

* Correlation Coefficient : 0.967

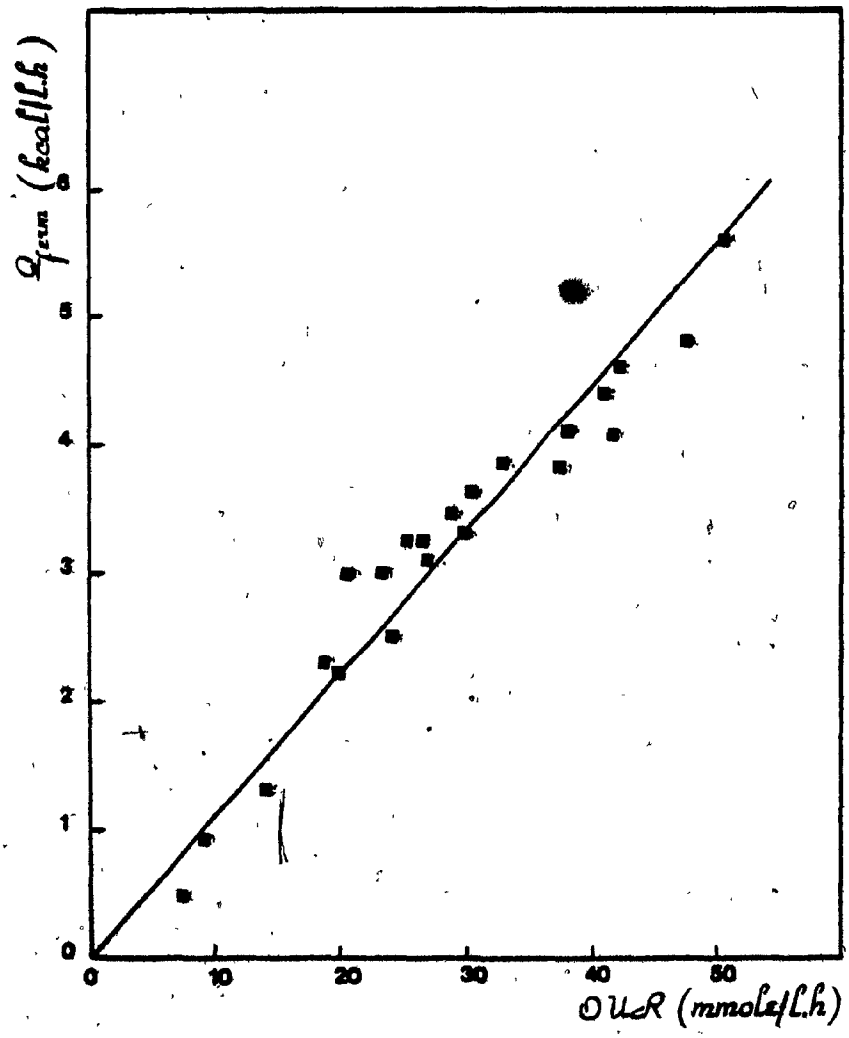
Q_{prod} (kcal/l.h)
0
1
2
3
4
5
6
0
10
20
30
40
50
OUR (mmole/l.h)

Figure IV.35 · The Rate of Heat Production versus the Oxygen Uptake Rate for C. lipolytica grown on Hexadecane

* Correlation Coefficient : 0.982

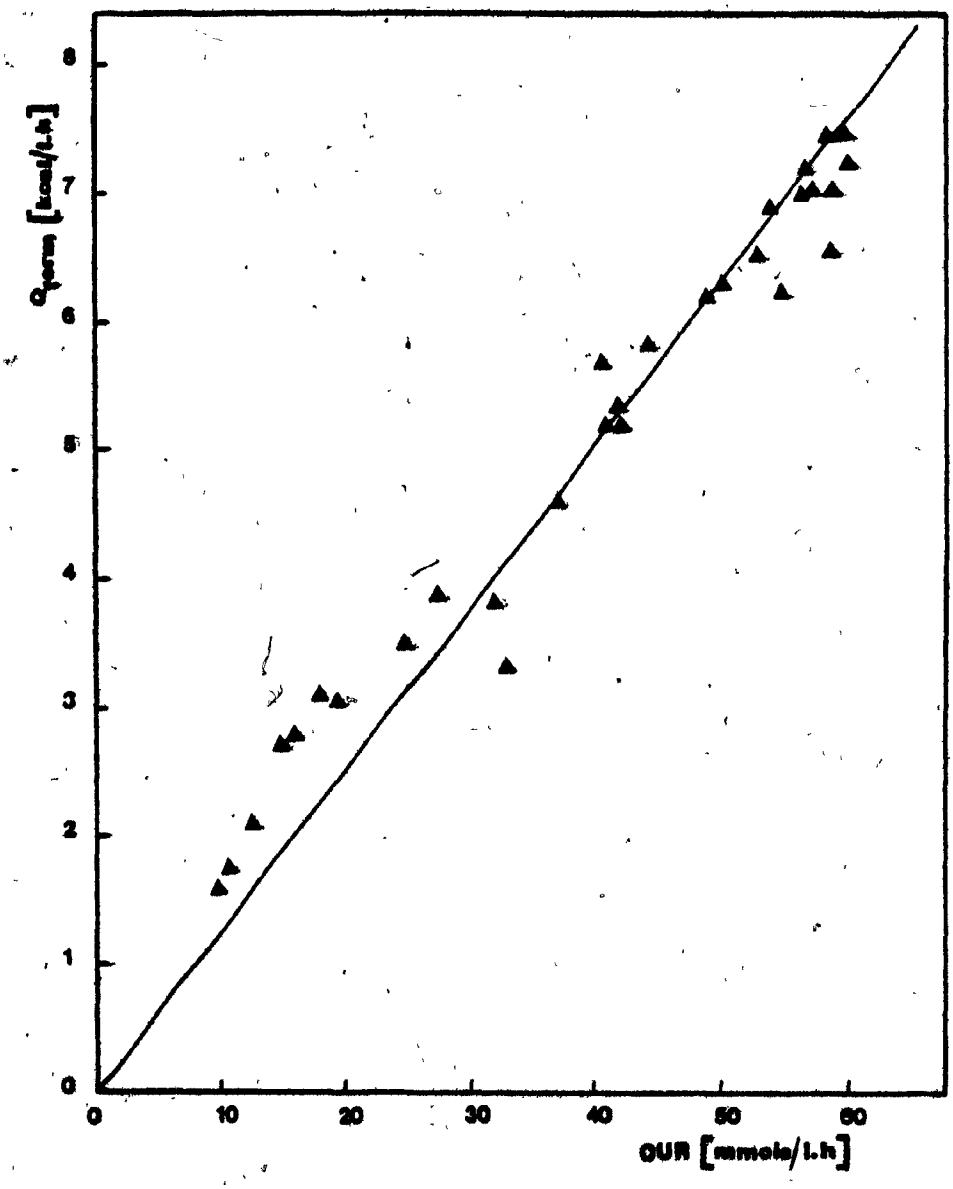
Q_{gross} [kcal/l.h]
0
1
2
3
4
5
6
7
8
0
10
20
30
40
50
60
OUR [mmole/l.h]

Figure IV.36 The Rate of Heat Production versus the Oxygen Uptake Rate for C. utilis grown on Glucose(Dynamic Calorimetry)

* Correlation Coefficient : 0.985

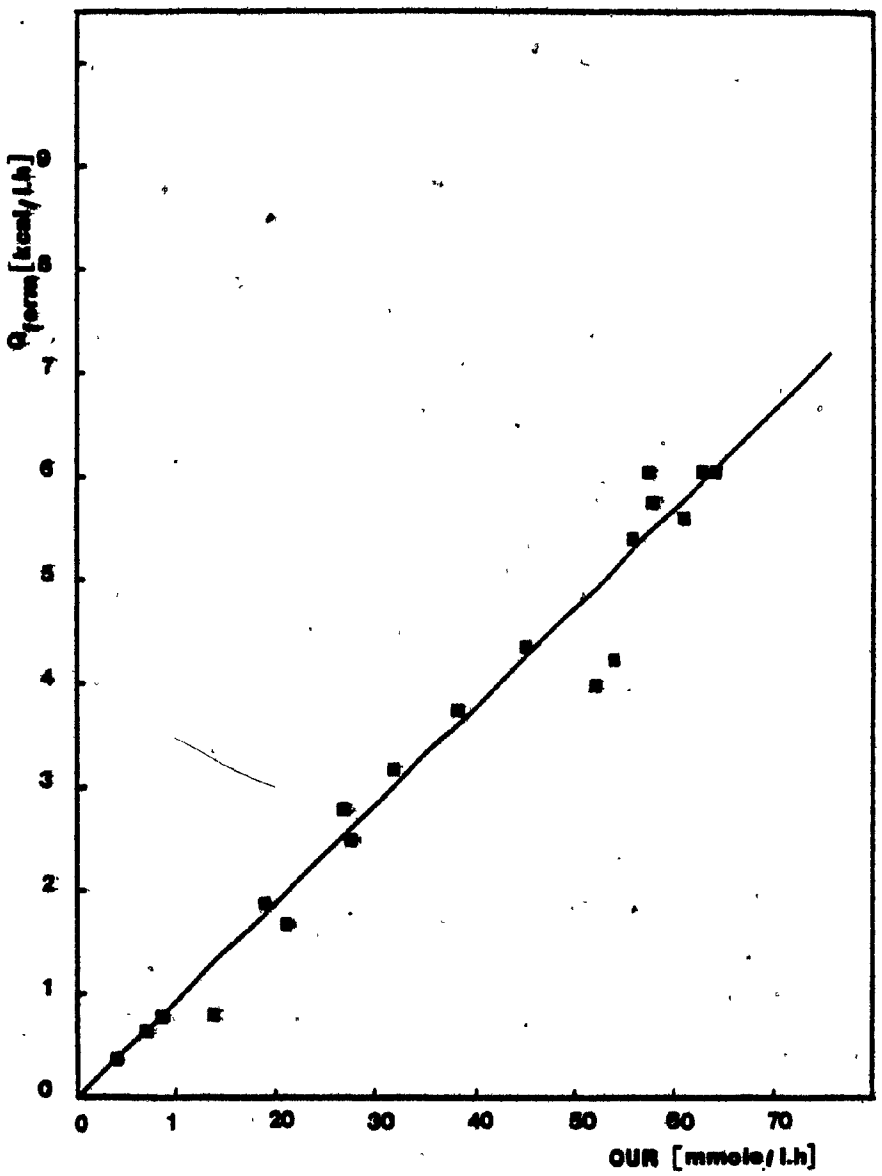
Q_{formo} [kcal/l.h]
0
1
2
3
4
5
6
7
0
1
20
30
40
50
60
70
OUR [mmole/l.h]

Figure IV.37 The Rate of Heat Production versus the Oxygen Uptake Rate for C. utilis grown on Glucose

* Correlation Coefficient : 0.988

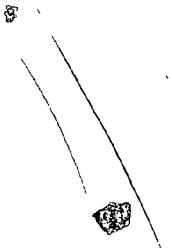

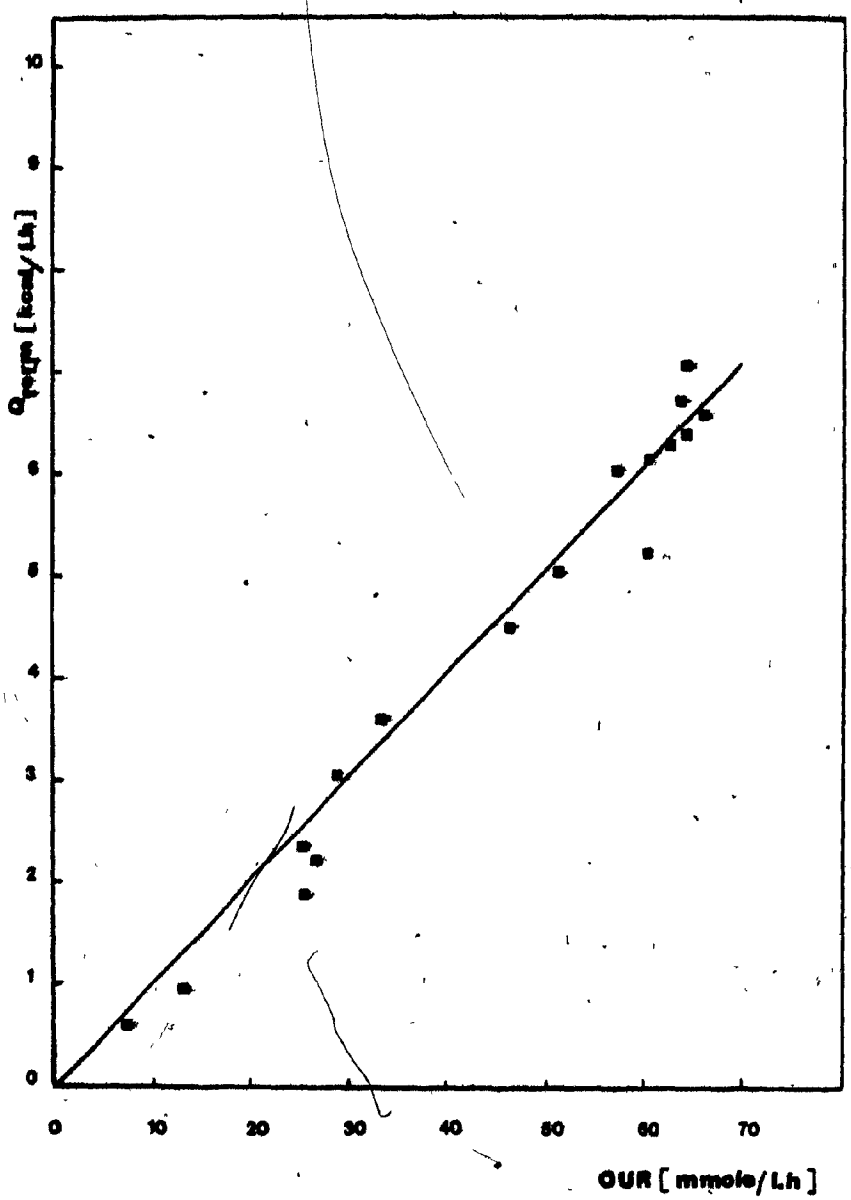
Q_{respo} [kcal/ l.h]
0
1
2
3
4
5
6
7
8
9
10
0
10
20
30
40
50
60
70
OUR [mmole/ l.h]

Figure IV.38 The Rate of Heat Production versus the Oxygen Uptake Rate for C. utilis grown on Glucose

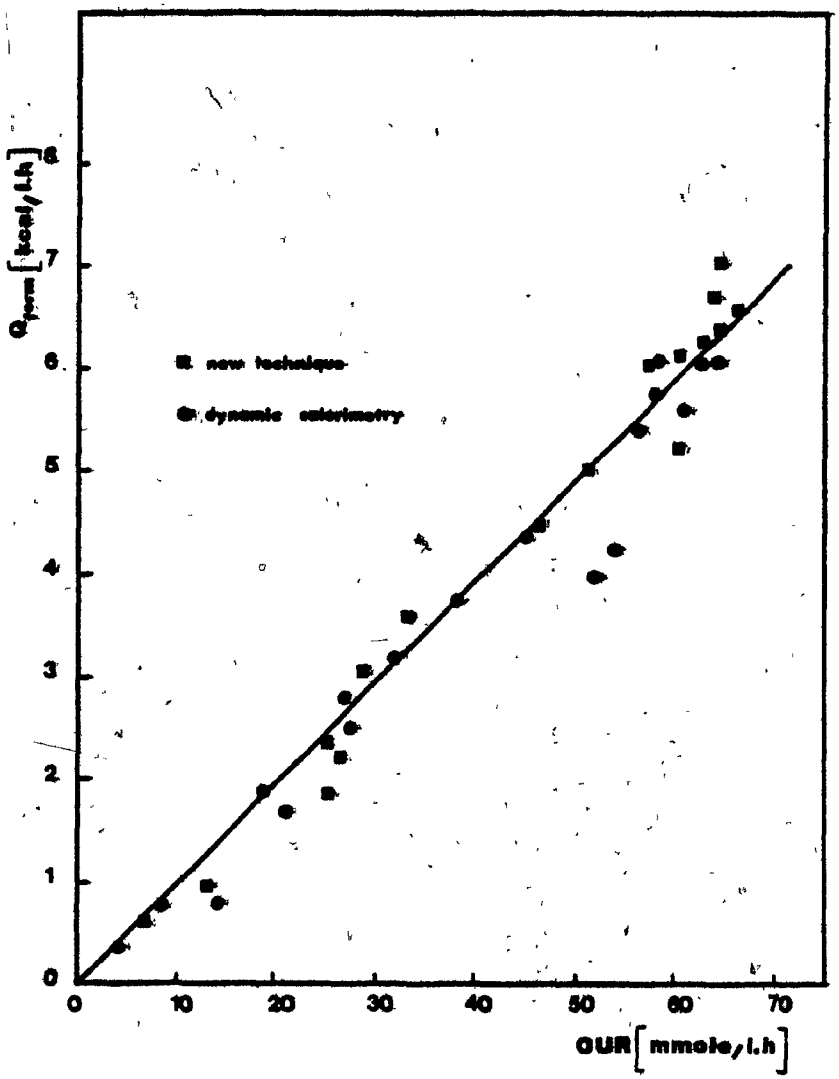
Q_{perm} [kcal/l.h]
0
1
2
3
4
5
6
7
8
new technique
dynamic calorimetry
0
10
20
30
40
50
60
70
OUR [mmole/l.h]

Figure IV.39 The Rate of Heat Production versus the Oxygen Uptake Rate for C.utilis grown on Sucrose

* Correlation Coefficient : 0.957

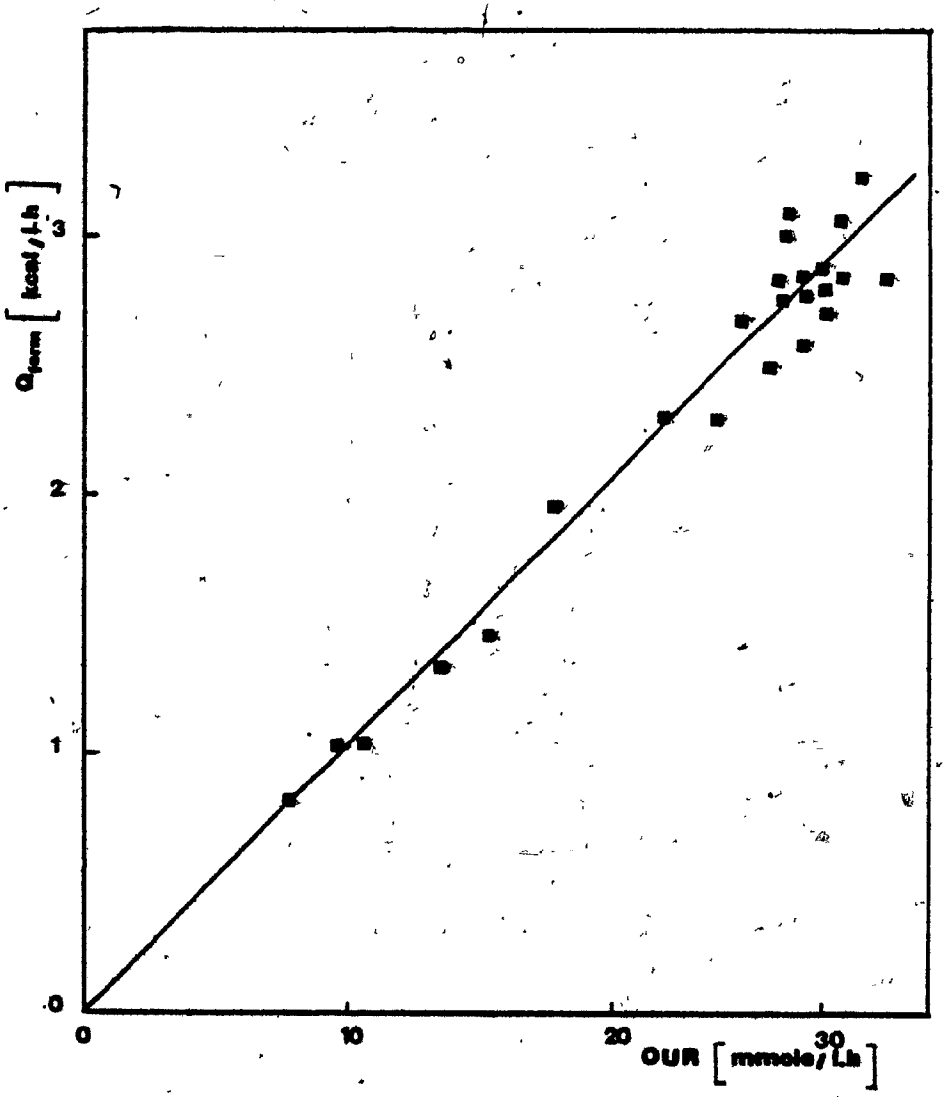
Q_{perm} [kcal/l.h]
0
1
2
3
0
10
20
30
OUR [mmole/l.h]

Figure IV.40 The Rate of Heat Production versus the Oxygen Uptake Rate for C.utilis grown on Ethanol

* Correlation Coefficient : 0.994

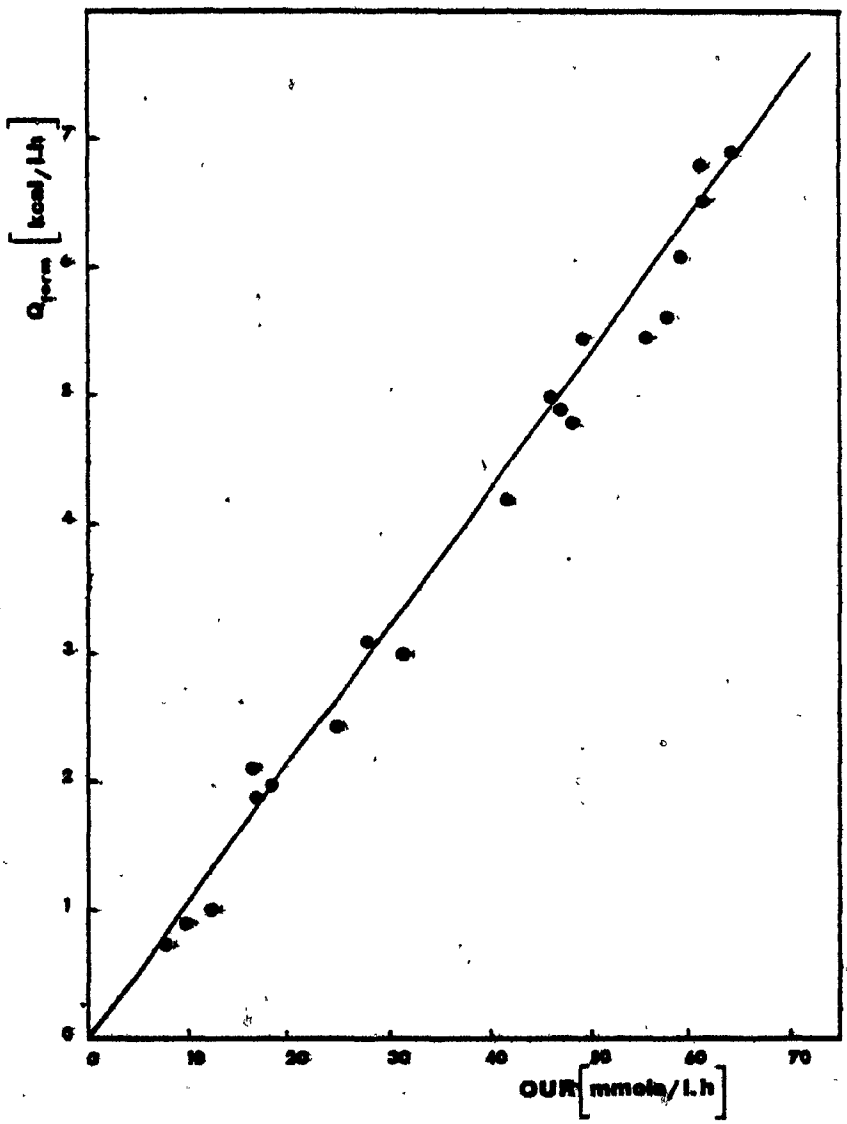
Q_{perm} [kcal/l.h]
0
1
2
3
4
5
6
7
0
10
20
30
40
50
60
70
OUR [mmole/l.h]

Figure IV.41 The Rate of Heat Production versus the Oxygen Uptake Rate for C.utilis grown on a 1 : 1 mixture of Glucose and Cellobiose

- Total Sugar Concentration : 30 g/l

* Correlation Coefficient : 0.979

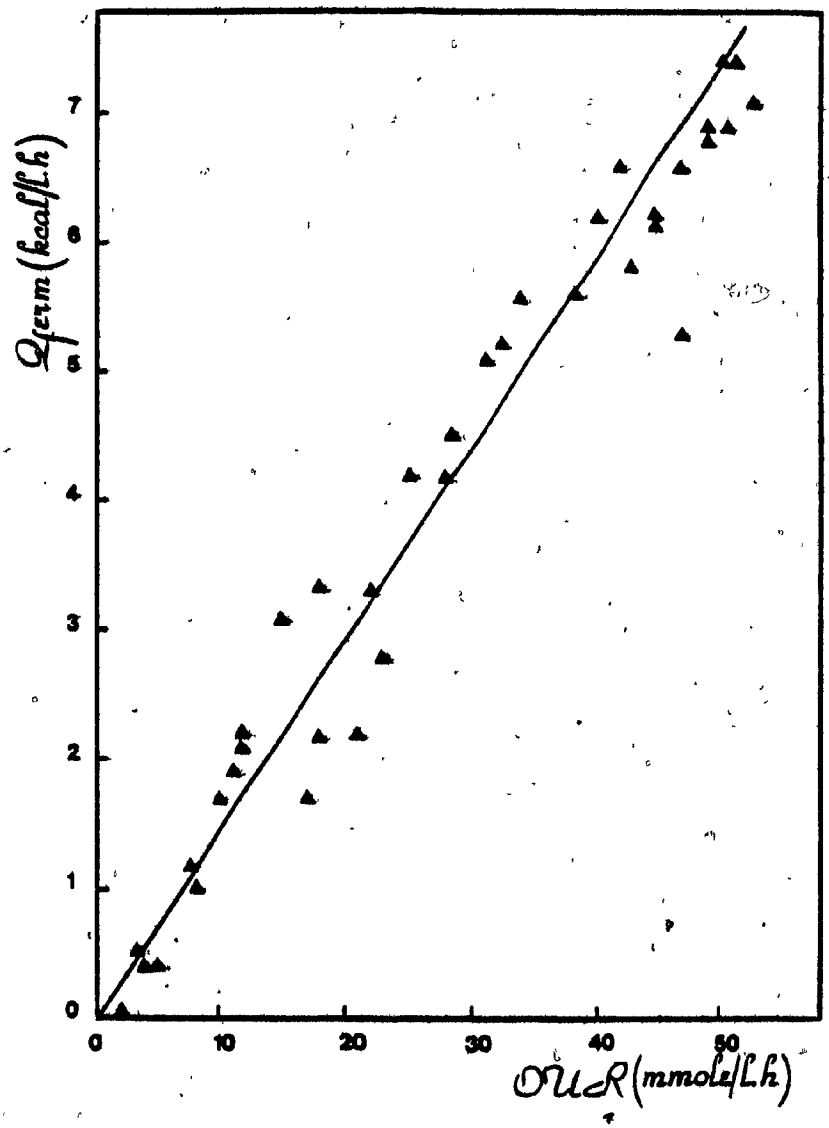
Q_{ferm} (kcal/L.h)
0
1
2
3
4
5
6
7
0
10
20
30
40
50
OUR (mmole/L.h)

Figure IV.42 The Rate of Heat Production versus the Oxygen Uptake Rate for Individual Experiments

$$Q_{ferm} = (0.111 \pm 0.02)\ \Delta O_2$$

Where

Q_{ferm} : Rate of Heat Production (kcal/l.h)

ΔO_2 : Oxygen Uptake Rate (mmol/l.h)

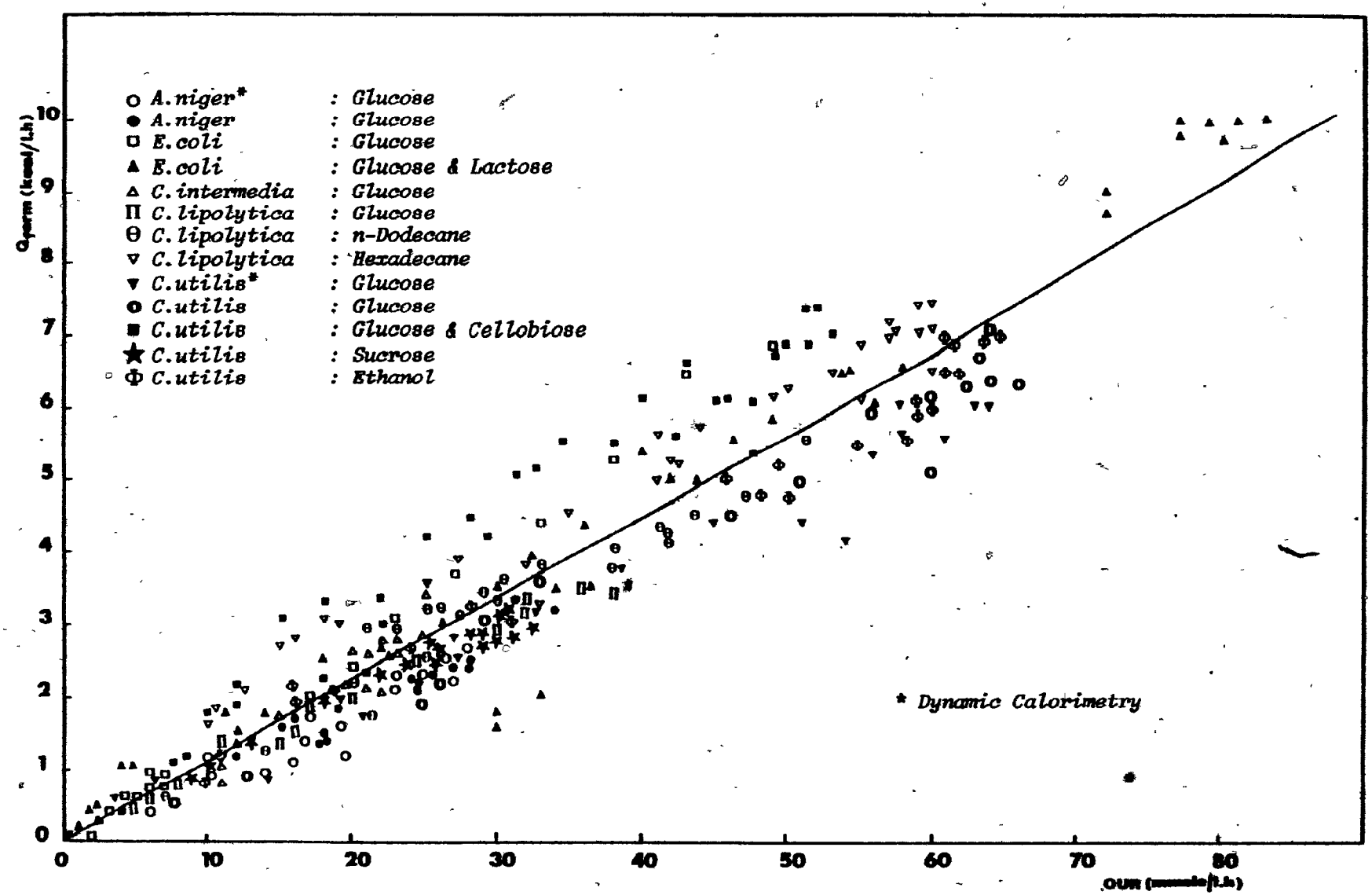
○ A.niger* : Glucose
● A.niger : Glucose
□ E.coli : Glucose
▲ E.coli : Glucose & Lactose
△ C.intermedia : Glucose
Π C.lipolytica : Glucose
Θ C.lipolytica : n-Dodecane
▽ C.lipolytica : Hexadecane
▼ C.utilis* : Glucose
○ C.utilis : Glucose
■ C.utilis : Glucose & Cellobiose
★ C.utilis : Sucrose
Φ C.utilis : Ethanol
* Dynamic Calorimetry
0 1 2 3 4 5 6 7 8 9 10
0 10 20 30 40 50 60 70 80

I. TOTAL HEAT RELEASED AND TOTAL OXYGEN CONSUMED

The total heat released and the total oxygen consumed during a batch growth period was found for individual cultures by integrating the curve shown in Figure IV.11 through Figure IV.24 using Simpson's rule. The results are expressed in Table IV.12 as kcal/l and mmol O_2/l of fermentation broth .

The total heat released and total oxygen consumed for hydrocarbon and ethanol fermentations are much higher in comparison with those for conventional carbohydrate fermentations . This behavior would certainly be expected as indicated in Table I . It is also important to note that higher heat release and oxygen consumption were observed for monosaccharide (glucose) fermentation with respect to disaccharide (sucrose) fermentation for the same organism. In general, values of the heat released are in the following descending order of substrates : hydrocarbons, alcohols, monosaccharides, and disaccharides .

When a plot of the total oxygen consumed versus the total heat produced was made (Figure IV.43), a straight line with a slope of 0.111 ± 0.02 kcal/mmol O_2 was fitted to the experimental data by the least squares method .

Figure IV.43 The Total Heat Released versus the Total Oxygen Consumed

$$\int_0^{t_f} Q_{ferm}\, dt \ (kcal/\ell) = \Delta H_{fo} \cdot \int_0^{t_f} \Delta O_2\, dt \quad (mmole/\ell)$$

where

ΔH_{fo} = 0.111 ± 0.02 (kcal/mmole O_2)

= 3.47 ± 0.62 (kcal/g O_2)

t_f = Fermentation Time

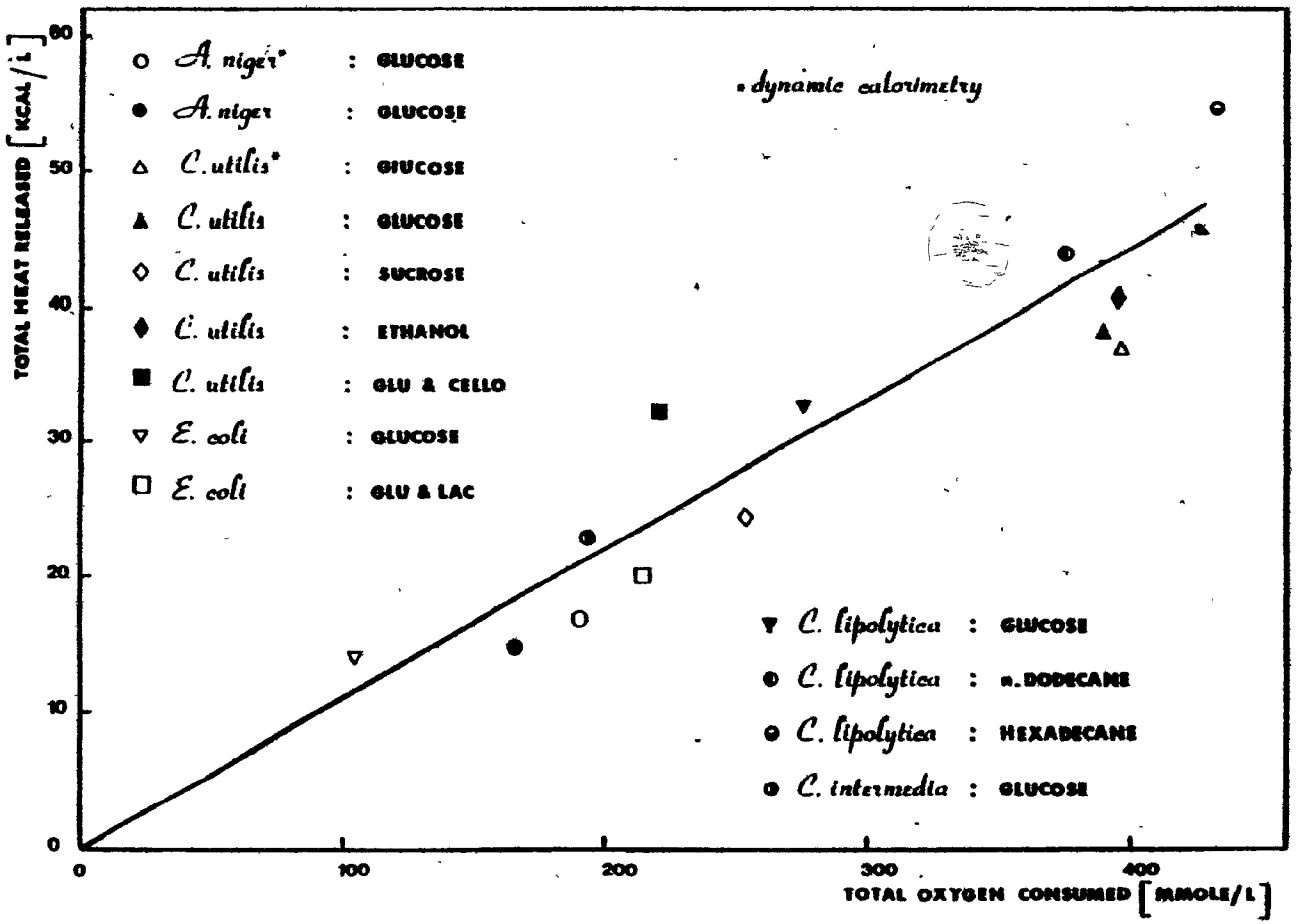
TOTAL HEAT RELEASED [KCAL/L]
TOTAL OXYGEN CONSUMED [MMOLE/L]
0
10
20
30
40
50
60
100
200
300
400
A. niger* : GLUCOSE
A. niger : GLUCOSE
C. utilis* : GLUCOSE
C. utilis : GLUCOSE
C. utilis : SUCROSE
C. utilis : ETHANOL
C. utilis : GLU & CELLO
E. coli : GLUCOSE
E. coli : GLU & LAC
C. lipolytica : GLUCOSE
C. lipolytica : n.DODECANE
C. lipolytica : HEXADECANE
C. intermedia : GLUCOSE
* dynamic calorimetry

TABLE IV.12

TOTAL HEAT RELEASED VERSUS TOTAL OXYGEN CONSUMED

Micro-organisms	Substrate	Total Heat (kcal/l)	Total Oxygen (mmole/l)	ΔH^{*}_{fo} (kcal/mmole)
A.niger *	Glucose	17.125	191.171	0.090
A.niger	Glucose	15.085	167.296	0.092
C.intermedia	Glucose	21.442	192.320	0.111
E.coli	Glucose	14.073	105.871	0.133
E.coli	Glucose & Lactose	33.063	277.981	0.119
C.lipolytica	Glucose	20.521	213.956	0.096
C.lipolytica	n-Dodecane	43.758	376.035	0.116
C.lipolytica	Hexadecane	55.712	423.654	0.131
C.utilis *	Glucose	37.087	397.304	0.093
C.utilis	Glucose	38.530	390.764	0.097
C.utilis	Sucrose	24.931	254.024	0.098
C.utilis	Ethanol	40.554	395.279	0.103
C.utilis	Glucose & Cellobiose	31.791	217.856	0.146

* Dynamic Calorimetry

J. SOME YIELD COEFFICIENTS OF SELECTED MICROBIAL CULTURES

Some important fermentation parameters used for the economic assessment of biomass production costs are the oxygen requirement per gram of dry cells (ΔH_{O_2}) , the thermal yield (ΔH_{fc}) , i.e. the heat evolved per gram cells on dry weight basis, and the cell yield defined as the weight of cell mass produced per weight of substrate consumed ($Y_{x/s}$) .

The experimental results indicated that ΔH_{O_2} is relatively independent of the type of micro-organism . For carbohydrate (glucose) fermentations, this ratio varied from 0.86 to 1.17 g O_2/g cell . In general, this ratio follows the descending order : bacteria, yeast, mold . The amount of oxygen required per gram of cells was confirmed to be dependent on the type of substrate used . While ΔH_{O_2} was 1.17 g O_2/g cell for the growth of *C. lipolytica* on glucose, it was experimentally determined to be 1.44 and 1.80 g O_2/g cell when this organism was grown on hexadecane and n-dodecane respectively. The highest value, 2.25 g O_2/g cell, was observed for *C. utilis* grown on ethanol while the lowest value, 0.62 g O_2/g cell, was established for the growth of *C. utilis* on sucrose .

The thermal yields for *C. intermedia, C. lipolytica, and C. utilis* grown on glucose were experimentally determined to be 3.53, 3.52, and 2.68 kcal/g cell respectively. The thermal yields for *C. lipolytica* grown on hexadecane and n-dodecane were established to be 5.92 and 6.55 kcal/g cell respectively. The thermal yield for the mold culture is lower than that for the yeast and bacterial cultures oxidizing the same substrate. The

value of ΔH_{fc} for *A. niger* grown on glucose ranged from 2.75 to 2.87 kcal/g cell . The thermal yield for the growth of *E. coli* on glucose was 3.62 kcal/g cell and was higher (4.37 kcal/g cell) when this organism was grown on a 1 : 1 mixture of glucose and lactose . The thermal yield ΔH_{fc} of *C. utilis* grown on a mixture of glucose and cellobiose was also found to be higher than that of *C. utilis* grown only on glucose under identical environmental conditions . In this case, the value of ΔH_{fc} for the combined substrate was experimentally determined to be 4.17 kcal/g cell.

The lowest value of ΔH_{fc}, 1.92 kcal/g cell, was observed for *C. utilis* grown on sucrose while the highest value, 7.23 kcal/g cell, was established for *C. utilis* grown on ethanol as a source of carbon .

The highest value of $Y_{x/s}$, 1.15, was determined for the growth of *C. lipolytica* on hexadecane while the lowest cell yield, 0.14, was observed for *A. niger* grown on glucose . As expected, the yeast-hydrocarbon combinations produce higher cell yield than yeast-carbohydrate fermentation .

All the above-mentioned coefficients were dependent on the substrate used and were relatively independent of the type of organism (Table IV.13) .

TABLE IV.13

THE YIELD COEFFICIENTS OF SELECTED MICROBIAL CULTURES

Micro-organism	Substrate	ΔH_{fc} (kcal/g cell)	ΔH_{O_2} (g O_2/g cell)	$Y_{x/s}$ (g cell/g substrate)
A. niger *	Glucose	2.76	0.98	0.17
A. niger	Glucose	2.74	0.97	0.14
C. intermedia	Glucose	3.53	1.01	0.18
E. coli	Glucose	3.61	0.87	0.16
E. coli	Glucose & Lactose	4.36	1.17	0.23
C. lipolytica	Glucose	3.51	1.17	0.32
C. lipolytica	n-Dodecane	6.55	1.80	0.80
C. lipolytica	Hexadecane	5.92	1.44	1.15
C. utilis	Glucose	2.68	0.86	0.45
C. utilis	Sucrose	1.92	0.62	0.39
C. utilis	Ethanol	7.22	2.54	0.26
C. utilis	Glucose & Cellobiose	4.16	0.91	0.47

* Dynamic Calorimetry

K. *ESCHERICHIA COLI* GROWN ON A DEFINED MEDIUM

An energy balance on the fermentation was attempted for the growth of *E. coli* on a mixture of glucose and lactose.

The initial total sugar concentration was 21.30 g/l (11.30 g/l glucose and 10 g/l lactose). A plot of the glucose concentration versus time is shown in Figure IV.16 .

After 15.6 hours, all of the sugar appeared to have been assimilated by the growing culture as indicated by the heat, oxygen and carbon dioxide curves (Figure IV.16). However, an increase of biomass concentration was noted after 15.6 hours which suggests that perhaps some partially oxidized accumulated catabolies might have been utilized then .

33.063 kcal/l were released during the 16 hour experiment. The final cell concentration was 7.57 g/l. The thermal yield is therefore 4.37 kcal per gram of cell dry weight.

During the experiment, 277.981 mmoles/l of oxygen were consumed while 273.636 mmoles/l of carbon dioxide were produced. These values were obtained by integrating the oxygen uptake rate and carbon dioxide production rate curves shown in Figure IV.16 using Simpson's rule.

The measurement of glucose concentration showed that 11.30 grams of glucose was completely utilized by the growing culture. If a carbon balance is made, the growth equation becomes :

$$11.30 \text{ Glucose} + \text{Lactose} + 8.89\ O_2 \longrightarrow 7.57 \text{ Cell} + 12.04\ CO_2$$

where the stoichiometric coefficients are in g/l . If it is assumed further that the cells are 50% carbon[38], then 6.05 g of lactose would be

needed to balance the equation

$$11.30\ \text{Glucose} + 6.05\ \text{Lactose} + 8.89\ O_2 \longrightarrow 7.57\ \text{Cell} + 12.04\ CO_2$$

An analysis of the experimental data showed that the values of the respiratory quotient (RQ), defined as the ratio of the carbon dioxide production rates(CPR) to the oxygen uptake rates (OUR), were close to unity (Figure IV.44).

A comparison between the rate of heat release and the carbon dioxide respiration rate revealed a linear relationship (Figure IV.45). The proportionality constant for this relationship is approximately equal to the proportionality constant, ΔH_{fo}, between the rate of heat release and the rate of oxygen uptake. This result is certainly to be expected since the RQ values are close to unity, which implies that the carbon dioxide production rates are more or less equal to the oxygen uptake rates.

However when the rate of heat production is plotted against the rate of carbon dioxide evolution, the correlation is not as good as when the rate of oxygen consumption is used (Figure IV.45).

Figure IV.44 The Correlation between the Oxygen Uptake Rate (OUR) and the Carbon Dioxide Production Rate (CPR)

Slope= RQ (Respiratory Quotient)= 1.02 ± 0.14

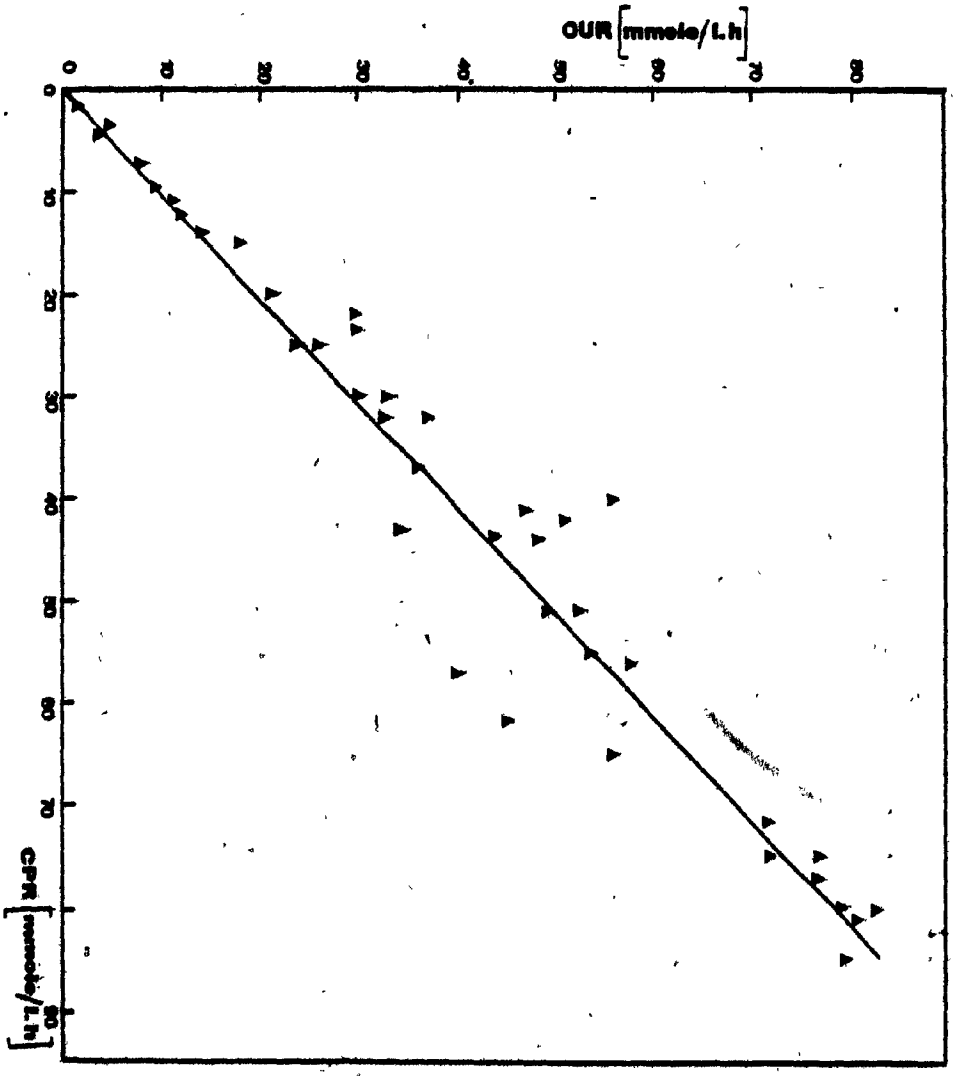
OUR [mmole/l.h]
0
10
20
30
40
50
60
70
80
CPR [mmole/l.h]

Figure IV.45 The Correlation between the Carbon Dioxide Production Rate (CPR) and the Rate of Heat Release

$$\text{Slope} = \Delta H_{fo}^{**} = 0.113 \pm 0.024 \text{ kcal}/\ell.h$$

(Correlation Coefficient = 0.96)

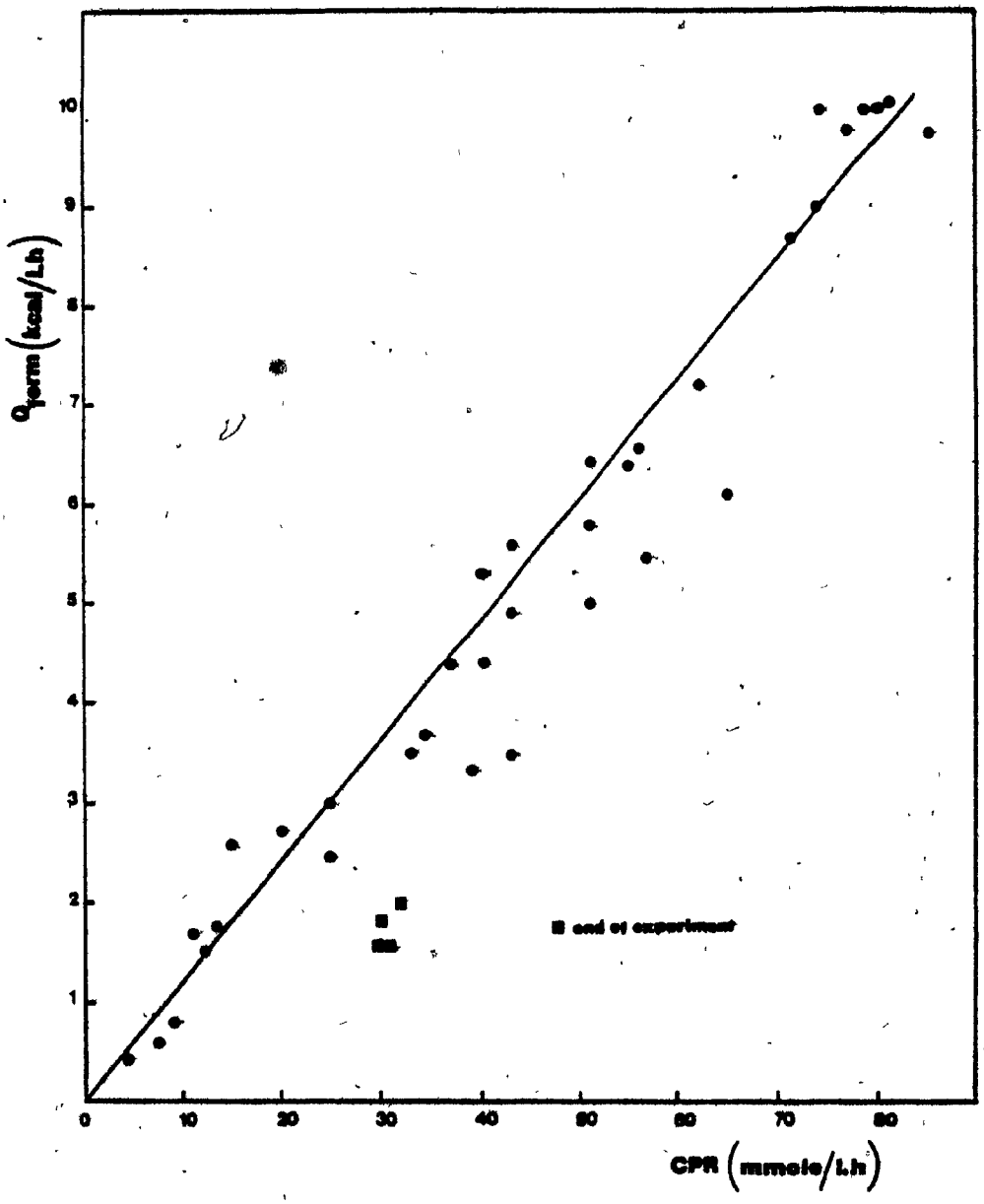
Q_{perm} (kcal/l.h)
CPR (mmole/l.h)
0
10
20
30
40
50
60
70
80
1
2
3
4
5
6
7
8
9
10
■ end of experiment

L. THERMODYNAMIC EVALUATION OF MICROBIAL GROWTH

The heat evolved, $\int_0^{t_f} Q_{ferm}\, dt$, from a fermentation which transforms nutrients to microbial cells and related products during a specific period of time, t_f, is given by :

$$\Delta Q = (-\Delta H_1) - (-\Delta H_2) \quad \ldots\ldots\ldots\ldots\ldots\ldots (120)$$

where $-\Delta H_1$ is the heat of combustion of substrates (kcal/l) and $-\Delta H_2$ is the heat of combustion of products (kcal/l) .

The terms on the right-hand side of Equation (120) are given by :

$$-\Delta H_1 = (-\Delta H_s)(-\Delta S) + (-\Delta H_N)(-\Delta N) \quad \ldots\ldots\ldots (121)$$

$$-\Delta H_2 = (-\Delta H_{cell})(\Delta X) + \Sigma_1(-\Delta H_{pi})(\Delta P_i) \quad \ldots\ldots\ldots\ldots (122)$$

where $-\Delta H_s$ is the heat of combustion of carbonaceous substrate (kcal/mole substrate), $-\Delta H_N$ is the heat of combustion of nitrogenous substrate (kcal/mole), $-\Delta H_{cell}$ is the heat of combustion of dry cells (kcal/g cell), $-\Delta H_{pi}$ is the heat of combustion of i^{th} product (kcal/mole i^{th} product), $-\Delta S$ is the amount of carbonaceous substrate consumed (mole), $-\Delta N$ is the amount of nitrogenous substrate consumed (mole), ΔX is the amount of cell material synthesized (g cell) and ΔP_i is the amount of i^{th} product formed (mole).

From Equations (120) to (122), it is evident that the heat of combustion of microbial cells could be estimated by measuring the heat

evolution of fermentation (ΔQ) and attempting the overall material balance for fermentation by monitoring the differences in the substrate concentration, biomass concentration, by-product concentration, and ammonia concentration during the growth of the culture .

Of particular interest are the industrial processes emphasizing biomass production, where only a small formation of organic by-products is desirable (less than 1 - 3 %). Furthermore, if the combustion of cells happens to yield ammonia in the reverse of the reaction of cell synthesis employing ammonia as a starting material[13], the second terms on the right-hand side of Equation (121) and (122) can be disregarded .

$$\Delta Q = (-\Delta H_s)(-\Delta S) - (-\Delta H_{cell})(\Delta X) \quad \text{.....(123)}$$

Equation (123), therefore, could be used to calculate the heat of combustion of microbial cells by measuring the heat evolution of fermentation. This application can be illustrated by calculating the heat of combustion of the *C. utilis* microbial cells grown on glucose .

It was assumed that after 14 hours of fermentation, 30 g/l of glucose substrate were completely oxidized by the growing culture. The total heat released was 38.530 kcal/l corresponding to 14.382 g/l of synthesized microbial cells. The heat of combustion of cells, therefore, is :

$$-\Delta H_{cell} = \frac{30 \times 3.74 - 38.538}{14.382}$$

$$= 5.12 \text{ kcal/g cell}$$

The heats of combustion of some different cultures are shown in Table IV.14. The lowest value, 3.32 kcal/g cell, was observed for the growth of *C. lipolytica* on hexadecane while the highest value, 5.96 kcal/g, was for *C. lipolytica* grown on n-dodecane .

The calculation of the heats of combustion for the growth of *A. niger, C. intermedia, E. coli, and C.utilis* on glucose and the growth of *C. utilis* on sucrose was not attempted since the relevant experiments were not carried to completion. Unfortunately the biomass was not examined by a specialized established experimental procedure for the heat of combustion due to unavailability of the appropriate instrumentation at the time when the fermentation experiments were carried out .

TABLE IV.14

THERMODYNAMIC EVALUATION OF MICROBIAL GROWTH

Organism	Substrate	Substrate Concentration (g/l)	$-\Delta H_s$ (kcal/g)	Total Heat (kcal/l)	Total Cell (g/l)	$-\Delta H_{cell}$ (kcal/g)
A. niger[1]	Glucose	30	3.74	17.1	6.9	-
A. niger	Glucose	30	3.74	15.0	5.4	-
C. intermedia	Glucose	30	3.74	21.4	6.20	-
E. coli	Glucose	20	3.74	14.0	4	-
E. coli	Glucose & Lactose	20	3.84	33.0	7.60	5.75
C. lipolytica	Glucose	25	3.74	20.5	5.9	-
C. lipolytica	n-Dodecane	7.44	11.34	43.7	6.8	5.96
C. lipolytica	Hexadecane	7.70	11.29	55.7	9.4	3.32
C. utilis	Glucose	30	3.74	38.5	14.3	5.12
C. utilis	Sucrose	30	3.94	24.9	12.9	-
C. utilis	Ethanol	20	7.102	40.5	5.6	-
C. utilis	Glucose & Cellobiose	30	3.74	31.7	7.6	3.58

1. Dynamic Calorimetry

CHAPTER V

DISCUSSION

A. MIXING POWER INPUT STUDIES

This work confirmed that the mechanical mixing power input of turbulent non-aerated agitated Newtonian as well as non-Newtonian liquids in fully baffled tanks varied with the cube of the impeller rotational speed. The power number, N_p, was 6.14 for the six-blade turbine used in this study. The results agree very well with the well-known work of Rushton et al[39].

For the non-Newtonian liquids, the mechanical power input also varied with N^3. This behavior appears to be consistent with the work of Calderbank and Moo-Young[40] who proposed the following equation for predicting the mixing power consumption (pseudoplastic behavior) :

$$N_p = \frac{P}{\rho_L N^3 d^5} = 160 \frac{W_I L_I (d - W_I)}{d^3} \quad \ldots\ldots (224)$$

It could be generalized that the power consumption for mixing in turbulent regime is proportional to N^3 for both Newtonian and non-Newtonian fluids. The power number, N_p, attained a value of about 6.0-6.15 for some non-Newtonian fluids examined in this study. Because the agitation power requirement in turbulent regime does not depend on the viscosity of the fluid, and because the density of many fermentation broths is very close

to that of water, it is expected that in non-gassed systems the mixing power input for fermentation broth is equal to the power input for water. This was observed by Mou and Cooney[11].

In plotting the experimental results for (P_g/P) and aeration number (Q/Nd^3), it was indicated that the change in the power ratio was dependent upon whether the aeration number was changed by altering the gas flow rate or the impeller rotational speed. The power ratio consistently decreased with increasing aeration number when the gas flow rate was varied at constant rotational speed of impeller. A non-linear correlation for the power ratio and the aeration number has been suggested (Figure IV.5) .

When the gas flow rate was kept constant at different points of a fairly wide range with N varied, the mechanical power input required to agitate a gas-liquid dispersion was still proportional to the cube of the impeller rotational speed (Figures IV.2 and IV.3) . Upon the completion of a regression analysis of all experimental data obtained in this study, it was demonstrated that the power ratio P_g/P is proportional to $Q^{-0.38}$. Therefore the aeration number exponent in Equation (63), m*, is -0.38 . This is consistent with the work of Cooney[41] and Hassan and Robinson[29].

Since both P_g and P have been shown to vary with N^3 , the power ratio P_g/P should be independent of N and constant at a specified gas flow rate . Based on this consideration, the value of Weber number exponent, n*, in Equation (63) can be determined to be -0.19 . The estimate of n* based on regression analysis showed that the experimental value of n* is very close to the predicted value based on the aeration number exponent. This

is illustrated in Figure IV.6 .

In addition to the mixing power input, there is a certain amount of energy introduced into the aerated system by the bubbling gas . When P_{bub} , estimated from Equation (15), is of significant magnitude, the value of $(P_g/P)(Q/N\,d^3)^{0.38}$ is not necessarily constant . The effect of isothermal expansion of the bubbling gas into the gas-liquid dispersion can be neglected only when the ratio of the gas flow rate over the liquid volume is smaller than 1/6 (m^3/second/m^3) as indicated by Hassan and Robinson[29]. This condition is quite easy to fulfill for many practical applications .

As mentioned previously, the experimental results in this study confirmed that both P_g and P in the turbulent regime are proportional to N^3 for some pseudo-plastic behavior fluids. However, the P_g/P ratio was appreciably different for non-Newtonian liquids compared to the corresponding ratio for Newtonian solutions. The CMC (carboxy-methyl-cellulose) solution data in Figure IV.6 were best fitted by a straight line whose slope is very close to that for Newtonian solutions. In effect, the constant C* and n* do not merely reflect geometric parameters but also depend on the charateristics of fluids . This could perhaps be explained by the fact that the ratio P_g/P is also dependent on the Hedstrom number[42] .

The comparison of experimental results with the theoretical predictions available in the literature and with the original one reported in this study was illustrated in Table V.1 . In general, the proposed correlation of $(P_g/P)(Q/N\,d^3)^{0.38}$ with Weber number is more useful than

TABLE V.1

THE COMPARISON OF EXPERIMENTAL RESULTS WITH THE THEORETICAL PREDICTION (MIXING POWER INPUT RATIO)

Solution	Calderbank et al[30,31] (P_g/P)	Pharamond et al[27] (P_g/P)	This Work (P_g/P)	Experiment (P_g/P)
Water	0.543	0.581	0.531	0.536
Methanol (10%)	0.543	0.581	0.513	0.522
Methanol (25%)	0.543	0.581	0.540	0.544
Ethylene Glycol (8%)	0.543	0.581	0.507	0.514

* Rotational Speed = 600 rpm

* Air Flow Rate = 10.128 ℓ/min

those available so far. Admittedly, this proposed correlation has not been tested for different scales of operation and for different system geometries. The correlating procedure reported herein is justified if the following conditions apply :

- The power of mixing is proportional to the density which in turn is directly related to gas hold-up .

- Hold-up is related to bubble size[30,31] which in turn is related to Weber number .

B. FERMENTATIVE HEAT STUDIES

Following the testing and calibration of the technique developed as part of this work for the purpose of continuously measuring the heat given off during a fermentation process, the technique was used for selected typical culture growth experiments. Several cultures representing bacterial, mold and yeast aerobic fermentation processes were grown on substrates representative of different levels of energy available for bio-oxidation. Monosaccharides, disaccharides, paraffinnic hydrocarbons and ethanol were selected as substrates of industrial large-scale application and interest.

Results of the selected growth experiments are graphically depicted in Figures IV.11 to IV.25 where three quantitives are plotted against time; heat release rate, oxygen consumption rate, and biomass concentration. It is essential to include the latter if the former two are expressed in terms of liter^{-1} hour^{-1} so that a physically and practically meaningful expression of the two rates can be derived in corresponding units of gram^{-1} hour^{-1} for any given time. Unfortunately, some results of experiments published earlier[5,8,11,41,43] do not include the culture biomass growth data making a meaningful interpretation and comparison of results impossible. It is very tempting to express the experimental results in the units corresponding to those found in the overall and partial heat balance equations which invariably use units of kcal per liter or kcal per liter per hour for the following reason : except for the fermentative heat, the other heat parameters are specified on the basis of unit volume. Unit volume, however, becomes meaningless when the heat

produced is a function of something else included in this volume. In the case of fermentation broth, the suspended "solid" particles of biomass are actually generating the heat. As it happens, the same "unit volume" produces an entirely different amount of heat when it contains only inoculum micro-organism cells as compared to the more advanced phases of fermentation when the cell concentrations are much higher. In this work both rate values expressed in terms of $liter^{-1}$. $hour^{-1}$ as well as $gram^{-1}$. $hour^{-1}$, are listed for the peaks for the rate of heat production and oxygen consumption rate respectively in Table IV.10 for convenience .

B.1 Correlation of the Rate of Microbial Heat Evolution with the Rate of Oxygen Consumption

During the course of the experiments, the rate of heat production has been found to correlate well with the rate of oxygen consumption. The correlation has a general form :

$$Q_{ferm} = \Delta H_{fo} \cdot \Delta O_2$$

where ΔH_{fo} is a proportionality constant with the units kcal/mmol O_2. This type of correlation was applicable for all thirteen experiments using five different micro-organisms grown on a variety of substrates. The correlation was also valid for the diauxic system, i.e. a system where two different sources of carbon are utilized by a culture in a sequential mode.

The proportionality constant, ΔH_{fo}, appeared to be relatively

dependent on the substrate used and on the type of organism (Table IV.11). Variation of ΔH_{fo} with the organism used would be expected since the constant value for ΔH_{fo} represents a constant efficiency in using the available free energy. This efficiency can vary depending on many circumstances. According to experimental results, the values of ΔH_{fo} vary from 0.092 kcal/mmol O_2 for mold to 0.135 kcal/mmol O_2 for bacteria. This observation agrees well with the results obtained by Cooney[41]. During the lag phase and/or the end of cultivation experiment, some fermentations (Figures IV.27 and IV.32) exhibited a large deviation from the general trend. A great deal of fundamental knowledge on the metabolic pattern of each culture used in this study would have to be gathered in order to elucidate this problem. The scatter of recorded data, however, could also be due to the experimental error which is relatively large when smaller quantities are measured.

The accuracy of ΔH_{fo} estimates depend on the measurement of the oxygen uptake and the fermentative heat values.

$$\frac{\epsilon(\Delta H_{fo})}{\Delta H_{fo}} = \pm \frac{\epsilon(OUR)}{OUR} \pm \frac{\epsilon(Q_{ferm})}{Q_{ferm}} \qquad \text{..... (125)}$$

when Equation (115) is used for computing the oxygen uptake rate, the error in the oxygen uptake rate $\epsilon(OUR)$ originated from the oxygen and carbon dioxide analyzers is :

$$\epsilon(OUR) = \pm F_N/V_L \left\{ 2\, \delta P_{O_2}^{out} + \delta P_{CO_2}^{out} \right\} \qquad \text{..... (126)}$$

where $\delta P_{O_2}^{out}$ and $\delta P_{CO_2}^{out}$ are the instrument errors for the oxygen and carbon dioxide analyzers respectively.

Under typical experimental conditions, F_{in} = 8.4 ℓ/min, V_L = 9 ℓ, $P_{O_2}^{out}$ = ± 0.0717% , and $P_{CO_2}^{out}$ = ± 0.004%, giving and error, ε(OUR) = ± 2.91 mmol/ℓ.h . This could indicate a significant error in the value of the OUR data for the first 3 to 5 hours of the culture experiment and/or during the end of the experiment when the OUR values are relatively small.

The error in the rate of heat evolution could be estimated by examining the measurements of $U_2A_2^*$, $(Q_{agi} + Q_{bub} - Q_{surr})$ and the voltage across the immersion heater. The ratio $\varepsilon(Q_{ferm})/Q_{ferm}$ depends on the values of Q_{ferm} and varies from 7.2% to 0.2% when Q_{ferm} ranges from 2.9 to 22.3 kcal/ℓ.h. For the sake of simplicity, the ratio $\varepsilon(Q_{ferm})/Q_{ferm}$ was evaluated to be 1.41% as indicated in Table IV.5.

For the growth of *A. niger* on glucose, 4 hours after inoculation, when the OUR value was estimated to be 18.919 mmol/ℓ.h , the ratio $\varepsilon(\Delta H_{fo})/\Delta H_{fo}$ becomes :

$$\frac{\varepsilon(\Delta H_{fo})}{\Delta H_{fo}} = \pm \ 16.79\ \%$$

The value of ΔH_{fo} was experimentally established to be 0.0964 kcal/mmol O_2, the confidence interval for the value of ΔH_{fo} is (0.080-0.112) kcal/mmol O_2. This calculation illustrates that when the fermentative heat and oxygen consumption are relatively small, a more inaccurate estimation of ΔH_{fo} can be expected.

In order to minimize the error due to the OUR data, an oxygen analyzer and carbon dioxide analyzer with greater accuracy and stability would have to be employed for monitoring the concentrations of oxygen and carbon dioxide in the out-going gas stream. This suggestion is difficult to implement due to the restricted choice of available instruments and due to the complexity of the analytical procedures involved.

Another important experimental parameter is the carbon dioxide production rate (CPR).

$$CPR = \frac{F_N}{V_L}\left[\frac{p_{CO_2}}{1 - p_{CO_2}^{out} - p_{O_2}^{out}} - 0.00042\right] \quad \ldots\ldots\ldots (127)$$

The error in the carbon dioxide production rate (CPR) attributable to the oxygen and carbon dioxide analyzers is :

$$\varepsilon(CPR) = \pm \frac{F_N}{V_L}\left(2\,\delta p_{CO_2}^{out} + \delta p_{O_2}^{out}\right) \quad \ldots\ldots\ldots\ldots\ldots (128)$$

Under typical experimental conditions the error in the carbon dioxide production rate is 1.57 mmol/l.h . The measurement of the CPR data is therefore more accurate than that of OUR.

Unfortunately, the correlation of heat released with carbon dioxide evolved has been indicated as less satisfactory[5] and therefore it has not been attempted in this study . An illustration of this correlation is shown in Figure IV.45 for the growth of *E. coli* on a mixture of glucose

and lactose. When the rate of heat production is plotted versus the rate of carbon dioxide production, the correlation is not as good as when the oxygen consumption is used. This may be observed by comparing the carbon dioxide and oxygen data in the appropriate figures (Figures IV.32 and IV.45). While the correlation coefficient of the linear relationship between the heat release and the carbon dioxide production is 0.963 , the correlation coefficient of the relationship between the heat release and the oxygen consumption is 0.98 which indicates a better fit to the experimental data. For the heat release and the carbon dioxide production correlation, it was further observed that the experimental data obtained exhibited a large deviation from the general regression line (Figure IV.45) when the culture passed the exponential growth phase. Such a phenomenon indicates a significant change in the ratio of the heat releaesd to the carbon dioxide produced. The change in this ratio can be explained by considering material being oxidized at the time when the heat production and the carbon dioxide production rates were measured. If organic acids, for instance, were to accumulate during exponential growth on glucose and lactose and oxidized only when the sugar supply was completely depleted then at least two different values of the ratio (heat to CO_2 production rates) would be expected.

When attempting the correlation between the rates of heat production and CO_2 production, Cooney[41] also observed that the data for *E. coli*, *B. subtilis, and C. intermedia* grown on glucose after the exponential phase showed a large deviation from the general trend. The author suggested that the significant change in the ratio of the heat released and the carbon

dioxide produced could be due to the accumulation of some organic acids. Presumably these organic acids were only oxidized after the primary substrate (glucose) was completely exhausted. As a consequence, the ratio between the rate of heat production and the carbon dioxide production can vary significantly with the substrate being oxidized.

A similar conclusion was also reported by Zabriskie and Humphrey[44] when these investigators used the CPR for estimation of the biomass concentration instead of the OUR. This conclusion is supported by the fact that carbon dioxide is evolved during many metabolic processes. Only some of these processes are involved directly in producing energy for cellular growth. Therefore, carbon dioxide evolution and heat release are not expected to be correlated as closely as the heat release and oxygen consumption.

The correlation between the heat of fermentation and oxygen uptake reported herein did not take the heat of product formation into account. This approach is only acceptable if the product formed has an energy potential similar to the carbon substrate on a weight basis. If the product has an energy potential similar to or less than the biomass, the effect of product formation on thermal data cannot be considered negligible and the direct correlation of heat production and oxygen uptake is no longer valid. Alcohol and organic acid fermentation are typical examples of the first type of product formation, while antibiotic fermentations are typical of the second type. The good correlation obtained for each individual set of experimental data reported here demonstrate that the effect of product formation on thermal data for all fermentations examined in this study is quite negligible .

B.2 - Correlation of the Total Heat Released and the Total Oxygen Consumed

In general, the total heat released and total oxygen consumed for hydrocarbon fermentations are much higher compared with those for carbohydrate fermentations. This behavior can be explained by the fact that a carbohydrate furnishes some of the cell growth material carbon(C), hydrogen(H) and oxygen(O) in aqueous solution where the cells grow, while a hydrocarbon furnishes only C and H in a form which is practically insoluble in water. Oxygen must then be supplied from large quantities of atmospheric air blown into the process. As a consequence, the use of hydrocarbon substrates instead of carbohydrates, requires about two and a half times as much atmospheric oxygen and releases over twice as much heat in the reaction[1].

It is evident from Tables IV.12 and IV.13 that the oxygen consumed and heat released for the growth of *C. lipolytica* on n-dodecane and hexadecane are much higher than those of this organism grown on glucose. Using the same argument, it is to be expected that the oxygen consumed and the heat released for the disaccharide fermentation are lower than those of the monosaccharide and ethanol fermentation for the same micro-organism. The experimental results confirm this expectation (Tables IV.12 and IV.13).

When the total heat produced was plotted against the total oxygen consumed during a fermentation process, a linear relationship resulted:

$$\int_0^{t_f} Q_{ferm}\, dt = \Delta H^*_{fo} \times \int_0^{t_f} \Delta O_2\, dt$$

Similarly, the proportionality constant ΔH^*_{fo} depends on the type of organism and growth substrate used. This constant was found to be

slightly higher for bacteria than for yeasts and molds . Although only one line was drawn in Figure IV.43, it is observed that several lines may exist passing through the origin. It is expected that ΔH^*_{fo} can vary from organism to organism and further correlations characteristic for specific groups of micro-organisms, if possible at all, would be well beyond the scope of this study.

B.3 Comparison of Experimental Data with the Literature

The experimental data for the heat released per gram of oxygen consumed from this study agree well with the values from the literature. The proportionality constant , ΔH_{fo}, according to Minkevich and Eroshin[12], varies from 0.092 to 0.118 (kcal/mmol O_2) regardless of the type of substrate, microbial species, and effectiveness of cell growth when oxygen is the limiting factor. It is evident from Table IV.11 that the experimental data reported in this study correspond to the theoretical prediction from the work of Minkevich and Eroshin[12], and Imanaka and Aiba[13]. The constant ΔH_{fo} arrived at this work is slightly lower than the value obtained experimentally by Cooney et al[5] . It appears in the following correlation :

$$Q_{ferm} = (0.124 \pm 0.003) . \Delta O_2$$

The heat released per mole of oxygen consumed determined by Sedlaczek[45] is generally lower than the values observed in this study. The

significant difference between these values could be explained by the fact that Sedlaczek[45] used a medium rich in amino acids for his experiment. Consequently, less energy would probably be wasted by the growing culture as heat due to the lower demand for energy for growth because some of the preformed compounds for cell constituents would be readily available and need not be synthesized. This fact was also pointed out by Cooney[41].

When the values of total oxygen consumed in the course of the fermentation are plotted against the total energy dissipated as heat (Figure V.1), a straight line with a slope of (0.097 ± 0.014) kcal/mmol O_2 can be shown to fit the data of Sedlaczek[45]. In the work of Cooney et al[5] a straight line with a slope of 0.11 ± 0.01 kcal/mmol O_2 was found to fit the data (Figure V.2). Winzler and Baumberger[3] found the ratio of heat produced to oxygen consumed to be 0.104 and 0.144 kcal/mmol O_2 for Erythrocytes and Vibrio metchnikoff respectively. It is evident from Table IV.12 that the experimental data in this work are quite consistent with the fragmentary data reported by previous investigators. The comparison of the original experimental data and the data from the literature is summarized in Table V.1 .

The experimental results for the heat released per gram of dry microbial cells also agree well with those obtained by previous workers. The thermal yield, ΔH_{fc}, for yeast-carbohydrate fermentation processes was reported to range from 3.5 to 4.6 kcal/g cell[46] . The mean value of ΔH_{fc} for yeast-carbohydrate fermentations was experimentally determined by this study to be 3.47 kcal/g cell .

Figure V.1 The Total Heat Released versus the Total Oxygen Consumed (Data from Sedlaczek)

Slope = 0.097 ± 0.014 kcal/mmol O_2

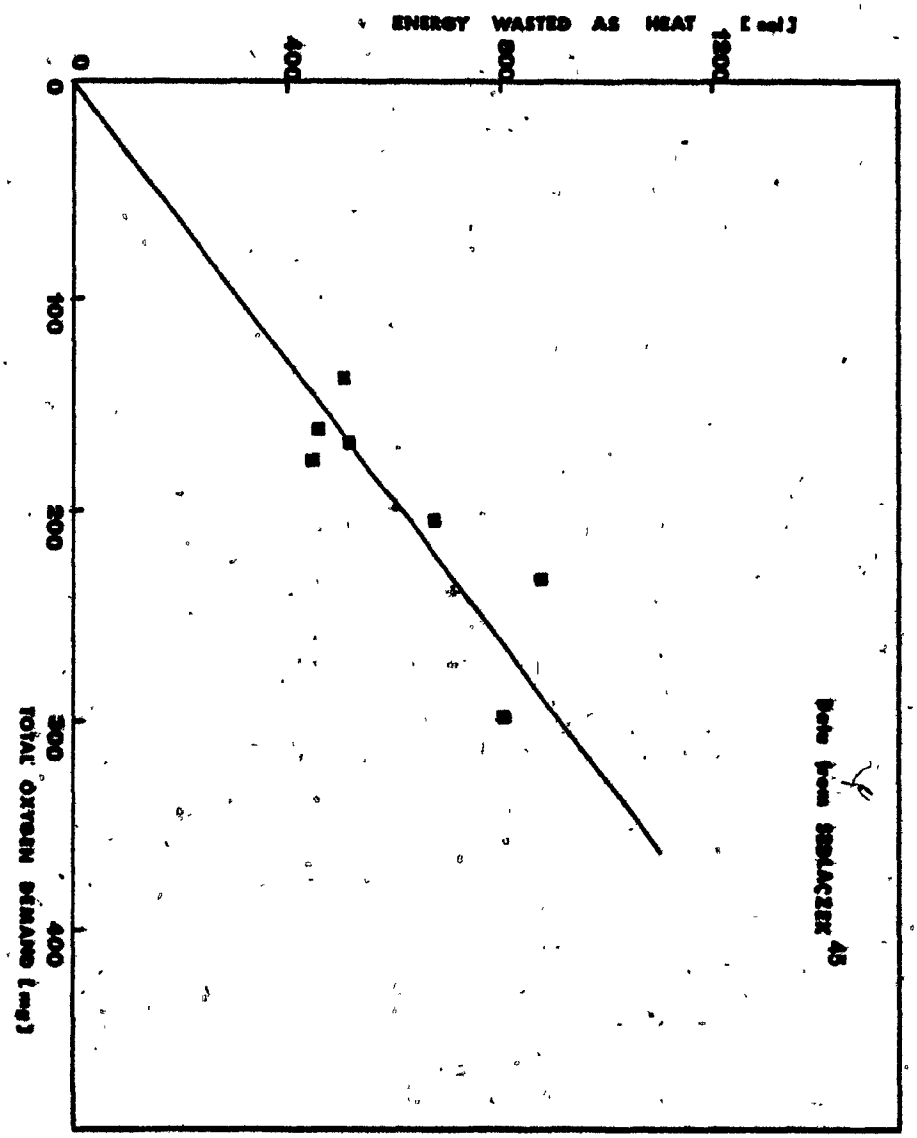
ENERGY WASTED AS HEAT [eq]
0
400
800
1200
0
100
200
300
400
TOTAL OXYGEN DEMAND [mg]
Data from REICHERT 45

Figure V.2 The Total Heat Released versus the Total Oxygen Consumed (Data from Cooney)

Slope = 0.11 ± 0.01 kcal/mmol O_2

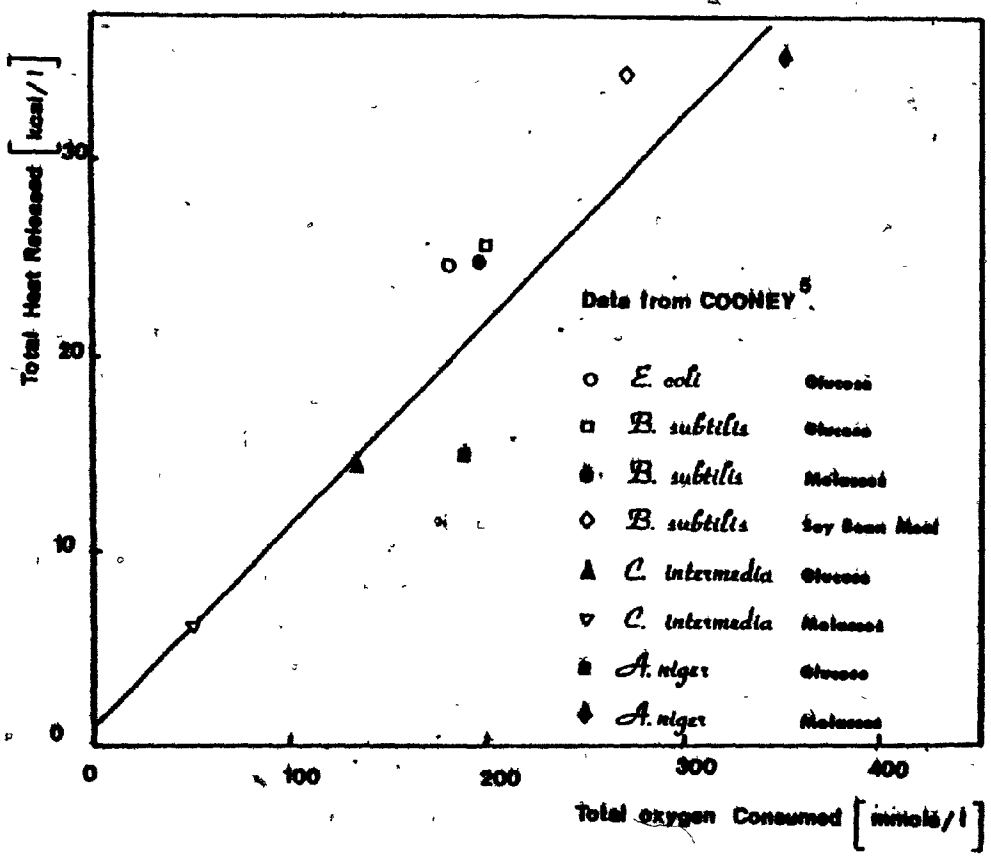
Total Heat Released [kcal/l]
30
20
10
0
0
100
200
300
400
Total oxygen Consumed [mmols/l]
Data from COONEY[5]
E. coli Glucose
B. subtilis Glucose
B. subtilis Molasses
B. subtilis Soy Bean Meal
C. intermedia Glucose
C. intermedia Molasses
A. niger Glucose
A. niger Molasses

TABLE V.2

COMPARISON OF LITERATURE AND EXPERIMENTAL DATA FOR THE FERMENTATIVE HEAT STUDY

Organisms	Substrate	ΔH_{fo} (kcal/g O_2)		ΔH_{fc} (kcal/g cell)	
		References	This Work	References	This Work
E.coli [41]	Glucose	5.0	4.21	4.73	3.62
E.coli [45]	Rich Medium	2.88	-	3.27	-
E.coli	Glucose & Lactose	-	3.77	-	4.37
S.typhi [45]	Rich Medium	2.69	-	2.95	-
S.sonnei [45]	Rich Medium	3.22	-	3.73	-
P.vulgaris [45]	Rich Medium	3.40	-	4.15	-
S.aureus [45]	Rich Medium	3.81	-	3.97	-
P.fluorescens [45]	Rich Medium	3.88	-	4.48	-
Yeast [46]	Wood Hydrolyzate	-	-	3.5-4.6	-
Yeast [47]	Glucose	-	-	3.87	-
S.marcescens [45]	Rich Medium	2.76	-	3.32	-
A.niger [41]	Glucose	2.82	2.87*, 2.88	2.60	2.75, 2.87*
A.niger [41]	Molasses	3.72	-	2.76	-

* Dynamic Calorimetry

TABLE V.2 (Cont)

Organisms	Substrate	ΔH_{fo} (kcal/g O_2)		ΔH_{fc} (kcal/g cell)	
		References	This Work	References	This Work
B. subtilis [41]	Glucose	3.90	-	2.94	-
B. subtilis [41]	Molasses	4.69	-	3.84	-
B. subtilis [41]	Soy Bean Meal	3.94	-	2.80	-
C. intermedia [41]	Glucose	3.59	3.50	5.45	3.53
C. intermedia [41]	Molasses	3.88	-	2.21	-
*C. utilis**	Glucose	-	2.94	-	-
C. utilis	Glucose	-	3.00	-	2.68
C. utilis	Sucrose	-	3.06	-	1.92
C. utilis	Ethanol	-	3.28	-	7.23
C. utilis	Glucose and Cellobiose	-	4.47	-	4.17
C. lipolytica	Glucose	-	3.25	-	3.52
C. lipolytica	n-Dodecane	-	3.50	-	6.55
C. lipolytica	Hexadecane	-	4.22	-	5.92

* Dynamic Calorimetry

The experimental results of this study indicated that the value of ΔH_{fc} for A. niger grown on glucose ranged from 2.75 to 2.87 kcal/g cell. Cooney [41] reported that ΔH_{fc} for A. niger grown on the same medium as was used in this work was 2.60 kcal/g cell .

The thermal yields for E. coli grown on glucose and a glucose medium enriched with amino acids were reported to be 3.27 and 4.73 kcal/g cell respectively[41,45] . The value of ΔH_{fc} for E. coli in this work was 3.62 kcal/g cell when glucose was used as a sole source of carbon. The thermal yield for E. coli grown on a 1 : 1 mixture of glucose and lactose was established to be 4.37 kcal/g cell .

Heat evolved during the bio-oxidation of hydrocarbons has been theoretically estimated to be more than double that evolved by a culture oxidizing an equivalent molar weight of carbohydrate (Table I) . The heat released corresponds to about 7.6 and 3 kcal per gram dry weight of biomass for hydrocarbon and carbohydrate fermentation respectively[1] . The mean value of the thermal yield for all the carbohydrate fermentations examined in this study was determined to be 3.25 kcal/g cell . In the case of hydrocarbon fermentations, the thermal yields for C. lipolytica grown on n-dodecane and hexadecane were 6.55 and 5.92 kcal/g cell respectively. These values are less than the crude theoretical prediction. The difference between the experimental values and the theoretical prediction could be explained by the fact that the predicted thermal yield (ΔH_{fc} = 7.6 kcal/g cell) was considered to be the mean value for different micro-organisms grown on different paraffinnic hydrocarbon substrates. This value was different from culture to culture as indicated before (Table IV.13).

In particular, Cooney and Makiguchi[2] used the value of 7 kcal/g cell as the thermal yield of hexadecane fermentations for the calculation of heat production during growth on selected carbon sources . The difference between the above values could be due to the fact that the thermal yield estimation is dependent on the cell yield (g cell/g substrate). For n-paraffinnic hydrocarbon fermentations, the thermal yield, ΔH_{fc}, was reported to range from 4.53 to 7.8 kcal/g cell when the cell yield varied from 1.4 to 1 . For a cell yield of 1.2 (g cell/g substrate), the thermal yield was reported to be 5.90 kcal/g cell [48] . The cell yield for a hexadecane fermentation was determined here to be 1.15 (g cell/g substrate). The thermal yield, H_{fc}, for C. lipolytica grown on hexadecane obtained in this study (5.92 kcal/g cell) agrees very well with that reported in the literature (5.90 kcal/g cell)[48] . The thermal yield of C. lipolytica grown on n-dodecane was also fairly consistent with the theoretical prediction.

Another confirmation of the validity of the results from the two hydrocarbon fermentations examined in this study can be illustrated by considering the cell yield coefficient (g cell/g substrate). These coefficients were determined to be 0.80 to 1.15 for the growth of C.lipolytica on n-dodecane and hexadecane respectively. The literature indicated that cell yields on hydrocarbon fractions range from 50 to 115 per cent[49,50]. A figure of 85 per cent was reported to be typical [51] . It is also reported here that C. lipolytica grown on hexadecane produces a higher cell yield than when it was grown on n-dodecane. This observation agrees well with the results cited in the literature. Takahashi et al[52] reported that the higher

boiling fractions of n-alkanes were more easily utilized by C. tropicalis than the lower boiling fractions, with n-octadecane and hexadecane showing the best assimilation and dodecane and tridecane being poorly assimilated.

Another already mentioned important parameter of a fermentation process is the amount of oxygen consumed per unit weight of cell produced. This ratio is useful in mass transfer calculations and estimation of cooling requirements through the use of a value of 0.11 ± 0.02 kcal per millimole oxygen consumed was obtained in this study.

From Table I, it is noted that carbohydrate fermentation require 0.8 mole O_2 per mole of microbial cell [1] . If the weight of ash is neglected as a component of the cell, the theoretical ratio ΔH_{O_2} for carbohydrate fermentations is 1.05 g O_2/g cell . The mean ratio ΔH_{O_2} was experimentally established here to be 0.955 g O_2/g cell (Table IV.13) for the carbohydrate fermentations . This value agrees well with the theoretical prediction.

In this work, the experimental value of ΔH_{O_2} was found to be 1.81 and 1.44 g O_2/g cell for the growth of C. lipolytica on n-dodecane and hexadecane respectively. The oxygen requirement per gram cell for yeast-hydrocarbon fermentation was reported to range from 1.52 g O_2/g cell to 2.42 g O_2/g cell when the cell yield varied from 115 to 85 per cent[15,53]. The values of ΔH_{O_2} obtained for the growth of C. lipolytica are relatively smaller than those reported in the literature. A difference between these values can be expected since the predicted value of ΔH_{O_2} was developed for different micro-organisms grown on different hydrocarbon substrates. This value can vary from culture to culture.

In general,the values of ΔH_{O_2} observed in this work were dependent

on the type of substrate and relatively independent of the type of micro-organism grown . This observation is consistent with the results from the work of Mateles[54].

The application of the experimental technique for determining the heats of combustion of different cultures is illustrated in Table IV.14 . The values of combustion heat ($-\Delta H_{cell}$) developed here were consistent with those reported by the previous workers. Prochazka, Payne, and Mayberry[55] indicated that the mean calorific content of the various micro-organisms they tested was 5.4 kcal/g of cells on ash-free, dry-weight basis; the range of variation was from 5.0 to 6.4 kcal/g . In an earlier study, Guenther[15] had used a value of 3.6 kcal/g of cells, dry weight, in the evaluation of heat production during hydrocarbon fermentations. Using the theoretical availability of electrons to calculate the heat of combustion of cells, Abbott and Clamen[56] derived a value of 5.38 kcal/g cells . Using a bomb calorimeter, Mennett and Nakayama[57] found a value of 4.8 kcal/g cell of ash-free cells, dry weight, for Pseudomonas fluorescens .

Another comparison can be made between the literature data and the results of this study by considering the fraction of the available energy wasted as heat . This comparison was based on E. coli grown on a 1:1 mixture of glucose and lactose .

There are two different ways of intepreting the experimental data. In the first approach it is assumed that a total of 21.30 gram/liter of glucose and lactose are completely oxidized by the growing culture. The total free energy change (the heat of combustion) resulting from the complete oxidation of this amount of sugar is 81.436 kcal/l .Experimentally determined

amount of heat released from the fermentation was 33.063 kcal/l (Table IV.12) corresponding to 0.406 of the total.

The second approach uses the stoichiometric equation derived by means of a carbon balance (Section IV.K). It is found that 17.35 of total sugar (11.3 g of glucose and 6.05 g of lactose) per liter would be needed to balance the equation. This approach assumes that the difference between the initial total sugar introduced (21.30 g/l) and the stoichiometric quantity of 17.35 g/l cited above may be accounted for by the presence of some accumulated metabolite. In this case, the total free energy change is 66.10 kcal per liter. This would then yield a fraction of energy wasted as heat equal to 0.500.

The fractions of energy wasted as heat calculated for both cases only represent a lower and upper limit for comparison . The actual value will lie between the two extremes . If the actual fraction of wasted energy is taken to be an average of the two extreme values, it is equal to 0.453 . This value derived here agrees well with those obtained by the previous workers [45,58] . The values found in the literature for E. coli range from 0.435 to 0.609 .

The good agreement between literature and the experimental data reported here confirms the validity of the results obtained which support the applicability of the experimental technique .

B. 4 Technical Problems Involved With Calorimetric Measurement

1. The Heat of Agitation

The heat of agitation, Q_{agi}, is equal to the power input introduced into mechanically mixed systems by the shaft (gas sparging power input can be neglected). The reasons for the changes in the power input into the fermentation broth during the batch growth are not completely understood[11]. As a consequence, Q_{agi} was calibrated before inoculation at the specified agitation and aeration rates and was then used throughout the fermentation in the calculation of Q_{ferm}. This procedure was extensively employed by many previous workers to determine the heat of fermentation[5,8,11]. In order to support the applicability of this procedure these authors[5,8,11] quoted the work of Ohyama and Endoh[25], and Michel and Miller[26] to conclude that the mixing power input for the turbulent regime does not depend on the physio-chemical properties of the fermentation broth except for the density of the solution. Taguchi and Miyamota[59] also observed that the correlation of Michel and Miller[26] is valid for turbulent agitation of Newtonian as well as non-Newtonian fluids. This observation implies that the mixing power input does not appear to vary appreciably during the course of fermentation even though some types of broths such as in the polysaccharide fermentation are known to exhibit highly non-Newtonian rheological properties. Goma[43] et al further observed that when the fermentation medium is a Newtonian fluid, the Einstein law is verified and the viscosity forces do not vary much. These investigators also measured the agitation work in the Newtonian fermentation broth and confirmed that the ratio $\Delta Q_{agi}/Q_{agi}$ is less than 1% when the

biomass concentration varies from 15 to 25 g/l . Most fermentative heat data developed here are for yeast culture broths, which have been established as Newtonian liquids[2]. The parameters corresponding to the Reynolds number and the power number (N_p) were used by many previous workers[2] without the modifications generally applied in the case of yeast culture broth. However, for the non-Newtonian fungal culture broths the usual corrections would be required.

In this work, the density and the surface tension of fermentation broth were measured periodically throughout the experiments in order to improve the correction for the agitation energy input introduced into the system. Usually, the density of fermentation broth does not change appreciably during fermentation for both carbohydrate and hydrocarbon fermentations (Table IV.8) . Cooney[41] observed that the density of fermentation broths remained unchanged for all of his cultures. The density of C. intermedia grown on hexadecane broth, for example, only fluctuates from 1.0008 g/cm^3 to 1.0048 g/cm^3 after 53 hours of fermentation. The surface tension, therefore, is the only parameter which needs to be measured during the fermentation. It is noted that the ordinate $(P_g/P)(Q/N\,d^3)$ increases by 15% as the impeller Weber number changes about 2.5 fold, so the mixing power ratio is relatively insensitive to the Weber number .

The measurements of surface tensions of the carbohydrate fermentation broths indicated that this parameter did not change appreciably during the experiment. Considering these observations, it is quite reasonable to assume that the mixing power input of yeast cultures grown on carbohydrate

media remained unchanged or varied insignificantly during the culture period. In the case of hydrocarbon fermentations, this problem becomes more complicated. The interfacial tension was found to decline sharply even though the mixing power input was held constant for the growth of C. lipolytica grown on hexadecane (Table IV.9). This phenomenon could be explained by the fact that the interfacial tension decrease was responsible for the reduction of the Sauter mean bubble diameter with resulting increase in interfacial area . The variation of the mixing power input during such fermentations would require more investigation. The shaft torque should be monitored accurately during the course of fermentation in order to minimize errors introduced by estimating and/or correcting the heat of agitation .

The effect of antifoam addition on the heat of agitation should not be neglected. It was investigated in this work as well as by Cooney[41], and Mou and Cooney[11] . Since this effect was pronounced at low antifoam concentrations, it could be avoided by using initial antifoam concentration greater than 300 mg/l. Before inoculation, such an antifoam concentration should be adjusted in the liquid broth and additional antifoam should only be used when really required during the experiment. No extra quantities of antifoam were required for most cultures used in this study except for the growth of C. lipolytica on glucose and hydrocarbons. In Figures IV.17 and IV.19 the experiments were terminated prematurely because of a foaming problem. In this case the heat production is approximately 33% below the earlier results for the growth of C. lipolytica on glucose. In this

experiment, it was observed that foaming occured several times during the fermentation. The aeration and flow patterns were significantly affected which in turn affected the mixing power input. Some previous investigators[60] already discovered that the mechanical mixing power input is quite different for non-foaming systems as compared to foaming ones. The deviation of the heat production data with the oxygen consumption from a straight line, therefore, would not be totally unexpected if there was no correction applied to the mixing power input under such a circumstance.

2. The Heat Dissipated by the Sparged Gas

The energy dissipated by the bubbling gas is directly proportional to the density of fermentation broth as shown in Equation (15) . This energy term is expected to be constant since the density of fermentation broth does not vary appreciably during fermentation for both carbohydrate and hydrocarbon fermentations. Furthermore, under the typical experimental conditions used in this study, the gas sparging power input can be safely neglected; $Q_{bub} = 0.037$ kcal/l.h (Appendix V). Volesky et al[8] neglected the changes in potential and kinetic energy when deriving a heat balance on the fermentor to calculate the fermentation heat released during bio-oxidation of a carbon substrate. Since these energy terms are very small in comparison with other heat terms, they were, therefore, also ommited in the overall heat balance in the work of Cooney et al[5] and Mou and Cooney[11] .

3. The Heat Loss to the Surroundings

The specific heat transfer coefficient U_1A_1 which determines the heat loss to the surroundings was evaluated experimentally before inoculation

and then used throughout the fermentation experiment without any corrections regardless of the slight changes of physical properties of fermentation broth. This procedure is justified considering the following :

- The changes in rheological properties of fermentation broth affect only the film heat transfer coefficient h_o (Equation {31}) .

- In Equation (41), the terms $\ln(r_1/r_o)/k_{01}$, $1/r_2\, h_\infty$, and $\ln(r_2/r_1)/k_{12}$ dominate the heat transfer. The term $1/r_o h_o$ can be neglected in Equation (41) to simplify the heat loss calculation since it is very small in comparison with the terms above (Appendix VII).

The theoretical calculation of the heat loss to the surroundings is illustrated an Appendix VII. In the absence of relevant experimental data, Equations (16) to (41) could be used for the heat loss calculation to within an acceptable accuracy. Even though there is a 36% difference between the measured value and the theoretical heat loss evaluation, it does not affect the overall heat balance appreciably. This is because the heat loss term is relatively small in comparison with the other heat energy terms measured for the overall heat balance equation . Overall error in the fermentation heat evaluation resulting from the heat loss error (35%) is corresponding very small,ranging from 0.3% to 3% .

The heat loss to the surroundings could also be directly measured by a heat flow sensor. The details of this procedure were reported elsewhere[61]. This approach , however, has not been attempted in this work because it would represent an unnecessary complication of the experimental procedure.

4. The Applicability of This Experimental Technique versus the Dynamic Calorimetric Technique

The overall accuracy of this measuring technique was experimentally determined to be - 1.41% while the percent difference between the known heat input and the amount of heat determined by the dynamic calorimetric technique was 2.2% (Tables IV.5 and IV.6).

Cooney et al[5] reported that the overall accuracy of their experimental technique was - 1.2% . It is evident from Tables IV.5 and IV.6 that the accuracy of both techniques is quite satisfactory when the fermentative heat is high. The fermentative heat data measured by these two techniques should thus compare well during the period of high fermentative heat production. Indeed, for two typical examples illustrated by experimental results depicted in Figures IV.29 and IV.38 . The ratio ΔH_{fo} developed by the new technique agreed quite well with the one developed by the dynamic calorimetric technique (Table IV.11).

Apart from the lower reliability and accuracy of the dynamic calorimetric technique as seen from experimental comparison of the two methods, the use of that technique represents a further experimental disadvantage. The technique requires continuous attention during fermentation experiments which can last for a few days . The temperature fluctuations resulting from its application may disturb the microbial metabolic activities. Furthermore, while the new technique can provide the fermentative heat data immediately, the dynamic calorimetric technique usually requires longer times. An initial period of 5-9 minutes is required to let the temperature rise reach a constant rate after the control system had been shut off.

Dynamic calorimetry is, therefore, not as efficient in determining reliably the heat evolution during the end of exponential growth phase when the rate of heat released may drastically decline in a relatively short period of time.

The technique utilized in this study is very suitable for the measurement of the heat of fermentation. If a correlation between the heat of fermentation and the biomass concentration was successfully attempted[62], the new technique could be used as an indirect sensor for determining the growth and biomass concentration during fermentation. It could also serve as a quantitative indicator of different metabolic activities and parameters. These are extremely important for industrial fermentations, particularly in processes designed to produce high cell densities.

CHAPTER VI

CONCLUSIONS AND RECOMMENDATIONS

A. CONCLUSIONS

1. The rate of heat released during growth correlates well with the rate of oxygen consumption. This correlation has the following form :

$$Q_{ferm} = \Delta H_{fo} \cdot \Delta O_2$$

where Q_{ferm} and ΔO_2 represent the rate of heat production and the rate of oxygen uptake respectively. The proportionality constant ΔH_{fo} was experimentally determined as 0.111 ± 0.02 kcal/mmol O_2 .

2. The constant ΔH_{fo} is dependent on the type of micro-organism, on the substrate used, and is independent of the growth rate.

3. The total heat released and the total oxygen consumed also correlated well as follows :

$$\int_0^{t_f} Q_{ferm}\, dt = \Delta H^*_{fo} \int_0^{t_f} \Delta O_2\, dt$$

$$\text{Total heat Released} = (\Delta H^*_{fo}) \times \text{Total Oxygen Consumed}$$

4. The constant ΔH^*_{fo} is approximately equal to ΔH_{fo}. It is also dependent on the type of micro-organism and substrate used .

5. The total heat released and the total oxygen consumed depend on the microbial culture and in general decrease with the decreasing free energy of the substrate .

6. The experimental data agree well with the theoretical prediction of Minkevich and Eroshin, and with the work of Imanaka and Aiba . The proportionality constant ΔH_{fo} is slightly lower than the one experimentally established by Cooney et al .

7. In absence of experimental data, the correlations derived in this study could be used to estimate the fermentative heat through the measurement of the oxygen uptake rate . The upper limit value of ΔH_{fo}(0.13 kcal/mmol O_2) is applied to the bacterial culture or the diauxic growth. On the other side, the lower limit value of ΔH_{fo}(0.09 kcal/mmol O_2) can be used to correlate the rate of heat released and the oxygen uptake rate for the mold culture. The mean value of ΔH_{fo}(0.11 kcal/mmol O_2) is applicable for the yeast culture .

8. The aforementioned correlation could be useful in the design of heat removal systems for the fermentor, espectially when complex substrate materials are used .

9. The energy dissipated by the bubbling gas could be neglected in any practical calculation for evaluation of the fermentation heat.

10. The mixing power input of the impeller shaft and the heat loss

to the surroundings did not fluctuate appreciably during the course of experiment for thirteen experiments examined in this study .

11. In the overall heat balance on the fermentor, the concept of the impeller Weber number should be used to correlate the mixing power input (P_g/P) for both Newtonian and non-Newtonian fluids in the turbulent regime .

B. ORIGINAL CONTRIBUTIONS

Several elements of this study are considered to be original contributions to knowledge in fermentation technology :

i. The design of the special temperature control system which can be applied to continuously monitor the heat evolution during a fermentation .

ii. The results of the measurement of the fermentative heat and the oxygen uptake for many different organisms grown on different carbon sources . This work also develops the fermentative heat data for typical hydrocarbon and alcohol fermentations which have not been reported elsewhere. The dual maxima phenomenon for the rate of heat released and the rate of oxygen consumption for the diauxic growth had not be previously reported .

iii. The derivation of correlations between the fermentative heat and

the oxygen uptake by the growing culture is very useful both for fermentation system design and process optimization. In addition, it could be extended into process control applications .

iv. The results of investigation of the mixing power input in gassed and ungassed systems for Newtonian and non-Newtonian liquids resulted in a semi-theoretical correlation for estimation of the mixing power input in gas-liquid dispersion systems. Because the proposed correlation for estimating the mixing power input is based on the dimensional analysis approach, it can be useful for the design and scaling-up of fermentor system .

C. RECOMMENDATIONS FOR FUTURE STUDY

Some interesting facets of the present project can be recommended for future study :

1. Applicability of the correlation proposed in this study for estimating the mixing power input in gas-liquid dispersion systems for different tank sizes and impeller designs (propeller, paddle, and different turbines).

2. The effect of surfactant concentration on the mixing power input in a gassed system .

3. The rheological properties (Newtonian or non-Newtonian behavior) of fermentation broth should be specified further during fermentation process for individual cultures. The viscosity should be measured in parallel with the mixing power input in order to confirm its effect on the latter. Inaccuracies in the estimation of the heat of agitation could thus be minimized .

4. A reliable method for measurement of mixing power input in a foaming system should be developed .

5. Mixing power input in a complex three-phase system (gas,liquid-oil, and solids) should be studied in more detail .

6. The described technique for measuring the heat of fermentation should be further extended to thermogenesis studies in fed-batch and continuous-flow cultures with other microbial strains of interest .

7. The multi-maxima behavior of the fermentative heat and oxygen uptake for diauxic growth should be examined further. This could lead to the use of fermentative heat as a process parameter to regulate and/or control the fermentation process .

8. The correlation between the rate of fermentation heat evolution and the biomass concentration should be investigated further . This

correlation could be useful as an additional physiological process variable in the fermentation process .

9. Further study of the effect of product formation on the heat evolution and its correlations . Anaerobic and product-oriented fermentations should be examined .

10. The validity of the resulting correlations should be investigated for the fermentation process when the desired end product of the fermentation is a product other than cell mass .

APPENDIX I

GROWTH MEDIA

The following growth media were used for the fermentations discussed in this study :

MEDIUM I : (used for *Aspergillis niger*)*

Component	gram / liter
Glucose	30.0
$(NH_4)_2SO_4$	4.0
$MgSO_4.7H_2O$	1.0
KH_2PO_4	3.0
Salt Solution[1]	4.0 ml
Temperature	30°C
pH	5.5

MEDIUM II : (used for *Candida intermedia*)*

Component	gram / liter
Glucose	30.0
Hexadecane	5.0
$(NH_4)_2SO_4$	10.0
KH_2PO_4	3.5
Na_2HPO_4	1.5
Yeast Extract	0.1
Temperature	30.0°C
pH	5.5

* C.L. Cooney, "Measurement of Heat Evolution During Fermentation" M.Sc. Thesis, M.I.T. (1968).

MEDIUM III : (used for *Candida utilis*) **

Component	gram / liter
Glucose	30.0
Sucrose	30.0
Glucose and Cellobiose	30.0
Ethanol	20.0
$(NH_4)_2SO_4$	2.5
$CaCl_2.2H_2O$	0.05
KH_2PO_4	2.5
$MgSO_4.7H_2O$	0.5
Temperature	30 °C
pH	4.5

MEDIUM IV : (used for *Escherichia coli*)*

Component	gram / liter
Glucose	20.0
Glucose & Lactose	20.0
$(NH_4)_2SO_4$	4.5
KH_2PO_4	7.0
K_2HPO_4	3.0
$MgSO_4.7H_2O$	0.1
$FeSO_4.H_2O$	0.005
Temperature	37 °C
pH	7

* C.L. Cooney, "Measurement of Heat Evolution During Fermentation" M.Sc. Thesis, M.I.T. (1968).

** Y. Alroy and S.R. Tannenbaum, Biotech. Bioeng., 14, 239 (1973).

MEDIUM V : (used for *Candida lipolytica*)***

Component	gram / liter
Glucose	25.0
n-Dodecane	5-10 ml
Hexadecane	5-10 ml
KH_2PO_4	7.0
$Na_2HPO_4.12\ H_2O$	1.2
$MgSO_4.7H_2O$	0.2
$(NH_4)_2SO_4$	4.0
$CaCl_2.2H_2O$	50 mg
NaCl	50 mg
$CuSO_4.5H_2O$	80 µg
KI	200 µg
$FeCl_3.6H_2O$	1 mg
$MnSO_4.2H_2O$	30 µg
$Na_2MoO_4.H_2O$	10 µg
$ZnSO_4$	80 µg
Boric Acid	200 µg
Yeast Extract	100 µg

1. One liter of trace salt solution was made such that one milliliter would contain the following :

Component	mgram / liter
$CuSO_4.5H_2O$	40.0
$FeSO_4.7H_2O$	150.0
$MnSO_4.H_2O$	400.0
$ZnSO_4.7H_2O$	400.0
$(NH_4)_6Mo_7O_{24}.4H_2O$	175.0

*** Chas. Pfizer Co., Brit. Patent, 1,203,006 (1970).

APPENDIX II

HEAT CAPACITY OF SYSTEM COMPONENTS

Component	Mass/liter of broth, kg/l	Specific heat, kcal/kg. °C	Heat capacity/ liter, kcal/l. °C
Fermentation broth[1]	1.01	1.00	1.01
Fermentor jar[2] (Pyrex)	0.382	0.20	0.0763
Stainless Steel[3] (Type 316)	0.152	0.12	0.0182
Total			1.1045

1. Based on 9.0 liter of fermentation broth
2. Based on 68% of the glass being in contact with the liquid
3. The weight of the impeller, shaft, pH electrode, immersion heater, and stainless steel baffles was estimated to be 1.368 kg

APPENDIX III

TABULATED RESULTS FOR MIXING POWER INPUT STUDY

III.1 Mixing power input for Newtonian fluids at 25°C .

III.2 The mixing power number for Newtonian fluids .

III.3 Mixing power input for non-Newtonian fluids .

III.4 The mixing power ratio versus the aeration number .

III.5 The $(P_g/P)N_A^{0.38}$ ratio versus the Weber number for Newtonian fluids .

III.6 The $(P_g/P)N_A^{0.38}$ ratio versus the Weber number for non-Newtonian fluids .

APPENDIX III.1

MIXING POWER INPUT FOR NEWTONIAN FLUIDS AT 25°C

Rotational Speed (rpm)	Mixing Power Input Per Unit Volume (kW/m^3)			
	Water	Methanol (25%)	Methanol (10%)	Ethylene Glycol (8%)
500	1.047	-	-	-
550	1.393	1.363	1.393	1.416
600	1.799	1.775	1.799	1.832
650	2.296	2.269	2.323	2.993
700	2.866	2.837	2.866	2.993
750	3.533	3.641	3.533	3.594
800	4.289	4.217	4.316	4.349

APPENDIX III.2

THE MIXING POWER NUMBER FOR NEWTONIAN FLUIDS

Rotational Speed (rpm)	The Mixing Power Number (N_p)			
	Water	Methanol (25%)	Methanol (10%)	Ethylene Glycol (8%)
500	6.117	-	-	-
550	6.114	6.210	6.158	6.167
600	6.082	6.230	6.125	6.144
650	6.105	6.270	6.220	6.200
700	6.102	6.270	6.145	6.105
750	6.116	6.220	6.159	6.172
800	6.118	6.25	6.200	6.154

APPENDIX III.3

MIXING POWER INPUT FOR NON-NEWTONIAN FLUIDS

Rotational Speed (rpm)	Mixing Power Input Per Unit Volume (kW/m^3)	
	CMC (0.4%)	CMC (0.67%)
550	-	1.3406
580	1.620	-
600	-	1.7746
640	2.173	-
650	-	2.269
680	2.626	-
700	-	2.808
740	3.405	-
750	-	3.5123
800	-	4.3161
820	4.637	-
850	5.144	-

APPENDIX III.4

THE MIXING POWER RATIO VERSUS THE AERATION NUMBER

Air Flow-Rate (l/min)	$(Q/nD^3)x100$ (dimensionless)	Mixing Power Ratio (P_g / P) Water	Methanol (25%)	Ethylene Glycol (8%)	Glycerol (40%)
14.54	5.981	0.449	0.456	-	0.473
13.65	5.613	0.464	-	0.471	-
12.75	5.245	0.478	0.485	-	0.486
11.86	4.877	0.493	-	0.485	-
10.89	4.519	0.507	0.529	-	0.514
10.13	4.165	0.536	-	0.514	-
9.27	3.813	0.550	0.558	-	0.554
8.34	3.429	0.565	-	0.557	-
7.35	3.021	0.594	0.603	-	0.622
6.45	2.653	0.623	-	0.600	-
5.49	2.258	0.667	0.676	-	0.662
4.59	1.888	0.696	-	0.685	-
3.62	1.488	0.753	0.765	-	0.757
2.71	1.114	0.840	-	0.828	-
2.50	0.886	0.869	-	-	-
1.79	0.782	0.927	-	-	0.946
1.50	0.738	0.985	0.941	-	-

* Rotational Speed = 600 rpm

APPENDIX III.5

The $(P_g/P)N_A^{0.38}$ ratio versus the Weber number for Newtonian fluids.

N_{We}	$(P_g/P)N_A^{0.38} \times 10$
1. Water :	
472.92	1.6320
562.81	1.5789
660.52	1.5323
766.05	1.4891
879.39	1.4506
1000.55	1.4154
2. Methanol (10%) :	
575.60	1.5939
685.01	1.5421
803.94	1.4960
932.38	1.4543
1070.33	1.4169
1217.80	1.3825
3. Ethylene Glycol (8%):	
624.04	1.5723
742.7	1.5211
871.60	1.4757
1010.85	1.4757
1160.41	1.3976
1320.29	1.3637

APPENDIX III.6

The $(P_g/P)N_A^{0.38}$ ratio versus the Weber number for non-Newtonian fluids.

N_{We}	$(P_g/P)N_A^{0.38} \times 10$
1. CMC(0.2%)	
684.50	1.4712
931.68	1.4136
1216.09	1.3686
1540.12	1.2849
2. CMC(0.4%)	
529.59	1.5126
644.83	1.4570
727.95	1.4238
862.08	1.3789
957.80	1.3515
1058.56	1.3261
1137.43	1.3081
3. CMC(0.6%)	
497.08	1.5476
591.56	1.4973
694.27	1.4525
805.19	1.4121
924.32	1.3756
1051.67	1.3423

APPENDIX IV

TABULATED RESULTS FOR FERMENTATIVE HEAT DATA

APPENDIX IV.1

A.niger grown on Glucose (pH=5.5 , T=30°C)

Dynamic Calorimetric Technique (Experiment 1)

No.	Time (h)	OUR (mmole/l.h)	Q_{Term} (kcal/l.h)	Biomass (g/l)
0	0	-	-	1.014
1	2	6.14	0.433	1.400
2	3	10.414	0.894	-
3	5.5	9.945	1.149	-
4	6	16.380	1.392	-
5	6.5	17.037	1.724	-
6	7	22.812	2.093	-
7	7.5	22.757	2.291	-
8	8	26.373	2.486	3.290
9	8.50	24.676	2.306	-
10	9	27.637	2.641	-
11	9.50	28.725	2.641	-
12	10	26.590	2.239	4.850
13	10.50	19.220	1.580	-
14	11	-	-	5.350
15	11.50	13.533	0.962	-
16	12	-	-	6.045
17	12.50	16.191	1.166	-
18	13	-	-	6.193
19	13.50	19.121	1.186	-

APPENDIX IV.2

A.niger grown on Glucose (pH= 5.5 , T= 30°C)

Dynamic Calorimetric Technique (Experiment 2)

No.	Time (h)	OUR (mmole/l.h)	Q_{term} (kcal/l.h)
0	0	-	-
1	3	6.044	0.228
2	4.5	9.023	0.301
3	5	12.034	0.854
4	5.75	16.225	1.479
5	7	23.980	2.105
6	7.5	26.952	2.731
7	8	29.920	3.126
8	8.5	32.880	3.200
9	9	35.860	3,482
10	9.5	35.860	3.482
11	10	35.860	3.200
12*	11	29.97	1.792
13*	11.5	26.980	1.425
14*	12	26.980	1.122
15*	12.5	26.980	1.479

* Wall Growth

APPENDIX IV.3

A.niger grown on Glucose (pH = 5.5 , T = 30 °C)

No.	Time (h)	OUR (mmole/l.h)	Q_{term} (kcal/l.h)	Biomass (g/l)
0	0	-	-	1.346
1	1	2.078	-	-
2	1.60	2.078	-	-
3	3.50	11.743	1.226	-
4	3.67	15.328	1.601	-
5	4	18.919	1.824	1.682
6	4.5	24.511	2.103	-
7	4.67	24.385	2.189	-
8	5	23.876	2.203	-
9	5.50	25.087	2.330	-
10	6	27.120	2.398	1.920
11	6.50	28.641	2.506	-
12	7	34.272	3.207	2.552
13	7.50	31.339	3.297	-
14	8	28.194	2.419	3.252
15	9	18.634	1.416	3.880
16	9.50	17.475	1.420	-
17	10	-	-	4.750
18	10.50	15.868	1.696	-
19	11	17.993	1.383	5.222
20	12	-	-	5.412
21	13	-	-	5.490

APPENDIX IV.4

C. intermedia grown on Glucose (pH=5.5 , T=30°C)

No.	Time (h)	OUR (mmole/l.h)	Q_{ferm} (kcal/l.h)	Biomass (g/l)
0	0	-	-	0.530
1	2	2.644	0.301	0.546
2	4	10.928	0.791	-
3	5	10.608	1.162	-
4	6	12.257	1.340	1.377
5	6.50	19.485	2.191	-
6	7	14.902	1.693	-
7	7.50	22.553	2.556	-
8	8	24.939	3.444	2.835
9	8.50	21.821	2.760	-
10	9.25	22.836	2.543	-
11	9.50	20.243	2.632	-
12	10	24.705	2.792	-
13	10.50	22.952	2.575	-
14	11	20.876	2.589	4.925
15	11.50	22.957	2.804	-
16	12	21.409	2.516	5.590
17	12.50	22.957	2.682	-
18	12.75	22.265	2.035	-
19	13	23.650	2.911	6.068
20	13.42	20.933	2.142	-

APPENDIX IV.5

E.coli grown on Glucose (pH=7 , T=37°C)

No.	Time (h)	OUR (mmole/l.h)	Q_{ferm} (kcal/l.h)	Biomass (g/l)
0	0	-	-	0.606
1	1.58	1.906	0.086	-
2	2.00	3.139	0.464	-
3	2.50	4.339	0.568	0.736
4	3.00	4.735	0.611	-
5	3.5	17.104	2.058	-
6	4.00	19.855	2.395	1.700
7	4.25	27.096	3.724	-
8	4.58	33.095	4.425	-
9	4.92	38.214	5.297	-
10	5.25	42.599	6.494	-
11	5.67	48.448	6.925	-
12	6.08	22.818	3.146	-
13	6.50	6.921	0.843	3.817
14	6.83	7.698	0.916	3.895
15	7.00	6.018	0.749	-
16	7.25	5.814	0.951	-
17	7.33	6.358	0.905	-

APPENDIX IV.6

E.coli grown on a mixture of Glucose and Lactose

No.	Time (h)	OUR (mmole/l.h)	Q_{ferm} (kcal/l.h)	Biomass (g/l)	Glucose Concentration (g/l)
1	0	-	-	0.625	11.30
2	1.25	-	-	0.705	10.30
3	4.92	-	-	0.725	10.20
4	6	0.469	-	-	-
5	7.33	1.259	0.203	0.837	10.00
6	7.50	4.625	0.511	-	-
7	8.50	-	-	1.160	-
8	9	4.351	0.423	-	-
9	9.50	7.612	1.051	1.340	9.38
10	9.83	9.296	1.028	-	-
11	10.17	11.287	1.773	-	-
12	10.50	11.736	1.532	1.852	8.67
13	10.67	13.827	1.753	-	-
14	11	18.136	2.598	-	-
15	11.33	21.477	2.695	-	-
16	11.42	23.289	2.459	-	-
17	11.50	26.389	3.044	1.936	7.18
18	11.83	29.900	3.484	-	-
19	12	32.213	3,886	-	-
20	12.17	35.925	4.443	-	-
21	12.50	42.505	5.017	2.664	4.95
22	12.58	43.636	4.902	-	-
23	12.75	46.564	5.321	-	-
24	12.83	48.259	5.634	-	-
25	13	48.699	5.873	-	-
26	13.17	53.318	6.463	-	-

APPENDIX IV.6 (Cont.)

No.	Time (h)	OUR (mmole/l.h)	Q_{ferm} (kcal/l.h)	Biomass (g/l)	Glucose Concentration (g/l)
27	13.33	53.933	6.449	-	-
28	13.50	58.264	6.597	4.532	0.611
29	13.58	40.441	5.437	-	-
30	13.67	35.925	3.459	-	-
31	13.83	55.795	4.414	5.088	0.022
32	14	56.409	6.125	-	-
33	14.17	72.276	8.716	-	-
34	14.33	72.446	9.013	-	-
35	14.50	77.196	9.877	6.304	0.002
36	14.75	77.022	10.032	-	-
37	14.83	78.906	10.019	-	-
38	15	83.287	10.196	-	-
39	15.17	81.644	10.109	-	-
40	15.33	79.259	9.777	-	-
41	15.50	45.389	5.290	7.568	0.005
42	15.58	34.307	3.529	-	-
43	15.67	32.801	2.020	-	-
44	15.75	30.553	1.837	-	-
45	16	30.165	1.623	-	-
46	16.08	30.034	1.584	-	-

APPENDIX IV.7

C.lipolytica grown on Glucose (pH = 5.5 , T = 30°C)

No.	Time (h)	OUR (mmole/l.h)	Q_{ferm} (kcal/l.h)	Biomass (g/l)
0	0	-	-	1.560
1	2	5.015	0.554	1.760
2	2.50	5.120	0.569	-
3	3	5.906	0.607	-
4	3.50	7.931	0.803	-
5	4	8.705	0.969	2.343
6	5.75	11.244	1.406	-
7	6	15.939	1.622	-
8	6.50	14.938	1.425	3.610
9	7	16.952	1.789	-
10	7.50	20.494	2.059	-
11	8.08	24.637	2.487	-
12	9	30.306	2.918	5.496
13	9.50	31.958	3.181	-
14	10	35.973	3.469	-
15*	10.50	38.434	3.376	-
16*	11	37.524	3.376	5.834
17*	11.5	40.587	3.249	-
18*	12.10	39.814	3.098	-
19*	12.50	32.228	3.345	-

* Foaming problem

Experiment was terminated earlier due to foaming problem . The final cell concentration after 24 hours is 11.280 g / l .

APPENDIX IV.8

C.lipolytica grown on n-Dodecane (pH = 5.5 , T = 30°C)

No.	Time (h)	OUR (mmole/l.h)	Q_{ferm} (kcal/l.h)	Biomass (g/l)
0	0	-	-	0.902
1	2	0.979	-	-
2	2.83	3.353	-	-
3	3.08	3.682	-	-
4	9.25	18.825	2.301	2.045
5	9.33	19.544	2.243	-
6	9.83	20.675	2.991	-
7	10.00	22.920	2.992	-
8	10.50	25.532	3.268	-
9	10.58	26.275	3.271	-
10	11.00	28.731	3.434	-
11	11.08	30.220	3.334	-
12	11.75	30.407	3.621	-
13	11.83	32.640	3.847	2.928
14	12.08	38.239	4.117	-
15	13.25	37.934	3.840	-
16	13.42	41.860	4.150	-
17	13.92	41.332	4.406	-
18	14.17	43.518	4.594	-
19	15.00	47.343	4.798	5.235
20	16.00	51.429	5.598	-
21	17.00	27.424	3.152	6.360
22	17.08	24.471	2.549	-
23	17.25	21.477	1.747	-
24	17.50	13.946	1.311	6.823
25	18.00	9.215	1.152	6.675
26	19.00	6.947	0.657	-

APPENDIX IV.9

C.lipolytica grown on Hexadecane (pH=5.5,T=30^{0}C)

No.	Time (h)	OUR (mmole/l.h)	Q_{ferm} (kcal/l.h)	Biomass (g/l)
0	0	-	-	0.560
2	4.67	9.735	1.585	0.833
3	5.17	10.489	1.787	-
4	6.25	15.277	2.670	-
5	6.67	16.332	2.788	1.163
6	7.17	17.642	3.146	-
7	7.67	19.334	3.047	-
8	8.67	25.098	3.472	2.045
9	9.17	27.239	3.923	-
10	9.67	31.896	3.864	-
11	10.17	33.383	3.335	-
12	10.67	37.062	4.651	3.015
13	11.08	40.955	5.028	-
14	11.17	42.403	5.192	-
15	11.42	40.593	5.728	-
16	11.84	42.176	5.323	-
17	12.17	44.393	5.852	-
18	12.59	48.816	6.180	-
19	12.67	50.255	6.299	5.575

APPENDIX IV.9 (Cont.)

No.	Time (h)	OUR (mmole/l.h)	Q_{ferm} (kcal/l.h)	Biomass (g/l)
20	13.08	52.897	6.533	-
21	13.58	54.364	6.929	-
22	14.00	57.001	6.987	-
23	14.33	59.603	7.135	-
24	14.67	57.001	7.059	7.397
25	14.75	59.314	7.034	-
26	15.00	56.709	7.201	-
27	15.17	60.044	7.487	-
28	15.33	58.873	7.478	-
29	15.67	59.126	6.521	8.430
30	16.17	55.089	6.129	9.410

APPENDIX IV.10

C.utilis grown on Glucose (pH=4.5 , T=30°C)
Dynamic Calorimetry Technique

No.	Time (h)	OUR (mmole/l.h)	Q_{ferm} (kcal/l.h)
0	0	-	-
1	1	0.395	0.038
2	2	4.147	0.398
3	3	7.165	0.642
4	4	8.723	0.795
5	5.33	21.285	1.699
6	6	27.408	2.478
7	6.50	26.802	2.784
8	7	31.616	3.225
9	7.50	38.233	3.744
10	8	44.828	4.374
11	8.50	-	4.772
12	9	55.966	5.389
13	9.50	60.849	5.624
14	10	58.130	5.766
15	10.50	57.705	6.069
16	11	63.756	6.069
17	11.50	63.190	6.069
18	12	53.821	4.230
19	12.50	51.399	3.994
20	13	18.712	1.919
21	13.50	14.027	0.795

APPENDIX IV.11

C. utilis grown on Glucose (pH=4.5 , T= 30°C)

No.	Time (h)	OUR (mmole/l.h)	Q_{ferm} (kcal/l.h)	Biomass (g/l)
0	0	-	-	0.746
1	1.17	7.185	0.612	-
2	2.00	-	●	1.036
3	2.17	13.285	0.944	-
4	5.00	25.549	2.333	2.092
5	6.00	28.758	3.050	-
6	6.58	33.212	3.577	-
7	7.00	46.213	4.495	3.858
8	7.50	51.063	5.036	-
9	8.00	57.249	6.074	-
10	8.50	60.643	6.162	-
11	9.00	62.453	6.318	8.180
12	9.50	63.504	6.753	-
13	10.0	66.042	6.618	11.708
14	10.08	64.245	6.450	-
15	10.58	64.380	7.085	-
16	11.00	60.341	5.255	13.840
17	11.67	26.138	2.241	-
18	12.00	25.156	1.882	14.382

APPENDIX IV.12

C.utilis grown on Sucrose (pH = 4.5 , T = 30°C)

No.	Time (h)	OUR (mmole/l.h)	Q_{ferm} (kcal/l.h)	Biomass (g/l)
0	0	-	-	1.144
1	2	-	-	1.228
2	2.25	8.221	0.781	-
3	2.50	10.607	1.043	-
4	3	13.356	1.358	-
5	3.50	15.333	1.465	-
6	4	17.750	1.967	1.904
7	4.5	21.991	2.305	-
8	5.5	24.295	2.305	-
9	6	29.903	2.704	3.580
10	6.17	30.667	3.086	-
11	6.50	31.303	3.221	-
12	7	29.457	2.777	-
13	7.50	29.457	2.855	-
14	8	29.264	2.585	6.192
15	8.17	30.030	2.799	-
16	8.50	28.498	3.109	-
17	9	30.030	2.860	-
18	9.50	32.292	2.832	-
19	10	30.763	2.842	9.440
20	10.50	28.373	2.821	-
21	11	26.395	2.668	-
22	11.50	26.074	2.499	-
23	12	26.965	2.672	12.456
24	12.50	-	-	12.980

APPENDIX IV.13

C.utilis grown on Ethanol (pH=4.5 , T=30°C)

No.	Time (h)	OUR (mmole/l.h)	Q_{term} (kcal/l.h)	Biomass (g/l)
0	0	-	-	0.438
1	2	7.316	0.768	-
2	2.50	9.648	0.891	-
3	3.17	11.643	1.077	-
4	4.00	15.927	-	0.666
5	4.58	16.700	1.915	-
6	6.00	15.927	2.100	0.998
7	6.50	18.049	1.977	-
8	7.00	-	1.829	-
9	8.00	24.368	2,456	1.544
10	8.50	27.696	3.155	-
11	9.08	30.860	2.995	-
12	9.50	41.519	4.190	-
13	10.0	46.942	4.913	2.624
14	10.25	47.843	4.781	-
15	10.50	46.017	5.000	-
16	11.00	49.052	5.236	-
17	11.42	55.521	5.451	-
18	12.00	57.935	5.608	4.010
19	12.50	63.918	6.923	-
20	13.00	59.419	6.099	4.870
21	13.50	61.524	6.491	-
22	14.00	61.524	6.797	5.610

APPENDIX IV.14

C.utilis grown on Glucose and Cellobiose (pH = 4.5 , T = 30°C)

No.	Time (h)	OUR (mmole/l.h)	Q_{ferm} (kcal/l.h)	Biomass (g/l)	Glucose Concentration (g/l)
0	0	-	-	0.32	15.5
1	1.25	2.216	0.082	-	-
2	1.50	3.393	0.529	-	-
3	2	4.762	0.420	-	-
4	2.42	4.230	0.420	0.467	15.0
5	3	8.061	1.033	-	-
6	3.58	7.796	1.166	-	-
7	3.75	-	-	0.703	14.8
8	4.17	10.066	1.770	-	-
9	4.50	11.301	1.911	-	-
10	4.67	12.065	2.113	0.986	14.0
11	5.42	11.901	2.207	-	-
12	5.67	15.342	3.099	1.456	13.5
13	6	17.828	3.351	-	-
14	6.33	21.759	3.323	-	-
15	6.58	24.893	4.159	-	-
16	6.67	28.375	4.533	2.285	12.3
17	7	30.777	5.116	-	-

APPENDIX IV.14 (Cont.)

No.	Time (h)	OUR (mmole/l.h)	Q_{ferm} (kcal/l.h)	Biomass (g/l)	Glucose Concentration (g/l)
18	7.25	32.519	5.231	-	-
19	7.33	38.234	5.577	-	-
20	7.42	34.166	5.577	-	-
21	7.58	40.016	6.179	-	-
22	7.67	42.729	6.613	3.555	9.10
23	7.75	45.715	6.186	-	-
24	7.83	42.421	5.759	-	-
25	8	45.041	6.176	-	-
26	8.25	47.344	6.609	-	-
27	8.42	48.997	6.918		
28	8.33	51.062	6.901	5.660	3.90
29	9	53.180	7.074	-	-
30	9.33	51.113	7.410	-	-
31	9.42	51.278	7.410	-	-
32	9.50	48.921	6.859	7.623	0.155
33	9.67	46.672	5.299	-	-
34	9.83	27.862	4.255	-	-
35	9.92	23.282	2.941	-	-
36	10.08	17.943	2.240	-	-
37	10.17	20.762	2.225	7.630	0.048
38	10.50	17.079	1.756	-	-

APPENDIX V

CALIBRATION FOR INSTRUMENTS

V.1 Calibration for Strain-Gauge Dynamometer (SGD) .

V.2 Calibration for Carbon Dioxide Analyzer .

V.3 Calibration for EMF Converter .

V.4 Calibration for Electronic Controller .

V.5 Calibration for Thermocouple .

V.6 Calibration for Thermistor .

V.7 Calibration for Air Rotameter .

V.8 Calibration for Cooling Water Rotameter .

APPENDIX V.1

CALIBRATION FOR SGD. (25°C)

I = 25 mA
Gain = 200

Weight (grams)	de (μv)	de (volt)	Torque (kg-cm)
200	21	0.0042	0.511
300	30	0.0060	0.766
400	41.5	0.0083	1.022
500	50.0	0.010	1.278
800	70.0	0.014	1.788
1000	100.0	0.020	2.555
1200	120.0	0.024	3.066
1500	150.0	0.030	3.832
1700	170.0	0.034	3.832
2000	197.5	0.0395	5.110
2678	212.5	0.0425	6.843
2878	232	0.0464	7.354
3378	282.5	0.0565	8.63
3578	302.5	0.0605	9.143
3728	317	0.0635	9.526
3878	331.5	0.0663	9.91
4378	381.0	0.0762	11.187
4578	400.0	0.080	11.698

Note : Torque = Weight * Length (Length = 1.006" = 2.55524 cm)

APPENDIX V.2

CALIBRATION FOR CARBON DIOXIDE ANALYZER

Scale Reading	% CO_2	mvolt
0	0	0
26.5	1.18	27.10
52	3.01	53.80
70	4.99	71.80
74.50	5.45	76.50
100	10	10

$$Y_{CO_2} = 8.9 \times 10^{-3} \, de^{1.47554}$$

Correlation Coefficient = 0.99703

APPENDIX V.3

CALIBRATION FOR EMF CONVERTER

dc (mvolt)	milliampere
0.96	10
1.15	15
1.35	20
1.55	25
1.75	30
1.95	35
2.15	40
2.34	45
2.55	50

APPENDIX V.4

CALIBRATION FOR ELECTRONIC CONTROLLER

Scale reading	milliampere
0	10
10	14
20	18
30	21.8
40	26
50	30
60	34
70	38
80	42.1
90	45.9
100	50

APPENDIX V.5

THE CALIBRATION FOR THERMOCOUPLE

Temperature (^{o}C)	Output (mvolt)	Temperature (^{o}C)	Output (mvolt)
20	0.96	22	1.06
23.50	1.13	26.56	1.33
26.80	1.35	27.0	1.36
27.50	1.38	28.0	1.40
29.0	1.44	29.50	1.46
30.0	1.49	31.0	1.54
31.65	1.57	31.80	1.58
32.0	1.60	32.50	1.625
33.0	1.65	34.00	1.700
35.0	1.75	36.00	1.800
37.0	1.850	38.0	1.900
39.0	1.960	40.0	2.01
42.0	2.12	45.0	2.28
47.0	2.39	48.0	2.44
49.0	2.49	50.0	2.55
51.0	2.60	-	-

APPENDIX V.6

THE CALIBRATION FOR THERMISTOR

Temperature (°C)	Output (mvolt)	Temperature (°C)	Output (mvolt)
18.80	72.64	18.65	72.77
19.73	67.45	19.64	67.95
20.0	66.17	19.90	66.62
19.97	66.30	20.30	64.66
20.35	64.44	20.68	62.70
20.62	63.05	21.33	59.50
22.0	56.07	22.36	54.23
22.28	54.57	22.82	51.85
23.48	48.43	23.42	48.70
24.30	44.19	24.36	43.77
25.10	39.86	25.17	39.50
26.00	35.09	26.94	29.94
26.88	30.30	27.83	25.09
27.77	25.43	28.53	21.28
28.50	21.30	29.60	15.15
29.65	14.93	30.30	11.36
30.80	8.50	31.46	4.75
32.05	1.30	32.10	1.05
32.25	0.30	32.28	0.00

APPENDIX V.7

CALIBRATION FOR AIR ROTAMETER

Scale Reading	Elapsed Time (Second)	Volume (ft^3)	Flow Rate (l/min)
2	434	0.5	1.957
3	287.5	0.5	2.955
4	215	0.5	3.951
5	169.5	0.5	5.012
6	141.7	0.5	5.995
7	120.6	0.5	7.044
8	105.9	0.5	8.022
9	93.3	0.5	9.105
10	83.9	0.5	10.125
11	76.8	0.5	11.060
12	70.8	0.5	11.998
13	65.6	0.5	12.949
14	61.0	0.5	13.926
15	57.0	0.5	14.903
16	53.5	0.5	15.878

APPENDIX V.8

CALIBRATION FOR COOLING WATER ROTAMETER

Scale Reading	Volume(mℓ)	Elapsed Time	Flow Rate(ℓ/h)
7.5	400	42.7"	33.724
7	400	46.6"	30.901
6.5	400	50.7"	28.402
5.5	400	55.8"	25.806
5	400	1'2.2"	23.151
4.5	400	1'9.7"	20.660
4	400	1'11.9"	18.159
3.5	400	1'34"	15.319
3	400	2'14.5"	10.706
2.5	400	2'52.9"	8.329
2	400	4'5"	5.878
1	100	3'13.7"	1.859

APPENDIX VI

CALCULATION OF THE ENERGY DISSIPATED BY THE BUBBLING GAS

The energy dissipated by the bubbling gas could be estimated by the following equation :

$$Q_{bub} = \frac{Q\,\rho_G}{V_L}\frac{U_{in}^2}{2} + V_s g\,\rho_L$$

In the typical condition of this study,

ρ_G : 0.0753 lb/ft^3 1.21 x 10^{-3} g/cm^3 (air)

g : 980 cm/sec^2

ρ_L : 1 g/cm^3 (broth density)

V_L : 9 liters (operating volume of fermentation broth)

d_o : 0.3 cm (sparger hole diameter)

D : 0.21 cm (diameter of tank)

Q : 8.505 l/min (gas flow rate)

V_s : 0.409 cm/sec (superficial velocity $Q/\pi D^2/4$)

U_{in}: 2.10^3 cm/sec (sparger hole velocity of gas)

(i) The potential energy change per unit volume :

$$\Delta PE = V_s g\,\rho_L = 40.08\ W/m^3 = 0.034\ kcal/l.h$$

(ii) The kinetic energy change per unit volume :

$$\Delta KE = (Q\rho_G/V_L)U_{in}^2/2 = 0.0038\ W/l = 0.0033\ kcal/l.h$$

The energy dissipated by the sparging gas , therefore , is

$$Q_{bub} = \Delta PE + \Delta KE = 0.037\ kcal/l.h$$

The gas sparging power input, obviously, can be neglected .

APPENDIX VII

THEORETICAL CALCULATION FOR THE HEAT LOSS TO THE SURROUNDINGS

Thermal conductivity (Glass,Pyrex)	k_{01} = 0.63 BTU/h.ft.^{o}F
Thermal conductivity (Styrofoam)	k_{12} = 0.23 BTU/h.ft^{2}.^{o}F/inch
Thermal conductivity (Water)	k_{w} = 0.360 BTU/h.ft.^{o}F
Thermal conductivity (Air)	k_{air} = 0.015 BTU/h.ft.^{o}F
Specific heat (Water)	C_p = 1.0 kcal/kg.^{o}C
Density (Water)	ρ = 1.0 g/cm^{3}
Viscosity (Water)	μ = 0.007975 g/cm.sec
Inner radius of fermentor	r_o = 11.1 cm
Outer radius of fermentor	r_1 = 12.1 cm
Impeller rotational speed	N = 700 rpm
Impeller diameter	d = 7.4 cm
Inner diameter of fermentor	D = 22.2 cm
Fermentor height	L = 43.5 cm

1. $\ln(r_1/r_o)/k_{01}$ = $\ln(12.1/11.1)/0.63$
   = 0.13692 (h.ft.^{o}F/BTU) **********

2. $\ln(r_2/r_1)/k_{12}$ = $\ln(14.6/12.1)/(0.23/12)$
   = 9.79910 (h.ft.^{o}F/BTU) **********

3. $h_o D/k_f$ = $0.74 (N d^2 \rho/\mu)^{2/3} (C_p \mu/k_f)^{1/3}$

APPENDIX VII

THEORETICAL CALCULATION FOR THE HEAT LOSS TO THE SURROUNDINGS

Thermal conductivity (Glass,Pyrex)	k_{01} = 0.63 BTU/h.ft.^{o}F
Thermal conductivity (Styrofoam)	k_{12} = 0.23 BTU/h.ft^{2}.^{o}F/inch
Thermal conductivity (Water)	k_{w} = 0.360 BTU/h.ft.^{o}F
Thermal conductivity (Air)	k_{air} = 0.015 BTU/h.ft.^{o}F
Specific heat (Water)	C_{p} = 1.0 kcal/kg.^{o}C
Density (Water)	ρ = 1.0 g/cm^{3}
Viscosity (Water)	μ = 0.007975 g/cm.sec
Inner radius of fermentor	r_{o} = 11.1 cm
Outer radius of fermentor	r_{1} = 12.1 cm
Impeller rotational speed	N = 700 rpm
Impeller diameter	d = 7.4 cm
Inner diameter of fermentor	D = 22.2 cm
Fermentor height	L = 43.5 cm

1. $\ln(r_1/r_o)/k_{01}$ = $\ln(12.1/11.1)/0.63$
   = 0.13 (h.ft.^{o}F/BTU) **********

2. $\ln(r_2/r_1)/k_{12}$ = $\ln(14.6/12.1)/(0.23/12)$
   = 9.79 (h.ft.^{o}F/BTU) **********

3. $h_o D/k_f$ = $0.74 (N.d^2 \rho/\mu)^{2/3} (C_p \mu/k_f)^{1/3}$

$$N_{Re} = \frac{d^2 N \rho}{k_f} = \frac{(7.4)^2 \text{ (cm}^2\text{) (700/60) (1/sec) (1) (g/cm}^3\text{)}}{0.007975 \text{ (g/cm.sec)}}$$

$= 0.80 \times 10^5$

$(N_{Re})^{2/3} = 1858$

$(C_p \mu/k_f) = 4.8$ (Water at 30°C)

$(C_p \mu/k_f)^{1/3} = 1.68$

$h_o D/k_f = (0.74)(1858.31652)(1.68979)$

$= 2323$

$h_o = 2323.72 \times 0.360 / (22.2/30.48)$ BTU/ft^2.h.°F

$h_o = 1148$ BTU/ft^2.h.°F

$1/r_o h_o = 1/(11.1/30.48)(1148.54585)$ ft.h.°F/BTU

$= 0.0023$ ft.h.°F/ BTU **********

4. $h_\infty L/k_f = Nu_f = C\ (Gr_f.Pr_f)^m$

$T_f = \frac{T_\infty + T_w^*}{2}$

$= (30 + 24)/2 = 27°C = 89.24\ °F$

$Pr_f = 0.72$ (Air at 90 °C)

$\frac{g \beta \rho^2}{\mu^2} = 1.80 \times 10^6$ 1/ft^3.°F (Air at 90°F)

$Gr = g \beta \rho^2 (T_w^* - T_\infty) L^3/\mu^2$

$Gr_f = 1.80 \times 10^6 (30 - 24)(212/100)(43.5/30.48)^3$

$= 0.66 \times 10^8$

$Gr_f.Pr_f = 0.47 \times 10^8$

From Table II, m = 0.25 and C = 0.59

$h_\infty L / k_f = 0.59\ (0.47919 \times 10^8)^{0.25}$

$= 0.59 \times 0.83201 \times 10^2$

$= 49$

$h_\infty = (49.08859)(k_f)/L$

$= (49.08859)(0.015)/(43.5/30.68)$ BTU/ft.^{2} h. $^\circ$F

$= 0.51$ BTU/ft^2.h. $^\circ$F

$(1/r_2 h_\infty) = 1/(14.6/30.48)(0.51932)$ ft.h.$^\circ$F/BTU

$= 4$ ft.h.$^\circ$F/BTU **********

$1/r_o h_o + \ell n(r_1/r_o)/k_{01} + \ell n(r_2/r_1)/k_{12} + 1/r_2 h_\infty = 0.002 + 0.13 + 9.79 + 4.01$

$= 13.95$ h.ft.$^\circ$F/BTU

$= 9.38$ h.m.$^\circ$C /kcal **********

$$U_1 A_1 \simeq \frac{2\pi L(1 + r_2/L)}{V_L(1/r_o h_o + \ell n(r_1/r_o)/k_{01} + \ell n(r_2/r_1)/k_{12} + 1/r_2 h_\infty}$$

$U_1 A_1 \simeq 2\pi(0.435)(1 + 14.6/43.5)/(9 \times 9.38316)$

$\simeq 0.043$ kcal/ℓ.h.$^\circ$C **********

The experimental value of $U_1 A_1$ was determined as 0.068 kcal/ℓ.h.$^\circ$C . The difference between the experimental and theoretical value of $U_1 A_1$ would certainly be expected since the heat sink could not been taken into consideration in this calculation .

APPENDIX VIII

A SAMPLE CALCULATION FOR THE FERMENTATIVE HEAT AND THE OXYGEN CONSUMPTION

Experimental Data :

Organism	*C. lipolytica*
Substrate	n-Dodecane
Fermentation time	14.17 hours
Air Flow Rate (F_{air})	8.40420 ℓ/min
Impeller Rotational Speed (N)	800 rpm
Ambient Air Temperature (T_{amb})	26.40 ^{o}C
Liquid Broth Temperature (T)	29.93 ^{o}C
Inlet Air Temperature	29.98 ^{o}C
Inlet Temperature of Cooling Water (T_c)	17.20 ^{o}C
Heat Activated by the dc Power Supply (E)	26.25 volt dc
Immersion Heater Resistance	7.29 Ω
Oxygen Concentration in the Exit Gas Stream	19.416 %
CO_2 Concentration in the Exit Gas Stream	0.7 %
Heat Transfer Coefficient $U_2A_2^*$	1.15517 kcal/ℓ.h.^{o}C

A. THE RATE OF OXYGEN CONSUMPTION

The oxygen uptake rate (OUR) was calculated by the following equation :

$$OUR = \frac{F_N}{V_L}\left[\frac{p_{O_2}^{in}}{1 - p_{O_2}^{in} - p_{CO_2}^{in}} - \frac{p_{O_2}^{out}}{1 - p_{O_2}^{out} - p_{CO_2}^{out}}\right] \quad \ldots\ldots (1)$$

where F_N the molal flow rate of inert (N_2) gas was calculated as 0.79 times inlet air flow rate. For a fermentor aerated with water-saturated air, Equation (1) becomes :

$$OUR = \frac{F_N}{V_L}\left[0.26507 - \frac{p_{O_2}^{out}}{1 - p_{O_2}^{out} - p_{CO_2}^{out}}\right] \quad \ldots\ldots (2)$$

where

$p_{O_2}^{in}$ = 0.20946

$p_{CO_2}^{in}$ = 0.00033

OUR = Oxygen uptake rate (mmol /ℓ.h)

F_N = Gas flow rate (ℓ/min)

V_L = Volume of liquid in fermentor (ℓ)

Under typical condition of experiments, the operating volume broth is 9ℓ and the ingoing gas flow rate equals 8.40420 ℓ/min and if the concentrations of oxygen and carbon dioxide in the out-going gas stream were measured to be 0.19416 and 0.007 , respectively . The value of the oxygen uptake rate (OUR) was calculated as :

$$OUR = \frac{2116.534 \times 8.40420}{9}\left(0.26507 - \frac{0.19416}{1 - 0.19416 - 0.007}\right)$$

$OUR = 43.518$ mmol /ℓ.h **********

B. THE RATE OF HEAT EVOLUTION

* $Q_{agi} + Q_{bub} - Q_{surr} = 1.0748$ kcal/ℓ.h

* $Q_{ferm} = U_2 A_2^* (T - T_c) - E^2 \times 0.86042/(9)(7.29) - 1.0748$

$Q_{ferm} = 1.15517(29.93 - 17.20) - (26.25)^2/76.2535 - 1.0748$

$Q_{ferm} = 4.594$ kcal/ℓ.h **********

C. THE VALUE OF PROPORTIONALITY CONSTANT ΔH_{fo}

$\Delta H_{fo} = Q_{ferm} / OUR$

$\Delta H_{fo} = 0.1056$ kcal/ mmol O_2 **********

APPENDIX IX

DESIGN OF THERMISTOR CIRCUIT

It is necessary to obtain a linear relationship of the temperature rise as a function of time in the control element IJKL (Figure II.1) . This will enable the evaluation of dT/dt and hence the transient heat term $\Sigma_i M_i C_{pi} dT/dt$ as specified in Equation (116) .

Starting with the thermistor used in the temperature controller, the variation in the thermistor resistance as a function of temperature must first be evaluated. This was done by connecting the thermistor immersed in a variable temperature bath to a gaurded Wheatstone bridge. The balancing of the bridge legs to give null current detection will specify the resistance of the thermistor at the particular temperature. Given the accuracy of the resistance measurement it is necessary to maintain an equally accurate temperature constancy of the variable temperature water bath. This was possible using the constant temperature water circulator.

From the data obtained, the following equation was possible :

$$R \simeq 0.005497 \exp\left(\frac{3813.636}{T_K}\right) \quad \ldots\ldots\ldots\ldots (1)$$

The accuracy of Equation (1) being ± 0.1% . From the proposed relationship it is apparent that the millivolt response to the change in resistance would be non-linear. In order to obtain a linear millivolt output as a function of temperature of the bridge circuit of Figure A.IX.1 may be used. The requirements of the bridge are as follows :

1. Output across R_M = 0 mv at 32 °C
2. Output across R_M = 4 mv at 32.7 °C
3. $R_1 = R_T$ at 32 °C
4. $R_2 = R_3 = R_T$ at 32.35 °C

By substitution of the temperature conditions R_1, R_2, R_3 and R_T were evaluated from Equation (1) and found to be :

R_1 = 1470.5 ohms

$R_2 = R_3$ = 1449.4 ohms

R_T = 1428.8 ohms

The expression for the current i across R_M is given by the bridge equation :

$$i = \frac{e(R_1R_3 - R_TR_2)}{R_M (R_1 + R_2)(R_T + R_3) + R_TR_1(R_2+R_3) + R_2R_3(R_T+R_1)} \quad (2)$$

Since $R_M = V/i$ with e = 1.5 volt (depends on the power supply to the circuit) and V = 4 mv, substitution in Equation (2) gives R_M = 854.2 Ω thus specifying the bridge completely .

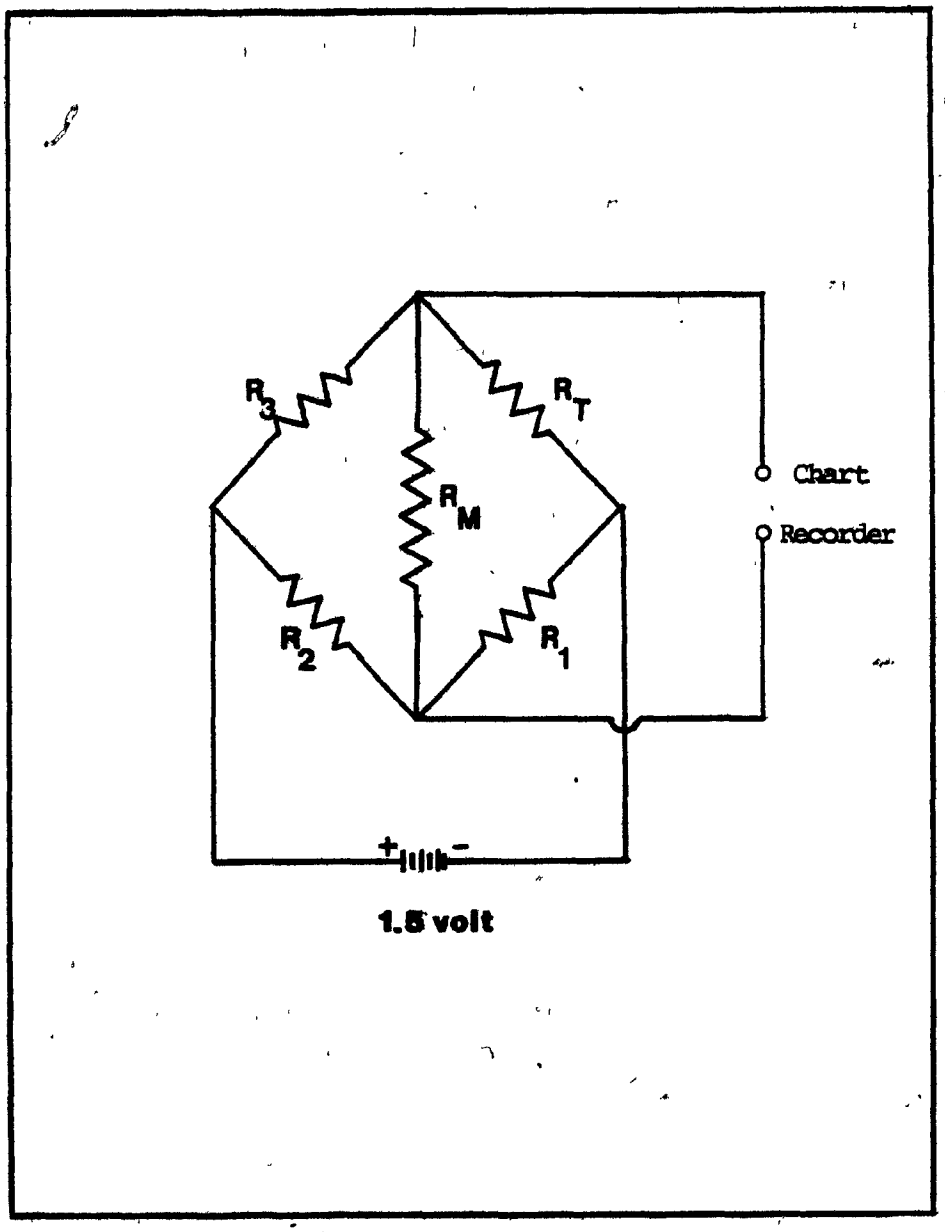

Figure A.IX.1 : Design of Thermistor Circuit

APPENDIX X

COMPONENTS OF ATMOSPHERIC AIR[1]

(Exclusive of water vapour)

Constituent	Content (%) By Volume	Content (ppm) By Volume
N_2	78.084±0.004	
O_2	20.946±0.002	
CO_2	0.033±0.001	
A	0.934±0.001	
Ne		18.18±0.04
He		5.24±0.004
Kr		1.14±0.01
Xe		0.087±0.01
H_2		0.5
CH_4		2
N_2O		0.5±0.1

1. Weast, R.C., "Handbook of Chemistry and Physics" CRC Press, Cleveland, Ohio (1946)

NOMENCLATURE

Some symbols defined in the text and used only once are not listed here.

Symbol	Meaning
A	Cross-Sectional Area
A_o	Base Area of Heat Transfer
C	Proportionality Constant in Equation (34)
C_1	Proportionality Constant in Equation (47)
C_1^*	Proportionality Constant in Equation (63)
C_2	Proportionality Constant in Equation (50)
C_{air}	Heat Capacity of Air
C_c	Heat Capacity of Cooling Water
C_p	Heat Capacity
C_w	Heat Capacity of Water
d	Impeller Diameter
D	Tank Diameter
d_i	Inner Diameter of Hollow Shaft
d_o	Outer Diameter of Hollow Shaft
de	Potential Generated Between the Terminals of the Bridge
E	Young's Modulus
F_{in}	Inlet Gas Flow Rate
F_{out}	Outlet Gas Flow Rate

F_N	Molal Flow Rate of Inert (N_2) Gas
G	Modulus of Rigidity
g	Gravitational Acceleration
g_c	Conversion Factor
h	Liquid Height
h_{or}	Heat Transfer Coefficient at the Fermentor Wall
h_r	Heat Transfer Coefficient at the Ambient Insulation Interface
h_∞	Heat Transfer Coefficient on the Ambient Side
I	Current of Immersion Heater
I_p	Polar Moment of Inertia
K	Constant in Equation (65)
K_1	Constant in Equation (32)
K_2	Function of Aeration Number defined in Equation (44)
K_c	Gain of Controller
K_M	Gain of Measurement Device (Thermocouple)
K_p	Gain of Programmble Power Supply
K_α	Constant in Equation (81)
K^*_α	Constant in Equation (88)
K_s	Gauge Factor
k_f	Thermal Conductivity of Fluid Evaluated at the Mean Film Temperature
k_{01}	Thermal Conductivity of Region 01
k_{12}	Thermal Conductivity of Region 12
k_{02}	Thermal Conductivity of Region 02

L	Length of Reactor
m	Reciprocal of Poisson's Ratio
m^*	Exponent in Equation (63)
M	Torque of Impeller Shaft
n^*	Exponent in Equation (63)
N	Rotational Speed of Impeller Shaft
OUR	Oxygen Uptake Rate
p	Total Pressure
$p_{CO_2}^{in}$, $p_{CO_2}^{out}$	Concentrations of CO_2 in Inlet and Outlet Gas
$p_{O_2}^{in}$, $p_{O_2}^{out}$	Concentrations of O_2 in Inlet and Outlet Gas
p_w^{in}, p_w^{out}	Concentrations of Water in Inlet and Outlet Gas
P	Mechanical Agitation Power in Ungassed Liquid
P_g	Mechanical Agitation in Gas-Liquid Dispersion
P_w	Vapor Pressure of Water
Q	Gas Flow Rate
Q_c	Flow Rate of Cooling Water
Q_{agi}	Heat of Agitation
Q_{bub}	Heat Dissipated by the Bubbling Gas
Q_{con}	Heat Removal by the Action of Controller
Q_{evp}	Heat of Evaporation
Q_{sen}	Sensible Heat Loss

Q_{surr}	Heat Loss to the Surroundings
Q^1_{surr}	Heat Loss to the Surroundings in the Radial Direction
Q^2_{surr}	Heat Loss to the Surroundings in the Axial Direction
Q^3_{surr}	Heat Sink
Q^B_{surr}	Heat Loss to the Surroundings from the Top Plate
Q^T_{surr}	Heat Loss to the Surroundings from the Bottom of the Reactor
$\bar{Q}_{pss}$	Constant Average Power Dissipated by the Immersion Heater
$\tilde{Q}_{pss}$	Fluctuating Power Dissipated by the Immersion Heater
Q_{pss}	Power Dissipated by the Immersion Heater
q_o	Heat Flux Defined in Equation (28)
q_{01}	Heat Flux in Region 01
r	Radial Co-ordinate from Fermentor Axis
r_o	Radius of Fermentor Jar
r_1	Outer Radius of Fermentor Jar
r_2	Outer Radius of Insulation
R_3	Outer Radius of Insulation (r_2)
T	Temperature of fermentation Broth
$\bar{T}$	Constant Average Temperature of Fermentation Broth
$\tilde{T}$	Fluctuating Temperature of Fermentation Broth
T_{amb}	Temperature of the ambient air
T_c	Temperature of Inlet Cooling Water

T_{in}	Temperature of Entering Air
T_{out}	Temperature of Exiting Air
T_w	The Average Coolant Temperature
T_w^*	Temperature at Surface of a Wall
T_∞	Temperature of Fluid Far Removed from Heat Source
U_1^*	Over Heat Transfer Coefficient Defined in Equation (29)
U_{in}	Sparger Hole Velocity
U_{out}	Bubble Velocity
U_1A_1	Overall Heat Transfer Coefficient for Determination of the Heat Loss to the Surroundings
U_2A_2	Overall Heat Transfer Coefficient for Cooling Surfaces
V	Volume
V_1	Electric Potential Applied
V_2	Voltage of Immersion Heater
V_L	Liquid Volume
V_S	Superficial Gas Velocity
V_b	Volume of a Bubble
Y	Humidity of Air
Y_{in}	Humidity of Inlet Gas Stream
Y_{out}	Humidity of Outlet Gas Stream
W	The Work Required to Push the Bubble from the Sparger to the Top of the Liquid Height
W_{air}	Mass Flow Rate of Air
W_I	Impeller Blade Width

DIMENSIONLESS GROUPS

G_v	Geometrical Number = $d^2 W_I / h.D^2$
Gr	Grashof Number = $g\beta\rho^2 (T_w^* - T_\infty) L^3/\mu^2$
Pr	Prandtl Number = $C_p \mu / k_f$
N_A	Aeration Number = $Q/N.d^3$
N_P	Mixing Power Number = $P.g_c/\rho_L N^3 d^5$
N_{Re}	Impeller Reynolds Number = $N\, d^2 \rho_L/\mu$
Nu	Nusselt Number = $h_o D/k_f$
N_{We}	Impeller Weber Number = $N^2 d^3 \rho_L/\sigma$

GREEK LETTERS

α	Constant Defined in Equation (68)
β	Temperature Coefficient of Volume Expansion
γ	Shear Strain
ΔH	Heat of Combustion
ΔH_{fc}	(Thermal Yield) Heat Evolved Per Gram of Dry Biomass
ΔH_{fo}	Ratio of Heat Released and Oxygen Consumed
ΔH_{fo}^*	Ratio of Total Heat Released and Total Oxygen Consumed
ΔH_{fo}^{**}	Ratio of Heat Released and CO_2 Evolved
ΔH_{O_2}	Gravimetric Oxygen Requirement Per Gram of Dry Biomass

ΔO_2	Oxygen Uptake Rate
ΔW	Amount of Dried Biomass per Unit Volume per Unit Time
ΔQ_{ferm}	Heat Generation per 1 gram of Dried Cells
ε	Strain
θ	Angle of Twist per Unit Length of the Shaft
λ	Latent Heat of Evaporization
μ	Absolute Viscosity
μ	Viscosity of Fluid at the Walls of Vessel
ρ	Mass Density
ρ_C	Density of Cooling Water
ρ_D	Density of Aerated Liquid
ρ_G	Density of Gas
ρ_∞	Density of Fluid far from the Heat Source
ρ_L	Density of Liquid
τ	Time Constant defined in Equation (80)
τ^*	Time Constant Defined in Equation (87)
σ	Surface Tension (also Weight Part of Carbon in Equation [97-107])
ϕ	Angle of Twist
Φ	Gas Hold-up
ω	Angular Velocity
$\Sigma_i M_i C_{pi}$	Heat Capacity of System Components (Appendix II) (Fermentation Broth + Fermentor Jar + Stainless Steel)

REFERENCES

1. Bennett, I.C., Hondermarck, J.C. and Todd, J.R., Hydrocarbon Processing 3, 104 (1969).
2. Cooney, C.L. and Makaguchi, N., Biotechnol. Bioeng. Sypm. 7, 65 (1977).
3. Winzler, R.J. and Baumberger, J.P., Journal of Cellular and Comparative Physiology 12, 183 (1938).
4. Sedlaczek, L., Czerniawki, E. and Zablocki, B. , Bulletin de L'Academic Polonaise des Sciences 5, 295 (1965).
5. Cooney, C.L., Wang, D.I.C. and Mateles, R.I., Biotechnol. Bioeng. 11, 269 (1969) .
6. Battley, E.H., Physiologia Plantarum 13, 674 (1960) .
7. Forrest, W.W., Journal of Scientific Instruments 38, 143 (1961) .
8. Volesky, B., Luong, H.T. and Thambimuthu, K.V., Can. J. Chem. Eng. 56, 526 (1978) .
9. Eriksson, R. and Wadsö, I., Proc. 1st Eur. Biophyys. Congr. IV, 319, Wien Med. Akad. (1971) .
10. Eriksson, R. and Holme, T., " Advances in Microbial Engineering ", Biotech. Bioeng. Sypm. 4, 581 (1973).
11. Mou, D.G. and Cooney, C.L., Biotechnol. Bioeng. 18, 1371 (1976).
12. Minkevich, I.G. and Eroshin, V.K., Folia Microbiol. 13, 376 (1973).
13. Imanaka, T. and Aiba, S., J. Appl. Chem. Biotechnol. 26, 559 (1976).
14. Thaysen, A.C., " Food " 14, 116 (1945).
15. Guenther, K.R., Biotechnol. Bioeng. 7, 445 (1965).
16. Lehrer, I.H., Ind. Eng. Chem, Process Design Develop. 7, 226 (1968).

17. Miller, D.N., AIChE J. 20, 445 (1974).

18. Bird, R.B., Stewart, W.E. and Lightfoot, E.N., " Transport Phenomena ", J. Wiley & Sons, N.Y. (1960).

19. Bird, R.B., Stewart, W.E. and Lightfoot, E.N., " Transport Phenomena ", J. Wiley & Sons, N.Y. (1960).

20. Seider, E.N. and Tate, G.E., Ind. Eng. Chem. 28, 1429 (1936)

21. Brooks, G. and Su, G., Chem. Eng. Prog. Symposium Series 56, 237 (1960).

22. McAdams, W.H., " Heat Transmission " 3rd Ed., McGraw-Hill, N.Y. (1954).

23. Rushton, J.H., Costich, E.W. and Everett, H.J., Chem. Eng. Prog. 46, 395 (1950) .

24. Blakebrough, N. and Sambamurthy, K., J. Appl. Chem. 14, 413 (1964) .

25. Ohyama, Y. and Endoh, K., Chem. Eng. (Japan) 19, 2 (1955).

26. Michel, B.J. and Miller, S.A., AIChE J. 8, 262 (1962).

27. Pharamond, J.C., Roustan, M. and Roques, H., Chem. Eng. Sci. 30, 907 (1975).

28. Clark, M.W. and Vermeulen, T., UCRL- 10996, Uni. Calif., Berkeley (1963) .

29. Hassan, I.T.M. and Robinson, C.W., AIChE J. 23, 48 (1977) .

30. Calderbank, P.H., Trans. Inst. Chem. Engrs., 37, 443 (1958).

31. Calderbank, P.H., Trans. Inst. Chem. Engrs., 38, 173 (1959).

32. Timoshenko,S. and MacCullough, G.H., " Elements of Strength of Material ", 3rd Ed., D. van Nostrand, Princeton, N.J. (1949).

33. Amundson, N.R., Aris. R., Kalman, N.R. and Lapidus, L., " Fundamental Ideas and Applications of Optimization Techniques in Design and Control ", AIChE Special Lecture Notes, Cleveland, Ohio (1960) .

34. Aris, R. and Amundson. N.R., Chem. Eng. Sci. 7, 121 (1958).

35. Aris, R. and Blakemore, N., Chem. Eng. Sci. 17, 591 (1962).

36. Lapidus, L. and Koepke, R., Chem. Eng. Sci. 16, 252 (1961).

37. Fiechter, A. and Meyenburg, K.V., Biotechnol. Bioeng. 10, 535 (1968).

38. Servizi, J.A. and Bogan, R.H., Journal of Water Pollution Control Federation 36, 607 (1964).

39. Rushton, J.H., Costich, E.W. and Everett, H.J., Chem. Eng. Prog. 46, 467 (1950).

40. Calderbank, P.H. and Moo-Young, M., Trans. Inst. Chem. Eng. 37,26 (1959).

41. Cooney, C.L., "Measurement of Heat Evolution During Fermentation", M.Sc. Thesis, MIT (1968).

42. Headstrom, B.O.A., Ind. Eng.Chem. 44,651 (1952).

43. Goma, G., Ribot, D. and Pourciel, J.B., "Heat Balance, Analytical Tool in Fermentation", Paper Presented at Fifth International Fermentation Symposium, Berlin (1976).

44. Zabriski, D.W. and Humphrey, A.E., AIChE J. 24, 138 (1978).

45. Sedlaczek, L., ACTA Microbiologica Polonica 13, 101 (1964).

46. Wiley, A.J., "Food and Feed Yeast", Industrial Fermentation , 1, Leland A. Underkofler and Richard J. Hickey, Chemical Publishing Co., Inc., New York, N.Y., 307-343 (1954).

47. Harrison, J.S., Process Chemistry 2, 41 (1967).

48. Wang, D.I.C., Chem. Eng. 75, 99 (1968).

49. Vary, P.S. and Johnson, M.J., Abstract Q1, Amer. Chem. Soc., 154th National Meeting, Chicago, September 11-14 (1967).

50. Wodzinski, R. S. and Johnson, M.J., Abstract Q2, Amer. Chem. Soc., 154th National Meeting, Chicago, September 11-14 (1967).

51. Humphrey, A.E., "Single Cell Protein" , MIT Press, Cambridge, Mass.(1968).

52. Takahaski, J. Kobayashi, K., Kawabata, Y., and Yamada, K., Agri. Biol. Chem. 27, 836 (1963).

53. Darlington, Q.A., Biotechnol. Bioeng. 5, 241 (1964).

54. Mateles, R.I., Biotechnol. Bioeng. 18, 581 (1971).

55. Prochazka, G.J., Payne, W.J., and Mayberry, W.R., Biotechnol. Bioeng. 15, 1007 (1973).

56. Abbott, B.J. and Clemmen, A., Biotechnol. Bioeng. 15, 117 (1973).

57. Mennett, R.H. and Nakayama, T.O.M., Appl. Microbiol. 22, 772 (1971).

58. Czerniawski, E., Sedlaczek, L., and Zablocki, B., Bulletin de L'Academie Polonaise Des Sciences, 13, 291 (1965).

59. Taguchi, H. and Miyamota, S., Biotechnol. Bioeng. 10, 535 (1966).

60. Loiseau, B., Midoux, N. and Charpentier, J.C., AIChE J. 23, 931 (1977).

61. Gerashchenko, A., "The Basis of Thermometry", Kiev, Naukovo (1971).

62. Wang, H.Y., Cooney, C.L.,and Wang, D.I.C., "Dynamic Calorimetry of *S. Cerevisiae*", Unpublished Paper (Private Communication).